

# Protura from Hainan Island, China: new species, checklist and distribution

Yun Bu<sup>1,2</sup>, Yan Xiong<sup>3</sup>, Yun-Xia Luan<sup>2,4</sup>, Wen-Ying Yin<sup>2</sup>

**1** Natural History Research Center, Shanghai Natural History Museum, Shanghai Science & Technology Museum, Shanghai, 200041, China **2** Institute of Plant Physiology and Ecology, Chinese Academy of Sciences, Shanghai, 200032, China **3** Shanghai Information Center for Life Sciences, Shanghai Institute of Nutrition and Health, Shanghai Institutes for Biological Sciences, Chinese Academy of Sciences, Shanghai 200031, China **4** Guangdong Provincial Key Laboratory of Insect Developmental Biology and Applied Technology, Institute of Insect Science and Technology, School of Life Sciences, South China Normal University, Guangzhou, 510631, China

Corresponding author: Yun-Xia Luan ([yxluan@scnu.edu.cn](mailto:yxluan@scnu.edu.cn))

---

Academic editor: L. Deharveng | Received 9 March 2019 | Accepted 25 August 2019 | Published 9 October 2019

<http://zoobank.org/53FD6801-C4B5-4C09-B61B-47210DE937A7>

---

**Citation:** Bu Y, Xiong Y, Luan Y-X, Yin W-Y (2019) Protura from Hainan Island, China: new species, checklist and distribution. ZooKeys 879: 1–21. <https://doi.org/10.3897/zookeys.879.34404>

---

## Abstract

More than 1500 proturan specimens from Hainan Island are systematically studied. An annotated list of all species of Protura from Hainan Island is provided and their geographical distribution is discussed. The genus *Paracondeellum* is reported from Hainan Island for the first time, and *Paracondeellum paradisum* sp. nov. is described. The type species *Paracondeellum dukouense* (Tang & Yin, 1988) is redescribed based on syntype, and the lectotype and paralectotype are designated. The characters of the genus *Paracondeellum* are redefined, and the two known species are compared in detail. The Protura fauna of Hainan Island is mainly composed of species from the Oriental region, with 91% of the species belonging to the families Berberentulidae and Eosentomidae.

## Keywords

distribution, diversity, *Paracondeellum*, new species, taxonomy, type specimen

## Introduction

Protura is a group of tiny soil-dwelling arthropods with more than 800 described species (Bu et al. 2012, 2017; Galli et al. 2018). The diagnosis, distribution, and key to 76 known genera and seven families of Protura worldwide were recently given by Galli et al. (2018). So far, there are 214 species belonging to 43 genera recorded in China (Bu et al. 2012, 2017; Qian et al. 2018).

Hainan Island is the second largest island of China and is located off the southernmost point of the mainland (18°10'–20°10'N, 108°37'–111°03'E; Fig. 1). The tropical forest landscape on Hainan Island is one of the hotspots for biodiversity in China, with a high floral diversity and over 6000 species of insects recorded (Huang 2002). In recent years, many rare insects, such as belonging to Zoraptera, have been found on Hainan Island (Yin et al. 2015).

There are several previous publications on the Protura from Hainan Island. The first study reported 14 species of Eosentomidae from Hainan (Yin 1986). Then, eight species of the genus *Kenyentulus* (Berberentulidae) were described (Yin 1987). Later, 24 species of Protura were recorded in Hainan Province with *Fujientomon dicestum* Yin, 1977 and *Pseudanisentomon yongxingense* Yin, 1988 included (Yin 1999, 2002). In 2004, the Protura from Jianfengling Mountain were investigated again. In 2005, *Amphientulus sinensis* Xiong, Xie & Yin, 2005 was described and seven new records and three undetermined species were newly added (Xiong 2005; Xiong et al. 2005). One of these undetermined species was subsequently described as *Anisentomon hainanense* Xiong, Bu & Yin, 2008 (Xiong et al. 2008).

In 2011 and 2017, we investigated the soil fauna of Hainan Island on several occasions and collected many proturan specimens. In the present paper, Protentomidae is recorded for the first time and one new species of genus *Paracondeillum* Yin, Xie & Zhang, 1994 is identified and described. We checked the syntypes of the type species of *Paracondeillum dukouense* (Tang & Yin, 1988), designated a lectotype and paralectotype, and redescribed it in detail. In addition, based on more than 1500 proturans collected in Hainan Island from 1984 to 2017, a checklist is presented and the distribution of Protura on Hainan Island is summarized.

## Materials and methods

Most of specimens were collected between 1984 and 2004, and more recent specimens were collected during the expeditions in 2011 and 2017. All localities sampled so far are listed in Table 1 and shown in Figure 1. All specimens were extracted by means of the Tullgren funnels from soil and humus samples and preserved in 75% ethanol. They were mounted on slides using Hoyer's solution and dried in an oven at 50 °C.

Observations were made with a phase contrast microscope (Leica DM 2500). Photos were taken by a digital camera (Leica DMC 4500). Line drawings were made using a drawing tube. All specimens are deposited in the collections of Shanghai

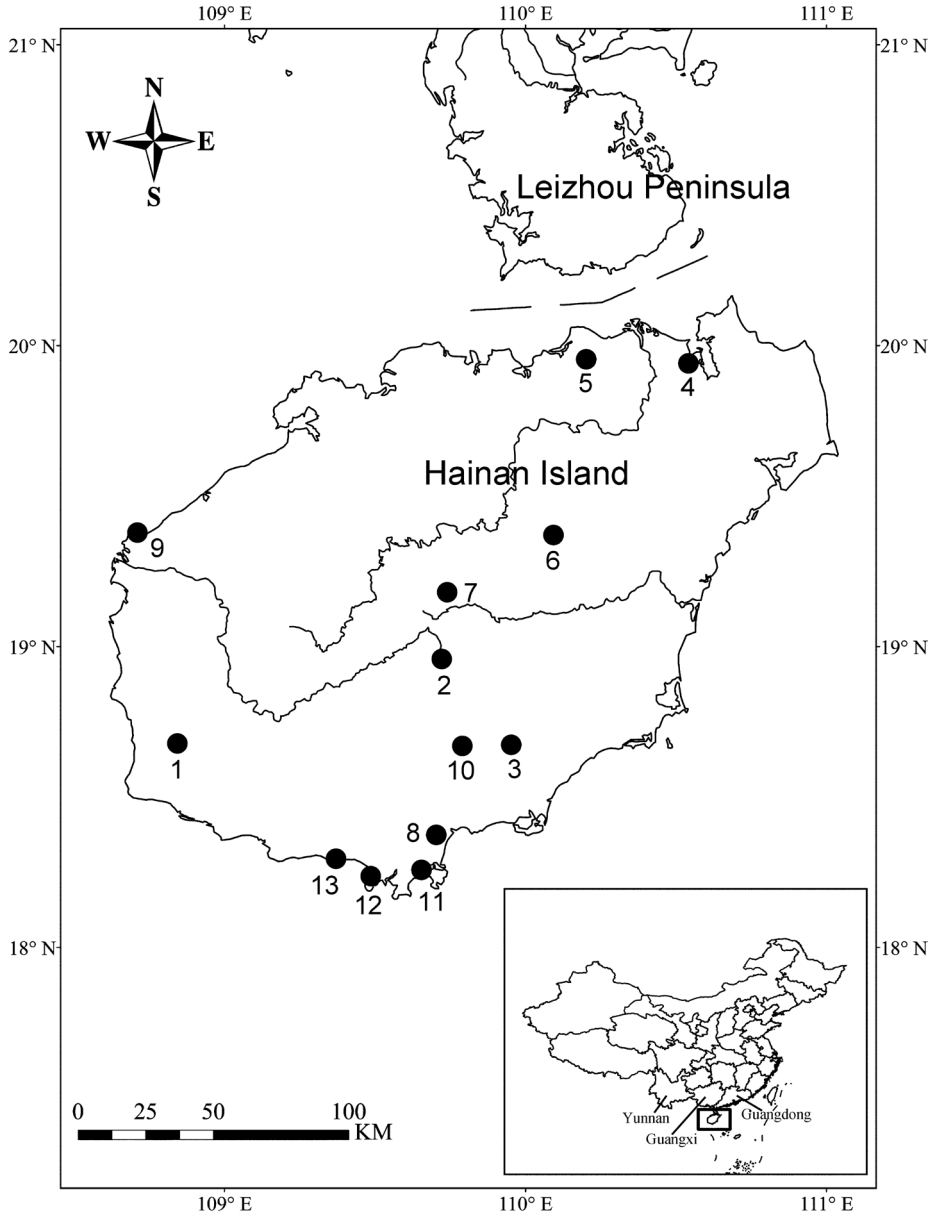


**Figure 1.** The sampling localities in Hainan Island. Numbers 1–13 indicate the localities listed in Tables 1, 5.

Natural History Museum (SNHM) and Shanghai Entomological Museum (SEM), Shanghai, China.

Abbreviations used in the text follow the paper by Bu and Yin (2007). Head setae and pores are named according to Rusek et al. (2012) and Shrubovych (2014). The arrangement of the taxa follows the system proposed by Yin (1999).

**Table 1.** The sampling localities of Protura in Hainan Island.

Number	Locality	Coordinates	Altitude (m)	Sampling years
1	Ledong County, Jianfengling National Natural Reserve	18°23'–18°52'N, 108°44'–109°02'E	120–330	1984, 1993, 2003, 2004
2	Wuzhishan City, Wuzhishan National Natural Reserve	18°49'–18°59'N, 109°32'–109°43'E	800–1200	1984, 1985, 2004, 2011
3	Wuzhishan City, Diaoluoshan National Natural Reserve	18°43'–18°58'N, 109°43'–110°03'E	500–1000	1985, 2004
4	Haikou City, Dongzhaigang National Natural Reserve	19°51'–20°01'N, 110°32'–110°37'E	20	2004
5	Haikou City, Crater National Geological Park	19°55'N, 110°12'E	223	2003
6	Tunchang County, Meiling Mountain	19°22'N, 110°04'E	150–230	2003
7	Tunchang County, Limu Mountain	19°17'N, 109°77'E	600–1000	2003
8	Baoting County, Ganshenling Provincial Natural Reserve	18°39'N, 109°66'E	500	2003
9	Changjiang County, Qizi bay	19°21'N, 108°40'E	15	2011
10	Baoting, Qixianling National Forest Park	18°42'N, 109°40'E	150	2017
11	Sanya City, Yalong Bay Tropical Paradise Forest Park	18°15'N, 109°38'E	200	2017
12	Sanya City, Luhuitou Park	18°13'N, 109°29'E	80	2017
13	Sanya City, Sanya bay	18°17'N, 109°22'E	5	2017

## Results

### Taxonomy

#### Family Protentomidae Ewing, 1936

#### Genus *Paracondeillum* Yin, Xie & Zhang, 1994

**Diagnosis.** Habitus short and robust. Pseudoculi circular without lever. Calyx of maxillary glands globular and smooth. Foretarsal sensilla of the exterior side reduced; interior sensilla *b'* absent. Abdominal appendages I–II two-segmented each with four setae, III uni-segmented with two setae. Tergites II–VII without or with few anterior setae. Sternites II–III each with three posterior setae. Sternites IV–VII each with nine posterior setae; sternite VIII with four setae in one row. Female squama genitalis short, with pointed acrostyli (Yin 1999; Galli et al. 2018).

**Distribution.** South China (Sichuan, Yunnan, Hainan).

**Remarks.** *Paracondeillum* Yin, Xie & Zhang, 1994 was originally separated from the genus *Condeillum* Tuxen, 1963. They have similar shapes of pseudocellus and maxillary gland, and the presence of setae *Pc* on sternites IV–V, but they can be easily separated by the chaetotaxy of tergite I (seta *P5* absent in *Paracondeillum* but present in *Condeillum*) and sternite VIII (four setae in *Paracondeillum* vs six setae in *Condeillum*). In addition, *Paracondeillum* can be distinguished from the genus *Neocondeillum* Tuxen & Yin, 1982 by the shape of pseudocellus (posterior lever absent in *Paracondeillum* but present in *Neocondeillum*) and the chaetotaxy of sternites IV–V (setae *Pc* present in *Paracondeillum* but absent in *Neocondeillum*).

***Paracondeellum paradisum* Bu & Yin, sp. nov.**

<http://zoobank.org/A723F8F3-18BF-420F-885E-29EA34F782D7>

Figures 2–4; Tables 2, 4

**Diagnosis.** *Paracondeellum paradisum* sp. nov. is characterized by two pairs of *A*-setae on tergite I, one pair of *A*-setae, and eight pairs of *P*-setae on tergites II–VI, absence of *A*-setae and *P2a* seta on tergite VII, tergites IX and X with 12 and 10 setae, respectively, absence of seta *d4* on dorsal side of head, and female squama genitalis short, with conical acrostylus.

**Material examined.** Holotype, female (slide no. HN-SY-P2017016) (SNHM), China, Hainan, Sanya City, Yalong Bay Tropical Paradise Forest Park, soil of the tropical rain forest, 200 m elev., 18.25°N, 109.63°E, 22-III-2017, Y. Bu collector. Paratypes, 1 female (slide no. HN-SY-P2017071) (SNHM), same data as holotype.

**Description.** Holotype: body length 570 µm, yellow-brown, foretarsus darker (Fig. 4A).

**Head.** Elliptic, length 80 µm, width 50 µm (Fig. 2A). Head setae short, rostrum slightly protruded. Setae *d6* and *sd6* present, *d4* and *sd4* absent, *d6* and *d7* length 6 µm and 7 µm respectively. Pores *cp* and *fp* present. Pseudoculus oval, without lever, length 8 µm, width 6.5 µm. PR = 10 (Fig. 2B). Canal of maxillary gland short, with globular calyx and short sausage-like posterior dilation. CF = 10 (Figs 2C, 4B). Labial palpus well developed, with four setae and apical tuft, without basal sensillum (Fig. 2D). Maxillary palpus with two subequal seta-like sensilla (Fig. 2E).

**Foretarsus.** Length 31 µm, claw length 9 µm, TR = 3.4; empodium length 2 µm, EU = 0.22. Dorsal sensilla *t-1* and *t-2* slender and long, BS = 0.63; *t-3* short and spatulate, not reaching base of claw (Fig. 2G). Exterior side with only sensilla *a*, *b* and *f* present; *a* spatulate, *b* and *f* short (Fig. 2F). Interior sensilla *a'* and *c'* short sword-like, *b'* absent. Relative length of sensilla:  $t-2 > t-1 > c' > t3 > a > a' > (b = f)$  (Fig. 2F, G). Length of middle tarsus 15 µm; claw length 10 µm. Length of hind tarsus 17 µm; claw length 12 µm.

**Thorax.** Thoracic chaetotaxy given in Table 2. Setae 1 and 2 on pronotum subequal in length, 6 µm and 7 µm respectively (Fig. 2H); mesonotum with seven pairs of posterior setae, *P5a* minute; metanotum with six pairs of posterior setae, *P5a* absent; setae *P1*, *P1a*, *P2* on mesonotum 6 µm, 1 µm, 7 µm, respectively; *P1a* on meso- and metanotum short, pin-shaped (Fig. 2H). Prosternum without seta *A2*. All setae on thoracic sternites of normal shape. Pores on thorax not observed.

**Abdomen.** Abdominal chaetotaxy given in Table 2. Tergite I with two pairs of anterior setae (*A1*, *A5*) and six pairs of posterior setae, *A5* short, sensillum-shaped (Fig. 2I). Tergites II–VI with one pair of anterior (*A1*) and eight pairs of posterior setae, *P2a* present and *P3a* absent (Figs 2J, 3A, 4E, F). Tergite VII without anterior setae and with eight posterior setae, *P2a* absent and *P3a* present (Figs 3B, C, 4E, F). Accessory setae *P1a* on tergites I–V short pin-shaped (4 µm), on tergites VI–VII normal (5 µm). Accessory setae *P2a* and *P4a* always pin-shaped, 2 µm in length. *P3a* on tergite VII

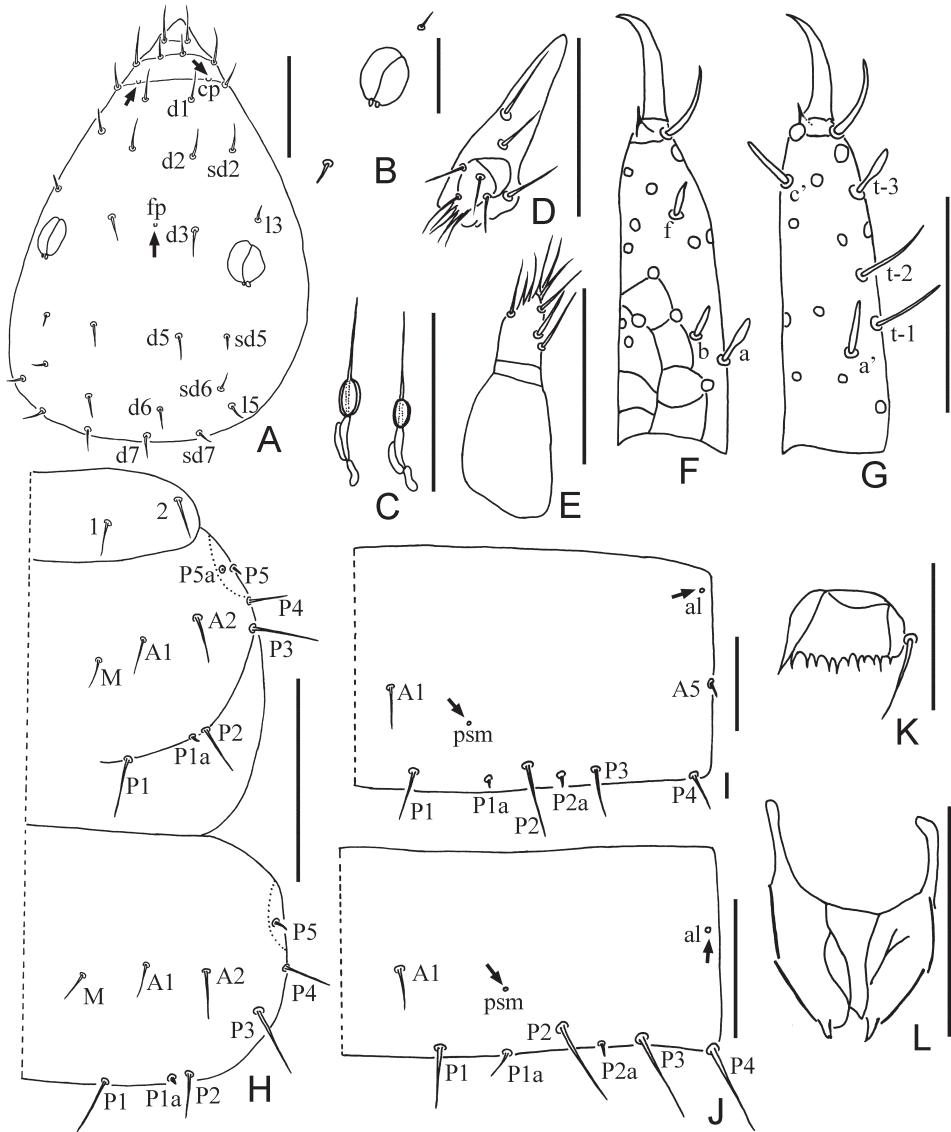


**Figure 2.** *Paracondeellum paradisum* sp. nov., holotype **A** head, dorsal view (*cp* = clypeal pore, *fp* = frontal pore) **B** pseudoculus **C** canal of maxillary gland **D** labial palpus **E** maxillary palpus **F** foretarsus, exterior view **G** foretarsus, interior view **H** dorsal thorax, right side **I** tergite I, right side (*al* = anterolateral pore, *psm* = posterosubmedial pore) **J** tergite VI, right side **K** comb **L** female quama genitalis. Arrows indicate pores. Scale bars: 10 µm (**B**, **K**); 20 µm (**A**, **C–J**, **L**).

of normal shape and 5 µm long (Fig. 4E, F). Tergite VIII with two pairs of anterior setae (*A1*, *A3*) (Fig. 4C). Posterior central seta *Pc* present on sternites IV–VII, sensillum shaped, 4–5 µm long (Figs 3A, C, 4F). *P1a* on sternites IV–VI short, pin-shaped (Fig. 3A), on sternite VII setiform (Fig. 3C).

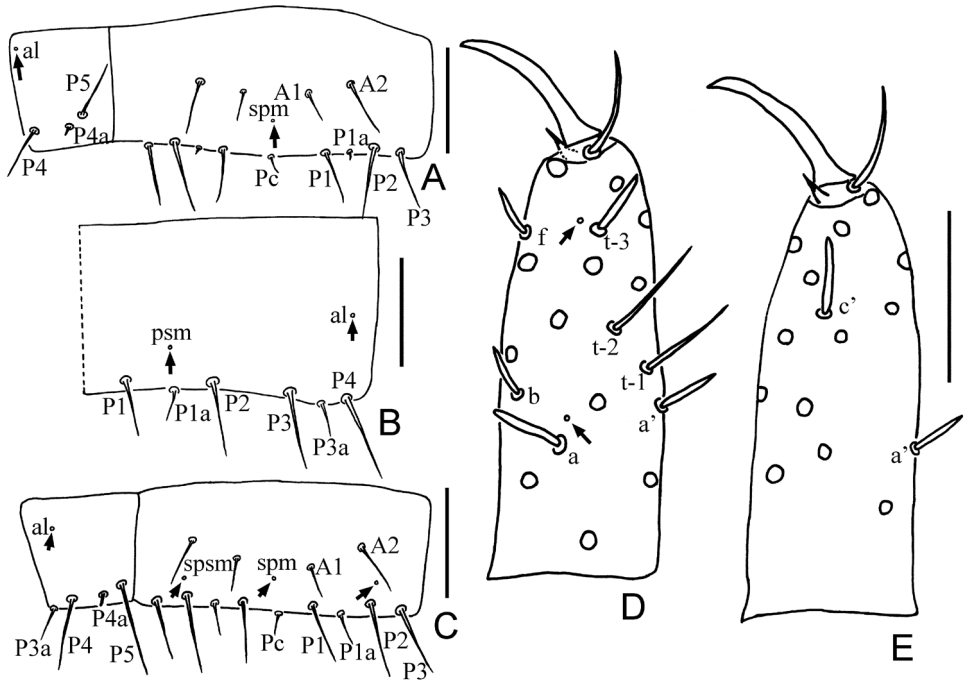


**Figure 3.** **A–C** *Paracondeellum paradisum* sp. nov., holotype **A** sternite VI (spm = sternal posteromedial pore) **B** tergite VII, right side **C** sternite VII (spsm = sternal posterosubmedial pore). **D–E** *Paracondeellum dukouense* (Tang & Yin, 1988) holotype **D** foretarsus, exterior view **E** foretarsus, interior view. Arrows indicate pores. Scale bars: 20  $\mu$ m.

Tergites I–VII with pores *psm* and *al* (Fig. 2I, J), VIII with pores *psm* only, IX–XI without pores, XII single median pore. Sternites I–VI each with single posteromedial pore *spm* (Figs 3A, 4F), VII with three posteromedial pores (Figs 3C, 4F), VIII with single posteromedial pore (Fig. 4D), IX–XI without pores, XII with one pair of anterolateral *sal* pores.

Abdominal appendages typical of the genus. Subapical setae and apical setae on appendage III 11  $\mu$ m and 5  $\mu$ m long respectively. Striate band on abdominal segment VIII reduced to a single serrate line (Fig. 4D). Comb on abdomen VIII rectangular, with 10 teeth, 10  $\mu$ m wide (Fig. 2K). Female squama genitalis short, with conical acrostylus (Fig. 2L).

**Etymology.** Latin “paradisum”, after “Paradise Forest Park” where type specimens were collected.

**Distribution.** China (Hainan)

**Remarks.** The genus *Paracondeellum* Yin, Xie & Zhang, 1994 is endemic to China and was previously known by a single species, *P. dukouense*, from Sichuan and Yunnan provinces. *Paracondeellum paradisum* sp. nov. differs from *P. dukouense* in the shape of foretarsal sensilla, pseudoculus, and female squama genitalis, and in the body chaetotaxy. A comparison of the morphology of these two species is given in Table 4.

**Table 2.** Adult chaetotaxy of *Paracondeellum paradisum* sp. nov.

	Segment	Dorsal		Ventral	
		Formula	Setae	Formula	Setae
Th.	I	4	1, 2	(2+2)/6	AI, M PI, 2, 3
	II	6/14	A2, 4, M	(4+2)/4	AI, 2, M
			PI, 1a, 2, 3, 4, 5, 5a		PI, 2
	III	6/12	A2, 4, M	(6+2)/4	AI, 2, 3, M
			PI, 1a, 2, 3, 4, 5		PI, 2
	Abd.	I	4/12	AI, 5	4/2
PI, 1a, 2, 2a, 3, 4				PI	
II–III		2/16	AI	4/3	AI, 2
			PI, 1a, 2, 2a, 3, 4, 4a, 5		Pc, 2
IV–VI		2/16	AI	4/9	AI, 2
			PI, 1a, 2, 2a, 3, 4, 4a, 5		Pc, 1, 1a, 2, 3
VII		0/16		4/9	AI, 2
			PI, 1a, 2, 3, 3a, 4, 4a, 5		Pc, 1, 1a, 2, 3
VIII		4/14	AI, 3	4	
			PI, 1a, 2, 2a, 3, 3a, 4		I, 2
IX		12	1, 1a, 2, 2a, 3, 4	4	I, 2
X		10	1, 2, 2a, 3, 4	4	I, 2
XI	6		6	I, 2, 3	
XII	9		6		

***Paracondeellum dukouense* (Tang & Yin, 1988)**

Figures 3, 5; Tables 3, 4

**Diagnosis.** *Paracondeellum dukouense* (Tang & Yin, 1988) is characterized by the one pair of *A*-setae on tergite I, absence of *A*-setae and *PIa* seta on tergites II–VI, absence of *A*-setae and nine pairs of *P*-setae (*P2a* present) on tergite VII, tergites IX and X with 14 and 12 setae respectively, absence of seta *d4* on head, and female squama genitalis with pointed acrostylus.

**Material examined.** Lectotype, female (slide no. 1), paralectotype, female (slide no. 2) (SEM), China, Sichuan, Dukou City (currently, Panzhihua City), Jinjiang County, soil under grass, 1155 m elev., 26.55N, 101.85E, 26-IX-1985, B.W. Tang and G.T. Jin collectors. We designated as the lectotype the female on slide no. 1 and the other female on slide no. 2 as the paralectotype.

**Redescription.** Body length of holotype 880 µm and paratype 720 µm; yellow-brown, with foretarsus darker (Fig. 5A).

**Head.** Elliptic, length 93–100 µm, width 70 µm. Dorsal setae longer than subdorsal and lateral ones, rostrum slightly protruded (Fig. 5C). Setae *d6* and *sd6* present, *sd6* sensillum-shaped; *d4* and *sd4* absent; *d6* and *d7* 11 µm and 6 µm long, respectively (Fig. 5C). Pores *cp* and *fp* present. Pseudoculus round, without lever, length 13 µm, width 11 µm. PR = 7.2–7.7 (Fig. 5C). Canal of maxillary gland short, with globular calyx and sausage-like posterior dilation. CF = 13.3–14.3 (Fig. 5B). Labial palpus well developed, with four setae and apical tuft, without basal sensillum. Maxillary palpus with two subequal sensilla.

**Foretarsus.** Length 46–50 µm, claw length 15–17 µm, TR=2.9–3.1; empodium length 4–5 µm, EU=0.24–0.33. Dorsal sensilla *t-1* and *t-2* slender and long, BS=0.66;

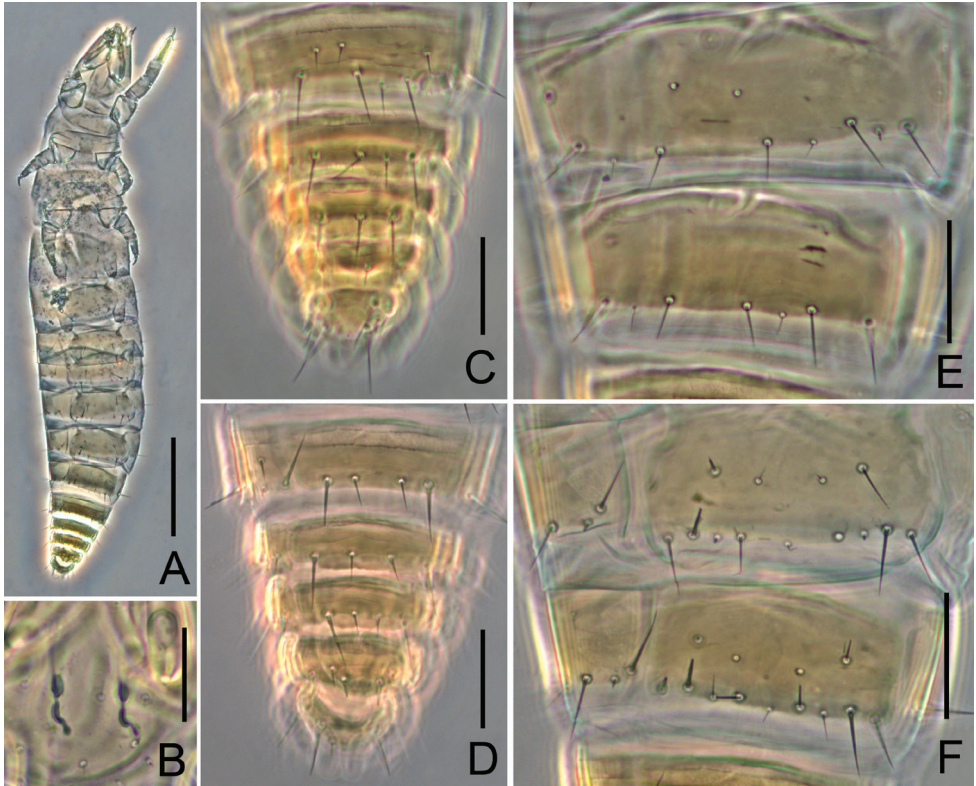


**Figure 4.** *Paracondeellum paradisum* sp. nov., holotype **A** habitus **B** canal of maxillary gland **C** tergites VIII–XII **D** sternites VIII–XII **E** tergites V–VII **F** sternites VI–VII. Scale bars: 100  $\mu\text{m}$  (**A**); 20  $\mu\text{m}$  (**B–F**).

*t-3* short sward-like, nearly reaching base of claw (Fig. 3D). Exterior slide with only sensilla *a*, *b* and *f* present; *a* spatulate, *b* and *f* short sward-like (Fig. 3D). Interior sensilla *a'* and *c'* short sward-like, *b'* absent (Fig. 3E). Relative length of sensilla:  $t-2 > t-1 > c' > a > t3 > a' > (b = f)$  (Fig. 3D, E). Length of middle tarsus 20  $\mu\text{m}$ ; claw length 12  $\mu\text{m}$ . Length of hind tarsus 23  $\mu\text{m}$ ; claw length 15  $\mu\text{m}$ .

**Thorax.** Thoracic chaetotaxy given in Table 3. Setae *1* and *2* on pronotum subequal in length, 10  $\mu\text{m}$  long; mesonotum with seven pairs of posterior setae, *P5a* minute; metanotum with six pairs of posterior setae, *P5a* absent; setae *P1*, *P1a*, *P2* on mesonotum 10  $\mu\text{m}$ , 1.5  $\mu\text{m}$ , 14  $\mu\text{m}$  respectively; *P1a* on meso- and metanotum short, pin-shaped. Prosternum with anterior seta *A2* (Fig. 5D), meso- and metasternum each with four posterior setae (Fig. 5E), metasternum with six anterior setae. All setae on sterna normal. Pores on thorax not detectable.

**Abdomen.** Abdominal chaetotaxy given in Table 3. Tergite I with one pair of anterior setae (*A5*) and six pairs of posterior setae, *A5* short, sensillum-shaped. Tergites II–VI without anterior setae and seven pairs of posterior setae, *P2a* present, *P1a* and *P3a* absent (Fig. 5F). Tergite VII without anterior setae and with nine pairs of posterior setae, both *P2a* and *P3a* present (Fig. 5G). Accessory setae *P2a* and *P4a* on tergites II–VII short, sensillum-shaped, 4  $\mu\text{m}$  in length, *P1a* and *P3a* on tergites VII normal,



**Figure 5.** *Paracondecellum dukouense* (Tang & Yin, 1988), holotype **A** habitus **B** canal of maxillary gland **C** head, dorsal view **D** prosternum **E** mesosternum **F** tergite VI **G** tergites VII–VIII **H** sternite VI **I** sternite VII **J** sternite V **K** tergites VIII–XII **L** sternites VIII–XII. Arrows indicate pores. Scale bars: 20 µm.

9–10 µm in length (Fig. 5F, G). Tergite VIII with three pairs of anterior setae (*A1*, *A3*, *A5*) and seven pairs of posterior setae, *P3a* short (5 µm) (Fig. 5G, K, L). Posterior central seta *Pc* present on sternites IV–VII slender, 8–9 µm long (Fig. 5H–J). *P1a* on sternites IV–VI short pin-shaped, 2 µm long (Fig. 5H, J), on sternite VII as normal seta, 9 µm long (Fig. 5I). Sternites IX and X with short *P3a* seta (Fig. 5L), which had been omitted in original description.

Tergites I–VII with pores *psm* and *al*, VIII with pores *psm* only, IX–XI without pores, XII with single median pore. Pores on sternites I–VI not observed due to the opacity of the old specimens (Fig. 5H, J); three posteromedial pores observed on sternite VII (Fig. 5I), VIII with posteromedial pore (Fig. 5L), IX–XI without pores, XII with one pair of *sal* pore.

Abdominal appendages typical of the genus. Subapical setae and apical setae on appendage III 12–13 µm and 6–8 µm long, respectively. Striate band on abdominal segment VIII reduced to a single serrate line (Fig. 5G, K, L). Comb on abdomen VIII

**Table 3.** Adult chaetotaxy of *Paracondeellum dukouense* (Tang & Yin, 1988).

Segment		Dorsal		Ventral	
		Formula	Setae	Formula	Setae
Th.	I	4	1, 2	(4+2)/6	A1, 2, M
			P1, 2, 3		
	II	6/14	A2, 4, M	(4+2)/4	A1, 2, M
			P1, 1a, 2, 3, 4, 5, 5a		P1, 2
	III	6/12	A2, 4, M	(6+2)/4	A1, 2, 3, M
			P1, 1a, 2, 3, 4, 5		P1, 2
Abd.	I	2/12	A5	4/2	A1, 2
			P1, 1a, 2, 2a, 3, 4		P1
	II-III	0/14		4/3	A1, 2
			P1, 2, 2a, 3, 4, 4a, 5		Pc, 2
	IV-VI	0/14		4/9	A1, 2
			P1, 2, 2a, 3, 4, 4a, 5		Pc, 1, 1a, 2, 3
	VII	0/18		4/9	A1, 2
			P1, 1a, 2, 2a, 3, 3a, 4, 4a, 5		Pc, 1, 1a, 2, 3
	VIII	6/14	A1, 3, 5		
			P1, 1a, 2, 2a, 3, 3a, 4	4	1, 2
	IX	14	1, 1a, 2, 2a, 3, 3a, 4	4	1, 2
	X	12	1, 2, 2a, 3, 3a, 4	4	1, 2
XI	6		6	1, 2, 3	
XII	9		6		

**Table 4.** Comparison between *Paracondeellum paradisum* sp. nov. and *P. dukouense* (Tang & Yin, 1988).

	<i>Paracondeellum paradisum</i> sp. nov.	<i>P. dukouense</i>
body length (µm)	570	720–880
pseudoculus (µm)	8	13
foretarsus (µm)	31	46–50
sensilla <i>b</i> and <i>f</i>	short, rod-like	longer, sward-like
sensillum <i>t-3</i>	short and spatulate	longer, sward-like
<i>A</i> -setae on tergite I	4 ( <i>A1</i> , <i>A5</i> )	2 ( <i>A5</i> )
<i>A</i> -setae on tergites II–VI	2 ( <i>A1</i> )	0
<i>P</i> -setae on tergites II–VI	16 ( <i>P1a</i> present)	14 ( <i>P1a</i> absent)
<i>P</i> -setae on tergite VII	16 ( <i>P2a</i> absent)	18 ( <i>P2a</i> present)
<i>A</i> -setae on tergite VIII	4 ( <i>A1</i> , <i>A3</i> )	6 ( <i>A1</i> , <i>A3</i> , <i>A5</i> )
setae on tergite IX	12 ( <i>P3a</i> absent)	14 ( <i>P3a</i> present)
setae on tergite X	10 ( <i>P3a</i> absent)	12 ( <i>P3a</i> present)
<i>A</i> -setae on prosternum	2 ( <i>A2</i> absent)	4 ( <i>A2</i> present)

rectangular, with 10 teeth, 12–13 µm wide (Fig. 5K). Female squama genitalis short, with pointed acrostylus.

**Etymology.** Named for Dukou City (now Panzhihua City, Sichuan Province) where type specimens were collected.

**Distribution.** China (Sichuan, Yunnan).

**Remarks.** *Paracondeellum dukouense* was originally described based on two syntypes (Tang and Yin 1988). In the original description (Tang and Yin 1988) and in the monograph of Yin (1999), most important characters such as foretarsal sensilla, pseudoculus, maxillary gland, as well as body chaetotaxy were briefly described and illustrated. After careful study of type specimens under a modern phase contrast microscope with higher resolution, we find that sensillum *c*' is present on the foretarsus and

that some of the setae on the body were previously ignored due to the lower resolution of the microscope used. We correct here these mistakes in the original description and supplement the description of head chaetotaxy, the porotaxy, and the shapes of setae on the body. Table 4 compares *P. dukouense* with the new species.

**List of species from Hainan Island**  
**Family Protentomidae Ewing, 1936**

*Paracondeellum paradisum* sp. nov.

**Description.** The description is given above.

**Family Berberentulidae Yin, 1983**

*Baculentulus tienmushanensis* (Yin, 1963)

**Material examined.** 1 male, 1 mj, locality 3, 19-I-1985, coll. G. T. Jin & Z. Y. Liu. 4 females, 1 mj, locality 5, 26-II-2003; 1 female, locality 1, 14-I-2004; 10 females, 6 mj, locality 2, 27-I-2004, coll. Y. Xiong. 1 mj, locality 11, 22-III-2017, coll. Y. Bu.

**Distribution.** Widely distributed in China (Hainan, Zhejiang, Shanghai, Jiangxi, Anhui, Hubei, Sichuan, Chongqing, Guizhou, Yunnan, Ningxia, Gansu, Shaanxi, Henan, Hebei, Liaoning, Neimenggu).

*Kenyentulus ciliciocalyci* Yin, 1987

**Material examined.** 5 females, locality 1, 27-XI-1984, coll. G. T. Jin & Z. Y. Liu. 1 female, VI-1993; 1 female, IV-1994, locality 1, coll. C. H. Liao. 9 females, 2 males, locality 5, 26-II-2003; 1 female, locality 6, 2-III-2003; 1 female, locality 5, 15-VI-2003; 6 females, 1 male, locality 1, 6-X-2003; 9 females, 2 males, 13 mj, locality 1, 14-I-2004; 7 females, 3 males, locality 1, 15-I-2004; 1 female, locality 1, 14-IV-2004; 2 females, 5 males, 1 mj, locality 1, 15-VII-2004, coll. Y. Xiong. 2 females, 1 male, 2 mj, locality 9, 20-III-2011, coll. Y. Bu & C. W. Huang. 14 females, 10 male, 1 mj, locality 11, 22-III-2017; 3 males, locality 12, 17-X-2017, coll. Y. Bu.

**Distribution.** Widely distributed in China (Hainan, Zhejiang, Hunan, Sichuan, Chongqing, Guizhou, Yunnan, Shaanxi).

*Kenyentulus dolichadeni* Yin, 1987

**Material examined.** 3 females, locality 2, 14-XI-1984, coll. G. T. Jin & Z. Y. Liu.

**Distribution.** China (Hainan, Zhejiang, Guangxi, Guizhou, Hubei, Sichuan, Jiangxi).

***Kenyentulus hainanensis* Yin, 1987**

**Material examined.** 4 females, 1 male, locality 1, 30-XI-1984; 2 females, 2 males, locality 2, 14-XI-1984; 1 male, 2 mj, locality 3, 19-I-1985, coll. G. T. Jin & Z. Y. Liu.

**Distribution.** China (Hainan, Guangdong).

***Kenyentulus henanensis* Yin, 1983**

**Material examined.** 2 female, 1 male, locality 2, 19-XI-1984, coll. G. T. Jin & Z. Y. Liu.

**Distribution.** Widely distributed in China (Hainan, Zhejiang, Jiangxi, Henan, Hubei, Guizhou, Yunnan, Ningxia).

***Kenyentulus japonicus* (Imadate, 1961)**

**Material examined.** 2 females, locality 2, 14-XI-1984; 5 females, 5 males, locality 1, 25-XI-1984, coll. G. T. Jin & Z. Y. Liu.

**Distribution.** Widely distributed in China (Hainan, Zhejiang, Jiangsu, Shanghai, Jiangxi, Anhui, Hunan, Sichuan, Guizhou, Yunnan, Shaanxi); Japan.

***Kenyentulus jianfengensis* Yin, 1987**

**Material examined.** 4 females, locality 1, 1-XII-1984, coll. G. T. Jin & Z. Y. Liu. 2 females, 1 male, 1 mj, locality 1, 6-X-2003; 7 females, 5 males, 2 mj, locality 1, 15-I-2004; 1 mj, locality 3, 27-I-2004; 3 females, 1 males, 1 mj, locality 1, 14-IV-2004; 7 females, 9 males, locality 1, 15-VII-2004, coll. Y. Xiong.

**Distribution.** China (Hainan, Guizhou).

***Kenyentulus jinghongensis* Yin, 1983**

**Material examined.** 3 females, locality 1, 25-XI-1984, coll. G. T. Jin & Z. Y. Liu.

**Distribution.** China (Hainan, Yunnan, Guizhou).

***Kenyentulus minys* Yin, 1983**

**Material examined.** 2 females, 2 males, locality 1, 19-XI-1984, coll. G. T. Jin & Z. Y. Liu.

**Distribution.** China (Hainan, Yunnan, Guangxi, Jiangxi)

***Amphientulus sinensis* Xiong, Xie & Yin, 2005**

**Material examined.** 1 female, locality 1, 17-XII-2002; 1 female, locality 2; 8 females, 4 males, 1 mj, locality 3, 27-I-2004, coll. Y. Xiong.

**Distribution.** China (Hainan, Guangdong).

**Family Sinentomidae Yin, 1965*****Sinentomon erythranum* Yin, 1965**

**Material examined.** 1 female, 1 male, 1 mj, locality 5, 26-II-2003; 1 mj, locality 1, 6-X-2003; 7 females, locality 1, 15-VII-2004, coll. Y. Xiong. 1 female, 1 LI, locality 13, 16-X-2017; 1 LI, locality 12, 17-X-2017, coll. Y. Bu.

**Distribution.** Widely distributed in South China (Hainan, Shanghai, Jiangsu, Zhejiang, Anhui, Fujian, Guangxi, Guangdong, Hunan, Guizhou, Yunnan).

**Family Fujientomidae Yin, 1996*****Fujientomon dicestum* Yin, 1977**

**Material examined.** 1 female, locality 5, 26-II-2003, coll. Y. Xiong.

**Distribution.** China (Hainan, Shanghai, Jiangsu, Zhejiang, Anhui, Ningxia).

**Family Eosentomidae Berlese, 1909*****Eosentomon actitum* Zhang, 1983**

**Material examined.** 8 females, 6 males, 2 mj, locality 1, XII-1984; 24 females, 24 males, 27 mj, locality 3, 23-I-1985, coll. G. T. Jin & Z. Y. Liu. 2 females, 3 males, locality 8, 22-II-2003, coll. Y. Xiong. 2 females, 3 mj, locality 11, 22-III-2017, coll. Y. Bu.

**Distribution.** China (Hainan, Guangdong, Sichuan).

***Eosentomon hainanense* Yin, 1986**

**Material examined.** 40 females, 33 males, 2 mj, locality 1, 25-XI-1984, coll. G. T. Jin & Z. Y. Liu. 2 females, VI-1993, locality 1, coll. C. H. Liao. 1 female, 5 males, locality 8, 22-II-2003; 4 females, 1 male, locality 6, 2-III-2003; 1 female, 3 males, 4 mj,

locality 5, 15-VI-2003; 19 female, 15 males, 8 mj, locality 1, 7-X-2003; 33 females, 31 males, 15 mj, locality 1, 14-I-2004; 1 male, locality 3, 960 m elev., 27-I-2004; 8 females, 8 males, 1 mj, locality 1, 15-VII-2004, coll. Y. Xiong.

**Distribution.** China (Hainan, Yunnan).

***Eosentomon iban* Imadate, 1965**

**Material examined.** 2 females, 2 males, locality 1, 27-XI-1984, coll. G. T. Jin & Z. Y. Liu.

**Distribution.** China (Hainan); Malaysia, Brunei.

***Eosentomon jinhongense* Yin, 1982**

**Material examined.** 2 females, 1 male, locality 2, 14-XI-1984, coll. G. T. Jin & Z. Y. Liu.

**Distribution.** China (Hainan, Yunnan).

***Eosentomon margarops* Yin & Zhang, 1982**

**Material examined.** 1 female, 2 males, 1 mj, locality 5, 26-II-2003; 1 female, 1 male, 2 mj, locality 5, 15-VI-2003; 1 female, 2 males, locality 1, 6-X-2003; 6 females, 3 males, 1 mj, locality 1, 15-I-2004; 2 females, 1 male, 1 mj, locality 2, 820 m elev., 27-I-2004; 3 females, 2 males, 2 mj, locality 3, 1000 m elev., 27-I-2004; 2 females, 1 male, locality 1, 14-IV-2004; 2 females, locality 1, 15-VII-2004, coll. Y. Xiong. 1 female, locality 10, 23-III-2017, coll. Y. Bu.

**Distribution.** China (Hainan, Guangdong, Sichuan).

***Eosentomon novemchaetum* Yin, 1965**

**Material examined.** 1 female, locality 11, 22-III-2017, coll. Y. Bu.

**Distribution.** China (Hainan, Shanghai, Jiangsu, Anhui, Jiangxi, Liaoning, Shaanxi)

***Eosentomon orientale* Yin, 1965**

**Material examined.** 1 female, locality 1, 25-XI-1984, coll. G. T. Jin & Z. Y. Liu.

**Distribution.** Widely distributed in China (Hainan, Shanghai, Jiangsu, Zhejiang, Anhui, Jiangxi, Hubei, Hunan, Guangxi, Guangdong, Sichuan, Chongqing, Guizhou, Ningxia, Shaanxi, Liaoning).

***Eosentomon sakura* Imadate & Yosii, 1959**

**Material examined.** 5 females, 3 males, locality 1, 25-XI-1984, coll. G. T. Jin & Z. Y. Liu. 13 females, 7 males, 9 mj, locality 8, 22-II-2003; 1 female, 1 mj, locality 5, 20-I-2003; 8 females, 13 males, 7 mj, locality 5, 26-II-2003; 1 female, 1 male, locality 6, 2-III-2003; 2 females, 5 males, 2 mj, locality 5, 15-VI-2003; 2 females, 1 mj, locality 1, 6-X-2003; 3 females, 1 male, 2 mj, locality 7, 13-VII-2003; 5 females, 2 males, 2 mj, locality 1, 15-I-2004; 46 females, 45 males, 29 mj, locality 4, 23-I-2004; 12 females, 20 males, 10 mj, locality 2, 820 m elev., 27-I-2004; 5 females, 5 males, 2 mj, locality 1, 500 m elev., 27-I-2004, coll. Y. Xiong. 1 male, locality 2, 20-III-2011, coll. Y. Bu & C. W. Huang. 8 females, 7 males, 3 mj, locality 11, 22-III-2017, coll. Y. Bu.

**Distribution.** Widely distributed in China (Hainan, Shanghai, Jiangsu, Zhejiang, Anhui, Jiangxi, Hubei, Hunan, Guangxi, Guangdong, Yunnan, Sichuan, Fujian, Guizhou, Taiwan, Hong Kong, Shaanxi).

***Eosentomon shanum* (Zhang, 1984)**

**Material examined.** 2 females, 1 male, locality 4, 23-I-2004; 1 female, 2 males, locality 1, 14-IV-2004; 5 females, 1 mj, locality 1, 15-VII-2004, coll. Y. Xiong.

**Distribution.** China (Hainan, Guangxi, Hunan, Jiangxi).

***Eosentomon spanum* Yin, 1986**

**Material examined.** 1 female, 1 male, locality 1, 27-XI-1984, coll. G. T. Jin & Z. Y. Liu.

**Distribution.** China (Hainan).

***Eosentomon tropicum* Yin, 1986**

**Material examined.** 5 females, locality 1, 25-XI-1984, coll. G. T. Jin & Z. Y. Liu. 1 female, VII-1993, locality 1, coll. C. H. Liao. 1 female, 3 males, 3 mj, locality 8, 22-II-2003; 4 females, 3 males, 4 mj, locality 1, 6-X-2003; 2 mj, locality 1, 15-I-2004; 3 females, 1 male, locality 1, 15-VII-2004, coll. Y. Xiong. 2 females, locality 11, 22-III-2017, coll. Y. Bu.

**Distribution.** China (Hainan).

***Eosentomon xishaense* Yin, 1988**

**Material examined.** 2 females, locality 1, 27-XI-1984, coll. G. T. Jin & Z. Y. Liu. 1 mj, VI-1993, locality 1, coll. C. H. Liao. 1 female, locality 5, 20-I-2003; 3 mj, locality

1, 14-IV-2004; 4 females, 2 males, locality 1, 15-VII-2004, coll. Y. Xiong. 1 female, locality 9, 20-III-2011, coll. Y. Bu & C. W. Huang. 2 females, 1 male, 1 mj, locality 11, 22-III-2017; 1 male, locality 10, 23-III-2017, coll. Y. Bu.

**Distribution.** China (Hainan, Xisha Islands, Yongxing Island).

***Eosentomon yanshanense* Yin & Zhang, 1982**

**Material examined.** 2 females, locality 1, 25-XI-1984, coll. G. T. Jin & Z. Y. Liu. 2 females, 4 males, 7 mj, locality 6, 2-III-2003; 9 females, 3 males, 10 mj, locality 4, 23-I-2004; 2 females, 2 males, locality 1, 14-IV-2004; 2 females, 1 mj, locality 1, 15-VII-2004, coll. Y. Xiong.

**Distribution.** China (Hainan, Guangxi, Guangdong, Fujian, Jiangxi, Hunan, Hubei, Yunnan).

***Eosentomon zhanjiangense* Zhang, 1983**

**Material examined.** 2 females, locality 1, 19-I-1985, coll. G. T. Jin & Z. Y. Liu. 1 females, 2 males, locality 1, 14-IV-2004, coll. Y. Xiong.

**Distribution.** China (Hainan, Guangdong).

***Anisentomon hainanense* Xiong, Bu & Yin, 2008**

**Material examined.** 1 female, 1 male, locality 1, 6-X-2003, coll. Y. Xiong.

**Distribution.** China (Hainan).

***Anisentomon quadrisetum* Zhang & Yin, 1981**

**Material examined.** 1 female, 1 male, locality 1, 7-X-2003, 14 females; 7 males, locality 1, 14-I-2004, coll. Y. Xiong. 1 male, 1 mj, locality 11, 22-III-2017, coll. Y. Bu.

**Distribution.** China (Hainan, Guangxi, Guangdong).

***Neanisentomon yuenicum* Zhang & Yin, 1984**

**Material examined.** 1 female, locality 1, 14-IV-2004, coll. Y. Xiong. 1 female, 1 male, locality 10, 23-III-2017, coll. Y. Bu.

**Distribution.** China (Hainan, Guangdong).

***Paranisentomon tuxeni* (Imadate & Yosii, 1959)**

**Material examined.** 6 females, 1 mj, locality 3, 1000 m elev., 27-I-2004, coll. Y. Xiong.

**Distribution.** China (Hainan, Hubei, Hunan, Jiangxi, Anhui, Guizhou, Shaanxi).

***Pseudanisentomon paurophthalmum* Zhang & Yin, 1984**

**Material examined.** 1 female, 1 mj, locality 11, 22-III-2017, coll. Y. Bu.

**Distribution.** China (Hainan, Guangxi).

***Pseudanisentomon molykos* Zhang & Yin, 1984**

**Material examined.** 5 females, 2 males, 1 mj, locality 1, 6-X-2003; 1 female, locality 1, 14-IV-2004, coll. Y. Xiong.

**Distribution.** China (Hainan, Guangdong, Guangxi, Yunnan).

***Pseudanisentomon sininotiale* Zhang & Yin, 1984**

**Material examined.** 2 females, locality 1, 27-XI-1984, coll. G. T. Jin & Z. Y. Liu. 2 females, 4 males, locality 4, 23-I-2004; 1 male, locality 3, 600 m elev., 27-I-2004, coll. Y. Xiong.

**Distribution.** China (Hainan, Guangxi, Hunan).

**Discussion.** The 34 species of Protura recorded from Hainan Island belong to 11 genera and five families (Protentomidae, Berberentulidae, Sinentomidae, Fujientomidae and Eosentomidae) (Table 5). Most species (91%) belong to Eosentomidae (21 species) and Berberentulidae (10 species), while the other three families are represented by one species each. Both Berberentulidae and Eosentomidae are widely distributed in China and have high species richness. In contrast, Sinentomidae, Protentomidae, and Fujientomidae each has fewer species occurring in China. Undoubtedly, proturans found in Hainan Island are mainly related to the fauna of Oriental Region and are distinctly different from those from Russian Far East and Siberia (Bu et al. 2014; Shrubovych 2014), which are dominated by the family Acerentomidae.

By comparing the species distribution, we found that the Protura fauna of Hainan Island is closely related to those of neighboring mainland regions (Yin 1999; Szeptycki 2007), and there are 13, 10, and 11 species shared with Guangdong, Guangxi, and Yunnan provinces, respectively (Fig. 1; Table 5), which is consistent with the geological history of Hainan Island (Wang 1991; Zhang and Fang 2012). Until the Quaternary period (2.5 million years ago), Hainan Island was still connected with Leizhou Peninsula of Guangdong Province. In the Middle Pleistocene, fault depression led to the separation of Hainan Island from the mainland. With sea level fluctuations, Hainan Island was connected to or separated from the mainland for several times. Since the

**Table 5.** The list of proturan species from Hainan Island and their distribution in Hainan Island and three neighboring mainland provinces.

Classification	Species	Hainan	Guangdong	Guangxi	Yunnan
<b>Acerentomata Yin, 1996</b>					
<b>Protentomidae Ewing, 1936</b>					
<i>Paracondeellum</i> Yin, Xie & Zhang, 1994	<i>P. paradisum</i> sp. n.*	11**			
<b>Berberentulidae Yin, 1983</b>					
<i>Baculentulus</i> Tuxen, 1977	<i>B. tienmushanensis</i> (Yin, 1963)	2, 3, 5, 11			+
<i>Kenyentulus</i> Tuxen, 1981	<i>K. ciliciocalyci</i> Yin, 1987	1, 5, 6, 9, 11, 12			+
	<i>K. dolichadeni</i> Yin, 1987	2			
	<i>K. hainanensis</i> Yin, 1987	1, 3	+		
	<i>K. henanensis</i> Yin, 1983	2			+
	<i>K. japonicus</i> (Imadate, 1961)	2			+
	<i>K. jianfengensis</i> Yin, 1987	1, 2			
	<i>K. jinghongensis</i> Yin, 1983	1			+
	<i>K. minys</i> Yin, 1983	1		+	+
<i>Amphientulus</i> Tuxen, 1981	<i>A. sinensis</i> Xiong, Xie & Yin, 2005	1, 3	+		
<b>Sinentomata Yin, 1996</b>					
<b>Sinentomidae Yin, 1965</b>					
<i>Sinentomon</i> Yin, 1965	<i>S. erythranum</i> Yin, 1965	1, 5, 12, 13	+	+	+
<b>Fujientomidae Yin, 1996</b>					
<i>Fujientomon</i> Yin, 1977	<i>F. dicesum</i> Yin, 1977	5			
<b>Eosentomata Yin, 1996</b>					
<b>Eosentomidae Berlese, 1909</b>					
<i>Eosentomon</i> Berlese, 1909	<i>E. actitum</i> Zhang, 1983	1, 3, 8, 11	+		
	<i>E. hainanense</i> Yin, 1986*	1, 3, 5, 6, 8	+		+
	<i>E. iban</i> Imadate, 1965	1			
	<i>E. jinhongense</i> Yin, 1982	2			+
	<i>E. margarops</i> Yin & Zhang, 1982	1, 2, 3, 5, 10	+		
	<i>E. novemchaetum</i> Yin, 1965	11			
	<i>E. orientale</i> Yin, 1965	1	+		+
	<i>E. sakura</i> Imadate & Yosii, 1959	1, 2, 4–8, 11	+	+	+
	<i>E. shanum</i> (Zhang, 1984)	1, 4		+	
	<i>E. spanum</i> Yin, 1986*	1			
	<i>E. tropicum</i> Yin, 1986*	1, 8, 11			
	<i>E. xishaense</i> Yin, 1988	1, 5, 9–11			
	<i>E. yanshanense</i> Yin & Zhang, 1982	1, 4, 6	+	+	+
	<i>E. zhanjiangense</i> Zhang, 1983	1	+		
<i>Anisentomon</i> Yin, 1977	<i>A. hainanense</i> Xiong, Bu & Yin, 2008*	1			
	<i>A. quadrisetum</i> Zhang & Yin, 1981	1, 11	+	+	
<i>Neanisentomon</i> Zhang & Yin, 1984	<i>N. yuenicum</i> Zhang & Yin, 1984	1, 10	+		
<i>Paranisentomon</i> Zhang & Yin, 1984	<i>P. tuxeni</i> (Imadate & Yosii, 1959)	3			
<i>Pseudanisentomon</i> Zhang & Yin, 1984	<i>P. paurophthalmon</i> Zhang & Yin, 1984	11		+	
	<i>P. molykos</i> Zhang & Yin, 1984	1	+	+	
	<i>P. sinintiale</i> Zhang & Yin, 1984	1, 4		+	

\* Species known only from Hainan Island so far.

\*\* Numbers indicate the localities given in Table 1.

end of the Quaternary period, due to the drastically rise of sea level, Hainan Island has been separated from the mainland without interruption.

Among the mainland regions neighboring Hainan Island, the Protura fauna of Yunnan Province has been systematically studied (Zhang et al. 1996; Yin et al. 2000), and nearly 80 species were reported from that province, with the Berberentulidae and Eosentomidae having fairly high diversity (Zhang et al. 1996; Yin et al. 2000). In this

study, we found the diversity of Protura fauna from Hainan Island is very similar to that from Yunnan Province. The only difference is the presence of family Hesperentomidae in Yunnan, which is absent in Hainan Island.

Sampling localities in Hainan Island are still sparse, and additional collection of proturans should be made in the future, so as to reveal the true diversity and provide a better understanding of the biogeography of Protura on the Hainan Island.

## Acknowledgements

We give our cordial gratitude to Mr Gentao Jin, Mr Zuyao Liu, Mr Chonghui Liao, Mr Bowei Tang, and Mr Chengwang Huang for their help in the collection of specimens, to Mr Yiming Yang for his help in preparation of slides, to Mr Rongdong Xie for his identification of part specimens and to Dr Yi Bai for his help in preparation of the map of Hainan Island. We also appreciate Professor José G. Palacios-Vargas for his linguistic corrections to the manuscript as well as his valuable advice. Special thanks are given to Dr Julia Shrubovych and Dr Loris Galli for their valuable comments and review of the manuscript. This research was supported by the National Natural Science Foundation of China (no. 31772509, 31471958 and 31772510), the Natural Science Foundation of Shanghai (no. 17ZR1418700), and the Open Project of Shanghai Key Lab for Urban Ecological Processes and Eco-Restoration (no. SHUES2019A11).

## References

- Bu Y, Gao Y, Luan YX, Yin WY (2012) Progress on the systematic study of basal Hexapoda. Chinese Bulletin of Life Sciences 24 (2): 130–138. [in Chinese with English abstract]
- Bu Y, Potapov MB, Yin WY (2014) Systematic and biogeographical study of Protura (Hexapoda) in Russian Far East: new data on high endemism of the group. ZooKeys 424: 19–57. <https://doi.org/10.3897/zookeys.424.7388>
- Bu Y, Qian CY, Luan YX (2017) Three newly recorded species of Acerentomata (Hexapoda: Protura) from China, with analysis of DNA barcodes. Entomotaxonomia 39(1): 1–14. <https://doi.org/10.11680/entomotax.2017001>
- Bu Y, Yin WY (2007) Two new species of *Hesperentomon* Price, 1960 from Qinghai Province, northwestern China (Protura: Hesperentomidae). Acta Zootaxonomica Sinica 32(3): 508–514.
- Galli L, Shrubovych J, Bu Y, Zinni M (2018) Genera of the Protura of the world: diagnosis, distribution, and key. ZooKeys 772: 1–45. <https://doi.org/10.3897/zookeys.772.24410>
- Huang FS (2002) Insect Fauna of Hainan Forest. Science Press, Beijing, 1063 pp. [In Chinese]
- Qian CY, Bu Y, Luan YX (2018) DNA barcoding and an updated key to the genus *Hesperentomon* (Protura: Acerentomata: Hesperentomidae), with a new species from Northwest China. Zootaxa 4462(4): 523–534. <https://doi.org/10.11646/zootaxa.4462.4.5>

- Rusek J, Shrubovych J, Szeptycki A (2012) Head porotaxy and chaetotaxy of order Acerentomata (Protura). *Zootaxa* 3262: 54–61. <https://doi.org/10.11646/zootaxa.3262.1.5>
- Shrubovych J (2014) Identification and character analysis of the Acerentomidae (Protura) of the northeastern Palearctic (Protura: Acerentomidae). *Zootaxa* 3755(2): 136–164. <https://doi.org/10.11646/zootaxa.3755.2.2>
- Szeptycki A (2007) Catalogue of the world Protura. *Acta Zoologica Cracoviensia* 50 (1): 1–210. <https://doi.org/10.3409/000000007783995417>
- Tang B, Yin WY (1988) Three new species of Protura from Sichuan Province. *Zoological Research* 9(3): 309–315. [in Chinese with English abstract]
- Wang XF (1991) Geology of Hainan Island III, Structural Geology. Science Press, Beijing, China, 138 pp. [in Chinese]
- Xiong Y (2005) The community diversity of soil animals in the tropical and subtropical forests and the phylogeny of Collembola. PhD Thesis, East China Normal University, Shanghai, 139 pp. [in Chinese with English abstract]
- Xiong Y, Bu Y, Yin WY (2008) A new species of *Anisentomon* from Hainan, Southern China (Protura: Eosentomidae). *Zootaxa* 1727: 39–43. <https://doi.org/10.11646/zootaxa.1727.1.4>
- Xiong Y, Xie RD, Yin WY (2005) First record of the genus *Amphientulus* Tuxen, 1981 (Protura: Acerentomidae) from China, with description of a new species. *The Raffles Bulletin of Zoology* 53 (1): 1–5.
- Yin WY (1986) Three new species and a new record of *Eosentomon* from Hainan Island, China (Protura: Eosentomidae). *Contribution from Shanghai Institute of Entomology* 6: 135–140. [in Chinese with English abstract]
- Yin WY (1987) Four new species of *Kenyentulus* from hainan Island. *Zoological Research* 8(2): 149–157. [in Chinese with English abstract]
- Yin WY (1999) Fauna Sinica. Arthropoda. Protura. Science Press, Beijing, 510 pp.
- Yin WY (2002) Protura. In: Huang FS (Ed.) *Insect Fauna of Hainan Forest*. Science Press, Beijing, 24–27. [In Chinese]
- Yin WY, Xie R, Imadaté G (2000) Protura of Yunnan, Southwest China, with description of four new species (Protura: Eosentomata), In: Aoki J, Yin WY, Imadaté G (Eds) *Taxonomical Studies on the Soil Fauna of Yunnan Province in Southwest China*, Tokai University Press, Tokyo, 117–131.
- Yin WY, Xie R, Zhang J (1994) Phylogeny and biogeography of *Condeellum* group. (Protura: Protentomidae). *Entomologia Sinica* 1(3): 195–240. <https://doi.org/10.1111/j.1744-7917.1994.tb00245.x>
- Yin ZW, Li LZ, Wu C (2015) New and little known species of *Zorotypus* Silvestri (Zoraptera: Zorotypidae) from China. *Zootaxa* 4007(4): 557–566. <https://doi.org/10.11646/zootaxa.4007.4.6>
- Zhang J, Xie R, Yin WY (1996) Study on diversity of Protura from Yunnan province. *Zoological Research* 17(2): 139–146. [in Chinese with English abstract]
- Zhang LS, Fang XQ (2012) Paleogeography of China, the Formation of Natural Environment in China. Science Press, Beijing, 425 pp. [In Chinese]



# Systematics of Scelioninae (Hymenoptera, Platygastroidea): new synonymy, distribution, and species

Norman F. Johnson<sup>1,2</sup>, Luciana Musetti<sup>1</sup>, Lubomír Masner<sup>3</sup>

**1** Department of Evolution, Ecology & Organismal Biology, The Ohio State University, 1315 Columbus, Ohio 43212, USA **2** Department of Entomology, The Ohio State University, Columbus, Ohio 43212, USA **3** Agriculture and Agri-Food Canada, K.W. Neatby Building, Ottawa, Ontario, Canada

Corresponding author: Norman F. Johnson ([johnson.2@osu.edu](mailto:johnson.2@osu.edu))

---

Academic editor: A. Köhler | Received 2 August 2019 | Accepted 16 September 2019 | Published 9 October 2019

---

<http://zoobank.org/606FB61E-1590-468F-AAF4-1DFE10B49B44>

---

**Citation:** Johnson NF, Musetti L, Masner L (2019) Systematics of Scelioninae (Hymenoptera, Platygastroidea): new synonymy, distribution, and species. *ZooKeys* 879: 23–31. <https://doi.org/10.3897/zookeys.879.38788>

---

## Abstract

The genera *Doddiella* Kieffer, 1913 and *Aratala* Dodd, 1927 are treated as junior synonyms of *Aneuroscelio* Kieffer, 1913 following study of the rediscovered holotype of the type species *Aneuroscelio rufipes* Kieffer, 1913 (syn. nov.). The nine species previously recognized in *Doddiella* are all transferred to *Aneuroscelio* (comb. nov.). *Calliscelio schlingeri* (Masner & Johnson) is recognized as a junior synonym of *Calliscelio vitilevuensis* (Fullaway) (syn. nov.). *Huddlestonium exu* Polaszek & Johnson is recorded from Kenya, significantly expanding its known range from West Africa (Côte d'Ivoire, São Tomé). A new species of the genus *Tyrannoscelio* Masner, Johnson & Arias-Penna, *T. cerradensis* sp. nov., is described from Paraguay and the Center-West of Brazil (Mato Grosso). The depositories of the holotypes of five recently described are corrected.

## Keywords

*Caloteleia*, species descriptions, taxonomy, *Xentor*

## Introduction

Our knowledge of the diversity of parasitoid wasps in the superfamily Platygastroidea has grown by leaps and bounds over the past 25 years. Since the publication of the last hard-copy taxonomic catalogs for the group (Johnson 1992, Vlug 1995), the number of de-

scribed genera has grown by 18.5%, from 426 to 505, and the number of species-group taxa has increased an astonishing 68.4%, from 4184 to 7045. The most current online tabulation of the diversity reports 263 valid genera and slightly over 6000 valid species.

In the course of this rapid expansion, several small discoveries and mistakes have been made, most of which would be too minor to merit separate publication. The goal of this contribution is to address these issues and formally document them in the literature.

## Taxonomy

### Status of *Doddiella* Kieffer

In 1913 J.-J. Kieffer published the description of a new genus of scelionine from Aburi in the Gold Coast (present-day Ghana), dedicating it to the teenaged Alan P. Dodd of Queensland. The primary distinguishing characteristic for the new genus was cited as the absence of veins in the wings. This feature was thought to be shared, within the Scelionidae of the time, only with *Rielia* Kieffer, a genus today known as *Mantibaria* Kirby. Ironically, although he was the person intended to be honored, Kieffer's description was not sufficient for Dodd to recognize the genus, and he later described it anew under the name *Aratala* (Dodd 1927). Nine species are currently treated as valid taxa, and the genus is known from the Afrotropical, Oriental, Australian, and Neotropical regions, and also edging into the Palearctic in Egypt and Ethiopia. It is a striking and unmistakable creature, so much so that Masner erected for it the monobasic tribe *Doddiellini* in 1976. It has received a limited amount of taxonomic attention, having been mentioned in the literature 16 times. Identification keys have been published for the African and Palearctic species (Priesner 1951, Kononova and Kozlov 2008).

In the same year in which *Doddiella* first appeared, Kieffer also described the new genus *Aneuroscelio* from Murang'a (reported as MÉRANGA or Fort-Hall) in British East Africa, modern Kenya. This name languished in obscurity due to the inadequacy of Kieffer's description and lack of study of the single known specimen of the type species, *Aneuroscelio rufipes* Kieffer. The type specimen had not been examined because it was not found in the pinned and mounted collection in the Muséum national d'Histoire naturelle in Paris (see comments in Masner 1976: 56). Through the efforts and kindness of Dr. Claire Villemant of that institution, Kieffer's types from that paper have now been unearthed, preserved in vials of ethanol and kept separate from the rest of the collection. We have since mounted these specimens so that they can be studied and the taxonomic concepts of names they represent can be determined.

*Aneuroscelio rufipes* is a typical species of *Doddiella* (Fig. 1). Not only does it lack wing veins, but it possesses all of the characteristic features: a dense field of white setae on the gena, mesopleuron smooth and lacking almost all of the the typical sulci and foveae, netrion absent, metascutellum produced into a "blade-like projection," first metasomatic segment elongate, and the posterior margin of the second segment strongly raised and curved (Masner 1976). The two generic names are clearly synony-

mous. Masner (1976) anticipated this but could not resolve the issue without the type. Beyond the synonymy, the question then is which name is senior?

*Doddiella* was described in the pages of the Bollettino del Laboratorio di Zoologia Generale e Agraria della R. Scuole Superior d'Agricoltura in Portici in volume 7. The index for that volume cites the dates of publication of each article, and Kieffer's paper is dated 20 October 1913. The description of *Aneuroscelio* appeared as a contribution to the Hymenoptera section in "Voyage de Ch. Alluaud et R. Jeannel en Afrique Orientale (1911-1912)", and an insert in that book dates the article to 15 August 1913. Thus, the name *Aneuroscelio* has priority over the much better known *Doddiella*.

### ***Aneuroscelio* Kieffer**

*Aneuroscelio* Kieffer, 1913a: 14. Type: *Aneuroscelio rufipes* Kieffer, by monotypy and original designation. Kieffer, 1926: 266, 278 (description, keyed); Muesebeck & Walkley, 1956: 328 (citation of type species); Johnson, 1992: 336 (cataloged, catalog of world species).

*Doddiella* Kieffer, 1913b: 109. Type: *Doddiella nigriceps* Kieffer, by monotypy and original designation. **Syn. nov.** Kieffer, 1926: 266, 281 (description, keyed); Priesner, 1951 (key to African species); Muesebeck & Walkley, 1956: 348 (citation of type species); Masner, 1976: 6, 56 (description, keyed, synonymy); Galloway & Austin, 1984: 5, 77 (diagnosis, list of species described from Australia, keyed); Johnson, 1992: 367 (cataloged, catalog of species); Austin & Field, 1997: 36, 68 (structure of ovipositor system, discussion of phylogenetic relationships); Lê, 2000: 31, 87 (keyed, description); Rajmohana K., 2006: 115 (keyed); Kononova & Kozlov, 2008: 21, 181 (description, keyed, key to species of Palearctic region); Rajmohana, 2014: 6, 21 (description, keyed).

*Aratala* Dodd, 1927: 74. Type: *Aratala globiceps* Dodd, by monotypy and original designation. **Syn. nov.** Muesebeck & Walkley, 1956: 331 (citation of type species); Masner, 1976: 56 (junior synonym of *Doddiella* Kieffer).

### **List of species**

*Aneuroscelio aegyptiacus* (Risbec, 1950), **comb. nov.**  
 = *Aneuopria aegyptiaca* var. *microcephala* Risbec, 1954  
*Aneuroscelio dolabella* (Kozlov & Lê, 1986), **comb. nov.**  
*Aneuroscelio globiceps* (Dodd, 1927), **comb. nov.**  
*Aneuroscelio indicus* (Mukerjee, 1993), **comb. nov.**  
*Aneuroscelio kiefferi* (Priesner, 1951), **comb. nov.**  
*Aneuroscelio maindroni* (Risbec, 1955), **comb. nov.**  
*Aneuroscelio nigricephala* (Mukerjee, 1993), **comb. nov.**  
*Aneuroscelio nigriceps* (Kieffer, 1913b), **comb. nov.**  
*Aneuroscelio rufipes* Kieffer, 1913a  
*Aneuroscelio similis* (Priesner, 1951), **comb. nov.**

### Status of *Xentor schlingeri* Masner & Johnson

We described the genus *Xentor* in 2007 for three quite distinctive species from Fiji: *X. schlingeri* Masner & Johnson, *X. filicornis* Masner & Johnson, and *X. convexifrons* Masner & Johnson. On the basis of newly discovered characters, Talamas et al. (2016) synonymized *Xentor* under *Calliscelio* Ashmead, a speciose and cosmopolitan genus. We have later independently corroborated this hypothesis with molecular evidence (*unpublished data*). Accordingly, the three species of *Xentor* were transferred to *Calliscelio*. During a visit to the J. Linsley Gressitt Center for Research in Entomology at the Bernice Pauahi Bishop Museum (Honolulu) we discovered that the most distinctive species and the type species of *Xentor*, *C. schlingeri*, had already been described by D.T. Fullaway under the name *Caloteleia vitilevuensis* Fullaway (1939). Thus, the name *Xentor schlingeri* falls as a junior synonym of *Calliscelio vitilevuensis* (Fullaway), syn. nov.

### Corrections of holotype depositories

The collections in which the holotypes for the following species are deposited were reported incorrectly. The corrections are noted alongside the taxon name.

*Axea atai* Valerio & Yoder: The Natural History Museum, London, UK

*Axea dorothae* Valerio & Yoder: The Natural History Museum, London, UK

*Axea mwari* Valerio & Yoder: Nairobi National Museum, Nairobi, Kenya

*Oreiscelio magnipennis* Talamas: Nairobi National Museum, Nairobi, Kenya

*Paridris trispinosa* Talamas & Masner: The Natural History Museum, London, UK

### *Huddlestonium exu* Polaszek & Johnson is widespread in Africa

The genus *Huddlestonium* is a curious creature whose features demand an expansion of the boundaries of what is morphologically possible in the Platygastroidea (Masner et al. 2007). It clearly belongs to the superfamily as it possesses the characteristic ventral papillar sensilla on the apical claval segments of the female (the male is, as yet, undiscovered). However, it has no well-developed laterotergites and laterosternites on the metasoma and the female antenna is uniquely 13-merous. It was described from two collections, a single specimen from the Côte d'Ivoire and a short series of four specimens from the island of São Tomé, both collecting localities in western Africa. Among the extant fauna, it is most similar to the Neotropical genus *Plaumannion*, a group that is even rarer than *Huddlestonium* as it is known from only 3 specimens (one of which is broken). In terms of the fossil record, *Huddlestonium* bears a striking resemblance to the Eocene genus *Archaeoscelio* Brues (see Masner et al. 2007) and perhaps even to the recently described Cretaceous species *Geoscelio mckellari* Engel & Huang (Engel et al. 2017).

It was, therefore, of some surprise to find new specimens of *Huddlestonium* collected nearly 2000 miles east of São Tomé in western Kenya. One specimen (UCRC ENT 154639) was collected in Isecheno Nature Reserve (0.24°N, 34.87°E); and two (OSUC 192430, 232305) in Ruma National Park (0.65°S, 34.33°E). The specimens differ slightly from their west African counterparts, particularly in the closer proximity of the lateral ocelli to the margins of the compound eyes. We were initially tempted to treat these specimens as a new species. Despite the great distance separating the collecting localities, the morphological differences seem too slight to warrant that course of action, particularly given the small number of specimens at hand. The new data do indicate that *Huddlestonium* is much more widely distributed than previously known. Unfortunately, we remain ignorant of the hosts that they parasitize.

### A new species of *Tyrannoscelio* Masner, Johnson & Arias-Penna

The genus *Tyrannoscelio* is known from only two species: *T. genieri* Masner & Johnson from the southeastern Brazilian state of Espírito Santo, and *T. crenatus* Arias-Penna, known from two specimens from the opposite side of the continent, in the Colombian province of Caquetá. The genus is immediately recognizable on the basis of the expanded, crenellated frontal shelf, and the extraordinarily elongate mandibles. More subtly, though, the genus is notable for the presence of a distinct skaphion and the lack of a postmarginal vein in the forewing. Here we describe a third species of the genus, from central Paraguay and the Brazilian state of Mato Grosso.

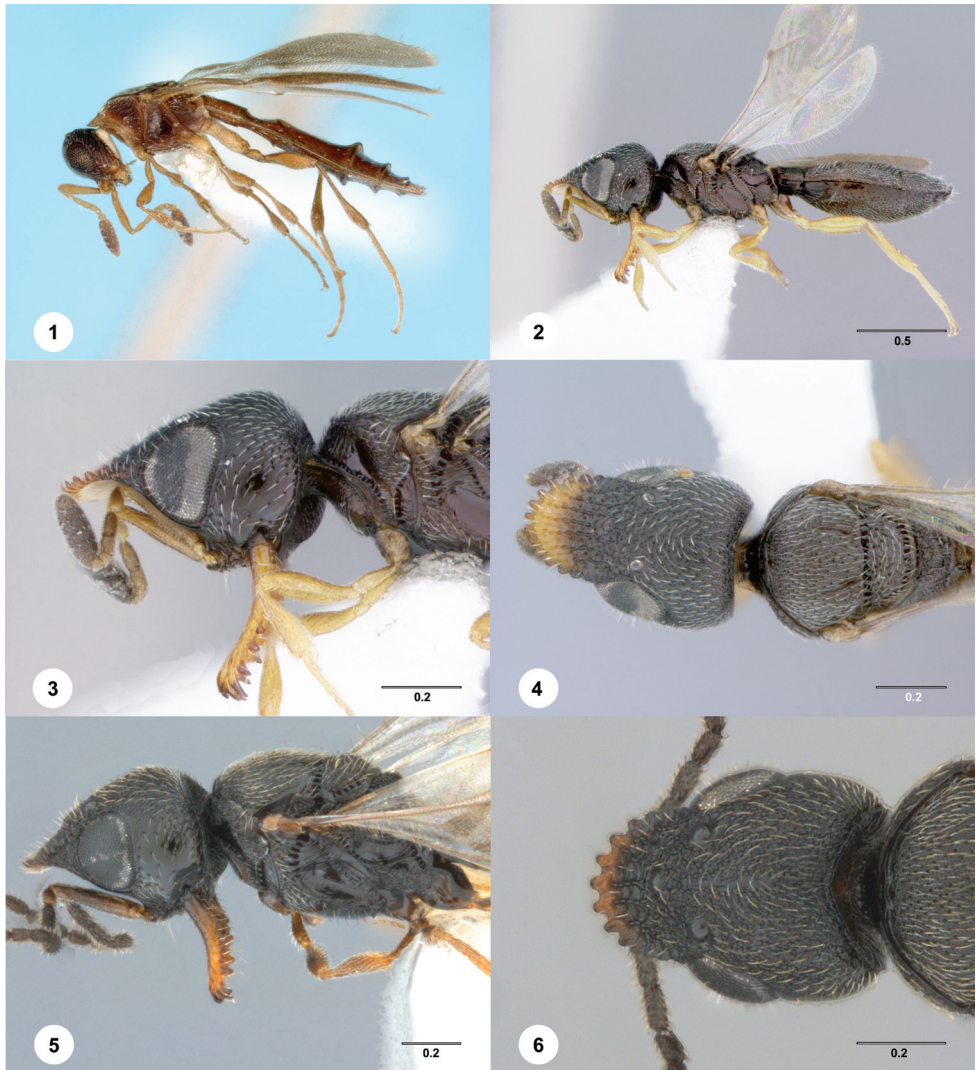
#### *Tyrannoscelio cerradensis* sp. nov.

<http://zoobank.org/D7781AC6-EB44-4863-BFAC-8FA15FE24A21>

Figs 2–6

**Diagnosis.** Similar to other known species in the genus, differing in the following characters. Body color: entirely dark brown except for brownish-yellow apex of frontal shelf. Frontal shelf: margined by 13–14 rounded teeth in female, ten in male. Median longitudinal furrow on vertex: weak, incomplete, visible only near occipital carina. Sculpture of vertex: rugose-reticulate, with superimposed coriaceous microsculpture. OOL: slightly less than ocellar diameter. Outer margin of mandible: with five to six teeth. Sculpture of mesoscutum: coriaceous, with longitudinal striae present only near transscutal articulation. Sculpture of mesoscutellum: rugose, with superimposed coriaceous microsculpture. Notauli: present only in posterior half of mesoscutum. Metascutellum shape: roughly triangular. Mesopleural carina: distinct, complete. Plicae on propodeum: well-developed. Felt field: present on S2.

**Material examined.** Holotype female: OSUC 232307, PARAGUAY: San Pedro, Cororo-Rio Ypane, XII-5/9-1983, Malaise Trap, M. Wasbauer coll. Deposited in California Department of Food and Agriculture (Sacramento). Paratypes: 3 males, OSUC



**Figures 1–6.** **1** Holotype of *Aneuroscelio rufipes* Kieffer. The flaring of the posterior margins of the metasomal segments is an artifact. **2–4** *Tyrannoscelio cerradensis* n.sp., holotype female (OSUC 232307). **2** lateral habitus **3** head and anterior mesosoma, lateral view **4** head and mesosoma, dorsal view. **5–6** *T. cerradensis* n.sp., male (OSUC 711174) **5** head and mesosoma, lateral view **6** head, dorsal view. Scale bars in millimeters.

711174, 786576, 786579. BRAZIL: Mato Grosso, Fazenda Formozinho, Mun. Tangará da Serra, 594 m, 14°29'33"S 57°55'49"W, 14.xii.2013, cerradão, flight int. trap, F. Génier & L. Sawaris, 2013-152 (CNCI).

**Etymology.** The specific epithet refers to the cerrado habitat in which the specimens were collected and is treated as an adjective.

**Comments.** Since the original description of *T. genieri* several additional specimens have been collected in the Brazilian state of Espírito Santo in or near the Soore-

tama Biological Reserve, the same area from which the species was described originally. The habitats are described on the specimen labels as semi-deciduous or primary lowland Atlantic forest. The additional species in the Center-West of Brazil, Paraguay, and Colombia suggests that the genus is very widely distributed and rare or perhaps restricted in its habitat preferences or timing of adult emergence.

### Key to species of *Tyrannoscelio*

- 1 Outer edge of mandible with three teeth near apex; mesosoma lighter in color than head and mesosoma; mesoscutum longitudinally rugose throughout (southeast Brazil) ..... *T. genieri*
- Outer edge of mandible with five to six teeth along its entire length; from dorsal view head, mesosoma, metasoma all dark brown; longitudinal sculpture on mesoscutum limited at most to area near transscutal articulation .... **2**
- 2 Metascutellum tridentate, lateral teeth distinct; mesoscutellum coriaceous (Colombia) ..... *T. crenatus*
- Metascutellum triangular, without lateral teeth; mesoscutellum with irregular longitudinal rugulae with superimposed coriaceous microsculpture (central-west Brazil, Paraguay) ..... *T. cerradensis*

### Acknowledgements

Thanks are due to C. Villemant (Paris) for finding the Kieffer holotypes and allowing us the opportunity to study them.

### References

- Austin AD, Field SA (1997) The ovipositor system of scelionid and platygastriid wasps (Hymenoptera: Platygastroidea): comparative morphology and phylogenetic implications. *Invertebrate Taxonomy* 11: 1–87. <https://doi.org/10.1071/IT95048>
- Dodd AP (1927) Notes on parasitic Hymenoptera from Australia, with descriptions of new species. *Memoirs of the Queensland Museum* 9: 63–75.
- Engel MS, Huang D, Alqarni AS, Cai C, Alvarado M, Breitzkreuz LCV, Azar D (2017) An apterous scelionid wasp in mid-Cretaceous Burmese amber (Hymenoptera: Scelionidae). *Comptes Rendus Palevol* 16: 5–11. <https://doi.org/10.1016/j.crpv.2016.03.005>
- Fullaway DT (1939) New species of proctotrupid wasps from the Bishop Museum collection of Samoan and Fijian insects. *Proceedings of the Hawaiian Entomological Society* 14: 209–221.
- Galloway ID, Austin AD (1984) Revision of the Scelioninae (Hymenoptera: Scelionidae) in Australia. *Australian Journal of Zoology Supplementary Series* 99: 1–138. <https://doi.org/10.1071/AJZS099>

- Johnson NF (1992) Catalog of world Proctotrupeoidea excluding Platygastriidae. *Memoirs of the American Entomological Institute* 51: 1–825.
- Kieffer JJ (1913a) Proctotrupidae, Cynipidae et Evaniidae. *Voyage de Ch. Alluaud et R. Jeannel en Afrique Orientale (1911–1912). Résultats scientifiques. Hyménoptères* 1: 1–35.
- Kieffer JJ (1913b) Nouveaux microhyménoptères de l'Afrique équatoriale. *Bollettino del Laboratorio di Zoologia Generale e Agraria della R. Scuola Superiore d'Agricoltura* 7: 105–112
- Kieffer JJ (1926) Scelionidae. *Das Tierreich*. Vol. 48. Walter de Gruyter & Co., Berlin, 885 pp.
- Kononova SV, Kozlov MA (2008) [Scelionids of the Palearctic (Hymenoptera, Scelionidae). Subfamily Scelioninae.] *Tovarishchestvo Nauchnykh Izdaniy KMK, Saint Petersburg*, 489 pp.
- Kozlov MA, Lê XH (1986) [New species of scelionids (Hymenoptera, Scelionidae) of the fauna of Vietnam.] *Trudy Zoologicheskogo Instituta Akademii Nauk SSSR* 159: 89–102.
- Lê XH (2000) Egg-parasites of family Scelionidae (Hymenoptera). *Fauna of Vietnam*, vol. 3. Science and Technics Publishing House, Hanoi, 386 pp.
- Masner L, Johnson NF. 2007. *Xentor*, a new endemic genus from Fiji (Hymenoptera: Platygastroidea: Scelionidae) and description of three new species. *Fiji Arthropods* 9: 11–20.
- Masner L (1976) Revisionary notes and keys to world genera of Scelionidae (Hymenoptera: Proctotrupeoidea). *Memoirs of the Entomological Society of Canada* 97: 1–87. <https://doi.org/10.4039/entm10897fv>
- Masner L, Johnson NF, Polaszek A (2007) Redescription of *Archaeoscelio* Brues and description of three new genera of Scelionidae (Hymenoptera): a challenge to the definition of the family. *American Museum Novitates* 3550: 1–24. [https://doi.org/10.1206/0003-0082\(2007\)3550\[1:ROABAD\]2.0.CO;2](https://doi.org/10.1206/0003-0082(2007)3550[1:ROABAD]2.0.CO;2)
- Muesebeck CFW, Walkley LM (1956) Type species of the genera and subgenera of parasitic wasps comprising the superfamily Proctotrupeoidea (order Hymenoptera). *Proceedings of the United States National Museum* 105: 319–419. <https://doi.org/10.5479/si.00963801.3359.319>
- Mukerjee MK (1993) On a collection of Scelionidae (Proctotrupeoidea: Hymenoptera) from Garhwal Himalayas, India. *Hexapoda* 5: 75–105.
- Priesner H (1951) New genera and species of Scelionidae (Hymenoptera, Proctotrupeoidea) from Egypt. *Bulletin de l'Institut Fouad I du Desert* 1(2): 119–149.
- Rajmohana K (2006) Studies on Proctotrupeoidea and Platygastroidea (Hymenoptera: Insecta) of Kerala. *Memoirs of the Zoological Survey of India* 21(1): 1–153. <https://doi.org/10.11609/JoTT.ZPJ.1570.2506-13>
- Rajmohana K (2014) A systematic inventory of Scelioninae and Teleasinae (Hymenoptera: Platygastriidae) in the rice ecosystems of north-central Kerala. *Memoirs of the Zoological Survey of India* 22: 1–72.
- Risbec J (1950) *Travaux du Laboratoire d'Entomologie du Secteur Soudanais de Recherches Agronomiques. Gouvernement Général de l'Afrique Occidentale Française*, Paris, 639 pp.
- Risbec J (1954) Chalcidoides et Proctotrupides de l'Afrique occidentale française. (3<sup>e</sup> Supplément). *Bulletin de l'Institut Français d'Afrique Noire* 16: 524–552.
- Risbec J (1955) Chalcidoides et Proctotrupides africains. *Bulletin de l'Institut Français d'Afrique Noire (A)* 17: 533–580.

- Talamas EJ, Johnston-Jordan D, Buffington ML (2016) *Calliscelio* Ashmead expands (Hymenoptera: Scelionidae). Proceedings of the Entomological Society of Washington 118: 404–423. <https://doi.org/10.4289/0013-8797.118.3.404>
- Talamas E, Johnson NF, van Noort S, Masner L, Polaszek A (2009) Revision of world species of the genus *Oreiscelio* Kieffer (Hymenoptera, Platyastroidea, Platygastridae). ZooKeys 6: 1–68. <https://doi.org/10.3897/zookeys.6.67>
- Talamas EJ, Masner L, Johnson NF (2013) Systematics of *Trichoteleia* Kieffer and *Paridris* Kieffer (Hymenoptera, Platyastroidea, Platygastridae). Journal of Hymenoptera Research 34: 1–79. <https://doi.org/10.3897/jhr.34.4714>
- Yoder MJ, Valerio AA, Masner L, Johnson NF (2009) Identity and synonymy of *Dicroscelio* Kieffer and description of *Axea*, a new genus from tropical Africa and Asia (Hymenoptera: Platyastroidea: Platygastridae). Zootaxa 2003: 1–45. <https://doi.org/10.11646/zootaxa.2003.1.1>



# A review of the genus *Pelodiaetus* Jeannel (Coleoptera, Carabidae, Anillini) of New Zealand, with re-description of the genus, description of a new species, and notes on the evolutionary history

Igor M. Sokolov<sup>1</sup>

<sup>1</sup> Systematic Entomology Laboratory, ARS, USDA, c/o Smithsonian Institution, P.O. Box 37012, National Museum of Natural History, Washington, DC 20013-7012, USA

Corresponding author: Igor M. Sokolov ([igor.sokolov@usda.gov](mailto:igor.sokolov@usda.gov))

---

Academic editor: B. Guéorguiev | Received 25 June 2019 | Accepted 30 August 2019 | Published 9 October 2019

---

<http://zoobank.org/668885D2-C218-4402-B430-8672EC98E81E>

---

**Citation:** Sokolov IM (2019) A review of the genus *Pelodiaetus* Jeannel (Coleoptera, Carabidae, Anillini) of New Zealand, with re-description of the genus, description of a new species, and notes on the evolutionary history. ZooKeys 879: 33–56. <https://doi.org/10.3897/zookeys.879.37684>

---

## Abstract

On the basis of new morphological data a re-description of the genus *Pelodiaetus* is provided, a new species of the genus *P. nunni* **sp. nov.** (Christchurch, Canterbury, South Island) is described, and *P. lewisi* Jeannel is proposed as a synonym of *P. sulcatipennis* Jeannel, **syn. nov.** A taxonomic key as well as distribution maps for species of *Pelodiaetus* are provided. Data on comparative morphology and biogeographical aspects of speciation in the genus *Pelodiaetus* and its morphological relatives from Australia and New Zealand are discussed.

## Keywords

Adephaga, biogeography, East Gondwana, identification key, new synonym, *Pelodiaetus*, syntopic co-occurrence

## Introduction

The genus *Pelodiaetus* was erected by Jeannel (1937) for tiny New Zealand anillines from the southern part of the South Island, characterized by the reduced number of setae (= eight) in the elytral series of umbilicate marginal pores, only one (posterior) elytral discal

seta, and a distinct elytral longitudinal groove (Jeannel 1937). The genus is composed of two species, *P. sulcatipennis* Jeannel and *P. lewisi* Jeannel, differing from each other in the details of their habitus, mainly in the shape of the pronotum. Later, in his main monograph, Jeannel (1963) recalculated the number of setae in the elytral series of umbilicate marginal pores and stated them as nine, a typical number for the majority of representatives of Anillini, thus rejecting the reduced state of this character. Meanwhile, the last reviser of the New Zealand anillines (Moore 1980) continued to consider the number of pores in the umbilicate series of elytra as incomplete with the seventh and eighth pores “obsolete or obsolescent,” and used this feature for distinguishing representatives of *Pelodiaetus* Jeannel from those of *Pelodiaetodes* Moore in his key for New Zealand anillines. In the same publication, Moore expressed doubts that the genus included two species and pointed out that “the two names may merely represent two extremes of a single species.”

The author had the opportunity to investigate the material on Anillini from the New Zealand Arthropod Collection and the private collection of JT Nunn, whose numerous collecting methods included a soil-washing technique that greatly enriched the number of subterranean species available for study. Preliminary sorting of the material of *Pelodiaetus* showed that this genus includes one undescribed species and one species that needs to be synonymized. In addition, thorough examination of elytral chaetotaxy revealed the discrepancy between the state of this character in the works of previous authors and its actual configuration. Altogether, the description of a new species and corrected re-description of the genus, along with comments on the status of described forms, serves as a basis for this paper.

## Materials and methods

This study is based on the examination of 83 specimens of *Pelodiaetus* from the New Zealand Arthropod Collection (NZAC), Auckland, New Zealand, and from the personal collection of John T Nunn (JTN), Dunedin, New Zealand. Verbatim label data are given for type specimens of all newly described taxa, with label breaks indicated by a slash (“/”).

## Measurements

All specimens were measured electronically using a Leica M420 microscope equipped with a Syncroscopy AutoMontage Photomicroscopy system (SYNCROSCOPY, Synoptics Ltd.). Measurements for various body parts, given in mm, are encoded as follows:

- LH** length of head, measured along midline from anterior margin of labrum to the virtual line connecting posterior supraorbital setae;
- WH** width of head, at level of anterior supraorbital setae;
- WP<sub>m</sub>** maximal width across pronotum;
- WP<sub>a</sub>** width across anterior angles of pronotum;
- WP<sub>p</sub>** width across posterior angles of pronotum;

- LP** length of pronotum from base to apex along midline;  
**WE** width of elytra, at level of 4<sup>th</sup> umbilicate setae;  
**LE** length of the elytra, from apex of scutellum to apex of left elytron;  
**SBL** standardized body length, a sum of LH, LP, and LE.

In addition, nine ratios between these measurements were calculated: WH/WPm, WPm/WE, WPa/WPp, WPm/WPp, WPm/LP, WE/SBL, WE/LE, LE/SBL, and LP/LE. All values are given as mean  $\pm$  standard deviation.

### Illustrations

Digital photographs of the dorsal habitus of new species were taken with the Auto-Montage system using a Leica M420 microscope. Line drawings of selected body parts were made using a camera lucida on an Olympus BX 50 microscope. Scanning electron micrographs were made with coating on an ESEM FEI Quanta 200.

### Dissections

Dissections were made using standard techniques. Genitalia were dissected from the abdomens of specimens previously softened in boiling water for 20–30 minutes. Contents of the abdomen were cleared using boiling 10% KOH for 2–3 minutes to remove internal tissues, and then washed in hot water before examination. After examination, genitalia were mounted on plastic transparent boards in dimethylhydantoin formaldehyde resin (DMHF, Steedman 1958) and pinned beneath the specimen. In some species, investigation of body parts was undertaken as follows. The whole specimen was cleared, using boiling 10% KOH for ~5 minutes, then washed and dissected. Disassembled body parts from one specimen were placed on a plastic transparent board, properly oriented, mounted in DMHF and pinned together with the specimen labels.

### Type material

The author had no opportunity to investigate the type material of the New Zealand anillines. The concept of *Pelodiaetus* used in the paper is based on the material identified by Moore during his work on New Zealand fauna of Anillina (Moore 1980).

### Species ranking

Criteria for recognizing new species were the following (Sokolov et al. 2004): two or more similar forms that are sympatric were considered separate species if they differed in genitalic morphology and at least one external character; allopatric forms that were

similar in external morphology were considered separate species if they differed in general form of the median lobe or the armature of the internal sac; allopatric forms were considered conspecific if they show intergradation of external characters and/or intergradation of the shape and armature of the median lobe. Therefore, morphological recognition of species was based on gross external characters, including forebody proportions, and form and structure of the elytra, and fine external characters, such as chaetotaxy of different body parts, structure of the labio-maxillar complex, shape of ventral sclerites, and patterns of forebody microsculpture. Genitalic characters included the form of the median lobe, the armature of the internal sac observed retracted inside the median lobe, the shape of spermatheca, and the structure of ovipositor sclerites.

### Terms and descriptions

The terms used in the paper and the scheme of descriptions follow that of the author's previous publications on New Zealand Anillini (Sokolov 2015, 2016). Numbering of the umbilicate pores of elytra follows that of Erwin (1974) and Giachino and Vailati (2011).

### Taxonomic treatment

**Order Coleoptera Linnaeus, 1758**

**Family Carabidae Latreille, 1802**

**Subfamily Trechinae Bonelli, 1810**

**Tribe Anillini Jeannel, 1937**

***Pelodiaetus* Jeannel, 1937**

*Pelodiaetus* Jeannel, 1937: 275 (type species *Pelodiaetus sulcatipennis* Jeannel, 1937, by original designation).

**Recognition.** The members of this genus are distinguished from the other New Zealand representatives of Anillina by the following combination of characters: eyes absent; head with long fronto-lateral carinae; antennae submoniliform, of moderate length; prosternal process slightly dilating to the blunt apex; pronotum cordiform, with prominent anterior angles and with short basal constriction anterior to the projected posterior angles; elytra with oblique longitudinal grooves; elytral apices slightly dehiscent with narrowly rounded sutural angles; pygidium exposed in apical half; 1<sup>st</sup> elytral discal seta indistinct, only slightly longer than surrounding vestiture, while 2<sup>nd</sup> and 3<sup>d</sup> discal setae always clearly visible; elytral margin with umbilicate series of 9 pores: the longest setae in the 2<sup>nd</sup>, 6<sup>th</sup>, and 9<sup>th</sup> pore positions, 7<sup>th</sup>, 8<sup>th</sup>, and 9<sup>th</sup> pores equidistant, not aligned, virtually forming obtuse isosceles triangle with 8<sup>th</sup> pore shifted towards disc. The developed fronto-lateral carinae, antennae of moderate length,

projected pronotal anterior angles, grooved elytra, exposed pygidium and small size separate *Pelodiaetus* from endogean *Hygranillus* Moore. Distinct posterior angles of pronotum, dilated prosternal process and grooved elytra distinguish the representatives of *Pelodiaetus* from the species of *Zeanillus* Jeannel. Umbilicate series of nine pores, slightly dehiscent apices of grooved elytra and exposed pygidium separate the members of *Pelodiaetus* from the species of *Nesamblyops* Jeannel. An absence of the distinct tubercle anterior to the posterior angles of the pronotum and the small size separate the species of *Pelodiaetus* from the species of *Pelodiaetodes* Moore.

**Description. Size.** SBL range 1.19–1.45 mm.

**Habitus.** Body form slightly convex, almost subparallel (Fig. 6), moderately elongate (WE/SBL range 0.31–0.35), head relatively wide, subequal to the width of pronotum (WH/WPm range 0.80–0.85), pronotum relatively wide, subequal to the width of elytra (WPm/WE range 0.79–0.88).

**Color.** Body rufo-testaceous or testaceous, appendages testaceous.

**Microsculpture.** Dorsal microsculpture of polygonal sculpticells with isodiametric mesh pattern throughout the dorsal surface. Development of microsculpture varies on different body parts. Head and disc of pronotum with shallow microlines, sometimes partially obliterated, while on elytra microlines are very distinct, forming well-pronounced sculpticells.

**Luster.** Body surface shiny.

**Macrosculpture.** Body surface sparsely and finely punctate.

**Vestiture.** Body surface covered with sparse yellowish short setae. Vestiture of elytra moderately long (around one-half length of discal setae).

**Fixed setae.** Primary head setae include a pair of clypeal (cs), a pair of frontal (fs), two pairs of supraorbital (ssa and ssp) and one pair of postorbital (pos) setae (Fig. 1A, B). Mentum with two pairs of long primary (paramedial and lateral) setae (Fig. 1C, D, pms, lms). Submentum with three pairs of long primary setae (lss, prss) and a few additional shorter setulae (Fig. 1C, D). Pronotum with two long primary lateral setae (midlateral, ls, and basilateral, bs) on each side (Fig. 2A, B). Elytra with two distinct discal setae (Fig. 4, ed5 and ed6), first discal seta (ed3) barely visible, scutellar (ed2) and apical (ed8) setae of normal sizes. Last three (7<sup>th</sup>, 8<sup>th</sup>, and 9<sup>th</sup>) pores (eo7, eo8, and eo9) of umbilicate series equidistant, not aligned, with 8<sup>th</sup> pore shifted towards the disc and virtually forming an obtuse isosceles triangle, the longest setae of umbilicate series in the 2<sup>nd</sup>, 6<sup>th</sup>, and 9<sup>th</sup> pore positions (Fig. 4). Fifth visible sternite of male with two and of female with four setae along the posterior margin.

**Head** (Fig. 1A, B). Anterior margin of clypeus (cl) straight. Frontal area flat without tubercle medially near frontoclypeal suture. Fronto-lateral carinae distinct and long (fcc).

**Eyes.** Eyes absent.

**Antennae.** Submoniliform, 11-segmented, extended to about posterior margin of pronotum. Antennomeres 1 and 2 elongate, of equal length and 1.3–1.4 times longer than antennomere 3, which is slightly elongate and 1.1 times longer than antennomere 4. Antennomeres 4–10 globose, last antennomere conical and 1.7–1.8 times longer than penultimate antennomere.

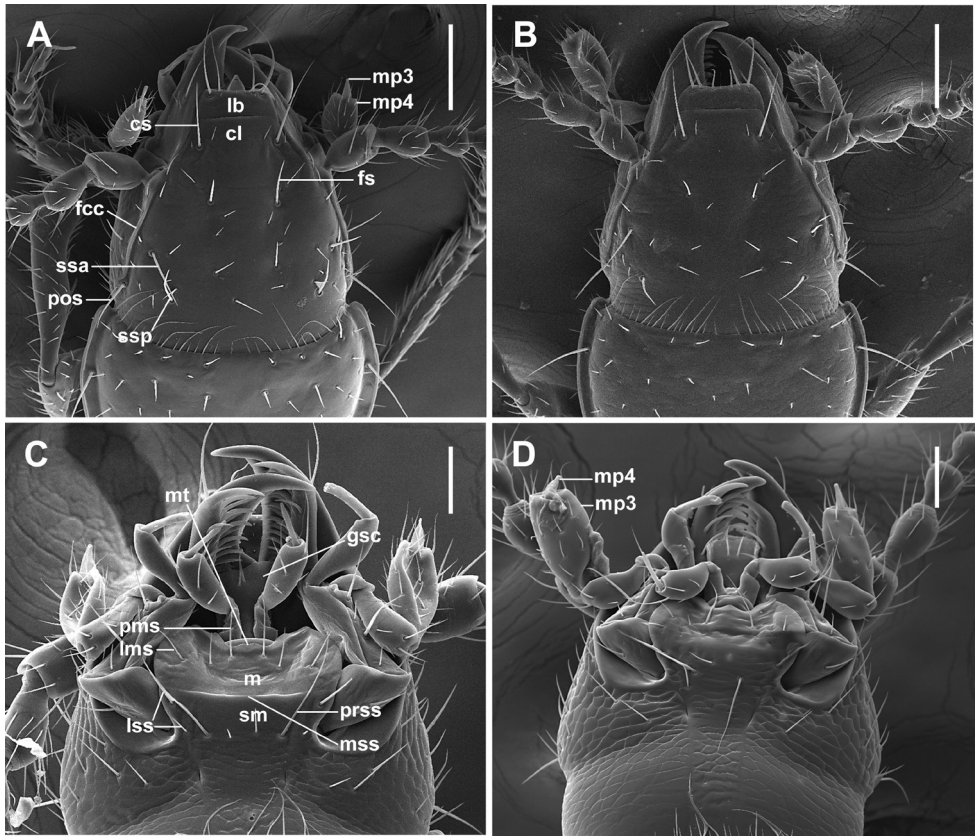


**Figure 1.** SEM illustrations of head, dorsal aspect, and labial complex, ventral aspect, of *Pelodiaetus* species. **A, C** *P. sulcatipennis* **B, D** *P. nunni*. Abbreviations: cl – clypeus; cs – clypeal seta; fcc – fronto-clypeal carina; fs – frontal seta; gsc – glossal sclerite; lb – labrum; lms – lateral mental seta; lss – lateral submental setae; m – mentum; mp3 – maxillary palpomere 3; mp4 – maxillary palpomere 4; mt – mental tooth; mss – mental-submental suture; pms – paramedial mental seta; pos – postorbital seta; prss – primary basal submental seta; sm – submentum; ssa – anterior supraorbital seta; ssp – posterior supraorbital seta. Scale bars: 0.1 mm (**A, B**); 0.05 mm (**C, D**).

**Labrum** (Fig. 1A, B). Labrum (lb) transverse with almost straight, entire anterior margin with six setae apically, increasing in size from the central pair outwards.

**Labium** (Fig. 1C, D). Labium with almost obliterated blunt mental tooth (mt); mentum (m) and submentum (sm) split, with mental-submental suture (mss). Glossal sclerite (gsc) without paraglossae, bisetose.

**Prothorax.** Pronotum (Fig. 2A, B) cordiform, slightly convex, arcuately constricted posteriorly and moderately sinuated anterior to posterior angles, with wide marginal gutter (mg). Posterior margin of pronotum shallowly concave medially and oblique laterally. Anterior angles narrowly rounded, distinctly projecting forward. Posterior angles rectangular, projecting outwards, bearing basolateral seta anterior to

angles. Widths across anterior margin slightly to moderately greater than between posterior angles at the level of basilateral setae (WPa/WPp range 1.11–1.40). Prosternum (Fig. 2CD) slightly protruding at the anterior margin medially, there with a group of longer setae relative to other prosternal vestiture. Prosternal intercoxal process (psp) unmarginated, slightly dilated apically and widely rounded at apex.

**Scutellum** (Fig. 2A, B). Externally visible, triangular, with rounded apex.

**Elytra** (Fig. 4). Elytra subdepressed, relatively long (LE/SBL from 0.56 to 0.60 among specimens) with oblique longitudinal grooves. Humeri rounded, forming an oblique angle with the longitudinal axis of body. Elytral basal margination lacking (Fig. 2A, B). Apical half of elytra without subapical sinuation. Sutural angle of elytron narrowly rounded, making apices of elytra slightly dehiscent (Fig. 4).

**Hind wings.** Absent.

**Pterothorax** (Fig. 3A). Metaventricle (mtv) moderately short, distance between meso- and metacoxae approximately equals diameter of mesocoxa. Metanepisternum (mte) slightly elongate, rectangle, with anterior margin shorter than outer margin. Metendoventrite (mes) with reduced anterior part and with lateral arms. Lateral arms U-shaped with widely divergent branches.

**Legs** (Fig. 5). Legs of moderate length, not elongated. Prothoracic legs of males with first 2 tarsomeres (ta1–2) moderately dilated apico-laterally with one row of oval articulo-setae (as) (Stork 1980) on the ventral surface. Protibiae (Fig. 5A) with antenna cleaner (ac) of type B (Hlavac 1971), with both anterior (asr) and posterior (psr) apical setal rows long and with concave apico-lateral notch. Length of anterior spur (asp) slightly smaller than length of 1<sup>st</sup> tarsomere (ta1). Profemora moderately swollen. Mesotibiae (Fig. 5B) with one long row of modified ventral setae (msms) at apical half, two terminal spurs and tibial brush (msb). Metafemora unmodified, metatibiae (Fig. 5C) with one row of modified ventral setae (mtms) in apical half, with two terminal spurs (mts) and tibial brush (mtb). Tarsi pentamerous, 1<sup>st</sup> and 5<sup>th</sup> tarsomeres are the longest, 2<sup>nd</sup>–4<sup>th</sup> tarsomeres of equal length on the tarsi of all legs, 1<sup>st</sup> tarsomere shorter than combined length of 2<sup>nd</sup>–4<sup>th</sup> tarsomeres. Tarsal claws simple, untoothed.

**Abdominal ventrites.** Five visible abdominal ventrites: 2<sup>nd</sup> ventrite longest, 1.7–2.0 times longer than 3<sup>rd</sup> or 4<sup>th</sup>, 3<sup>rd</sup> and 4<sup>th</sup> equal in length; the last, 5<sup>th</sup>, 1.6–1.8 times longer than 4<sup>th</sup>. Intercoxal process of 2<sup>nd</sup> ventrite of moderate width, constricted anteriorly, subparallel before blunt apex (Fig. 3A, ipa).

**Male genitalia** (Fig. 7). Median lobe of aedeagus anopic, elongate, slightly twisted and moderately arcuate. Apex of median lobe unmodified, only slightly enlarged in dorsal view. Internal sac with weakly sclerotized copulatory sclerites represented by flagellum-like structures combined at their basal or apical parts with small sclerotized plates of various size (ds). Ostial fields or spines of internal sac absent. Parameres bi-setose. Left paramere large and broad, evenly tapered to apex, right paramere moderately long. Ring sclerite ovoid, conically tapered apically with slightly elongated, triangular, handle-like extension.

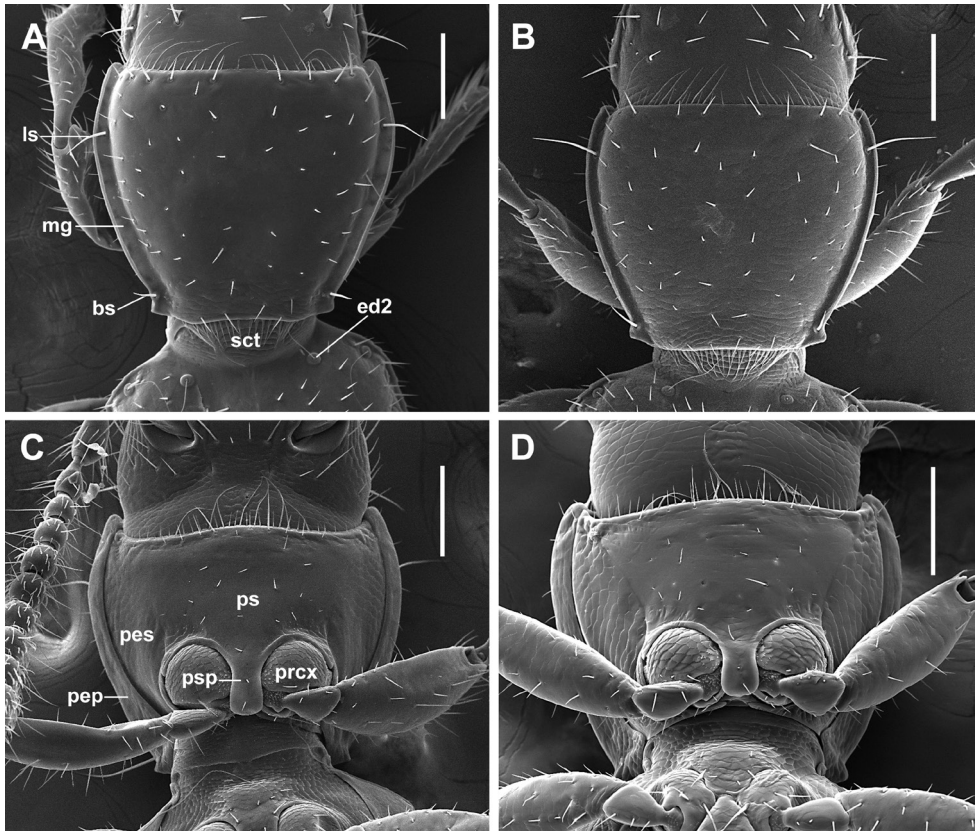


**Figure 2.** SEM illustrations of pronotum, dorsal aspect, and prothorax, ventral aspect, of *Pelodiaetus* species. **A, C** *P. sulcatipennis* **B, D** *P. nunni*. Abbreviations: bs – basilateral pronotal seta; ed2 – scutellar seta; ls – midlateral pronotal seta; mg – marginal pronotal gutter; pep – proepipleuron; pes – proepisternum; prcx – procoxa; ps – prosternum; psp – prosternal intercoxal process; sct – scutellum. Scale bars 0.1 mm.

**Female internal genitalia.** Gonocoxite 1 asetose (Fig. 3B, gc1). Gonocoxite 2 falciform (gc2), 1.8–2.1 times longer than its basal width, moderately curved, with two ensiform (es) and one apical nematiform (ns) setae. Laterotergite (lt) with six or seven setae. Spermatheca (sp) small, weakly sclerotized (Fig. 3B, 7DH), of bean-shape. Length of spermathecal gland (sg) much greater than length of spermatheca. Spermathecal duct (sd) very long.

**Included taxa.** The genus comprises two species: *P. sulcatipennis* Jeannel, and *P. nunni* sp. nov.

**Geographic distribution.** The species of *Pelodiaetus* are known from the lowlands of three regions of the South Island of New Zealand (Fig. 8): Canterbury, Otago, and Southland. In Otago representatives of the genus deeply penetrate inland along the Clutha River valley.

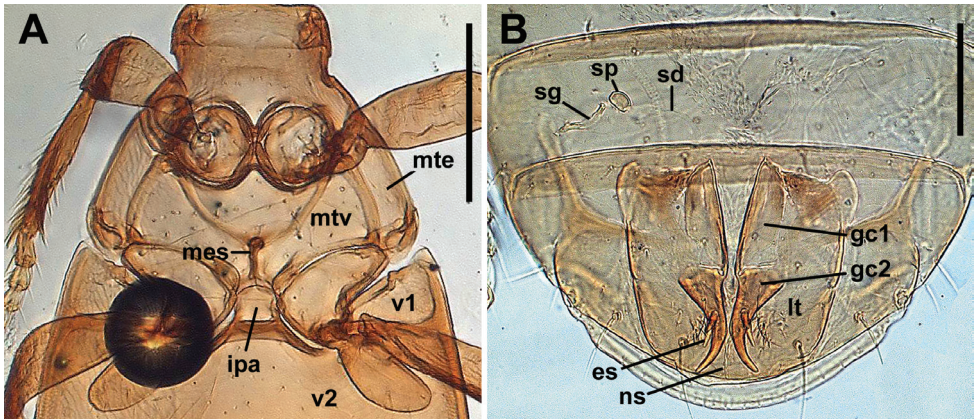


**Figure 3.** Digital images of pterothorax of *Pelodiaetus sulcatipennis* (A) and last abdominal ventrites with female genitalia (B), ventral aspect. Abbreviations: ipa – intercoxal process of abdominal ventrite 2; mes – metendosternite; mte – metanepisternum; mtv – metaventrite; v1-v2 – abdominal ventrites 1-2; es – ensiform seta; gc1 – gonocoxite 1; gc2 – gonocoxite 2; lt – laterotergite; ns – nematiform seta; sd – spermathecal duct; sg – spermathecal gland; sp – spermatheca. Scale bars: 200  $\mu$ m (A); 100  $\mu$ m (B).

**Habitat.** According to the label information, all specimens of *Pelodiaetus* were collected from washed soil samples, except one specimen, which was collected under a stone after rain. Collections were made in a vast spectrum of habitats: from improved pasture and tussocks to conifer (kahikatea and podocarp) and broadleaf (*Neopanax* and beech) forests. Beetles were collected during most months of the year, except February, July, and August.

**Relationships.** Morphologically, the closest relative of *Pelodiaetus* among the New Zealand anillines is *Pelodiaetodes*, the two genera together forming a distinct New Zealand lineage of Anillini. Both genera share developed fronto-lateral carinae, distinct pronotal posterior angles, a dilated prosternal process, nine setae in the elytral umbilical series of pores, longitudinal elytral grooves, and are distinguished by the combination of these characters from any other New Zealand Anillina. Compared with overseas Anillini it seems reasonable to group the members of *Pelodiaetus* with other anillines having grooved elytra, including the Australian *Illaphanus* Macleay and the Madagascan *Bulirschia* Giachino, *Malagasytyphlus* Giachino, and *Malagasydipnus* Giachino (Giachino 2005, 2008). Based on similarity between New Zealand *Pelodiaetus* and Australian *Illaphanus*, Jeannel (1937: 276–277) postulated that both genera had a common ancestor, and their ancestral stock inhabited East Gondwana at the time when it included modern territories of Australia, Tasmania, and, partly, New Zealand. I agree with Jeannel’s opinion and consider the representatives of the Australian genus *Illaphanus* as the sister-taxon to the members of the New Zealand *Pelodiaetus*-lineage.

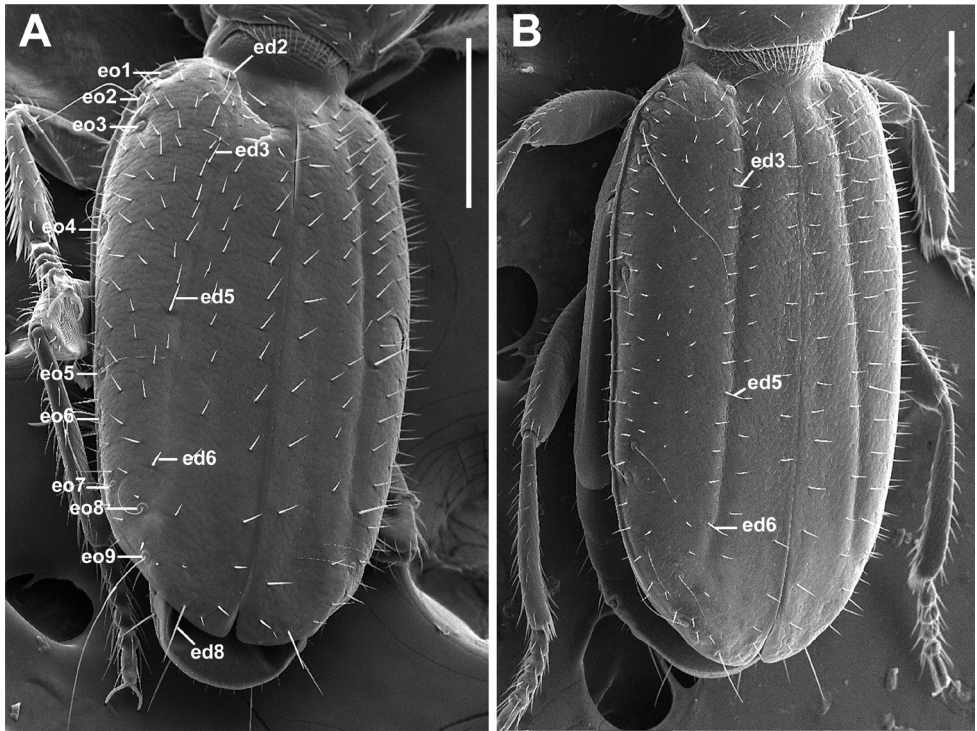


**Figure 4.** SEM illustrations of chaetotaxy of elytra, dorso-lateral aspect, of *Pelodiaetus* species. **A** *P. sulcatipennis* **B** *P. nunni*. Abbreviations: ed2 – scutellar seta; ed3 – 1<sup>st</sup> discal seta; ed5 – 2<sup>nd</sup> discal seta; ed6 – 3<sup>d</sup> discal seta; ed8 – apical seta; eo1–9 – setae 1–9 from the umbilical series. Scale bars 0.2 mm.

**A key for identification of adult representatives of *Pelodiaetus* from New Zealand**

- 1 Eyes lacking (Fig. 6). Posterior angles of pronotum distinct, projected outwards, without denticle anterior to them (Fig. 2A, B). Prosternal process dilating to blunt apex (Fig. 2C, D). Elytra with longitudinal grooves and uneven discal setae: 1<sup>st</sup> discal seta not distinguishable from surrounding vestiture, noticeably shorter than distinct 2<sup>nd</sup> and 3<sup>d</sup> discal setae, which are clearly visible (Fig. 4). Umbilicate series of nine pores (Fig. 4) ..... **2**
- Other combination of characters..... **other genera of New Zealand Anillini**
- 2 Male with distal sclerites (ds) of internal sac long (Fig. 7A), formed as a long flagellum with strongly sclerotized compact basal area. Females with spermatheca moderately elongated, > 2.5 times longer than wide (Fig. 7D). Beetles from the Port Hills Range (Fig. 8, white circles), of coastal central-eastern Canterbury ..... ***P. nunni* sp. nov.**
- Males with distal sclerites (ds) of internal sac short (Fig. 7E), not longer than a half of the length of median lobe; sclerites without compact basal congestion. Females with spermatheca slightly elongated, <2.0 times longer than wide (Fig. 7H). Beetles from Stewart Island, Southland, Otago and foothills of southern Canterbury (Fig. 8, yellow circles) ..... ***P. sulcatipennis* Jeannel**

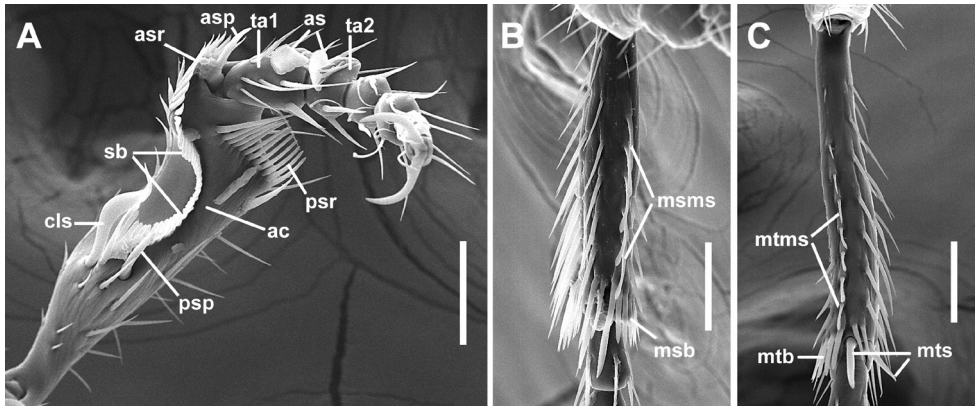


**Figure 5.** SEM illustrations of structural features of legs of *Pelodiaetus sulcatipennis*, ventral aspects. **A** left protarsus and protibia **B** right mesotibia **C** left metatibia. Abbreviations: ac – antenna cleaner; as – adhesive setae; asp – anterior spur; asr – anterior setal row; cls – clip seta; msb – mesotibial brush; msms – mesotibial modified seta; mtb – metatibial brush; mtms – metatibial modified seta; mts – metatibial spur; psp – posterior spur; psr – posterior setal row; sb – setal band; ta1–ta2 – tarsomeres 1–2. Scale bars: 0.05 mm.

***Pelodiaetus nunni* sp. nov.**

<http://zoobank.org/FEFE7294-B8BE-406B-89E8-6D98B26F6D62>

Figs. 1B, D, 2B, D, 4B, 6B, 7A–D, 8

**Type material.** HOLOTYPE, male, in NZAC, labeled: / New Zealand MC Ahuriri SR Port Hills 31 May 08 / Washed soil sample, broad-leaf forest / NZMS 260 M36: 797303 455m /.

PARATYPES (7 specimens, in NZAC, JTN), 4 males and 2 females labeled same as holotype; 1 female labeled: / New Zealand MC Ahuriri SR Port Hills 7 Apr 07 / Washed soil sample, broad-leaf forest /.

**Specific epithet.** The specific epithet is a Latinized eponym in the genitive case, and is based on the surname of John T. Nunn, the collector of this species.

**Type locality.** New Zealand, South Island, Canterbury, Port Hills Range.

**Recognition.** Adults of this species (Fig. 6B) are practically indistinguishable from the adults of *P. sulcatipennis* (Fig. 6A) and are distinguished from the latter by the structure of male and female genitalia.

**Description.** With character states of the genus as summarized above.

**Size.** Small to medium for genus (SBL range 1.25–1.32 mm, mean 1.30 ± 0.028 mm, n = 6).

**Habitus.** Body form subdepressed, subparallel, moderately elongate (WE/SBL 0.33 ± 0.012), head comparatively wide for genus (WH/WPm 0.84 ± 0.011), pronotum of moderate width in comparison to elytra (WPm/WE 0.83 ± 0.045).

**Color.** Body color rufo-testaceous, appendages testaceous.

**Prothorax.** Pronotum moderately long (LP/LE 0.41 ± 0.011) and comparatively elongate (WPm/LP 1.19 ± 0.049), with lateral margins arcuately constricted posteri-

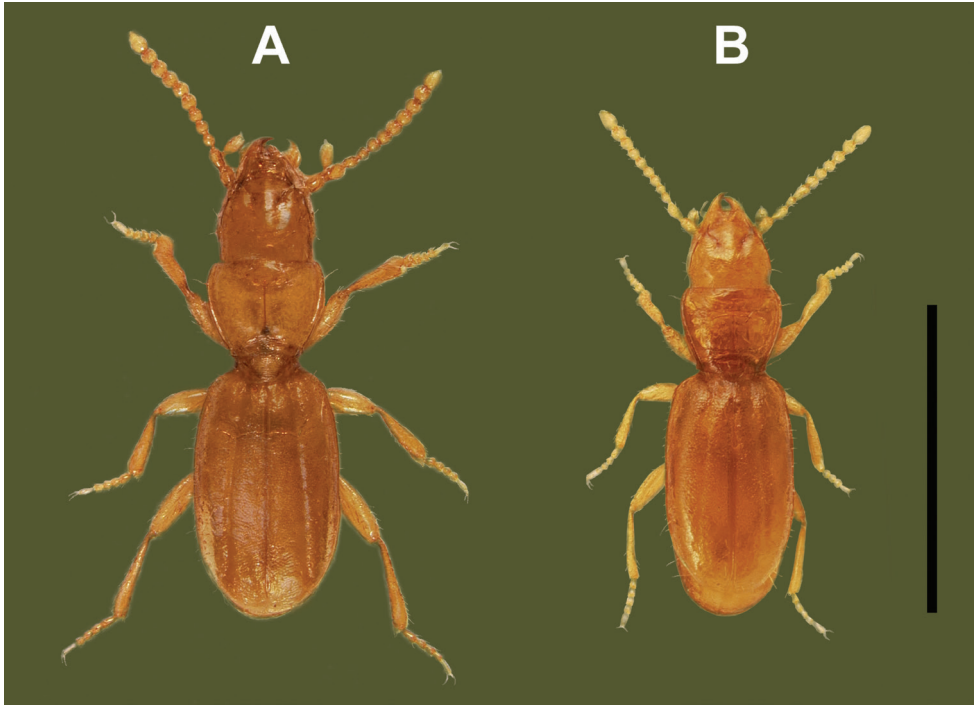


**Figure 6.** Digital images of habitus of *Pelodiaetus* species, dorsal aspect. **A** *P. sulcatipennis* (NZ, Otago, Outram) **B** *P. nunni* (NZ, Canterbury, Ahuriri Scenic Reserve). Scale bar: 1.0 mm.

only (WPm/WPp  $1.48 \pm 0.059$ ). Width between anterior angles slightly greater than between posterior angles (WPa/WPp  $1.21 \pm 0.080$ ).

**Elytra.** Slightly depressed along suture, comparatively long (LE/SBL  $0.57 \pm 0.004$ ) and moderately narrow (WE/LE  $0.58 \pm 0.019$ ). Lateral margins slightly divergent at basal third, subparallel at middle and evenly rounded to apex in apical third.

**Male genitalia.** Median lobe (Fig. 7A) with almost straight ventral margin and short apex with tapering tip. Sclerites of internal sac flagelliform, long, almost equal the length between apical and basal orifices, weakly sclerotized except basal enlargement.

**Female internal genitalia.** Spermatheca weakly sclerotized, moderately elongate (Fig. 7D). Spermathecal duct long without coils. Attachments of spermathecal duct and gland to spermatheca close together.

**Geographic distribution.** This species is known from the coastal Mid Canterbury area of Crosby et al. (1998), where its distribution is limited by Port Hills Range (Fig. 8, white circles).

**Habitat.** Specimens were collected from soil in a broadleaf forest.

**Relationships.** Based on the structure of male genitalia and spermatheca *P. nunni* is postulated to be the sister, more derived taxon of *P. sulcatipennis*.

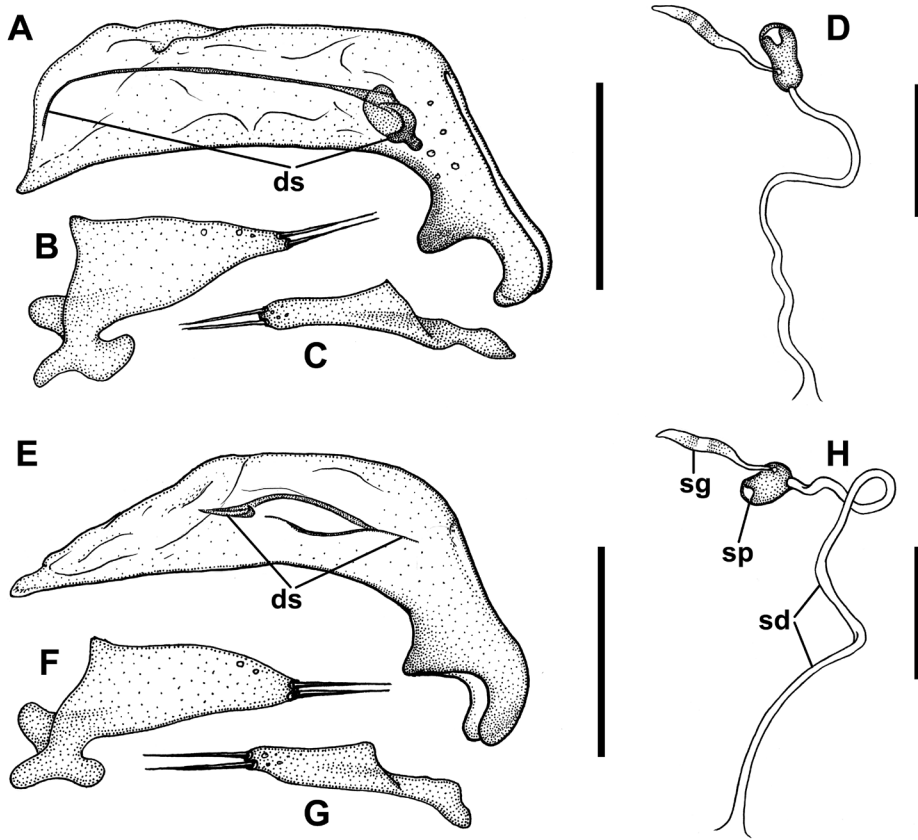


**Figure 7.** Line drawings of male genitalia and female spermathecae of *Pelodiaetus* species. *P. nunni* (NZ, Canterbury, Ahuriri Scenic Preserve): **A** median lobe, right lateral aspect **B** left paramere, left lateral aspect **C** right paramere, right lateral aspect **D** spermatheca. *P. sulcatipennis* (NZ, Otago, Outram): **E** median lobe, right lateral aspect **F** left paramere, left lateral aspect **G** right paramere, right lateral aspect **H** spermatheca. Abbreviations: ds – dorsal sclerites; sd – spermathecal duct; sg – spermathecal gland; sp – spermatheca. Scale bars: 0.1 mm (**A, B, C, E, F, G**); 0.05 mm (**D, H**).

### *Pelodiaetus sulcatipennis* Jeannel

Figs. 1AC, 2AC, 3, 4A, 5, 6A, 7E-H, 8, 9B-C

*Pelodiaetus sulcatipennis* Jeannel, 1937: 277 (original description); Jeannel 1963 (figures, key, distribution); Moore 1980 (key, distribution).

*Pelodiaetus lewisi* Jeannel, 1937: 277 (original description), **syn. nov.**; Jeannel 1963 (key, distribution); Moore 1980 (key, distribution).

**Investigated material.** Stewart Island: Ulva Island Nov-Dec 2003 /coastal forest litter (5 specimens).

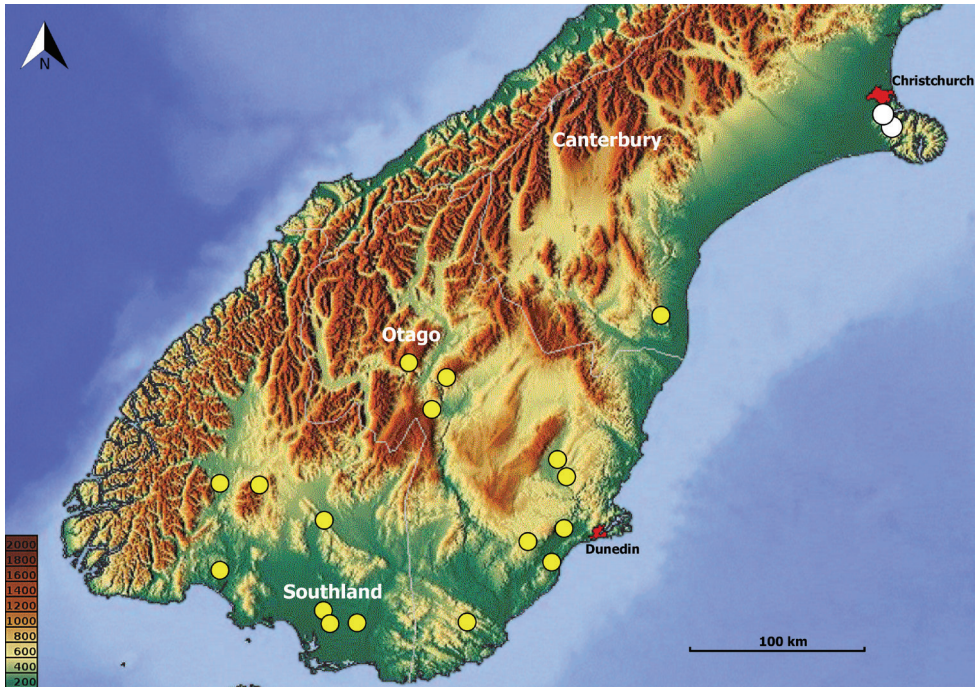


**Figure 8.** Map of southern half of South Island, New Zealand, showing positions of locality records for the species of *Pelodiaetus*: *P. nunni*, white circles; *P. sulcatipennis*, yellow circles. Elevation scale bars are given in meters.

Southland: Tussock Creek Forest Hill Res 1 Sep 07 / Washed soil sample. Wet Podocarp/broadleaf forest (4 specimens); New Zealand SL Forest Hill Res nr Edendale 1 Sep 07 / Washed soil sample. Kahikitea forest (3 specimens) ; New Zealand SL Alton Burn Tuatapere SR 16 Nov 08 / Washed soil sample, totara/beech forest / NZMS 260 D45: 992419 38m (4 specimens) ; New Zealand SL Tuatapere Domain Tuatapere SR 16 Nov 08 / Washed soil sample, beech forest / NZMS 260 D45: 993403 30m (1 specimen) ; New Zealand SL Tuatapere Scenic Reserve at Tuatapere Domain, 30m J.Nunn 16 Nov 08 / Molecular voucher # 104 Sokolov I.M 2009 (1 specimen); New Zealand SL Tuatapere Scenic Reserve at Tuatapere Domain, 30m J.Nunn 16 Nov 08 / Molecular voucher # 107 Sokolov I.M 2009 (1 specimen); New Zealand SL Bog Burn Taringatura Forest 2 Jan 09 / Washed soil sample, beech forest / NZMS 260 E45: 397596 250m (1 specimen); New Zealand SL Dunsdale Stream, Hokonui Hills, 110m, washed soil sample J.Nunn 26 April 08 / Molecular voucher # 100 Sokolov I.M 2009 (1 specimen); New Zealand MC Pudding Hill Reserve Mt. Hutt 700m J.Nunn 25 Oct 08 / Molecular voucher # 105 Sokolov I.M 2009 (1 specimen); SL Chloris Pass, Catlins 17 Jun 06 (7 specimens); Rakahouka 2 Sep 07 /Neaopanax forest (2 specimens).

Dunedin: Woodside Glen, Outram 18 Nov 06 (3 specimens); Sutton, Salt Lake 21 Jun 09 / tussock and improved pasture (2 specimens); Picnic Gulley, Taieri Mouth 18 May 06 / under stone after rain (29 specimens); New Zealand DN Start of Government Tck Waipori Valley / Washed soil sample 17 Dec 06 (1 specimen).

Central Otago: Logan Burn 900m 13 Dec 1982 / ex. *Oreobolus pectinatus* (3 specimens); Cromwell, Kawarau Gorge, Roaring Meg 500m 12 Mar 1959 (2 specimens); Garden V., Raggedy Range 10 Sept 68 / Raoulia (1 specimen); Alexandra Hills, the Knobbies 10 Sept 68 / Raoulia (1 specimen).

South Canterbury: Guns Bush Waimate 23 Dec 06 / Washed soil sample, broad-leaf forest (1 female).

**Discussion.** As mentioned above, the genus *Pelodiaetus* was established by Jeannel (1937) for two species: *P. sulcatipennis* and *P. lewisi*. Both species were collected together in Dunedin, Otago, by G Lewis, and, according to Jeannel (1937, 1963), they can be distinguished from each other by the shape of the pronotum and elytra. In their descriptions, Jeannel did not provide comparison of the genitalia of the two species, and obviously did not make the necessary measurements for comparison of above-mentioned body parts. He simply restricted description to two couplets of a key with very general diagnoses: a more transverse and rounded pronotum with shorter and more convex elytra for *P. sulcatipennis*, and a correspondingly less transverse and rounded pronotum, and narrower and more elongated elytra, for *P. lewisi*. This short and very general comparison, together with the same type locality, made the validity of two forms questionable. Later, Moore (1980), reviewing the New Zealand Anillini, paid attention to the presence of intermediates in the body shape between the two species and stated that both names may belong to extremes of the same species, but did not formally synonymize these taxa because of the scarcity of the available material.

Preparing this taxonomic review, I had an opportunity to investigate many more representatives of the genus. For analysis of the variation in body part proportions, measurements of 57 members of the genus were completed, including seven specimens of *P. nunni* and 50 specimens of *P. sulcatipennis*. Because of the wide range of *P. sulcatipennis*, the aim of this investigation was to compare main body ratios between the northeastern and southwestern parts of its range. All investigated ratios showed no difference between the two populations of *P. sulcatipennis*, as well as between the latter's populations and the representatives of *P. nunni*. At the same time, many ratios showed rather high interspecies variability; this was especially true for W/L – ratio of maximal width to length along the midline of the pronotum, one of the characters used by Jeannel for distinguishing his species. According to the obtained data, the variation in the proportions of the pronotum (Fig. 9) is similar across different species of *Pelodiaetus* (T-test for independent groups,  $p = 0.693$ ,  $n = 7$  for *P. nunni*, and  $n = 50$  for *P. sulcatipennis*) and between different populations of *P. sulcatipennis* (T-test for independent groups,  $p = 0.095$ ,  $n = 23$  for mid-eastern, and  $n = 27$  for south-western populations). The only difference between populations of *P. sulcatipennis* can be seen in the light shift towards the prevalence of specimens with a slightly more transverse pronotum in the southwestern part of range. However, this deviation lies within the error range and is not statistically significant (see above). The type locality of *P. sulcatipennis* and *P. lewisi* (Dunedin, Otago) is located exactly within the range of the mid-eastern population, thus supporting the point of view of Moore that both Jeannel's species may belong to extremes of a single species. In addition, in investigating male genitalia, I was unable to find any constant difference in the shape of the median lobe and in the armature of the internal sac. On the basis of this evidence, *P.*

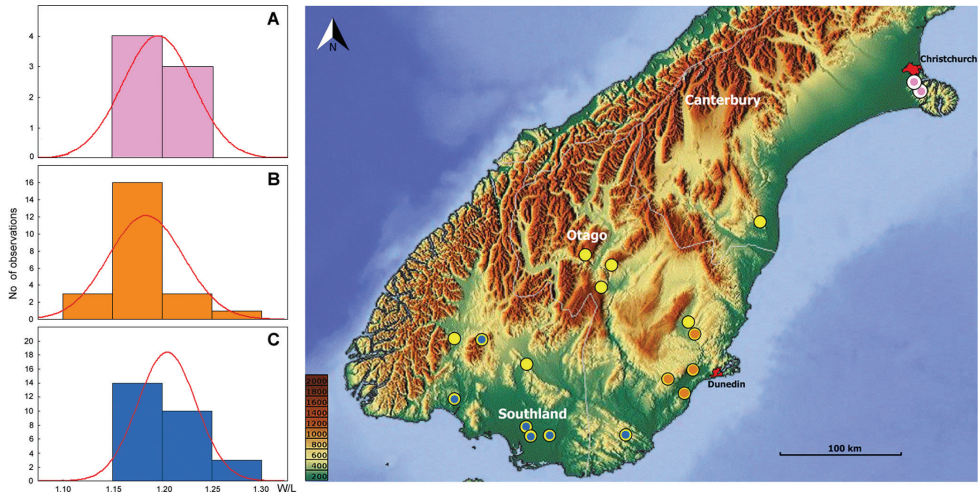


**Figure 9.** Variation in proportions of pronotum among different taxa and populations of *Pelodiaetus*. **A** – *P. nurni*; **B** – *P. sulcatipennis*, mid-eastern populations; **C** – *P. sulcatipennis*, south-western populations. Map of southern half of South Island, New Zealand, shows localities from where specimens were measured. Each species location dot (yellow or white) is identical to Fig. 8 but they are additionally marked with the appropriate bar graph color: pink, orange, and blue. X-axis values represent W/L – ratio of maximal width to length along the midline of pronotum. Red curve – expected normal distribution with sample mean and standard deviation. Elevation scale bars are given in meters.

*sulcatipennis* and *P. lewisi* should be considered as variations of the same species and be synonymized under the name of *Pelodiaetus sulcatipennis* Jeannel.

### *Pelodiaetus* sp.

**Material.** New Zealand: South Island, Nelson, Brightwater, Torpedo Pipe, May 1974 (1 female).

This locality lies far outside the range of *Pelodiaetus*. To confirm the locality and to clarify the taxonomic status of a local population more material including males is needed. At present the status of this specimen is uncertain and it is not considered in the following discussion.

## Discussion

### Range of the genus in the light of geological data and taxon-area concordant relationships

The range of *Pelodiaetus* species stretches across three regions of the South Island of New Zealand (Fig. 8) from Canterbury in the north through Otago and down to

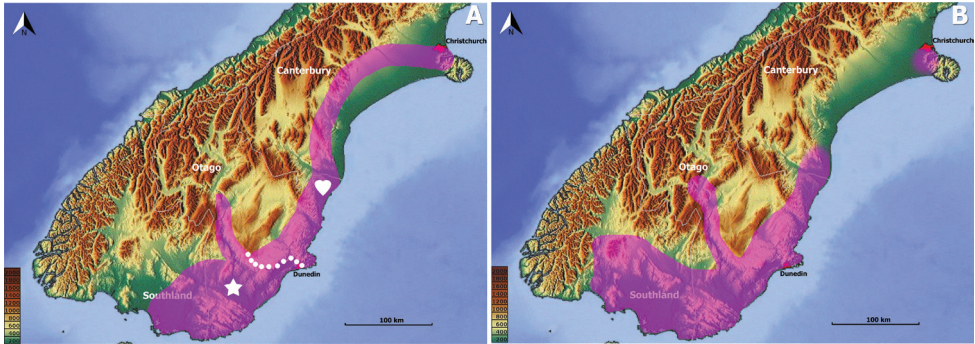


**Figure 10.** Map of southern half of South Island, New Zealand, showing ranges of subterranean non-montane Anillina. **A** – *Zeanillus* (combined ranges of subgenera *Zeanillus* s. str. (heart) and *Brounanillus* (star), white dots represent approximate boundary between taxon ranges); **B** – *Pelodiaetus*. Elevation scale bars are given in meters.

Southland and Stewart Island in the south. The members of the genus inhabit almost all the territory of the coastal lowlands, and in Otago penetrate deeply inland along the Clutha River valley. This rather large territory harbors only two species, one of which is endemic to the Christchurch area and the other of which occupies the rest of the genus range. Morphologically, the two species are almost identical and can be distinguished from each other only after dissection and genitalia investigation, suggesting that diversification between species took place relatively recently.

Geologically, the range of the genus is associated with old terranes composed of Paleozoic to Early Cretaceous volcanics or sediments (Mortimer 2004, Michaux 2009). The range of *P. sulcatipennis* occupies areas on older island arc-derived and oceanic terranes, namely, the Brook Street, the Murihuku, the Dun Mountain-Maitai, and part of the younger Rakaia Terrane (Wandres and Bradshaw 2005, Liebherr et al. 2011, Cooper and Ireland 2013). The range of the presumably more recently derived *P. nunni* is associated with the younger Rakaia Terrane only (Wandres and Bradshaw 2005, Liebherr et al. 2011, Cooper and Ireland 2013).

Search of concordant taxon-area relationships reveals that non-montane representatives of another anilline endogean taxon, the genus *Zeanillus*, demonstrate almost identical distribution to the members of the genus *Pelodiaetus* (Fig. 10). Indeed, the range of *Pelodiaetus* in its main contours repeats the range of the monotypic subgenus *Brounanillus* Sokolov (Fig. 10A, star), but, in comparison to the range of the latter, demonstrates evident features of northward and westward expansions. Interestingly, northward expansion of the range of *Pelodiaetus* corresponds to the range of the nomenclotypic subgenus *Zeanillus* (Fig. 10A, heart), a group of closely related species inhabiting coastal foothills of southern and central Canterbury. Similar to the members of *Pelodiaetus*, in the Christchurch area the members of *Zeanillus* s. str. are represented by their own endemic species *Z. phyllobius* (Broun). The similarity in general distribution and particular species ranges between the members of *Pelodiaetus* and *Zeanillus* may point to their at least partly shared evolutionary history in the South Island.

## Notes on the evolutionary history of *Pelodiaetus*

In the history of Zealandia (Mortimer et al. 2017), the remnant of which is New Zealand (Heads 2016), there was a critical time point for the local biota known as the Oligocene “drowning” (Haq et al. 1987, Stöckler et al. 2002). Depending on the scenario of maximal marine transgression, i.e., on how much the land of Zealandia was above sea level at that time, there exist two concepts of the shaping of modern New Zealand biota, called the “dispersal” and “vicariance” models (Heads 2016). One group of scientists assumes that complete submergence of subaerial lands with subsequent elimination of terrestrial biota took place and believes that all modern lineages arrived in New Zealand after the Oligocene (dispersal model) (Waters and Craw 2006, Landis et al. 2008, Wallis and Trewick 2009). Another group supports the idea that during maximum marine transgression, Zealandia was only reduced to a certain number of low-lying islands on which the Gondwanan-aged relict taxa survived drowning (vicariance model) (Lee et al. 2001, Knapp et al. 2007, Giribet and Boyer 2010, Conran et al. 2014). The second scenario implies that reduction in size of subaerial lands caused corresponding reduction in species diversity, and that these islands remained isolated for tens or hundreds of thousands of years, thus providing enhanced opportunities for geographic speciation (Cooper and Cooper 1995).

Contemporary distribution of the members of the genus *Pelodiaetus* and its relatives seems to fit better the vicariance model, because it is likely that their ancestors persisted on Zealandia after its rifting off and drifting away from Australia. The distribution of putative overseas relatives of *Pelodiaetus* serves as an indirect support for this assumption. As mentioned under the genus description, the members of *Pelodiaetus* are very similar to the members of the primarily Australian genus *Illaphanus* that comprises 29 species of small to medium-large (0.86–1.74 mm) beetles. Besides the Australian mainland, representatives of this genus are known from Tasmania and from the Lord Howe and Norfolk Islands (Giachino 2005). All *Illaphanus* species have grooved elytra, no denticle in front of the posterolateral angles of the pronotum, and, with some exceptions, are lacking the mental tooth in the labial complex. The state of the latter character in most cases distinguishes the members of *Illaphanus* from New Zealand representatives of *Pelodiaetus*, which are characterized by the blunt mental tooth. However, the state of the mental tooth varies within *Illaphanus*, and some species of *Illaphanus* with the developed mental tooth are almost indistinguishable from the members of *Pelodiaetus*. Notably, a small *Illaphanus* with the mental tooth, *Ill. norfolkensis* Giachino, occurs on Norfolk Island (Giachino 2005), which is famous for its endemic fauna of considerably older age than the island itself (Heads 2011). It has been hypothesized that endemic taxa surviving today on the island evolved on other former islands existing in the vicinity on the Norfolk Ridge, the strip of continental crust that extends from New Zealand to New Caledonia. During the breakup of East Gondwana, the Norfolk Ridge together with the Lord Howe Rise and the rest of Zealandia drifted away from Australia (Heads 2016). Hence, the occurrence of *Illaphanus* species on Norfolk and Lord Howe Islands supports the idea that *Pelodiaetus*-

like forms might have persisted on the territory that split from East Gondwana as the Zealandia continent ca. 84 Ma ago (Mortimer et al. 2019).

One more piece of evidence of the persistence of the representatives of the *Pelodiaetus* lineage in Zealandia is the geographical distribution of the members of *Pelodiaetodes*, presumably the sister-taxon to *Pelodiaetus* (Sokolov 2015). Externally, besides their large size, the members of *Pelodiaetodes* can be distinguished from the members of *Pelodiaetus* only by the well-developed denticle anterior to the posterolateral angles of the pronotum. This character is not known among the members of *Illaphanus* and other genera with grooved elytra and can be considered as an autapomorphy of *Pelodiaetodes*. The genus comprises two morphologically distinct subgenera; its modern distribution is disjunct and limited by the Northland Allochthon (Bradshaw 2004) on the North Island (nominotypical subgenus, four species) and one locality in the Oamaru region on the South Island (subgenus *Monosetodes* Sokolov, one species). Given that the lands of the Northland Allochthon were completely submerged during the late Oligocene and became subaerial only around the late- to mid-Miocene after subduction of the Pacific Plate under the Australian one (Bradshaw 2004), the later arrival of the members of *Pelodiaetodes* to the North Island can be assumed. The Oamaru region remained submerged from the Late Cretaceous to the early Oligocene, but some lands of this region were likely exposed during the Oligocene “drowning” from the late Oligocene to the early Miocene (Thompson et al. 2014), which is supportive of the idea of the late arrival of the members of *Pelodiaetodes* to the Oamaru region as well. The absence of *Pelodiaetodes*-like forms in Australia but their presence as two morphologically distinct taxa in New Zealand suggests that the genus *Pelodiaetodes* arose after the East Gondwana breakup, but before New Zealand acquired its modern contour, i.e., somewhere on the Zealandia continent. Apparently, the members of *Pelodiaetodes* managed to survive different epochs of Zealandia inundations including the Oligocene “drowning,” and finally reach the places of their modern distribution.

Additionally, it is worth mentioning a strange ecological pattern of co-occurrences of the members of *Pelodiaetus* with other anillines. In the examined material, I came across four cases of syntopic co-occurrences of New Zealand anillines. Three of these cases were related to *Pelodiaetus* species: namely, *Pelodiaetus nunni* co-occurred with *Z. (Zeanillus) phyllobius* (Broun) at Ahuriri (Christchurch area, Canterbury), *P. sulcatipennis* with *Z. (Zeanillus) nunni* Sokolov at Woodside Glen (Dunedin area, Central Otago), *P. sulcatipennis* with *Z. (Brounanillus) pallidus* (Broun) at Picnic Gully (Taieri Mouth, South Otago), and one case related to its sister-taxon, where *Z. (Nunnanillus) pellucidus* Sokolov co-occurred with *Pelodiaetodes (Monosetodes) nunni* Sokolov at Glen Warren Reserve (Oamaru, North Otago). In these examples, the co-occurring species were represented by two contrasting morphotypes, a small (first place in the listing above) and a large one. In all cases but one, a small species of the *Pelodiaetus* lineage co-occurs with a large one from the unrelated clade, i.e., a small *Pelodiaetus* lives together with a large *Zeanillus*. However, in the fourth case, on the contrary, a small *Zeanillus* lives with a large *Pelodiaetodes*. Generally, miniaturization is one of the ways of speciation in the Anillini allowing species to occur syntopically and to exploit resources more

effectively (Sokolov 2013, Andújar et al. 2017). Often these species are closely related and probably formed as a result of sympatric speciation, as was demonstrated for North American *Anillinus lescheni* Sokolov and Carlton and *A. stephani* Sokolov and Carlton (Sokolov et al. 2004), for some European *Typhlocharis* Dieck (Pérez-González and Zaballo 2013), and for Mexican *Zapotecanillus oaxacanus* Sokolov and *Z. nanus* Sokolov (Sokolov 2013). In the case described in this paper, the co-occurrence of small and large species belonging to unrelated taxa demonstrates evolutionary adaptations of representatives of different genera to living together in one community, and also suggests intermixture of different faunas, reflecting the complicated evolutionary history of endogean biota on the Zealandia continent. Apparently, the evolution of the local anilline community was accompanied by the subsequent extinction and replacement of one taxon with another, either because of dramatic historical events or as a result of species competition, or as a combination of both.

Comparison of species composition in Australia and New Zealand helps to explain the origin of the South Island anilline faunas. In Australia, as many as 29 (85.3%) of 34 known species of Anillini belong to the genus *Illaphanus*, the sister-taxon to the *Pelodiaetus* lineage. The same dominance of representatives of the *Pelodiaetus* lineage can be seen on the North Island, where four species (80.0%) of five recorded for the island belong to *Pelodiaetodes*. At the same time, on the South Island, only three species (20.0%) of 15 anillines belong to the *Pelodiaetus* lineage. The significant decline in the number of species of the *Pelodiaetus* lineage on the South Island suggests that the Anillini faunas of the two islands may have different origins. The presence of species with Australian roots on the North Island is in concord with well-documented southeastern Australia–New Zealand connections (Heads 2014, 2016). By contrast, on the South Island, the fauna of Anillini has been shaped by the representatives of *Zeanillus*, whose ancestors supposedly inhabited a territory of the Campbell Plateau (Sokolov 2016). The geological data show that the Campbell Plateau together with Marie Byrd Land formed the West Antarctic margin, rather distant from the Australia/Pacific Plate margin of East Gondwana (Siddoway 2008, Heads 2014). Thus, the anilline community of the South Island could have resulted from an intermixture of ancient endogean faunas from different parts of East Gondwana and perhaps was dramatically modified by the Oligocene “drowning.” The possibility that different parts of East Gondwana could harbor different terrestrial faunas seems plausible. Several recent investigations have demonstrated examples of diversification of ancient terrestrial groups that had taken place prior to major geological events that split ancient supercontinents (San Mauro et al. 2005, Muriénne et al. 2014, Heads 2014, Buckley et al. 2015).

## Acknowledgements

I am grateful to the staff of Louisiana State Arthropod Museum, LSU, Baton Rouge, and the former director, Christopher E. Carlton, and the curator, Victoria M. Bayless, for their diversified assistance and patience that made this paper pos-

sible, and, especially, for permission to use the Museum's equipment. I appreciate help with SEM imaging provided by the staff of the former Microscopy Center at Louisiana State University School of Veterinary Medicine (Baton Rouge, LA). I also would like to thank Richard A.B. Leschen (Landcare Research, Auckland, New Zealand) and John T. Nunn (Dunedin, New Zealand) for the loan of specimens in their care. Additionally, I am particularly thankful to Elisabeth Roberts (Museum Specialist, Systematic Entomology Laboratory, USDA, National Museum of Natural History, Washington, DC, USA), who checked the final version of manuscript for stylistic errors.

The mention of trade names or commercial products in this publication is solely for the purpose of providing specific information and does not imply recommendation or endorsement by the USDA; the USDA is an equal opportunity provider and employer.

## References

- Andújar C, Pérez-González S, Arribas P, Zaballos JP, Vogler AP, Ribera I (2017) Speciation below ground: Tempo and mode of diversification in a radiation of endogean ground beetles. *Molecular Ecology* 00: 1–18. <https://doi.org/10.1111/mec.14358>
- Bradshaw JD (2004) Northland Allochthon: an alternative hypothesis of origin. *New Zealand Journal of Geology and Geophysics* 47: 375–382. <https://doi.org/10.1080/00288306.2004.9515063>
- Buckley TR, Krosch M, Leschen RAB (2015) Evolution of New Zealand insects: summary and prospectus for future research. *Austral Entomology* 54: 1–27. <https://doi.org/10.1111/aen.12116>
- Conran JG, Mildenhall DC, Lee DE, Lindqvist JK, Shepherd C, Beu AG, Bannister JM, Stein JK (2014) Subtropical rainforest vegetation from Cosy Dell, Southland: plant fossil evidence for Late Oligocene terrestrial ecosystems, *New Zealand Journal of Geology and Geophysics* 57: 236–252. <https://doi.org/10.1080/00288306.2014.888357>
- Cooper A, Cooper RA (1995) The Oligocene bottleneck and New Zealand biota: genetic record of a past environmental crisis. *Proceedings of the Royal Society, B*, 261: 293–302. <https://doi.org/10.1098/rspb.1995.0150>
- Cooper AF, Ireland TR (2013) Cretaceous sedimentation and metamorphism of the western Alpine Schist protoliths associated with the Pounamu Ultramafic Belt, Westland, New Zealand. *New Zealand Journal of Geology and Geophysics* 56: 188–199. <https://doi.org/10.1080/00288306.2013.809776>
- Crosby TK, Dugdale JS, Watt JC (1998) Area codes for recording specimens localities in the New Zealand subregion. *New Zealand Journal of Zoology* 25: 175–183. <https://doi.org/10.1080/03014223.1998.9518148>
- Erwin TL (1974) Studies of the subtribe Tachyina (Coleoptera: Carabidae: Bembidiini), Part II: a revision of the New World-Australian genus *Pericompsus* LeConte. *Smithsonian Contributions to Zoology* 162: 1–96. <https://doi.org/10.5479/si.00810282.162>

- Giachino PM (2005) Revision of the Australian Anillina (Coleoptera, Carabidae, Bembidiini). In: Daccordi M, Giachino PM (Eds) Results of the Zoological Missions to Australia of the Regional Museum of Natural Sciences of Turin. II. Monografie del Museo regionale di Scienze naturali, Torino 42: 137–238.
- Giachino PM (2008) New genera and species of Anillina (Coleoptera Carabidae Bembidiini) from Madagascar and Seychelles Islands, with notes about their origin and distributions. Bollettino del Museo Civico di Storia Naturale di Verona, Botanica Zoologia 32: 91–136.
- Giachino PM, Vailati D (2011) Review of the Anillina of Greece (Coleoptera, Carabidae, Bembidiini). Biodiversity Journal, Monograph 1: 1–112.
- Giribet G, Boyer SL (2010) ‘Moa’s Ark’ or ‘Goodbye Gondwana’: is the origin of New Zealand’s terrestrial invertebrate fauna ancient, recent, or both? Invertebrate Systematics 24: 1–8. <https://doi.org/10.1071/IS10009>
- Haq BU, Hardenbol J, Vail PR (1987) Chronology of fluctuating sea levels since the Triassic. Science 235: 1156–1167. <https://doi.org/10.1126/science.235.4793.1156>
- Heads M (2011) Old taxa on young islands: a critique of the use of island age to date island-endemic clades and calibrate phylogenies. Systematic Biology 60: 204–218. <https://doi.org/10.1093/sysbio/syq075>
- Heads M (2014) Biogeography of Australasia: A molecular analysis. Cambridge University Press, Cambridge, 503 pp.
- Heads M (2016) Biogeography and evolution in New Zealand. CRC Press, Taylor & Francis Group, Boca Raton, 635 pp. <https://doi.org/10.1201/9781315368177>
- Hlavac TF (1971) Differentiation of the carabid antenna cleaner. Psyche 78: 51–66. <https://doi.org/10.1155/1971/927545>
- Jeannel R (1937) Les Bembidiides endogés (Col. Carabidae). Revue française d'Entomologie 3: 241–339.
- Jeannel R (1963) Monographie des “Anillini”, Bembidiides endogés [Coleoptera Trechidae]. Mémoires du Muséum national d'Histoire naturelle, Série A, Zoologie 28: 33–204.
- Knapp M, Mudaliar R, Havell D, Wagstaff SJ, Lockhart PJ (2007) The drowning of New Zealand and the problem of *Agathis*. Systematic Biology 56: 862–870. <https://doi.org/10.1080/10635150701636412>
- Landis CA, Campbell HJ, Begg JG, Mildenhall DC, Paterson AM, Trewick SA (2008) The Waipounamu Erosion Surface: questioning the antiquity of the New Zealand land surface and terrestrial fauna and flora. Geological Magazine 145: 173–197. <https://doi.org/10.1017/S0016756807004268>
- Lee DE, Lee WG, Mortimer N (2001) Where and why have all the flowers gone? Depletion and turnover in the New Zealand Cenozoic angiosperm flora in relation to palaeogeography and climate. Australian Journal of Botany 49: 341–356. <https://doi.org/10.1071/BT00031>
- Liebherr JK, Marris JWM, Emberson RM, Syret P, Roig-Junent S (2011) *Orthoglymma wangaepaka* gen.n., sp. n. (Coleoptera: Carabidae: Broscini): a newly discovered relict from the Buller Terrane, north-western South Island, New Zealand, corroborates a general pattern of Gondwanan endemism. Systematic Entomology 36: 395–414. <https://doi.org/10.1111/j.1365-3113.2011.00569.x>

- Michaux B (2009) Reciprocity between biology and geology: reconstructing polar Gondwana. *Gondwana Research* 16: 655–668. <https://doi.org/10.1016/j.gr.2009.06.002>
- Moore BP (1980) A synopsis of the New Zealand Anillini (Coleoptera: Carabidae: Bembidiinae), with descriptions of new genera and species. *New Zealand Journal of Zoology* 7: 399–406. <https://doi.org/10.1080/03014223.1980.10423793>
- Mortimer N (2004) New Zealand's geological foundations. *Gondwana research* 7: 261–272. [https://doi.org/10.1016/S1342-937X\(05\)70324-5](https://doi.org/10.1016/S1342-937X(05)70324-5)
- Mortimer N, Campbell HJ, Tulloch AJ, King RP, Stagpoole VM, Wood RA, Rattenbury MS, Sutherland R, Adams CJ, Collot J, Seton M (2017) Zealandia: Earth's hidden continent. *GSA Today*. Vol. 27, March/April. <https://doi.org/10.1130/GSATG321A.1>
- Mortimer N, van den Bogaard P, Hoernle K, Timm C, Gans PB, Werner R, Riefstahl F (2019) Late Cretaceous oceanic plate reorganization and the breakup of Zealandia and Gondwana. *Gondwana Research* 65: 31–42. <https://doi.org/10.1016/j.gr.2018.07.010>
- Murienne J, Daniels SR, Buckley TR, Mayer G, Giribet G (2014) A living fossil tale of Pangaean biogeography. *Proceedings of the Royal Society B* 281: 20132648. <https://doi.org/10.1098/rspb.2013.2648>
- Pérez-González S, Zaballos JP (2013) Four new species of *Typhlocharis* (*baetica* group) (Coleoptera: Carabidae: Anillini) from southwestern Iberian Peninsula with notes on their biogeographical and morphological implications. *Systematic Entomology* 38: 104–122. <https://doi.org/10.1111/j.1365-3113.2012.00649.x>
- San Mauro D, Vences M, Alcobendas M, Zardoya R, Mayer A (2005) Initial diversification of living amphibians predated the breakup of Pangaea. *The American Naturalist* 165:590–599. <https://doi.org/10.1086/429523>
- Siddoway CS (2008) Tectonics of the West Antarctic Rift System: New light on the history and dynamics of distributed intracontinental extension. In: Cooper AK, Barrett PJ, Stagg H, Storey B, Stump E, Wise W, and the 10<sup>th</sup> ISAES editorial team (Eds) *Antarctica: A keystone in a changing World*. Proceedings of the 10<sup>th</sup> International Symposium on Antarctic Earth Sciences. The National Academies Press, Washington, DC, 91–114. <https://doi.org/10.3133/ofr20071047KP09>
- Sokolov IM, Carlton CE, Cornell JF (2004) Review of *Anillinus* with descriptions of 17 new species and a key to soil and litter species (Coleoptera: Trechinae: Bembidiini). *Coleopterists Bulletin* 58: 185–233. <https://doi.org/10.1649/611>
- Sokolov IM (2013) A new genus and eight new species of the subtribe Anillina (Carabidae, Trechinae, Bembidiini) from Mexico, with a cladistics analysis and some notes on the evolution of the genus. *ZooKeys* 352: 51–92. <https://doi.org/10.3897/zookeys.352.6052>
- Sokolov IM (2015) Review of the species of *Pelodiaetodes* Moore (Coleoptera: Carabidae: Bembidiini: Anillina) of New Zealand. *Zootaxa* 3963: 561–582. <https://doi.org/10.11646/zootaxa.3963.4.4>
- Sokolov IM (2016) A taxonomic review of the anilline genus *Zeanillus* Jeannel (Coleoptera: Carabidae: Bembidiini: Anillina) of New Zealand, with descriptions of seven new species re-classification of the species, and notes on their biogeography and evolution. *Zootaxa* 4196: 1–37. <https://doi.org/10.11646/zootaxa.4196.1.1>

- Steedman HF (1958) Dimethyl hydantoin formaldehyde: a new water-soluble resin for use as a mounting medium. *Quarterly Journal of Microscopical Science* 99: 451–452.
- Stöckler K, Daniel IL, Lockhart PJ (2002) New Zealand Kauri (*Agathis australis* (D.Don) Lindl., Araucariaceae) survives Oligocene drowning. *Systematic Biology* 51: 827–832. <https://doi.org/10.1080/10635150290102474>
- Stork NE (1980) A scanning electron microscope study of tarsal adhesive setae in the Coleoptera. *Zoological Journal of the Linnean Society* 68: 175–306. <https://doi.org/10.1111/j.1096-3642.1980.tb01121.x>
- Thompson NK, Bassett KN, Reid CM (2014) The effect of volcanism on cool-water carbonate facies during maximum inundation of Zealandia in the Waitaki-Oamaru region. *New Zealand Journal of Geology and Geophysics* 57: 149–169. <https://doi.org/10.1080/00288306.2014.904385>
- Wallis GP, Trewick SA (2009) New Zealand phylogeography: evolution on a small continent. *Molecular Ecology* 18: 3548–3580. <https://doi.org/10.1111/j.1365-294X.2009.04294.x>
- Wandres AM, Bradshaw JD (2005) New Zealand tectonostratigraphy and implications from conglomeratic rocks for the configuration of the SW Pacific margin of Gondwana. In: Vaughan APM, Leat PT, Pankhurst RJ (Eds) *Terrane processes at the margins of Gondwana*. The Geological Society of London, London, 179–216. <https://doi.org/10.1144/GSL.SP.2005.246.01.06>
- Waters JM, Craw D (2006) Goodbye Gondwana? New Zealand biogeography, geology, and the problem of circularity. *Systematic Biology* 55: 351–356. <https://doi.org/10.1080/10635150600681659>

# New species of *Xiphoscelis* Burmeister, 1842 (Coleoptera, Scarabaeidae, Cetoniinae) from arid regions of South Africa and Namibia

Renzo Perissinotto<sup>1</sup>, Petr Šípek<sup>2</sup>

**1** School of Environmental Sciences, Nelson Mandela University, P.O. Box 77000, Port Elizabeth 6031, South Africa **2** Department of Zoology, Charles University, CZ- 128 44 Vinicna 7, Praha 2, Czech Republic

Corresponding author: Renzo Perissinotto ([renzo.perissinotto@mandela.ac.za](mailto:renzo.perissinotto@mandela.ac.za))

---

Academic editor: Andrey Frolov | Received 27 June 2019 | Accepted 28 August 2019 | Published 9 October 2019

---

<http://zoobank.org/D2A33EC1-971E-4CCA-B288-37BA8E186C59>

---

**Citation:** Perissinotto R, Šípek P (2019) New species of *Xiphoscelis* Burmeister, 1842 (Coleoptera, Scarabaeidae, Cetoniinae) from arid regions of South Africa and Namibia. ZooKeys 879: 57–89. <https://doi.org/10.3897/zookeys.879.37721>

---

## Abstract

Two new species of the southern African genus *Xiphoscelis* Burmeister, 1842 are recognised and described, *X. braunsi* **sp. nov.** from the Eastern and Western Cape Karoo (South Africa) and *X. namibica* **sp. nov.** from the Huns Mountains of southern Namibia and adjacent ranges in South Africa. These were previously overlooked and grouped together with *X. schuckardi* Burmeister, 1842, but further material and more in-depth analyses have now revealed their clear separation on the basis of key diagnostic features, including clypeal structure, metatibial spur development and aedeagal shape. The densely and coarsely costate elytral structure and the black to brown colour of these species are symplesiomorphies shared with a number of the most primitive genera among the African Cetoniinae. However, these characters also reflect the convergent adaptation to hot and arid conditions they share with several other species occurring in this region. Phylogenetic relationships of the genus with other Cetoniinae are explored using the larval characters highlighted in the description of the 3<sup>rd</sup> instar larva of *X. braunsi* **sp. nov.** The extraordinary hypertrophy observed in the male metatibial spur of species in this genus, and particularly in *X. schuckardi*, appears to represent a defence mechanism against potential predators on the ground, apart from playing a role during mating.

## Keywords

Afrotropical region, fruit chafers, identification key, immature stages, life cycle, Succulent Karoo, taxonomy, Xiphoscelidini

## Introduction

The genus *Xiphoscelis* has been recognised since its first description as characterised by unique features, such as a narrow mesometasternal process, enlarged metafemur, low subhumeral elytral arch, round pronotum and regularly costate elytra. To accommodate these, apparently plesiomorphic features, a supra-generic grouping was proposed with the aim of clustering together a variety of genera sharing the key characters. Burmeister (1842) suggested the name Xiphoscelidae, which was later converted to Xiphoscelidini by Schenkling (1921), in order to delineate a new tribal subdivision.

Krikken (1984) made substantial amendments to this tribe, by transferring several genera into or outside it, relying heavily on the lack/presence of mesometasternal protrusion and the degree of approximation of the mesocoxae. Apart from the proper Afrotropical genera, Krikken (1984) also included a few genera from the Madagascan subregion (i.e., *Scheinia* Ruter, 1957 and *Plochiliana* Ruter, 1978) and Australia (i.e., “Genus 1 (= *Pseudoclitria* auctorum” and other yet unnamed genera at that stage, Krikken 1984: 46–47). This was still largely reflected in the iconographic monograph of Sakai and Nagai (1998).

However, later Holm and Marais (1992) proposed the removal of most of the Afrotropical genera included by Krikken (1984), leaving only the genus *Xiphoscelis* and its immediate “precursors” (*Protoclita* and *Ischnostomiella*) in it, and the downgrade of the tribe to a subtribe. More recently, Beinhundner (2017) has included the following among the Afrotropical (excluding Madagascar) genera within this tribe: *Aporecolpa* Lansberge, 1886; *Ischnostomiella* Krikken, 1978; *Myodermidius* Bourgoïn, 1920; *Protoclita* Krikken, 1978; and *Xiphoscelis*.

As already pointed out by Krikken (1984), it is obvious that this supra-generic cluster is among the most uncertain of all the subdivisions currently recognised in the taxonomy of Cetoniinae. In his insightful account, this author articulated the following possibility: “A synapomorphy for the entire group is not available, and it may well be that most of the included groups (or even all of them) stand phylogenetically at the base of other tribes, which could ultimately lead to a complete dissolution of the tribe Xiphoscelidini” (Krikken 1984).

To complicate matters further, recent molecular analyses indicate that the phylogeny of Cetoniinae in general needs a substantial revision, as large incongruences with the traditional concepts are emerging (Šípek et al. 2016). This applies to all the major classification systems proposed to date, namely those of Schenkling (1921), Krikken (1984) and Holm and Marais (1992).

There are currently three species described within the genus *Xiphoscelis*, two of which (*X. lenxuba* Perissinotto, Villet & Stobbia, 2003 and *X. sneeubergensis* Perissinotto, Villet & Stobbia, 2003) were only recently separated from the type and only species previously recognised, *X. schuckardi* (Perissinotto et al. 2003, Beinhundner 2017). Further analyses of type specimens and availability of new material and data have now revealed that another two species need to be erected in order to account for the differences observed in the populations that were collectively grouped under *X. schuckardi* by Perissinotto et al. (2003). These are described here, along with an update of the

biology of the genus and the first detailed description of the 3<sup>rd</sup> instar larval stage of a species (*X. braunsi* sp. nov.) within the genus.

## Materials and methods

Holotype specimens of both *Xiphoscelis schuckardi* Burmeister, 1842 (♂, 17 mm total length, “Pr. b. sp. Sch.”) and *Xiphoscelis garipeana* Schaum, 1849 (nec Gory & Percheron) (♀, 15.8 mm total length, “Afr. Austr”) were studied in detail through high-resolution photographs kindly provided by Karla Schneider (MLUH) and Giulio Cuccodoro (MHNG), respectively.

Other specimens were obtained through field collections during the period 1995–2018 (R Perissinotto & L Clennell legit), or from museum and private collections (as per list provided below). Fresh specimens were either caught in flight using standard nets after rainfall events, excavated from underground or obtained after rearing third instar larvae collected in the wild under laboratory controlled-conditions. In the laboratory, larvae were kept in plastic containers of 1–5 L capacity, containing the natural soil and detrital material found in situ. Water was sprayed at the soil surface at regular intervals of about 1–2 weeks until pupation.

Data on distribution, period of adult activity and other biological information for all the species of the genus *Xiphoscelis* were also obtained from Péringuey (1907), Holm and Marais (1992), Sakai and Nagai (1998), Perissinotto et al. 2003 and Beinhundner (2017). The key geographic abbreviations used within the text are as follows: NAM = Namibia; WC = Western Cape Province (South Africa); NC = Northern Cape Province (South Africa); EC = Eastern Cape Province (South Africa).

As in previous works, the description of adult morphological characters follows the terminology of Krikken (1984) and Holm and Marais (1992). Specimen total length and maximum width were measured using a Vernier calliper, from the anterior margin of the clypeus to the apex of the pygidium and at the widest point of the elytra, respectively. Photos of specimen dorsal, ventral and lateral views were taken with a Nikon CoolPix S9700 digital camera with macro setting, while higher-resolution photos of specimen's clypeus, pygidium and male genitalia were obtained using a Nikon DigitalSight DS-Fi2 camera attached to a Nikon SMZ25 dissecting microscope. The background was removed from the photos using Microsoft Word 2010 (Picture Tools), in order to increase clarity of resolution. The Combine ZP Image Stacking Software by Alan Hadley (alan@micropics.org.uk) was used to obtain z-stacked composite images.

The identity of the larvae was confirmed by both rearing specimens to adulthood and by molecular match (COI) with adult specimens. Specimens for DNA extraction were stored in 96% ethanol immediately after capture. Genomic DNA from thoracic leg muscle tissue (both larvae and adults) was extracted non-destructively using a Qiagen Blood and Tissue Kit, following standard protocols. Voucher specimens are deposited at the NMCR. Partial sequences of the mitochondrial protein coding gene cytochrome oxidase subunit 1 (Cox1) were used in the study. For a detailed description of the laboratory protocol see Vondráček et al. (2018). The larval sequences proved to be identical to those

of the adults (100% match). The respective sequences will be submitted to the GenBank (NCBI) together with those of other Cetoniinae once the ongoing investigation of the phylogenetic relationships of South African Cetoniinae has been finalized.

Larval material was examined with an Olympus SZ9 and a Nikon SMZ 745 stereomicroscope, under which measurements were taken with an ocular grid. Habitus photographs were taken using a Canon EOS 70D camera fitted with Canon EF-S 60 mm f/2.8 Macro USM lens or Canon MP-E 65 mm f/2.8 1–5× macro lens. Microscopic slides were photographed using a Canon EOS 70D camera mounted on an Olympus SZ9 stereomicroscope. Partially-focused images of specimens were combined using Zerene Stacker (Zerene Systems LLC, Richland, USA). Structures examined using scanning electron microscopy (JEOL, Model 6380, Tokyo) were cleaned in 10% lactic acid for 24 h and submerged into a Sonorex ultrasonic bath (Bandelin electronics, Berlin) for 30 s, dried in a heating chamber, or using critical point drying, and mounted on aluminium plates. All pictures were digitally enhanced using Adobe Photoshop CC.

The terminology for larval description follows Böving (1936), Ritcher (1966) and Sawada (1991). Antennomeres I–IV were labelled with the respective abbreviations (an I–an IV). In order to give the most accurate information on chaetotaxy, hair-like setae of the cranium and other structures were classified by their relative size into two groups: medium to long (80–300 µm) and minute to short (5–40 µm or less).

To compare the observed larval morphological characters of *X. braunsi* sp. nov. with those of other cetoniines from various clades, a basic phylogenetic analysis based on a matrix of 77 larval morphological characters of 13 taxa was performed, as modified from Kouklík (2017) (Appendix 1). A heuristic parsimony analysis was carried out with PAUP version 4.0b10 (Swofford 2002), using 1000 random taxon additions and tree bisection-reconnection branch swapping. Missing data were coded with a question mark (?) and inapplicable characters as ‘en’ dash (–). The data matrix was prepared using Nexus data editor software and branch support was assessed by bootstrapping 1000 randomly selected trees (Felsenstein 1985). The TreeView and Winclada programs (Nixon 2002) were used to visualise the trees and character state optimisation.

Specimen repositories are abbreviated as follows:

- BMPC** Jonathan Ball and Andre Marais Private Collection, Cape Town, South Africa
- ISAM** Iziko South African Museum, Cape Town, South Africa
- MLUH** Martin Luther Universität Zoologische Sammlung, Halle, Germany
- MHNG** Muséum d’Histoire Naturelle, Genève, Switzerland
- NMCR** Národní Museum, Prague. Czech Republic
- SANC** South African National Collection of Insects, Pretoria, South Africa
- SRPC** Sébastien Rojkoff Private Collection, Sourcieux les Mines, France
- TGPC** Thierry Garnier Private Collection, Montpellier, France
- TMSA** Ditsong National Museum of Natural History (formerly Transvaal Museum), Pretoria, South Africa
- UCTC** University of Cape Town Entomological Collection, Cape Town, South Africa
- UKCR** Univerzita Karlova, Katedra Zoologie, Prague, Czech Republic
- ZMHB** Museum für Naturkunde der Humboldt Universität, Berlin, Germany

## Taxonomy

### *Xiphoscelis braunsi* Perissinotto & Šípek, sp. nov.

<http://zoobank.org/C4DB98B6-5EC0-4E16-8E00-87232F59E100>

Figs 1, 4, 8, 9

**Diagnosis.** This species differs from *X. schuckardi* by its matte, black to brown dorsal colouration (black and shiny in *X. schuckardi*) and the elytral costae which are weakly elevated and poorly visible, rather than prominent as in *X. schuckardi* (Figs 1, 3). The dorsal sculpture of *X. braunsi* is also scattered and shallow, in contrast to that of *X. schuckardi*, which is generally substantially denser and deeper. In *X. braunsi*, the anterior clypeal margin is deeply sinuate and its lateral margins smoothly rounded (Fig. 1D). In *X. schuckardi*, the anterior margin is moderately sinuate while the lateral margins are rather straight to arcuate (Fig. 3D). The total body length of *X. braunsi* falls within the range of 11–16 mm ( $N = 21$ ), while *X. schuckardi* normally exhibits a larger size of 14–22 mm ( $N = 26$ ).

Finally, the parameres of the two species are also different at the level of the inner apical end of the dorsal lobes, which is finely pointed in *X. braunsi*, but rather blunt in *X. schuckardi* (Figs 4, 6). The entire apical surface of the dorsal lobes is covered in relatively long setae in *X. braunsi*, while these are extremely short and barely visible in *X. schuckardi*. The diagnostic differences between *X. braunsi* and *X. namibica* are highlighted in the section below, under the description of the latter species.

**Description of holotype male.** (Figs 1A–E, 4A–C) **Size.** Length 14.8; width 7.7 mm.

**Body.** Black to dark brown, completely matte except for small worn ridges on elytral umbones (Fig. 1A); head and pronotum disproportionately small relative to abdomen size; metacoxa, abdominal sternites and pygidium protruding remarkably outside elytral margins; exhibiting scattered and shallow sculpture throughout dorsal surface associated with short to medium dark setae, becoming longer and denser on antero-lateral margins (Fig. 1A, C, D).

**Head.** Black to dark brown, with round sculpture on frons, becoming irregularly shaped on vertex; ultrafine rugosity across entire surface; long, erect black setae restricted to eye canthus and antennal pedicel; clypeus markedly bilobate and deeply concave, with anterior margin sharply elevated and lateral margins perfectly rounded both posteriorly and anteriorly; antennal clubs and flagellum black to dark brown, of normal cetonine length; pedicel dark brown, becoming lighter towards base.

**Pronotum.** Dark brown and matte, becoming blackish at margins; smoothly rounded at all margins except antero-lateral, which exhibit sharp angles leading to medio-apical, weakly elevated transversal protuberance; posterior margin forming straight line in front of scutellum; small, scattered round to horse-shoe punctures throughout surface, becoming denser towards lateral and anterior margins; thick, black, medium to long setae regularly distributed across entire surface and emerging at centre of punctures, becoming denser and longer at lateral margins (Fig. 1A, C).

**Scutellum.** Black on sides to dark brown on disc; isoscelic triangular with sharply pointed apex and deep but narrow lateral grooves; with regularly spaced horse-shoe

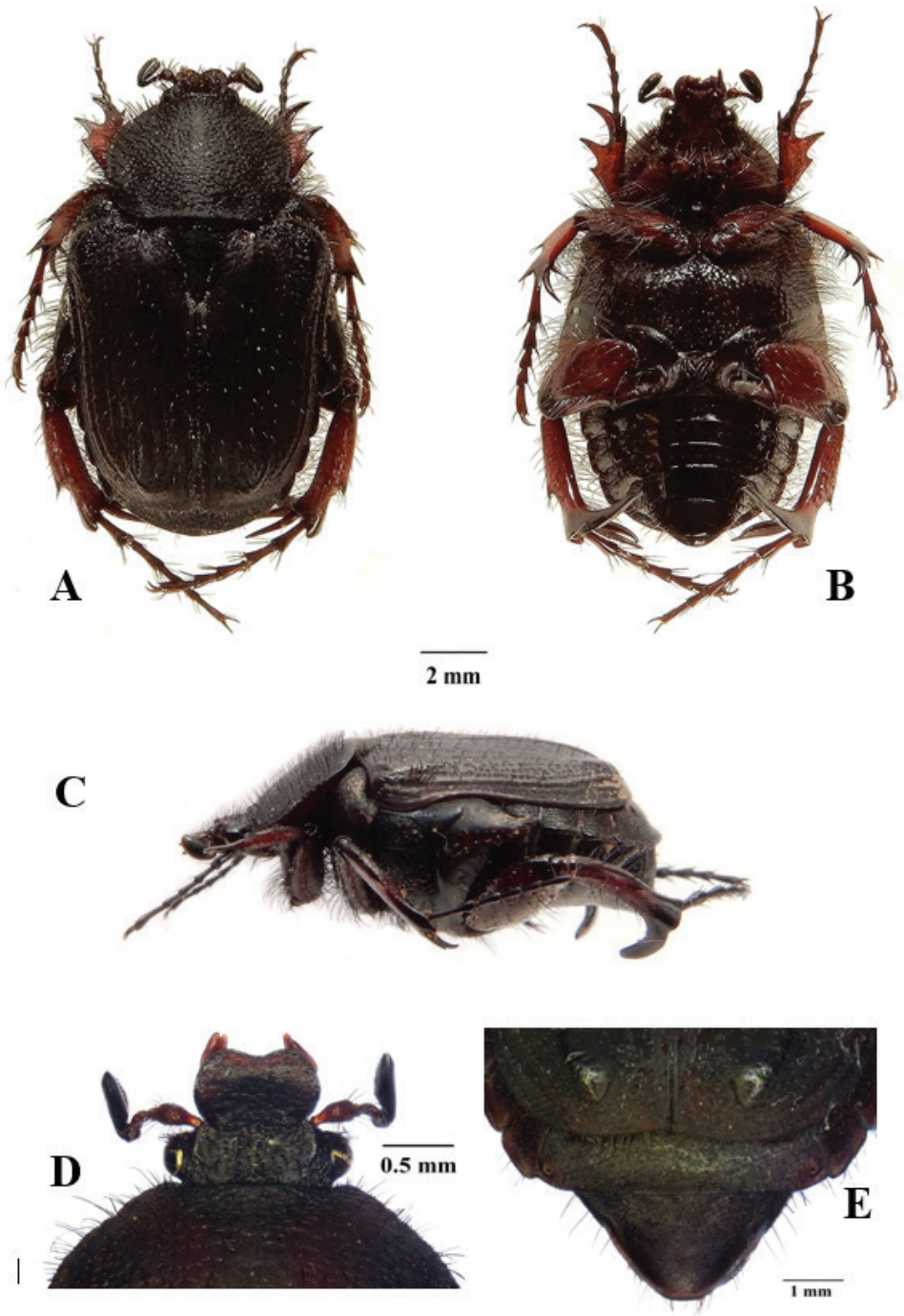


**Figure 1.** *Xiphoscelis braunsi* sp. nov., male: dorsal (A), ventral (B) and lateral (C) habitus; clypeus (D) and pygidium (E). Photographs by Lynette Clennell.

punctures restricted to basal and baso-lateral margins; dense line of short, light setae along basal margin, just below posterior pronotal margin (Fig. 1A).

**Elytron.** Black to dark brown, not covering entire abdomen and leaving external projection of sternites and pygidium partly exposed; subhumeral arch very low and postero-apical declivity extremely steep and abrupt; with costae 1–4 poorly elevated in basal two-thirds, becoming virtually flat in apical third; 5<sup>th</sup> costa and umbones raised, with latter showing shiny area on top; rest of surface matte and regularly sculptured with geminate striae along intercostal spaces 1–4, becoming round to horse-shoe beyond 5<sup>th</sup> costa; with sparse short, but thick and erect black setae across whole surface, except umbones; apex without spinal projection and weakly rounded (Fig. 1A, B).

**Pygidium.** Black at base gradually becoming dark brown towards apex; remarkably narrow and triangular in shape, with basal and baso-lateral margins sharply upturned; with dense, rugose sculpture on basal third, becoming scattered and round towards apex; with moderate central bulge and shallow, symmetric baso-lateral depressions; without pubescence on general surface but with lining of black, long setae along entire apical margin (Fig. 1E).

**Legs.** Tarsal segments consistently black and elongate, but tibiae reddish-brown with black tips and of normal cetoniine thickness and length; protibia tridentate, with proximal tooth drastically reduced; mesotibia bearing mid outer spine with four thick setae on its surface, two apical spines and two spurs of small to medium size; metatibia with extreme hypertrophic inner spine and spurs, inner spine 2–3 times as thick and 1.5 times as long as spurs; (Fig. 1A, B, C); femora reddish-brown with black edges and bearing long, thin setae; pro- and meso-femora of normal size, but metafemora hypertrophic.

**Ventral surface.** Shiny, reddish-brown to black; with thin and long dark setae on prosternum, coxae and all femoral margins, becoming shorter and more sparse on other surfaces, particularly abdominal sternites; all setae emerging at centre of small and round sculptures; mesometasternal process extremely small, not protruding forward or upwards and partly covered by coxal bases, reddish-brown to black, with scattered round punctures and thin setae on surface; abdominal sternites initially flat, but forming concavity at middle particularly in area of sternites 5–7.

**Aedeagus.** Parameres with dorsal lobes tapering gradually and smoothly towards apex, forming short spinal apical inner end, covering completely ventral lobes in dorsal view (Fig. 4A); exhibiting long, thin setae along entire apical margin (Fig. 4A–C); apical surface rounded-triangular in frontal view (Fig. 4C).

**Derivatio nominis.** This species is dedicated to the memory of Hans Brauns (1857–1929), renowned physician and entomologist, who during the early 20<sup>th</sup> century lived and collected extensively in the Willowmore District of the Eastern Cape Province. Most of the early specimens of the new species described here formed part of his collection.

**Description of female.** The only reliable and consistent external feature of sexual dimorphism in this species lies in the development of the metatibial internal apical spine and spurs, which are far less hypertrophic in the female, compared to the male. Also, like in most ceteroniines, the protibiae and protarsi are appreciably shorter in the female than in the male, and the abdominal sternites of the male are usually concave in the central area while those of the female tend to be flat or slightly convex.

**Distribution.** This species appears to be restricted to the Eastern and Western Cape provinces of South Africa. Apart from the long series collected at Willowmore by Brauns in the early part of the 20<sup>th</sup> century, specimens have recently been found in mountainous areas of the western part of the Eastern Cape and in the interior regions of the Western Cape, at altitudes > 500 m but not exceeding 1000 m asl. Thus, the species appears to follow the geographic range of the Cape Fold Belt, where it inhabits the lower slopes of its mountain ranges (Fig. 7).

**Biology.** Both literature and specimen data records report regular occurrences of association of this species with the southern harvester termite, *Microhodotermes viator* (e.g., Holm and Marais 1992, Perissinotto et al. 2003, Hans Brauns data labels). In particular, numerous larvae were collected recently at Worcester (Western Cape), from frass accumulations of *M. viator* that constructs heuweltjies, and reared successfully in the laboratory (Mike Picker, pers. comm.). However, this does not appear to be an obligatory or even predominant association, as most available records and observations are actually of a different nature. Both adults and larvae have most often been found in or around shrubs of a variety of karoid plants, like renosterbos, *Dicerotheramnus rhinocerotis*, or *Psilocaulon* sp. (RP pers. obs., Petr Malec pers. comm.).

**Remarks.** While the ventral habitus of this species is remarkably stable in colour, being predominantly reddish-brown, the dorsal surface ranges across two extreme varieties, one completely black (Fig. 9) and the other reddish-brown (Fig. 8). All the variations between these two extremes have been observed, with the populations at the eastern end of the distribution range normally showing a dominance of light forms and the westernmost populations exhibiting predominantly black habitus. Within the type series analysed in this study, the size ranges as follows: ♂ length 11.1–16.0 mm, width 5.3–8.5 mm ( $N = 13$ ); ♀ length 12.3–15.6 mm, width 5.9–8.3 mm ( $N = 8$ ).

**Type material.** **Holotype** (♂): South Africa, EC, Fullerton, 5 Jan 2017, R. Perissinotto & L. Clennell (ISAM). **Paratypes**: 1 ♂, Beauf. W., 1883, (ISAM: COL-A026571); 1 ♂, Algoa Bay, Capland, Dr Brauns (TMSA: CPH7888); 1 ♂, Capland, Willowmore, 1 Nov 1919, Dr Brauns (TMSA: CPH7883); 2 ♀, Capland, Willowmore, Jan 1916, Dr Brauns, *Hadotermes viator* Latr. (TMSA: CPH7882); 4 ♂, 1 ♀, Kliplaat, Capland, Dr Brauns, Jan 1911 (TMSA: CPH7889); 2 ♂, Willowmore, Capland, Dr Brauns, Jan 1909 (TMSA: CPH7881); 1 ♂, Willowmore, Capland, Dr Brauns, Jan 1909, *Xiphoscelis rufa*, J. Krikken ms 1985 - Paratype, *Xiphoscelis gariepena* G & P. (TMSA); 1 ♂, Willowmore, Capland, Dr Brauns, Jan 1909, *X. gariepena* G. & P., Cum typo comp. (TMSA); 1 ♀, Willowmore, Capland, Dr Brauns, 20 Nov 1902 (TMSA: CPH7880); 1 ♂, 2 ♀, No data (TMSA: CPH7885); 1 ♂, Willowmore, Capland, Dr Brauns, Jan 1909, *Xiphoscelis gariepena*, C. *Hadotermes viator* Haq., coll.

Jul. Moser (ZMHB); 1♂, Willowmore, Capland, Dr Brauns, 20 Nov 1902 (ZMHB); 1♀, Pr. b. sp. Meyer, coll. Nonfried Africa orient., coll. Jul. Moser (ZMHB); 1♂, 1♀, Willowmore District, Dec 1960, Dr Brown (BMPC); 1♂, Matjesfontein (C. C.), E. Simon 1893 (TMSA: CPH7886); 1♀, 5 May 1965 (TMSA: CPH7884); 1♂, Three Sisters, CP. RSA, 26 Oct 1973, N. J. Duke (TMSA: CPH7887); 1♂, South Africa, Western Cape, Matjiesfontein, 33°13'S, 20°35'E, Purcell leg. (SANC: COLS-12182); 1♂, South Africa W. Cape, Anysberg N. Res. 29 Oct 96, C. Price (BMPC); 1♀, South Africa E. Cape, Nr. Willowmore, 24 Dec 99, R. Perissinotto & L. Clennell (BMPC); 1♀, South Africa, EC, Antoniesberg, 23 Dec 2002, R. Perissinotto & L. Clennell (BMPC); 3♂, 1♀, South Africa, WC, Garcia Pass, 20 Jan 2016; 6♂, 2♀, South Africa, EC, Fullerton, 5 Jan 2017, R. Perissinotto & L. Clennell; 2♂, 2♀, South Africa, EC, Nr. Streytlerville, 18 Jun 2016, R. Perissinotto & L. Clennell; 5♂, 4♀, South Africa, EC, Sarah Baartman District (Dr Beyers Naudé Municipality), 15 km NW of Willowmore, 870 m, 5.I.2017, Malec & Šípek leg. (PMPC, PSPC); 1♂, 1♀, South Africa, Eastern Cape, Willowmore env., 3–4.I.2017, P. Malec & P. Šípek leg. (PSPC, NMCR: XS061RSA\_1); 1♀, South Africa, Eastern Cape, Willowmore env., 3–4.I. 2017, P. Malec & P. Šípek leg., Ex larva bred from wild larvae, P. Malec breeding; unspecified no. of specimens, South Africa (WC), Worcester, Sep 2017 [common in frass accumulations of *Microhodotermes viator* termites, heuweltjies] (Mike Picker, pers. comm.).

***Xiphoscelis namibica* Perissinotto, sp. nov.**

<http://zoobank.org/FA69288D-39FB-44C3-B900-E62AC514097F>

Figs 2, 5

**Diagnosis.** *Xiphoscelis namibica* can best be separated from both *X. schuckardi* and *X. braunsi* by the characteristics of its parameres, as it is the only species among the three to exhibit an apical protuberance on the inner margin of each dorsal lobe (Fig. 5A–C). There are also external morphological characters that can be used in the diagnosis of this species, the most prominent of which are clypeal shape and the size of the metatibial spurs. Unlike in the other two species, in *X. namibica* the anterior margin of the clypeus ranges from being weakly sinuate to straight, while the lateral margins are arcuate like those observed in *X. schuckardi* (Fig. 2D). The metatibial spines and spurs are generally hypertrophic in the genus *Xiphoscelis*, with the internal spine normally exceeding the thickness and length of the spurs by several fold and attaining extreme proportions in males (Perissinotto et al. 2003). In *X. namibica*, however, the metatibial spurs are as long as the inner spine in both sexes and neither of them reaches lengths comparable to those observed in the other two species under comparison (Figs 1–3).

**Description of holotype male.** (Figs 2A–E, 5A–C) **Size.** Length 14.3; width 8.0 mm.

**Body.** Completely black and matte, except for small worn ridges on elytral umbones (Fig. 2A); head and pronotum of normal proportions with respect to abdomen

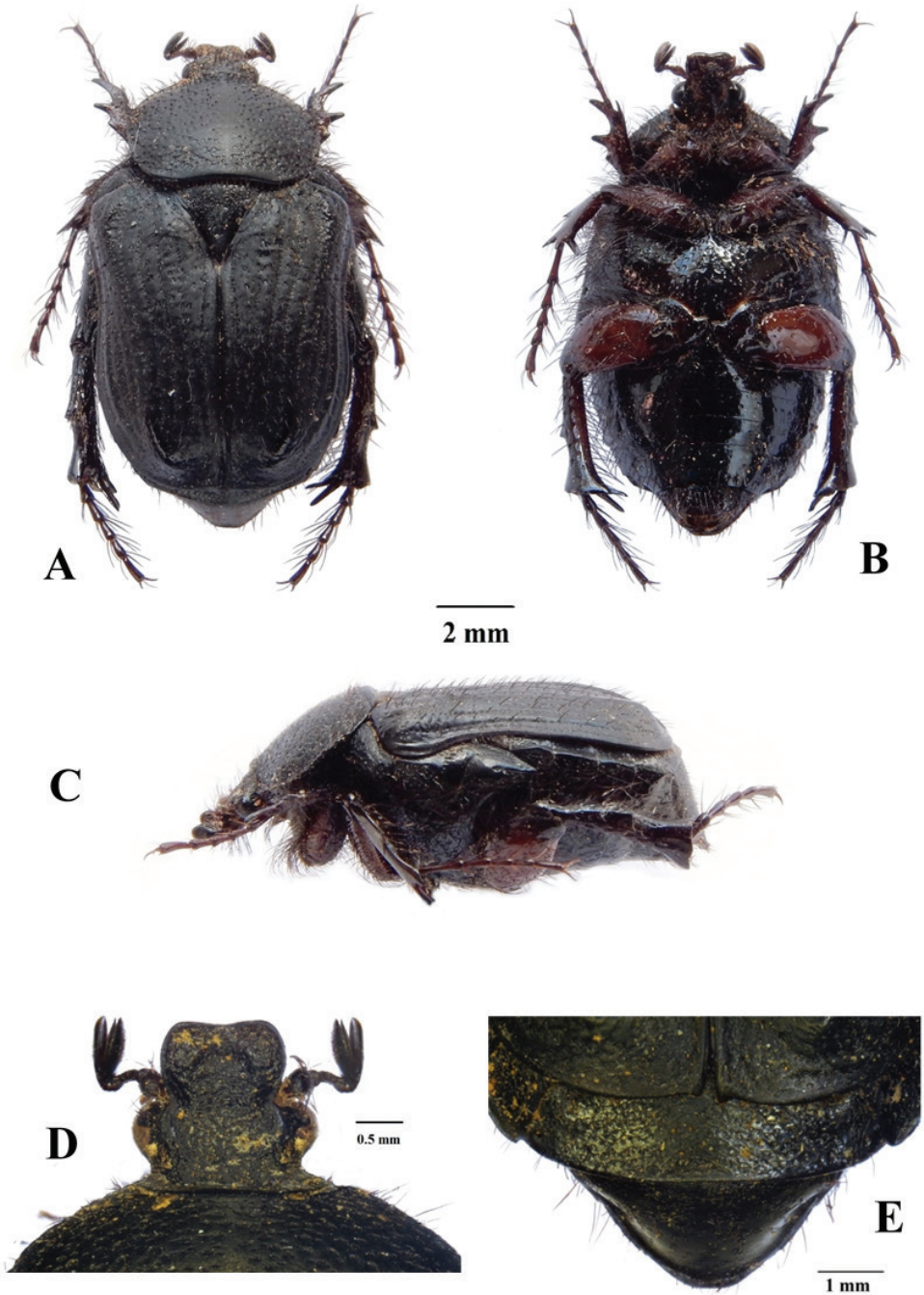


**Figure 2.** *Xiphoscelis namibica* sp. nov., male: dorsal (A), ventral (B) and lateral (C) habitus; clypeus (D) and pygidium (E). Photographs by Lynette Clennell.

size; metacoxa, abdominal sternites and pygidium moderately protruding outside elytral margins; with scattered and shallow sculpture throughout dorsal surface associated with short to medium dark setae, becoming longer and denser on antero-lateral margins (mostly fallen or broken due to specimen being retrieved from the field sometime after death, Fig. 2A, C, D).

**Head.** Entirely black, with coarsely round sculpture throughout surface; ultrafine rugosity across entire surface; long, erect black setae on eye canthus and antennal pedicel; clypeus weakly bilobate but deeply concave, with both anterior and lateral margins equally elevated, lateral margins smoothly rounded all around; antennal clubs, flagellum and pedicel black and of normal cetoniine length; pedicel becoming lighter and brown towards base.

**Pronotum.** Black and matte; regularly round in shape, except at antero-lateral margins, where sharp angles lead to medio-apical, moderately elevated transversal protuberance; posterior margin forming perfectly straight line in front of scutellum; round punctures regularly spaced across surface, but becoming more scattered on disc and denser at margins and on lateral declivities; thick, black, setae of medium length visible only on lateral margins (Fig. 2 A, C).

**Scutellum.** Completely black; isoscelic triangular with weakly rounded apex and lateral grooves absent on basal third but well developed along other two-thirds towards apex; with dense but irregularly shaped punctures on basal and baso-lateral margins, but absent on central part of disc and on apical third; few, thick and black erect setae scattered across basal third of surface (Fig. 2A).

**Elytron.** Completely black and matte, narrower than abdomen leaving apical projection of sternites and pygidium partly exposed; subhumeral arch very low and postero-apical declivity extremely steep and abrupt; all costae subequally and weakly elevated, with 5<sup>th</sup> and 6<sup>th</sup> costae and umbones raised; surface densely sculptured with geminate striae or round to irregular punctures along intercostal spaces, becoming very sparse and occasional on surface of costae; sparse short, but thick and erect black setae across whole surface, except umbones; apex with short but distinct spinal projection (Fig. 2A, B).

**Pygidium.** Completely black, narrow and broadly triangular in shape, with basal and lateral margins sharply upturned; with uniformly sparse horse-shoe sculpture across surface; convex with small baso-lateral depressions; without pubescence on general surface but with lining of black, long setae along lateral and apical margins (Fig. 2E).

**Legs.** All legs black in dorsal view, with tarsal segments elongate, but tibiae of normal cetoniine thickness and length; protibia tridentate, with proximal tooth reduced and other two teeth severely worn; mesotibia exhibiting mid outer spine, two apical spines and two spurs of small to medium size; metatibia with slightly hypertrophic inner spine and spurs, inner spine much thicker but shorter than spurs (Fig. 2A–C); femora reddish-brown at base, becoming black distally and at

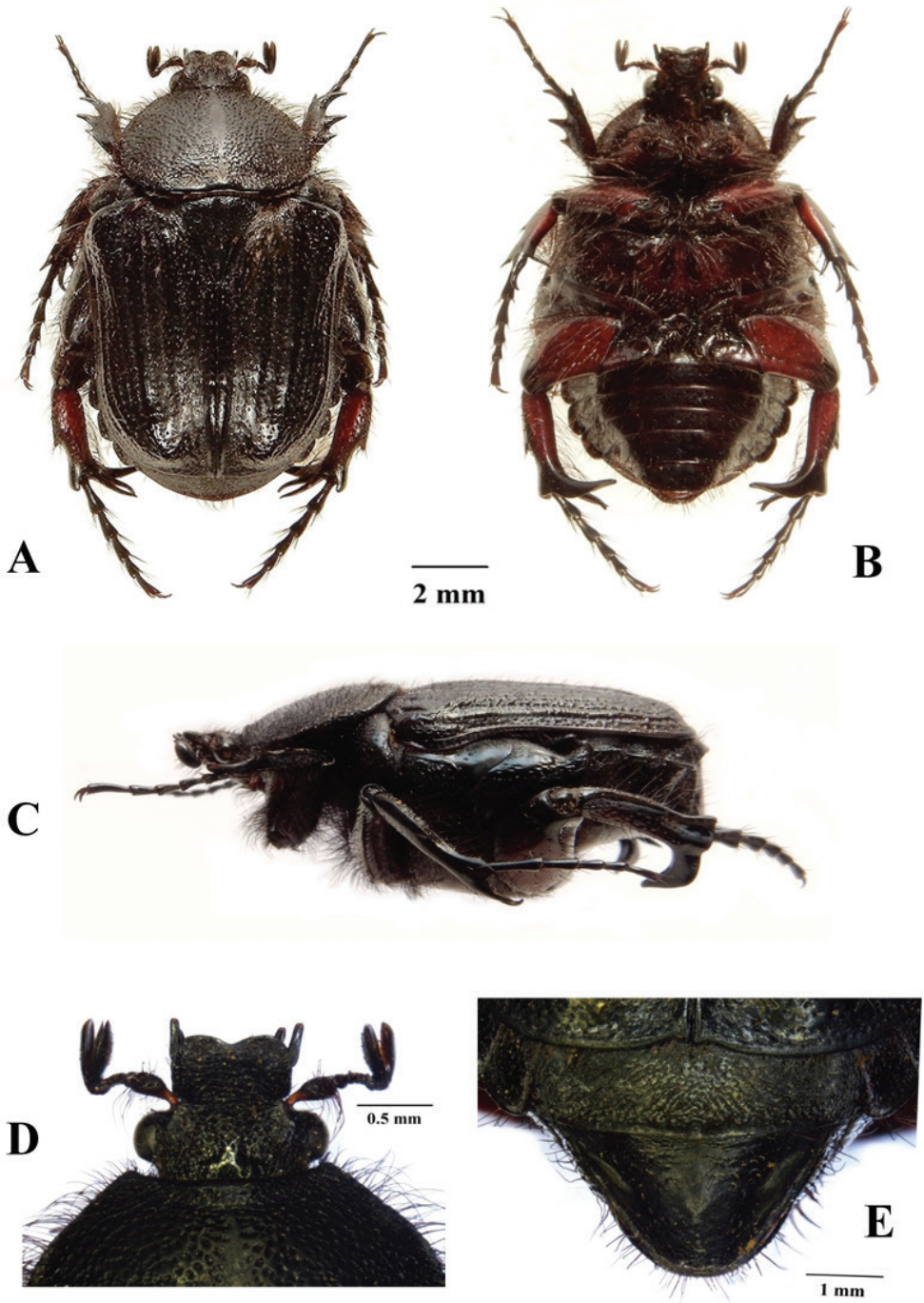


**Figure 3.** *Xiphoscelis schuckardi* Burmeister, 1842, male: dorsal (A), ventral (B) and lateral (C) habitus; clypeus (D) and pygidium (E). Photographs by Lynette Clennell.



**Figure 4.** *Xiphoscelis braunsi* sp. nov. (WC, Garcia Pass): dorsal (A), lateral (B) and frontal (C) views of aedeagus. Photographs by Lynette Clennell.



**Figure 5.** *Xiphoscelis namibica* sp. nov. (NAM, Namuskluft): dorsal (A), lateral (B) and frontal (C) views of aedeagus. Photographs by Lynette Clennell.

joints, bearing long, thin dark setae; pro- and meso-femora of normal size, but metafemora hypertrophic.

**Ventral surface.** Shiny and black, with reddish-brown areas restricted to part of coxae and basal portion of femora; with thin and long dark setae on prosternum, coxae and all femoral margins, becoming shorter and more sparse on other surfaces,



**Figure 6.** *Xiphoscelis schuckardi* Burmeister, 1842 (NC, Wallekraal): dorsal (A), lateral (B) and frontal (C) views of aedeagus. Photographs by Lynette Clennell.

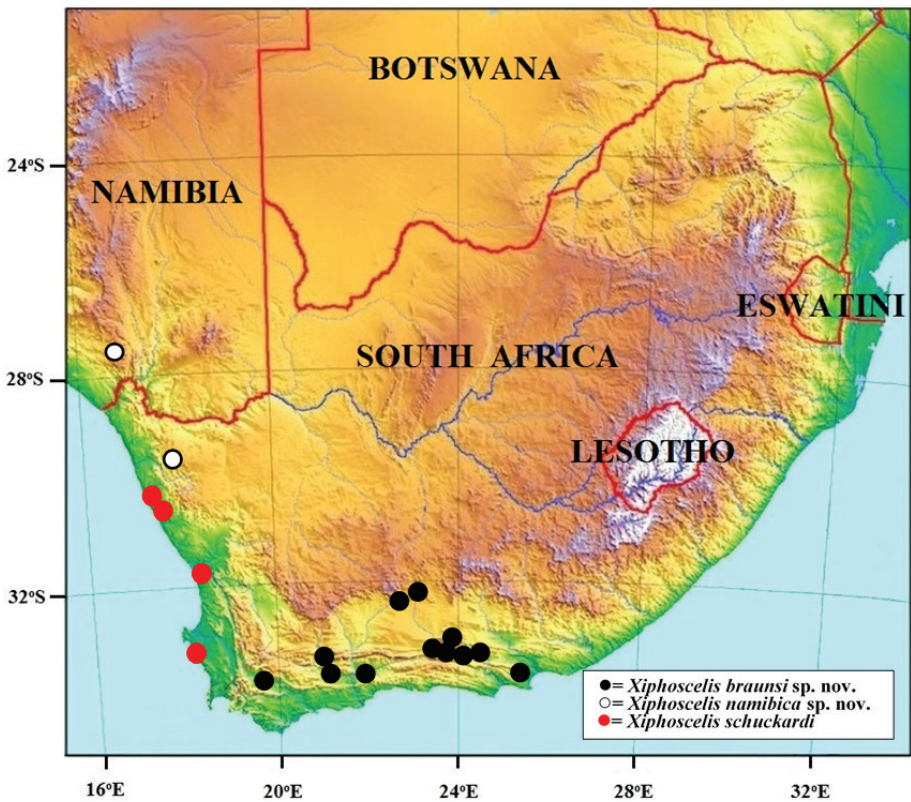


**Figure 7.** Known distribution range of *Xiphoscelis braunsi* sp. nov., *X. namibica* sp. nov. and *X. schuckardi* Burmeister, 1842 within southern Africa (Adapted from Mapsland: Copyright© 2019 Mapsland).



**Figure 8.** Reddish-brown female specimen of *Xiphoscelis braunsi* sp. nov. in its natural habitat at WilLOWmore, Dec 2005. Photograph by Lynette Clennell.

particularly abdominal sternites; all setae emerging at centre of small and round sculptures; mesometasternal process extremely small, not protruding forward or upwards and partly covered by coxal bases, black and with scattered round punctures and thin setae on surface; abdominal sternites slightly convex, becoming flat at middle particularly in area of sternites 5–7.

**Aedeagus.** Parameres with dorsal lobes tapering abruptly towards apex, forming steeply elevated apical spine at inner end, covering completely ventral lobes in dorsal view (Fig. 5A); exhibiting long, thin setae along entire apical margin (Fig. 5A–C); apical surface approximately circular in frontal view (Fig. 5C).

**Derivatio nominis.** With the exception of one female from O’Kiep (South Africa), so far, all the specimens known for this species and representing the type series originate from the same locality, in south-western Namibia. Hence the obvious geographic link to its name.

**Description of female.** Unlike with all the other species of the genus, it is virtually impossible to separate the two sexes of *X. namibica* on the basis of external morphology alone. This is because the metatibial internal apical spine and spurs of its male



**Figure 9.** Black male specimen of *Xiphoscelis braunsi* sp. nov. in its natural habitat at Worcester, Sep 2017. Photograph by Mike Picker.

(Fig. 2A–C) are just as poorly developed as those of the female: a truly unique situation within this genus, with essentially no detectable sexual dimorphism. The only characters where some difference can be observed with a well-trained eye are the relatively shorter protibial and protarsi of the female versus those of the male counterpart, as well as the slight concavity of the abdominal sternites in the male.

**Distribution.** So far, the few specimens known for this species have been collected mostly in south-western Namibia, near the town of Rosh Pinah, in the Namuskluft area at about 1200 m asl (Fig. 7). One female specimen is also known from O’Kiep, in the South African Northern Cape. Thus, the species appears to be an arid mountain specialist, possibly occurring throughout the Ai-Ais Huns Mountains, the Richtersveld range and nearby areas above the Great Escarpment.

**Biology.** The holotype and paratype series collected by Holm & Gebhardt in southern Namibia were all retrieved dead from middens of the southern harvester termite *Microhodothermes viator*. Given the very limited number of observations available for this species, it is not possible to establish whether or not this is a case of obligatory association, or again a rather opportunistic one.

**Type material. Holotype** (♂): Namibia, Namuskluft, 1200 m, 27°45’S, 16°53’E, 2–6 Apr 2002, in *Microhodothermes viator* middens, E. Holm & H. Gebhardt (ISAM). **Paratypes:** 3 ♂, 2 ♀, same data as holotype (BMPC); 1 ♀, South Africa, Northern Cape, O’Kiep 29°35’S, 17°52’E, 1885-11-10, L. Péringuey leg. (SANC-COLS-12181).



**Figure 10.** Male specimen of *Xiphoscelis lenxuba* Perissinotto, Villet & Stobbia, 2003 in its natural habitat in the Winterberg, Dec 2016. Photograph by Lynette Clennell.



**Figure 11.** Male specimen of *Xiphoscelis sneeubergensis* Perissinotto, Villet & Stobbia, 2003 in its natural habitat in the Compassberg, Jan 2017. Photograph by Lynette Clennell.

### Updated identification key to the species of *Xiphoscelis* Burmeister, 1842

- 1 Dorsal habitus completely black and shiny; elytral costae markedly elevated and visible; general dorsal sculpture dense and deep; body length 14–22 mm, larger than all other species; distribution: west coast lowlands of Western and Northern Cape ..... ***X. shuckardi* Burmeister, 1842** (Fig. 3)
- Dorsal habitus black or brown and matte or velutinous; elytral costae weakly elevated and dorsal sculpture scattered and shallow; body length 11–16 mm ..... **2**
- 2 Dorsal habitus exhibiting cretaceous markings ..... **3**
- Body without cretaceous markings ..... **4**
- 3 Cretaceous ornamentation extensive on elytral surface, pronotal margins and protruding areas of abdominal sternites; body covered in long, scattered black setae; distribution: high mountains of Eastern Cape Karoo, above Great Escarpment.... ***X. sneebergensis* Perissinotto, Villet & Stobbia, 2003** (Fig. 10)
- Cretaceous markings moderately developed on pronotal margins and occasionally present also on elytra, but very faintly; body velutinous and covered in dense, medium to long golden-brown or orange setae; distribution: eastern areas of Eastern Cape Karoo .....  
..... ***X. lenxuba* Perissinotto, Villet & Stobbia, 2003** (Fig. 11)
- 4 Dorsal habitus completely black and matte; metatibial internal apical spine as long as spurs in both sexes; anterior clypeal margin weakly sinuate to straight; distribution: south-western Namibia and adjacent areas of Northern Cape ...  
..... ***X. namibica* Perissinotto, sp. nov.** (Fig. 2)
- Dorsal habitus black or brown to reddish-brown; metatibial spurs and particularly inner apical spine hypertrophic in male; anterior clypeal margin strongly sinuate; distribution: Cape Fold Belt of the Western and Eastern Cape provinces ..... ***X. braunsi* Perissinotto & Šípek, sp. nov.** (Figs 1, 8, 9)

### Larval morphology

#### Description of third instar larva of *X. braunsi* sp. nov.

Figs 12–14

**Differential diagnosis.** The larvae of *Xiphoscelis braunsi* sp. nov. are characterised by the following characters: long and prolific chaetotaxy on cranium; frons with 2–3 posterior frontal setae, anterior and lateral frontal setae long; epipharynx with sensorial cone (left nesium) desclerotised, low, obtuse, reduced and plate-shaped; mandibles with an external tooth on lateral margin; lacinial unci unequally fused at their base, smaller uncus about three times shorter than the longer one; hypopharyngeal scleroma without trun-

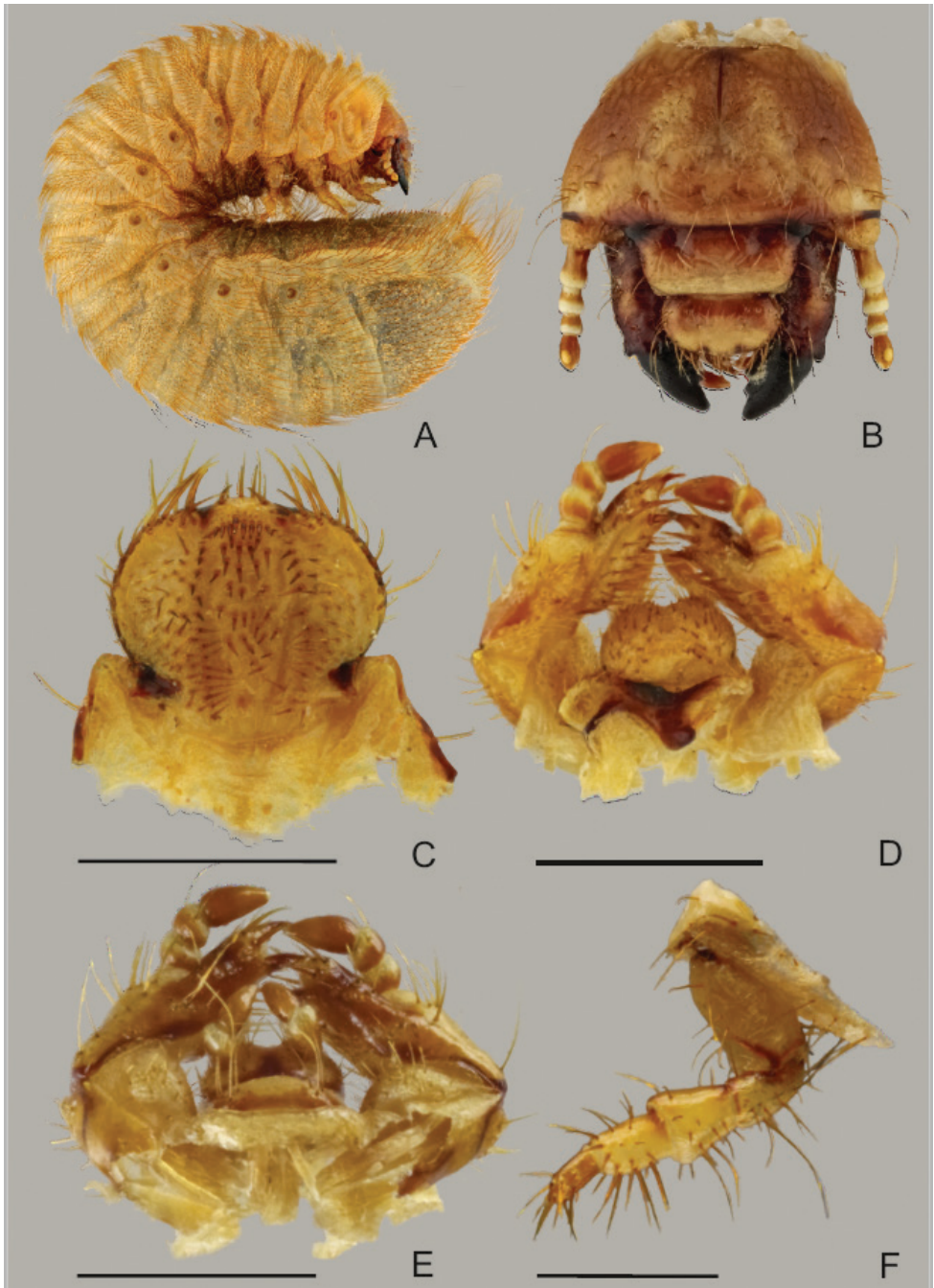


**Figure 12.** Last instar larva of *Xiphoscelis braunsi* sp. nov.: habitus (A), head capsule (B), epipharynx (C), maxillo-labial complex, dorsal view (D); maxillo-labial complex, ventral view (E), right metathoracic leg, anterior view (F). Scale bars: 1 mm.

cate process; pretarsi cylindrical with 11–12 setae, raster composed of 2 slightly sub-parallel rows of 14–20 pali, septula open posteriorly, narrow subtriangular to elliptical.

Larvae of *X. braunsi* sp. nov. differ from all known larvae of Cetoniinae *sensu stricto* by the absence of the hypopharyngeal truncate process. From those of *Meridioclita capensis* and *Heteroclita haworth* larvae of *X. braunsi* sp. nov. differ by the absence of the minute tip on the cylindrical pretarsi. Also, they can be separated from those of *Ichnestoma rostrata* by their only slightly emarginate frontal suture, by the trapezoidal clypeus and by the number of posterior frontal setae.

**Material studied.** Eight last instar larvae: EC, Sarah Baartman District (Dr Beyers Naudé Municipality), 15 km NW of Willowmore, 870 m, 5.I.2017. Fifteen larvae were collected in soil with organic debris under a shrub of *Psilocaulon* sp. (Mesembryanthemaceae), where also adult specimens were found together with larvae. No termites or ants were observed in the vicinity of the shrub. The identity of the larvae has been confirmed by rearing the remaining specimens to adulthood and by molecular match (COI) with adult specimens.

**General body.** Scarabaeiform (Fig. 12A); maximum length 30–35 mm; cranium yellowish-brown to brown, glabrous; body whitish with creamy shades; abdominal segments IX and X fused dorsally, ventrally separated by incomplete groove.

**Head capsule** (Fig. 12B). Maximum width 2.7–3.1 mm; surface of cranium shiny and glabrous, exhibiting sparse microsculpture with few irregular crooked lines; cranium yellowish-brown to brown; antennifer, postclypeus, posterior half of labrum and frontoclypeal border dark brown; mandibles brown with black apices and central pale-brown area; cranial chaetotaxy as summarized in Table 1; setae generally abundant, with groups of posterior, lateral and dorsoepicranial setae almost fused; lateral epicranial setation with numerous medium and short setae and one prominent anterior long seta; frontal sutures lyriform or slightly bisinuate; epicranial insertions of antennal muscles almost indistinct; anterior and lateral frontal setae long; clypeus trapezoidal to subrectangular, anteclypeal area narrow (less than  $\frac{1}{4}$  of entire clypeal area); postclypeus with one anterior and one pair of long lateral clypeal setae; stemmata present.

**Antennae** (Fig. 12B). Tetramerous (an I–IV), relative length of antennomeres: an I > an IV > an II > an III; first antennomere (an I) about length of an II and an III combined; antennomere III with ventral, apical projection exhibiting single sensory spot; last antennomere (an IV) with one dorsal, three ventral sensory spots and one single round, apical sensory field.

**Labrum** (Fig. 12B). Symmetrical, anterior margin trilobed with numerous setae; clithra present; dorsal surface of central part with two prominent setae on each side (one near labrum centre and one on lateral margin); posterior part of labrum with 1–3 medium sized setae on each side.

**Epipharynx** (Figs 12C, 13A). Haptomerum exhibiting convex zygum with transverse, broadly arcuate row of approximately 8–9 stout setae and another 1–2 rows of 2–4 stout and prominent setae posteriorly to main row; anterior portion of zygum with approximately 5–6 campaniform sensilla; haptomeral process and proplegmata absent; acroparia with medial labral lobe about half the size of lateral lobes; margin of medial

**Table 1.** Cranial chaetotaxy of the larva of *Xiphoscelis braunsi* sp. nov. Abbreviations: AAS = setae of anterior frontal angle; ACS = anterior clypeal setae; AES = anterior epicranial setae; AFS = anterior frontal setae; DES = dorsoepicranial setae; LCS = lateral clypeal setae; LES = lateral epicranial setae; LFS = lateral frontal setae; PES = posterior epicranial setae; PFS = posterior frontal setae.

Group of setae	Epicranium			Frons			Clypeus			
	DES	PES	AES	LES	PFS	LFS	AFS	AAS	ACS	LCS
Long/medium setae	5–9	1–5	1	9–15	2–30	1	1	1	1	2
Minute/short setae	13–23	3	–	3–6	–	–	–	–	–	–

labral lobe with 8 setae; lateral labral lobes with 8–10 setae; acanthoparia with 6–8 spine-like to hair-like setae, increasing in size from basal to apical part of acanthoparia; plegmata absent; chaetoparia asymmetric, right chaetoparia with 50–57 setae in total, left with 41–47 setae; chaetoparia with prominent row of 14–15 long and stout setae on each side; several more or less irregular rows of slender hair-like setae towards exterior margin of epipharynx; pedium covered with numerous irregular short but stout setae; gymnoparia absent; dextortorma subtriangular, short; right pternotorma absent or heavily reduced; laeotorma short and narrow; left pternotorma triangular and large; haptolachus with sensorial cone (left nesium) desclerotised, low and obtuse with four pores, but lacking sclerotized plate (right nesium); plate-shaped sclerite, phoba and crepis absent.

**Mandibles** (Fig. 13B–F). Asymmetrical, elongate and narrow, scissorial area about same length as molar area; scrobis with 9–13 setae, longitudinal furrow absent; external mandibular margin with prominent tooth-like projection in apical half; antero-lateral portion of dorsal mandibular surface with two prominent setae and 1–4 dorsomolar setae concealed in single rim on both mandibles; ventral surface with 4–5 ventromolar setae; stridulatory area with 27–32 transversal, uneven ridges; distance between distal ridges about twice as large as between proximal ones; left mandible with four scissorial teeth; second, third and fourth teeth of left mandible obtuse; right mandible with three well-developed scissorial teeth; distal molar lobe of left mandible oblique, dorsal end pointing strongly towards base of mandible; posterior margin of right mandibular calyx bilobed in medial view, both lobes subtriangular; dorsal lobe about twice as large as ventral; calyx of left mandible flattened medially, lateral borders emarginate, posterior margin convex; brustia with 3–4 setae on both mandibles.

**Maxilla** (Figs 12D–E, 15C–D). Dorsal surface of cardo with 9–12 setae, labacoparia with 16–24 setae; dorsomedial surface of stipes with 18–25 more or less slender hair-like setae, oblique row of 3–6 spine-like stridulatory teeth and anterior truncate process (blunt tubercle); postero-lateral part of stipes with 7–8 prominent long setae; ventral surface of stipes and mala brownish, setae prominent and mostly in desclerotised field; approximately 20 setae present on ventral surface of labacoparia; galea and lacinia entirely fused forming mala, galeo-lacinial suture indistinct, entirely absent on ventral surface; galear portion of mala with single falcate uncus and 5 long and stout hair-like setae in longitudinal rows, and 4 slender and shorter setae; lacinia with 15–20 long hair-like setae and two unequal unci fused at their base, smaller uncus

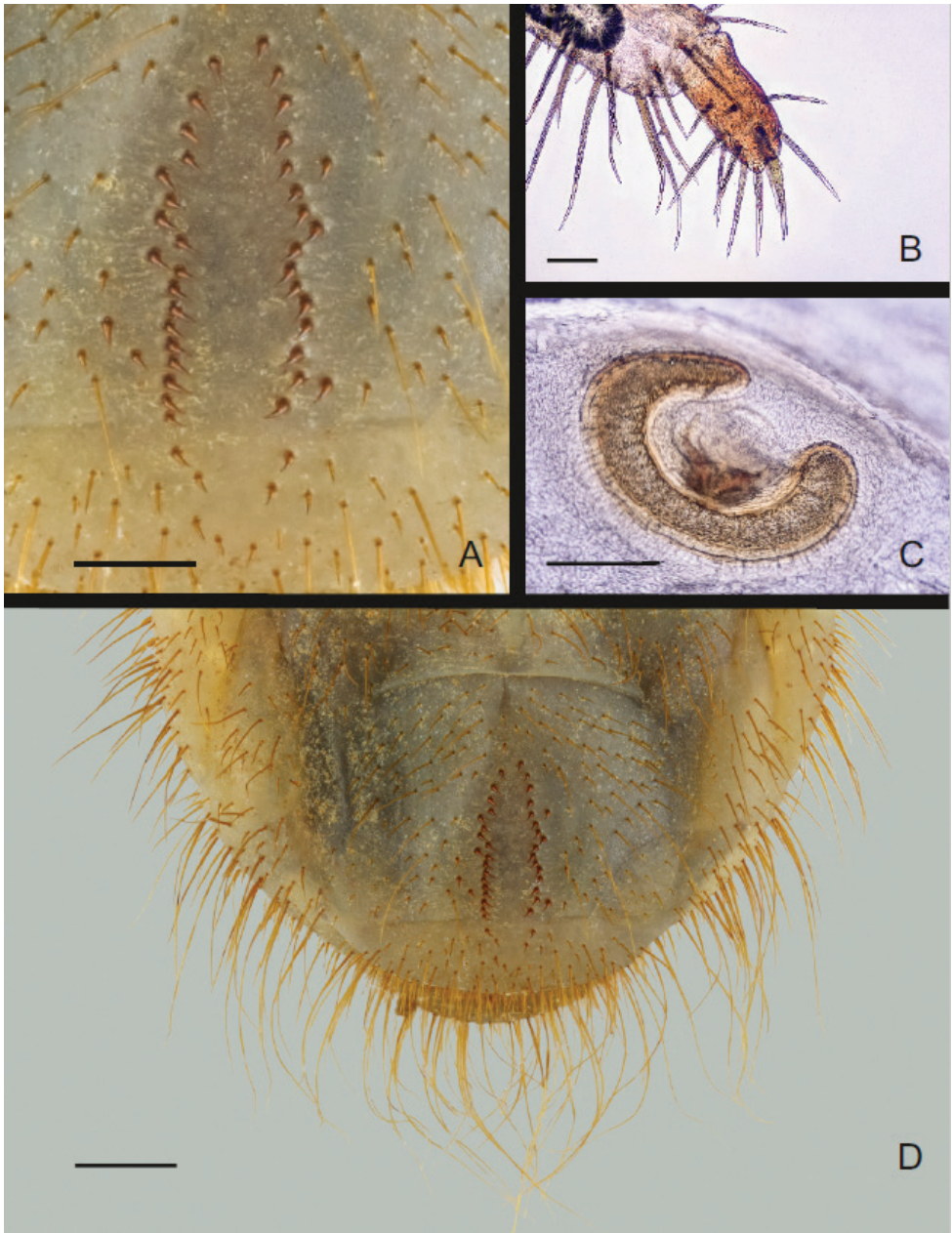


**Figure 13.** Last instar larva of *Xiphoscelis braunsi* sp. nov.: details of raster (**A**), right metapretarsus (**B**), thoracic spiracle (**C**) and general view of raster (**D**). Scale bars: 0.5 mm (**A**); 0.1 mm (**B, C**); 1 mm (**D**).

about  $\frac{1}{4}$  the length of the larger one; maxillary palps tetramerous, penultimate palpomere bearing two setae.

**Hypopharyngeal sclerome** (Figs 12C, 15A). Asymmetrical, narrow; truncate process rudimental or absent; left lateral lobe with irregular arcuate row of 5–8 prominent

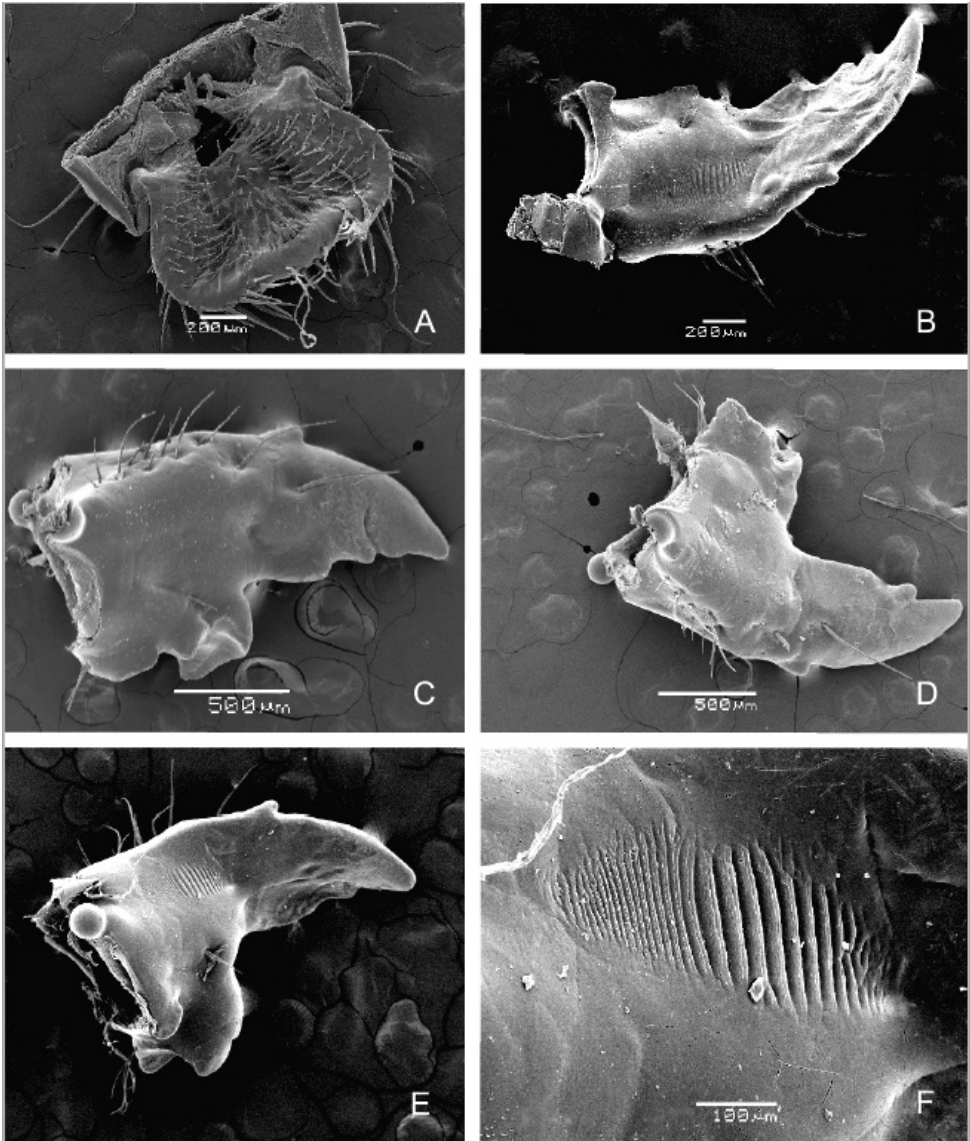


**Figure 14.** Last instar larva of *Xiphoscelis braunsi* sp. nov., SEM images: epipharynx (A); left mandible, ventral view (B); left mandible, dorsal view (C); right mandible, dorsal view (D); right mandible, ventral view (E); right mandible, ventral view - detail of stridulatory area (F).

setae, also two large setae proximal to right part of mesolateral margin of hypopharyngeal sclerome (remark: this structure is usually referred to as “tufts of tegumentary expansions” or “phoba”; however the SEM image shows a clear rim around each seta, Fig. 15A); both lateral lobes only feebly sclerotized with approximately 5–12 setae.

**Ligula** (Figs 12C, 15B). Dorsal surface with approximately 40 prominent setae, medial and proximal setae stout, almost conical, but setae on distal part and on lateral margin long and hair-like; base of ligula with proximal arcuate or transverse row of

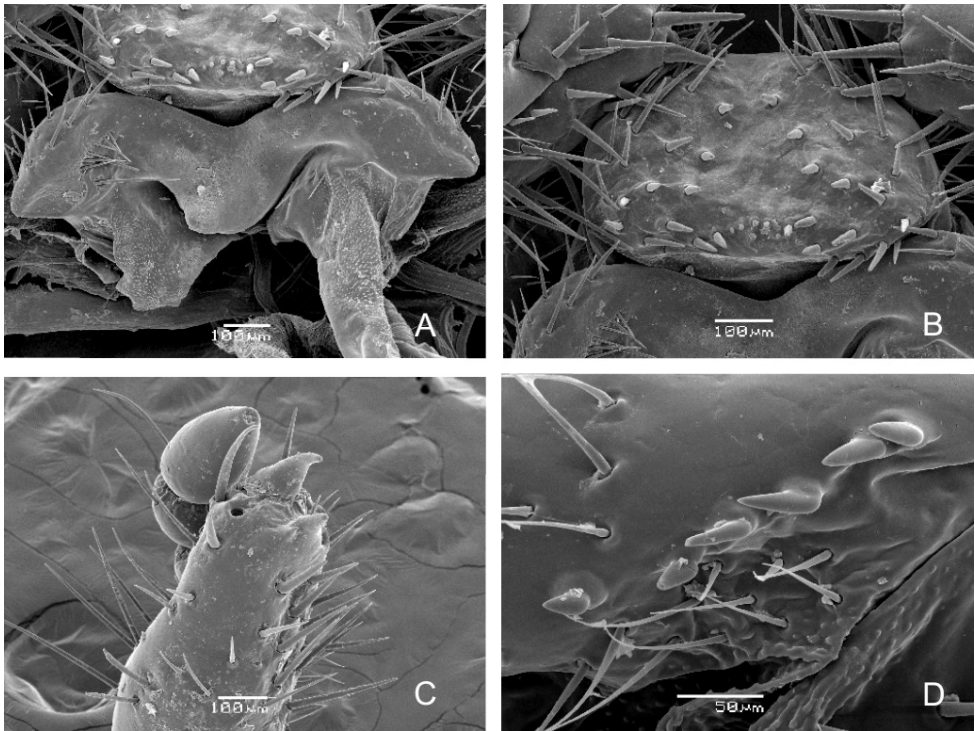


**Figure 15.** Last instar larva of *Xiphoscelis braunsi* sp. nov., SEM images: hypopharynx (A); ligula (B); mala with galear and lacinial unci (C); maxillar stridulatory teeth (D).

approximately 8–10 campaniform setae; labial palpi bimerous; proximal sclerite of prementum with 4 long, prominent setae on each side.

**Thorax** (Fig. 12A). Prothorax with single dorsal lobe, meso- and metathorax with three well-developed lobes; dorsi of each thoracic sublobe almost entirely covered with dense yellowish-brown setae, organized in approximately 3–6 rows; anterior rows with short setae, posterior row(s) with setae 3–5× longer; prothoracic sclerite well sclerotized, covering almost completely lateral portion of prothorax, bordered by dense line of setae; thoracic spiracle (Fig. 13C) with C-shaped respiratory plate; lobes of respiratory plate well separated with distance between lobes almost twice as large as maximum diameter of respiratory plate; respiratory plate with approximately 10–15 holes across diameter; bula with obtuse tubercle; all pairs of legs (Figs 12F) subequal in shape and size; pretarsi (Fig. 13B) cylindrical with 11–12 setae, claw absent.

**Abdomen** (Figs 12A, 13A, D). Nine-segmented; dorsum of abdominal segments I–VI with 3 sublobes, segments VII and VIII with only 2; each sublobe bearing 3–4 rows of setae; setation of abdominal segments I–VIII similar to that of thorax; abdominal spiracles similar to mesothoracic spiracle, all spiracles subequal in size, bula with obtuse tubercle; dorsum of last abdominal segment (segments IX and X fused) evenly covered by dense medium and long setae; anal slit transverse.

**Raster** (Fig. 13A, D). Palidium monostichous, with few irregular pali occasionally scattered around main row; raster composed of 2 slightly subparallel rows of 14–20 pali; pali with distal end dorsoventrally flattened distally, with pointed apices; septula open posteriorly, narrow subtriangular to elliptical, about 3 times longer than wide; tegilla sparsely setose but covering almost completely ventral surface of last abdominal segment; setae of tegilla and medium/long slender hair-like setae interspersed with few hamate setae and several long setae.

## Discussion

Apart from a number of characters that have led to believe that the genus *Xiphoscelis* may occupy a very primitive position in the phylogenesis of the Cetoniinae, species of the genus also exhibit a most unusual feature, represented by the extreme hypertrophy of structures in their metalegs. This is very prominent in males but less so in females and includes the femora, spurs and especially the inner spines, which are truly extraordinary in their thickness, length and sharpness in virtually all the species of the genus, possibly with the exception of *X. namibica* sp. nov. (Fig. 2 A–C).

Males of the largest species, *X. schuckardi* (Fig. 3 A–C), can inflict painful although superficial punctures on the skin of collectors when handled, by pushing through their metatibial inner spines with remarkable strength. This action generally escalates when gripping pressure is applied on their body (RP pers. obs, JB Ball & AP Marais pers. comm.). Such behaviour suggests a possible defence function for this apparatus, which may be used quite effectively against the various ground predators that occur in their natural habitat, such as lizards, agamas, geckos, frogs and toads as well as birds. Apart from this defence function, both inner spines and spurs are also involved in reproduction, as males have been observed exerting enhanced grip on females during mating using this apparatus (RP pers. obs.).

As reported earlier, all species of the genus are restricted to the south-western arid and semi-arid regions of southern Africa (Holm and Marais 1992, Perissinotto et al. 2003). The two species described in a previous revision by Perissinotto et al. (2003), *X. lenxuba* (Fig. 10) and *X. sneebergensis* (Fig. 11), seem to inhabit exclusively the mountainous region of the eastern Karoo, with the first occurring from the upper reaches of the Great Fish River Valley to the interior of the Winterberg range at altitudes < 1000 m, in the Albany Thicket Biome. On the other hand, *X. sneebergensis* is found at altitudes of 1500–2000 m asl in the Sneeberg and Bamboesberg ranges (Perissinotto et al. 2003, RP pers. obs.), in the upper bioregion of the Nama-Karoo Biome (Mucina and Rutherford 2006).

Following the description of the two new species here, it is evident that *X. schuckardi* is restricted to the lowlands of the South African west coast, from just north of Cape Town to the Namaqualand area of the Northern Cape (Fig. 7). The typical vegetation biome here can be classified as ranging from Fynbos of the Western Strandveld type to Succulent Karoo of the Namaqualand Sandveld type (Mucina

and Rutherford 2006). *Xiphoscelis braunsi* sp. nov. appears to be distributed across the entire belt of the Cape Fold Mountains, but at altitudes generally not exceeding 1000 m asl, in a wide variety of bioregions within the Succulent Karoo or Fynbos biomes. *Xiphoscelis namibica* sp. nov. inhabits the arid region of the Huns Mountains in Namibia and nearby ranges in the Northern Cape Province of South Africa, possibly including the Richtersveld (Fig. 7), in the Desert to Succulent Karoo biomes (Mucina and Rutherford 2006).

The frequently reported association with the termite *Microhodothermes viator* (Péringuey 1907, Holm and Marais 1992, Holm and Stobbia 1995), appears to apply only to the three species previously grouped under *X. schuckardi* (Perissinotto et al. 2003). However, at least for *X. braunsi* sp. nov. (Figs 1, 8, 9) this is not an obligatory association, as on several occasions both larvae and adults were found in detrital accumulations of non-termite origin, including leaf litter and aardvark dung (RP pers. obs.). Thus, larvae of this species (and possibly others in the genus) may actually exploit a suite of food sources as part of an opportunistic strategy aimed at utilising any accumulation of decomposing matter in their dry and resource-scarce habitats.

The Xiphoscelidini, or more accurately Xiphoscelidina (refer to Šípek and Král 2012 for further details), have been traditionally regarded as one of the most “primitive” or “basal” group of the Cetoniinae. Holm and Marais (1992) considered the genus *Xiphoscelis* as the “*Archaeopteryx*” among the fruit chafers. However, as pointed out previously, evidence in support of the Xiphoscelidina as an early clade in the cetoniine phylogeny has not been provided yet through any unambiguous morphological character. The latest molecular phylogenetic analysis of the Cetoniinae (Šípek et al. 2016) has questioned the classical interpretation of cetoniine phylogeny, suggesting a para- or polyphyletic structure for most of the tribes. At the same time, it has brought more insight into the intricate relationships within this group. In this analysis, the representatives of the tribes Osmodermatini, Taenioderini and Schizorhinini were identified as basal Cetoniinae “*sensu stricto*”. In other words, these groups have been identified as sister clades to the remaining clades, with the exception of the Trichiini and Valgini. Unfortunately, none of the putative representatives of Xiphoscelidina was present in the dataset.

Based on the description of the larval morphology of *X. braunsi*, we can conclude that the larvae of the genus *Xiphoscelis* are characterised by a remarkable subset of morphological characters: i.e., long and dense chaetotaxy of cranium; reduction of sense cone and plate-shaped sclerite of epipharynx; presence of an external tooth on lateral mandibular margin; shape and size of lacinial unci; shape of hypopharyngeal scleroma (especially the reduction of the truncate process); and shape of pretarsi. To allow an easy comparison of the morphological similarities of *Xiphoscelis* with other Cetoniinae larvae, a parsimony analysis of the larval morphology of 13 cetoniine genera, including *Xiphoscelis*, was performed (Fig. 16). *Osmoderma barnabita* Motschulsky, 1845 was used as an outgroup to root the tree and representatives of the tribes Cetoniini, Goliathini, Taenioderini were included in the analysis along with representatives of

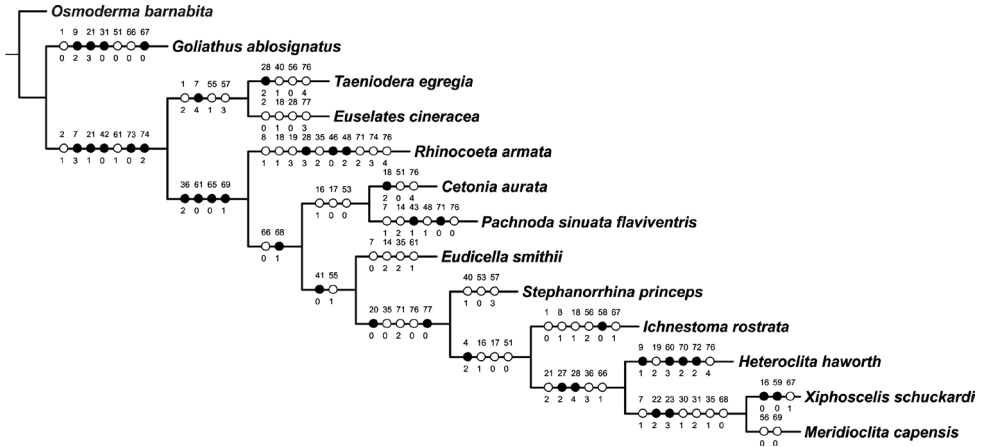


**Figure 16.** Strict consensus topology of 13 representatives of the Cetoniinae, based on a larval morphology dataset. Character states are marked on clades, with character number above each circle and state number below it; black circles indicate unique evolutionary events, while white circles denote reversals or parallelisms. Partitioned Bremer Support (PBS) values above 50% are indicated. The analysis was performed in order to highlight morphological similarities among representatives of distinct cetoniine clades.

other “enigmatic” genera from the southern part of Africa, such as *Rhinocoeta cornuta* (Fabricius, 1781), *Meridioclita capensis* Krikken, 1982 and *Heteroclita haworth* (Gory & Percheron, 1833).

The outcome shows that the larva of *X. braunsi* sp. nov. falls within a clade shared with *M. capensis* and *H. haworth* (Fig. 16). This clade is supported by the following key synapomorphies: 1) presence of long posterior frontal setae; and 2) absence of plate-shaped sclerite. *Meridioclita capensis* is identified as the sister species of *X. braunsi*, based on the prolific cranial chaetotaxy and the absence or wide reduction of right pretnotorma and laetotorma. *Ichnestoma rostrata* Janson, 1878 is identified as a sister species to the clade comprised of all the above-mentioned species based on cranial chaetotaxy, number of dorsal and ventral sensory spots on antenna and presence of a conspicuous outer tooth on lateral mandibular margin. These results question the hypothetical “basal” placement of *Xiphoscelis* among the Cetoniinae (e.g., Holm and Marais 1992, Perissinotto et al. 2003).

In the early taxonomic classifications of the Cetoniinae, the genera *Xiphoscelis*, *Ichnestoma*, *Heteroclita* and *Meridioclita* were all classified under the Xiphoscelidini (e.g., Burmeister 1842, Schenkling 1921). However, at least some of the alleged larval apomorphies may indeed represent the result of convergent evolution forced by the arid and seasonal conditions of their habitat as well as the soil-dwelling habits of their larvae. Unfortunately, the recent attempt by Kouklík (2017) to resolve the phylogenetic placement of *Xiphoscelis* and other Xiphoscelidini genera on the basis of molecular DNA analysis has generated contradictory results. More efforts are, therefore, needed in order to unravel the true phylogenetic relationships within this clade.

## Acknowledgements

The following museum curators, researchers and owners of private collections are thanked for kindly providing photos, data and material for analysis: Riaan Stals & Werner Strumpher (SANC), Ruth Müller (TMSA), Karla Schneider (MLUH), Giulio Cuccodoro (MHNG), Aisha Mayekiso (ISAM), Max Barclay (BMNH), Alain Drumont (ISNB), Dominik Vondráček (UKCR, NMCR), Jonathan Ball & Andre Marais (BMPC), Gerhard Beinhundner (GBPC), Thierry Garnier (TGPC), Petr Malec (PMPC), Mike Picker (UCTC) and Sébastien Rojkoff (SRPC). Dominik Vondráček and Ondřej Kouklík (UKCR) kindly allowed the use of some of their unpublished data in this manuscript. Thanks also to Lynette Clennell for preparing photos and illustrations included in this work. The Nelson Mandela University (Port Elizabeth, South Africa) is thanked for providing facilities and funding towards the completion of his work. Petr Šípek was financially supported by the Charles University Research Centre programme No. 204069 (Prague, Czech Republic). The Northern Cape Department of Environment and Nature Conservation, Cape Nature (Western Cape) and the Eastern Cape Department of Economic Development, Environmental Affairs and Tourism are thanked for providing permits and logistical assistance towards specimen and data collections.

## References

- Beinhundner G (2017) The Cetoniinae of Africa. Gerhard Beinhundner, Euerbach, 1199 pp.
- Bourgoin A (1920) Description d'un genre nouveau et d'une espèce nouvelle de Cétoine provenant des récoltes de Rohan-Chabot dans l'Afrique Australe. Bulletin du Muséum national d'Histoire naturelle 26(7): 627–628. <https://doi.org/10.5962/bhl.part.1211>
- Böving AG (1936) Description of the larva of *Plectris aliena* Chapin and explanation of new terms applied to the epipharynx and raster. Proceedings of the Entomological Society of Washington 38: 169–185.
- Burmeister H (1842) Handbuch der Entomologie 3, T.E.F. Enslin, Berlin, 830 pp.
- Fabricius C (1781) Species Insectorum exhibentes eorum differentias specificas, synonyma, auctorum, loca natalia, metamorphosia, adiectis observationibus, descriptionibus. CE Bohnii, Hamburg, 552 pp. <https://doi.org/10.5962/bhl.title.36509>
- Felsenstein J (1985) Confidence limits on phylogenies: an approach using the bootstrap. Evolution 39: 783–791. <https://doi.org/10.1111/j.1558-5646.1985.tb00420.x>
- Gory H, Percheron A (1833) Monographie des Cétoine set genres voisins, formant, dans les familles naturelles de Latreille, la division des Scarabées méliophiles. Paris: J.-B. Baillière, 302 pp. <https://doi.org/10.5962/bhl.title.8957>
- Holm E, Marais E (1992) Fruit chafers of southern Africa (Scarabaeidae: Cetoniini). Ekogilde, Hartbeespoort (South Africa), 326 pp.
- Holm E, Stobbia P (1995) Fruit Chafers of Southern Africa (*Scarabaeidae: Cetoniinae*). Appendix I. Giornale italiano di Entomologia 7: 289–300.

- Janson OE (1878) Notices of new or little known Cetoniidae No. 4. *Cistula Entomologica* 2(1875–1882): 299–304.
- Lansberge JW van (1886) Scarabaeides, Buprestides et Cerambycides de l’Afrique occidentale, envoyes au Musee de Leyde par MM.Veth et Van der Kellen (Note XIII). Notes from the Leyden Museum 8: 69–120.
- Kouklík O (2017) Larval morphology of Goliathini (Coleoptera: Cetoniinae) and its contribution towards the understanding of the group’s evolution. MSc. thesis, Dept. of Zoology, Charles University, Prague, 86 pp. [in Czech with English abstract]
- Krikken J (1978) Some peculiar Cetoniine beetles from South West Africa. *Zoologische Mededelingen Leyden* 53(24): 263–271.
- Krikken J (1982) Some unusual genera and species from Africa (Coleoptera: Cetoniidae). *Revue de Zoologie Africaine* 96(3): 529–538.
- Krikken J (1984) A new key to the suprageneric taxa in the beetle family Cetoniidae, with annotated lists of the known genera. *Zoologische Verhandelingen Leiden* 210: 3–75.
- Motschulsky Vde (1845) Remarques sur la collection de Coléoptères russes de Victor de Motschulsky. *Bulletin de la Société impériale des naturalistes de Moscou* 18: 1–127.
- Mucina L, Rutherford MC (2006) *The Vegetation of South Africa, Lesotho and Swaziland. Strelitzia 19.* South African National Biodiversity Institute, Pretoria, 807 pp.
- Nixon K C (2002) ‘WinClada, Version 1.0000.’ Published by the author, Ithaca, NY.
- Péringuey L (1907) Descriptive catalogue of the Coleoptera of South Africa (Lucanidae and Scarabaeidae). *Transactions of the South African Philosophical Society* 13: 1– 546. <https://doi.org/10.1080/21560382.1904.9525994>
- Perissinotto R, Villet MH, Stobbia P (2003) Revision of the genus *Xiphoscelis* Burmeister 1842 (Coleoptera Scarabaeidae Cetoniinae), with description of two new species and notes on its phylogeny and ecology. *Tropical Zoology* 16: 63–82. <https://doi.org/10.1080/03946975.2003.10531184>
- Ritcher PO (1966) *White Grubs and their Allies. A Study of North American Scarabaeoid Larvae.* Oregon State Monographs. Studies in Entomology Nr. 4. Oregon State University Press, Corvallis, 219 pp.
- Ruter G (1958). Contribution à l’étude des Cétonides malgaches. *Bulletin de la Société entomologique de France* 62: 30–33.
- Ruter G (1978) Contribution a l’étude des Cetonides. *Bulletin de la Société entomologique de France* 83: 125–137.
- Sakai K, Nagai S (1998) *The Cetoniine Beetles of the World.* Mushi-Sha’s Iconographic Series of Insects, Vol. 3. Mushi-Sha, Tokyo, pp. 421.
- Sawada H (1991) *Morphological and Phylogenetical Study on the Larvae of Pleurostict Lamellicornia in Japan.* Tokyo University of Agriculture Press, Tokyo, 132 pp. [+ 157 plates]
- Schaum H (1849) Observations critiques sur la famille des Lamellicornes mélitophiles (2e Partie). *Annales de la Société entomologique de France* (2)7: 241–295.
- Schenkling S (1921) Scarabaeidae: Cetoniinae. In: Junk W (Ed.), *Coleopterorum Catalogus.* W Junk, Berlin, 72: 1–431. [https://doi.org/10.1007/978-94-011-9697-0\\_1](https://doi.org/10.1007/978-94-011-9697-0_1)
- Šípek P, Fabrizi S, Eberle J, Ahrens D (2016) A molecular phylogeny of rose chafers (Coleoptera: Scarabaeidae: Cetoniinae) reveals a complex and concerted morphological evolu-

tion related to their flight mode. *Molecular Phylogenetics and Evolution* 101: 163–175. <https://doi.org/10.1016/j.ympev.2016.05.012>

Šípek P, Král D (2012) Immature stages of the rose chafers (Coleoptera: Scarabaeidae: Cetoniinae): a historical overview. *Zootaxa* 3323: 1–26. <https://doi.org/10.11646/zootaxa.3323.1.1>

Swofford DL (2002) 'PAUP\*: Phylogenetic Analysis Using Parsimony. Version 4.0b10.' Sinauer, Sunderland, MA.

Vondráček D, Venderová A, Král , Šípek P (2018) Phylogeography and DNA-based species delimitation provide insight into the taxonomy of the polymorphic rose chafer *Protaetia* (*Potosia*) *cuprea* species complex (Coleoptera: Scarabaeidae: Cetoniinae) in the Western Palearctic. *PLOS ONE* 13(2): e0192349. <https://doi.org/10.1371/journal.pone.0192349>

## Appendix I

Character states of the 77 morphological characters used in the analysis of larval similarity of 13 Cetoniinae genera (refer also to Fig. 16).

1. **Color of cranium:** 0 – black to dark brown, 2 – brown, 3 – light brown to yellowish
2. **Surface of cranium:** 0 – smooth or with very fine microsculpture, 1 – light to medium microsculpture, 2 – with coarse microsculpture
3. **Texture of cranial microsculpture:** 0 – more or less pitted, 1 – more or less linear
4. **Chaetotaxy of cranium:** 0 – light (short and/or very sparse setae), 1 – “standard Cetoniinae” type, 2 – dense (setae numerous and/or extraordinary long)
5. **Anterior end of epicranial suture:** 0 – originating at posterior end of frontal sutures, 1 – extending into frons, 2 – irregular, feebly visible
6. **Epicranial suture:** 0 – distinct, 1 – indistinct
7. **Frontal suture:** 0 – straight, 1 – straight, slightly emarginate, 2 – convex, 3 – concave, 4 – bisinuate
8. **Frontal suture:** 0 – distinct, 1 – indistinct
9. **Posterior angle of frontal sutures:** 0 – acute, 1 – right, 2 – obtuse
10. **Widest part of cranium:** 0 – at base of antennae, 1 – at approx. one-third of cranium, 2 – at middle of cranium
11. **Number of antennomeres:** 0 – 3, 1 – 4, 2 – 5
12. **Sensory spot on third antennomere:** 0 – present, 1 – absent
13. **Third antennomere:** 0 – with well-developed ventral and apical projection, 1 – ventroapical projection only feebly developed, 2 – ventroapical projection absent
14. **Stemmata:** 0 – present and pigmented, 1 – present without pigment, 2 – reduced, 3 – absent
15. **Setae on antennomeres:** 0 – present (at least on a single joint), 1 – absent
16. **Number of sensory spots on dorsal side of antenna:** 0 – 1, 1 – 2 or 3, 2 – 4 or more, 3 – 1 or 2 (if both character states 1 and 2 are present)
17. **Number of sensory spots on ventral side of antenna:** 0 – 0 to 3, 1 – 4 and more, 2 – 3 to 5 (if both character states 1 and 2 are present)

18. **Shape of clypeus:** 0 – trapezoidal, 1 – rectangular
19. **Preclypeus:** 0 – about  $\frac{1}{2}$  of area of entire clypeus, 1 – about  $\frac{1}{3}$  of area of entire clypeus, 2 – about  $\frac{1}{4}$  of area of entire clypeus, 3 – less than  $\frac{1}{4}$  of area of entire clypeus
20. **Anterior and lateral frontal setae:** 0 – medium long to long, 1 – minute, 2 – absent
21. **Posterior frontal setae:** 0 – absent or minute, 1 – one medium long to long seta, 2 – 2 or more medium to long setae, 3 – both long and short setae
22. **Number of long lateral epicranial setae:** 0 – absent, 1 – 1 or 2, 2 – 3 or more
23. **Dorso-epicranial setae:** 0 – 1 to 3 medium to long setae together with some minute setae, 1 – only minute setae, 2 – only medium to long setae, 3 – both long and short setae in abundance
24. **Shape of anterior labral margin:** 0 – asymmetric, 1 – slightly convex, 2 – strongly convex, 3 – slightly concave, 4 – trilobed
25. **Shape of sensory cone (second nesium):** 0 – ovoid, 1 – conical, 2 – not applicable
26. **Size of sensory cone (second nesium):** 0 – well developed, 1 – more or less reduced, 2 – absent, indistinct
27. **Size of third nesium (plate-shaped sclerome):** 0 – largely reduced, 1 – feebly sclerotized, reduced, 2 – absent
28. **Shape of third nesium (plate-shaped sclerome):** 0 – transverse, 1 – present on right and in front of sensory cone (shape of upturned and reversed capital letter “L”), 2 – present on left side of sensory cone, 3 – present in front and on both sides of the sensory cone (shape of reversed capital letter “U”), 4 – not applicable
29. **Dexiotorma:** 0 – straight and wide, 1 – bent at inner end, 2 – straight, narrow, 3 – reduced
30. **Right pternotorma:** 0 – present, 1 – absent
31. **Laeotorma:** 0 – present, 1 – reduced, 2 – only feebly developed
32. **Left pternotorma:** 0 – present, 1 – absent
33. **Number of sensilla on haptolachus:** 0 – four, 1 – five, 2 – six or more
34. **Clithra:** 0 – absent, 1 – only single clithrum present, 2 – two clithra present
35. **Setae of acanthoparia:** 0 – directly on lateral margin, with swollen base, 1 – directly on lateral margin, without distinctly swollen base, 2 – away from margin and slightly towards center of epipharynx
36. **Pedium:** 0 – absent, 1 – reaching < 25% of central part of epipharynx, 2 – reaching 25–50% of central part of epipharynx, 3 – reaching 51–75% of central part of epipharynx, 4 – reaching > 75% of central part of epipharynx
37. **Chaetoparia of epipharynx:** 0 – reaching only to level of laeo- and pternotorma, 1 – extending posteriorly behind level of laeo- and pternotorma
38. **Crepis:** 0 – well developed, 1 – reduced, 2 – absent
39. **Zygum:** 0 – flat or transverse, 1 – high and conical, 2 – extending into tylus, 3 – absent
40. **Sensilla of zygum:** 0 – not grouped on projection, 1 – grouped on distinct projection, 2 – intermediate
41. **Number of setae on zygum:** 0 – six, 1 – seven, 2 – eight and more, 3 – intermediate
42. **Transverse row of prominent setae on zygum:** 0 – arcuate, 1 – right angled, 2 – angulate, 3 – not applicable

43. **Setae at inner margin of zygum:** 0 – approximately of same size and shape as setae in prominent row, 1 – different from setae in transverse row, 2 – not applicable, 3 – absent
44. **Setae of chaetoparia:** 0 – all setae of approximately same size and shape, 1 – chaetoparia with several rows of longer and stouter setae
45. **Number of teeth on scissorial area of left mandible:** 0 – two, 1 – three, 2 – four
46. **Last two teeth of left mandible:** 0 – fused, 1 – separated
47. **Number of teeth on scissorial area of right mandible:** 0 – two, 1 – three, 2 – four
48. **Second and third teeth of left mandible (number from the apex):** 0 – separated, 1 – fused, 2 – not applicable
49. **Mandibular teeth:** 0 – in single plain, 1 – second and third tooth oriented dorsoventrally
50. **Dorsomolar setae:** 0 – absent on both mandibles, 1 – absent on left mandible, 2 – present on both mandibles
51. **Tooth on external mandibular margin:** 0 – present, 1 – absent
52. **Ventromolar setae:** 0 – present on both mandibles, 1 – absent on both mandibles
53. **Mandibular shape:** 0 – falcate at least at apex, 1 – more or less straight
54. **Mandibular stridulatory area:** 0 – well developed with transverse ridges on entire area, 1 – developed, ridges only feebly developed, 2 – absent
55. **Shape of stridulatory area:** 0 – oval, 1 – oblong, 2 – intermediate
56. **Number of stridulatory ridges on mandible:** 0 – less than 10, 1 – 10 to 20, 2 – 20 or more, 3 – intermediate
57. **Extent of ventral asperities:** 0 – reaching towards ventral process of mandibles, 1 – not reaching towards ventral process of mandibles, 2 – reaching towards ventral process only on left mandible, 3 – reaching towards ventral process only on right mandible
58. **Shape of ventral asperities (obr. 17):** 0 – small tubercle, 1 – tooth-like process
59. **Hypopharyngeal scleroma:** 0 – symmetrical, without processes, 1 – asymmetric, with large process on right side
60. **Number of maxillar stridulatory teeth:** 0 – 0, with indistinct transverse ridges, 1 – 4 to 9, reduced, 2 – 4 to 9, well developed, 3 – 10 to 20
61. **Shape of stridulatory teeth:** 0 – short, with swollen base, 1 – long and sharp, 2 – obtuse tubercles, 3 – more than one type, 4 – intermediate shape
62. **Lacinia and galea:** 0 – fused, forming mala, 1 – separated
63. **Number of lacinial unci:** 0 – three, 1 – two, 2 – one or none
64. **Shape of legs:** 0 – short and stout, 1 – slender and long
65. **Relative length of legs:** 0 – each pair increasing in size from prothorax to metathorax, 1 – all pairs (sub)equal
66. **Legs: relative length of tibiotarsus and trochanter joints:** 0 – trochanter longer than pretarsus, 1 – trochanter shorter than pretarsus
67. **Shape of pretarsus:** 0 – falcate, pointed with pair of setae, 1 – conical, setae in apical half, 2 – conical, with numerous setae and small claw on apex, 3 – narrow, pointed and slightly bent, with swollen base and a pair of basal setae, 4 – almost reduced with pair of setae

- 68. Relative size of pretarsi:** 0 – all pairs equal in length, 1 – increasing in size from prothorax to metathorax, 2 – decreasing in size from prothorax to metathorax.
- 69. Tibiotarsi:** 0 – all pairs equal in shape and size, 1 – first two pairs similar, last pair of different size, 2 – all three pairs same in size but of different shape
- 70. Size of spiracles:** 0 – all spiracles (sub)equal, 1 – first or first and second abdominal spiracles distinctly smaller than thoracic spiracles, 2 – size decreasing posteriorly
- 71. Shape of thoracic spiracles:** 0 – concealed, arms of respiratory plate almost closed, 1 – open but opening between arms narrow, 2 – open with arms of spiracular plate well separated
- 72. 9<sup>th</sup> and 10<sup>th</sup> abdominal segments:** 0 – entirely fused, 1 – separated, 2 – partially fused
- 73. Palidium:** 0 – present, 1 – absent
- 74. Size of Palidium:** 0 – absent, 1 – short, 2 – of medium length, reaching middle of last abdominal segment, 3 – long, reaching almost end of last abdominal segment
- 75. Hamate setae:** 0 – present, 1 – absent
- 76. Setae of last abdominal segment (excluding raster):** 0 – long, hair-like, 1 – short, 2 – long, dorsoventrally flattened at distal margin, 3 – absent, 4 – mixture of long hair-like and short stout setae
- 77. Chaetotax (general appearance) of larva:** 0 – hairy, with numerous long setae. 1 – dense, covered in numerous short setae, 2 – standard “Cetoniinae” type, 3 – sparse



# Establishing a new species group of *Pseudopoda* Jäger, 2000 with the description of two new species (Araneae, Sparassidae)

He Zhang<sup>1</sup>, Peter Jäger<sup>2</sup>, Jie Liu<sup>1,3</sup>

**1** The State Key Laboratory of Biocatalysis and Enzyme Engineering of China, College of Life Sciences, Hubei University, Wuhan 430062, Hubei, China **2** Arachnology, Senckenberg Research Institute, Senckenberganlage 25, 60325 Frankfurt am Main, Germany **3** School of Nuclear Technology and Chemistry & Biology, Hubei University of Science and Technology, Xianning 437100, Hubei, China

Corresponding author: Jie Liu ([sparassidae@aliyun.com](mailto:sparassidae@aliyun.com))

Academic editor: Cristina Rheims | Received 3 April 2019 | Accepted 30 July 2019 | Published 9 October 2019

<http://zoobank.org/EE12E439-0F6A-4989-BDC5-3EB4F846043A>

**Citation:** Zhang H, Jäger P, Liu J (2019) Establishing a new species group of *Pseudopoda* Jäger, 2000 with the description of two new species (Araneae, Sparassidae). ZooKeys 879: 91–115. <https://doi.org/10.3897/zookeys.879.351110>

## Abstract

The huntsman spider genus *Pseudopoda* Jäger, 2000 contains 140 species worldwide, of which 61 have been described from China. In this paper, this knowledge is increased by the description of two new species from Yunnan Province in China. These new species, *P. physematosa* **sp. nov.** (♀) and *P. semilunata* **sp. nov.** (♂♀), are treated with five previously described ones, *P. bibulba* Xu & Yin, 2000 (♂♀), *P. signata* Jäger, 2001 (♂♀), *P. wu* Jäger, Li & Krehenwinkel, 2015 (♂♀), *P. yinae* Jäger & Vedel, 2007 (♂), and *P. yunnanensis* Yang & Hu, 2001 (♂♀), as the newly defined *Pseudopoda signata* species group. The *P. signata* group can be distinguished from other groups within *Pseudopoda* by the male palps with long, slightly broad, S-shaped embolus, small but distinct tegular apophysis, pronounced dRTA and reduced vRTA, and by the female with V-shaped or W-shaped anterior margins of lateral lobes, membranous and wide first winding, long and strongly curved SIDS (sclerotised internal duct system), the latter mostly covered by the first winding. The monophyly of this group is also supported by molecular phylogenetic results mainly based on Chinese *Pseudopoda* species. In addition, photographs of *P. bibulba* (♂♀), *P. signata* (♂♀), and *P. yunnanensis* (♂♀) are provided. *P. bibulba* is newly recorded from Guizhou Province and *P. signata* is newly recorded from Yunnan Province.

## Keywords

Biodiversity, systematics, taxonomy, huntsman spiders, China

## Introduction

Jäger (2000) proposed the huntsman spider genus *Pseudopoda* by re-describing *P. prompta* (O. Pickard-Cambridge, 1885) from Pakistan and India. Since then, no fewer than 140 species have been assigned to this genus, which is now known to occur in areas from South, East and Southeast Asia. Of this diversity, 61 species have been recorded from China (World Spider Catalog 2019). Known species are mainly collected in the leaf litter, underneath tree bark, under stones and on plants (Jäger and Vedel 2007).

Jäger (2001) established six species groups within the genus according to morphological evidences based on species mostly collected from Himalayas and nearby mountain ranges: *P. diversipunctata* group, *P. latembola* group, *P. martensi* group, *P. parvipunctata* group, *P. prompta* group, and *P. schwendingeri* group. Nevertheless, the monophyly of these groups has never been tested by any phylogenetical analysis. Cao et al. (2016) published a molecular phylogeny on Chinese *Pseudopoda* species based on COI and ITS2 genes data, focusing on DNA barcoding of this genus, without discussing species groups. Zhang et al. (2017) established the seventh *Pseudopoda* group (*P. daliensis* group including five species from Yunnan Province, China) based on morphological and molecular data which are mostly cited from Cao et al. (2016). So far, only 47 (33.57%) species were assigned to species groups, since it is challenging to group species exclusively according to morphological data of a limited set of species. Jäger (2001) described *P. signata* but did not assign it to any species group considering the female a transitional form between the *prompta* group and the *martensi* group. Here, we expand the baseline data for such decision by evaluating molecular (Fig. 1, edited from Zhang et al. 2017: fig. 1) as well as morphological evidence (see taxonomy), and establish the *P. signata* group, to which we assign seven species, two of which new to science, from Guizhou, Sichuan, and Yunnan provinces in China.

## Material and methods

All specimens were preserved in 75% ethanol and examined with an Olympus SZX16 stereomicroscope; details were further investigated with an Olympus BX51 compound microscope. Male and female copulatory organs were examined and illustrated after dissection from the spider bodies, vulvae were cleared with Proteinase K. Habitus photos were obtained using a Leica 205C digital microscope.

Leg measurements are shown as: total length (femur, patella, tibia, metatarsus, tarsus). The numbers of spines are listed for each segment in the following order: prolateral, dorsal, retrolateral, ventral (in femora and patellae, ventral spines are absent, and the fourth digit is omitted in the spination formula). The body size classes and illustration of schematic course of internal duct system follow Jäger (2001). The terminology used in the text and figure legends follows Quan et al. (2014). All measurements are in millimetres.

We evaluated the most recent phylogenetic evidence for relationships among various *Pseudopoda* species (Fig. 1, edited from Zhang et al. 2017: fig. 1). For detailed phylogenetic methods and abbreviations see Cao et al. (2016) and Zhang et al. (2017).

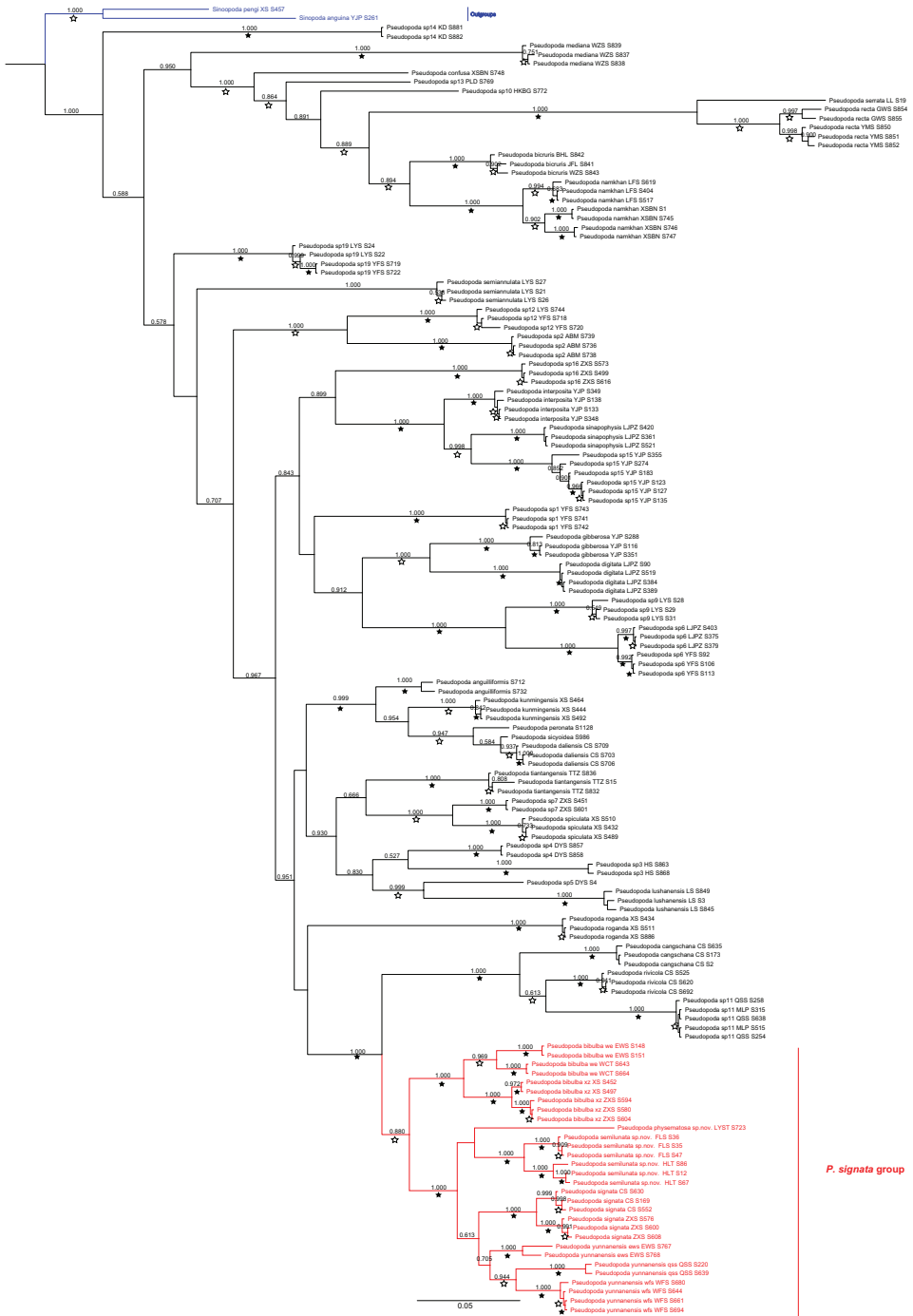


**Figure 1.** Bayesian tree based on the COI + ITS2 dataset including 144 *Pseudopoda* individuals belonging to 44 species. Numbers on nodes are posterior probabilities; bootstrap support from ML analyses is indicated as solid stars for values > 95%, open stars > 50–95%. Red clade indicates the *P. signata* group, blue clade indicates the outgroups. Phylogenetic tree cited from Zhang et al. (2017).

Abbreviations used throughout the text are given below.

Somatic morphology:

<b>ALE</b>	anterior lateral eyes;	<b>OS</b>	opisthosoma;
<b>AME</b>	anterior median eyes;	<b>Pa</b>	patella;
<b>CH</b>	clypeus height;	<b>PLE</b>	posterior lateral eyes;
<b>CO</b>	copulatory opening;	<b>PME</b>	posterior median eyes;
<b>dRTA</b>	dorsal part/branch of RTA;	<b>Pp</b>	palp;
<b>DS</b>	dorsal shield of prosoma;	<b>RTA</b>	retrolateral tibial apophysis;
<b>E</b>	embolus;	<b>SIDS</b>	sclerotised internal duct system;
<b>Fe</b>	femur;	<b>ST</b>	subtegulum;
<b>FD</b>	fertilisation duct;	<b>T</b>	tegulum;
<b>FW</b>	first winding;	<b>Ti</b>	tibia;
<b>Mt</b>	metatarsus;	<b>I, II, III, IV</b>	– legs I to IV;

**vRTA** ventral part/branch of RTA.

Institutes:

<b>CBEE</b>	Centre for Behavioural Ecology and Evolution, College of Life Sciences, Hubei University, Wuhan, China;
<b>HUST</b>	School of Nuclear Technology and Chemistry & Biology, Hubei University of Science and Technology, Xianning, Hubei, China;
<b>SWUC</b>	College of Life Sciences, Southwest University, Chongqing, China.

## Taxonomy

**Family Sparassidae Bertkau, 1872**

**Subfamily Heteropodinae Thorell, 1873**

**Genus *Pseudopoda* Jäger, 2000**

***Pseudopoda signata* group**

**Definition.** This group can be recognised by the combination of the following characters:

1. Embolus distinctly longer than tegulum, slightly S-shaped, arising from tegulum between 7- AND 9-o'clock-position (Fig. 2A);
2. Tegulum with distinctly short tegular outgrowth (Fig. 2A);
3. dRTA pronounced, vRTA short, dRTA two times longer than vRTA (Fig. 2A);
4. Anterior margins of lateral lobes bent medially, roughly “U” or “V”-shaped (Fig. 2B);
5. First winding membranous and wide, covering large part of the sclerotised internal duct system (Fig. 2D);

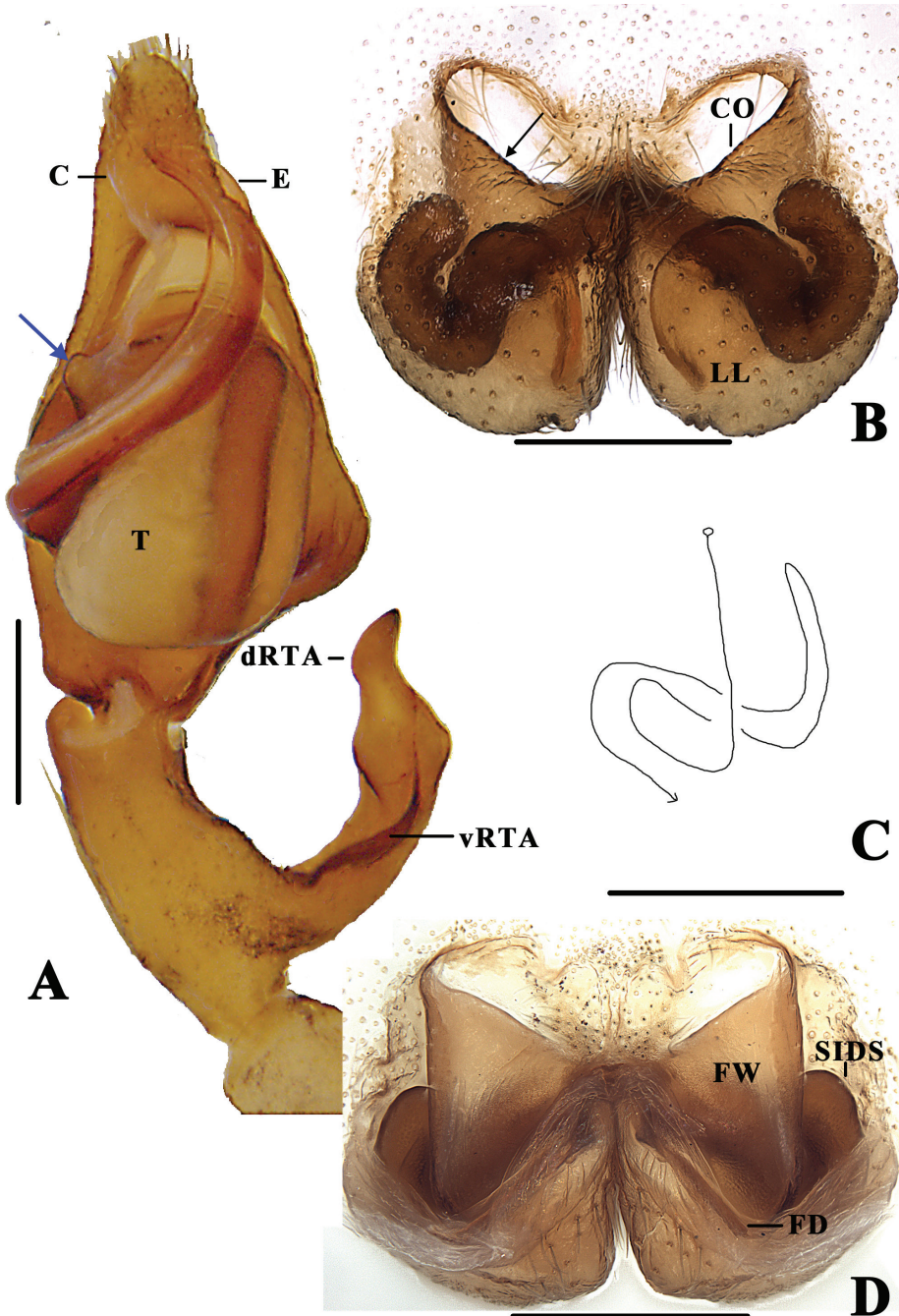


**Figure 2.** *Pseudopoda bibulba* Xu & Yin, 2000 **A** left male palp, ventral **B** epigyne, ventral **C** schematic course of internal duct system in right part, dorsal **D** vulva, dorsal. Black arrow pointing to anterior margin of lateral lobe, blue arrow to tegular outgrowth. Abbreviations: C–conductor; dRTA–dorsal retrolateral tibial apophysis; E–embolus; vRTA–ventral retrolateral tibial apophysis; T–tegulum; CO–copulatory opening; LL–lateral lobes; FD–fertilisation duct; FW–first winding; SIDS–sclerotised internal duct system. Scale bars: 0.5 mm.

6. Sclerotised part of internal duct system long, strongly curved, tube-shaped (Fig. 2D).

**Composition.** *P. bibulba* Xu & Yin, 2000, *P. physematosus* sp. nov., *P. semilunata* sp. nov., *P. signata* Jäger, 2001, *P. wu* Jäger, Li & Krehenwinkel, 2015, *P. yinae* Jäger & Vedel, 2007, *P. yunnanensis* Yang & Hu, 2001.

**Distribution.** China (Guizhou, Sichuan, Yunnan provinces) (Fig. 18).

### *Pseudopoda bibulba* Xu & Yin, 2000

Figs 2–4, 18

*Heteropoda bibulba* Xu & Yin, 2000: 37, figs 1–3 (description of female).

*Pseudopoda bibulba*: Jäger & Yin, 2001: 126 (transfer from *Heteropoda*); Jäger & Vedel, 2007: 15, figs 44–59 (description of male, redescription of female).

**Material examined. CHINA, Guizhou Province:** 3 females, Liupanshui City, Zhongshan District, Xianshui slope martyr cemetery, 26.61°N, 104.84°E, 1966 m, 11 April 2016, Yang Zhong, Yang Zhu & He Zhang leg. (CBEE, LJ02358-LJ02360); **Yunnan Province:** 19 males, 14 females, Kunming City, Xishan Scenic Area, 24.96°N, 102.63°E, 1975 m, 14 May 2014, Yang Zhong & Xiaowei Cao leg. (CBEE, LJ02361-LJ02393); 1 female, Kunming City, Xishan Scenic Area, 24.96°N, 102.63°E, 2204 m, 13 October 2016, Guiqiang Huang, Xiangbo Guo and Yanchao Wang leg. (CBEE, LJ02394); 19 males, 14 females, Chuxiong City, Zixishan Scenic Area, 25.01°N, 101.42°E, 2527 m, 15 May 2014, Yang Zhong & Xiaowei Cao leg. (CBEE, LJ02395-LJ02427); 5 males, 3 females, Nujiang Lisu Autonomous Prefecture, Lanping Bai Nationality Autonomous Prefecture, Mt. Erwu, 26.43°N, 99.41°E, 2377 m, 28 May 2014, Yang Zhong & Xiaowei Cao leg. (CBEE, LJ02428-LJ02435); 6 males, 5 females, Wei Xi Lisu Autonomous County, Pagoda of Cultural Prosperity, 27.18°N, 99.29°E, 2294 m, 26 May 2014, Yang Zhong & Xiaowei Cao leg. (CBEE, LJ02436-LJ02446).

**Diagnosis and Description.** See Jäger and Vedel (2007).

**Distribution.** China (Guizhou, new province record; Yunnan) (Fig. 18).

### *Pseudopoda physematosus* sp. nov.

<http://zoobank.org/8AD4A005-5F68-438F-997A-32F410F14B7A>

Figs 5–7, 18

**Type material. Holotype female: CHINA: Yunnan Province:** Lijiang City, Yongsheng County, Lingyuan Temple, 26.70°N, 100.78°E, 2305 m, 25 August 2013, Yang Zhong & Xiaowei Cao leg. (CBEE, LJ01667); **Paratypes:** 2 females, with same data as holotype. (CBEE, LJ01668-LJ01669).

**Etymology.** The specific name is derived from the Latin adjective *physematosus*, *-a*, *-um*, meaning swollen, referring to the shape of SIDS in dorsal view (Fig. 5C); adjective.

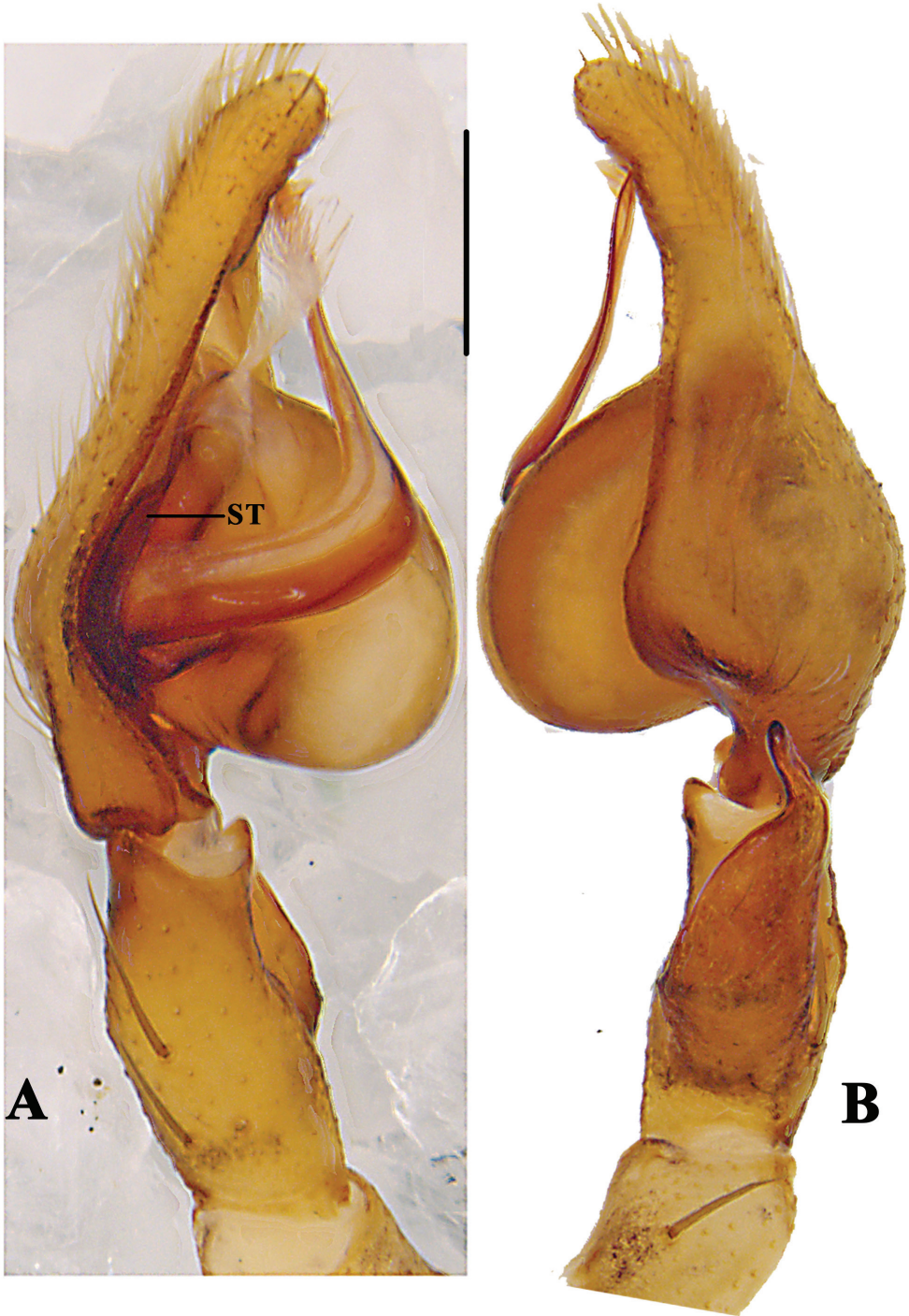


**Figure 3.** *Pseudopoda bibulba* Xu & Yin, 2000 **A** left male palp, prolateral **B** same, retrolateral. Abbreviation: ST—subtegulum. Scale bar: 0.5 mm.

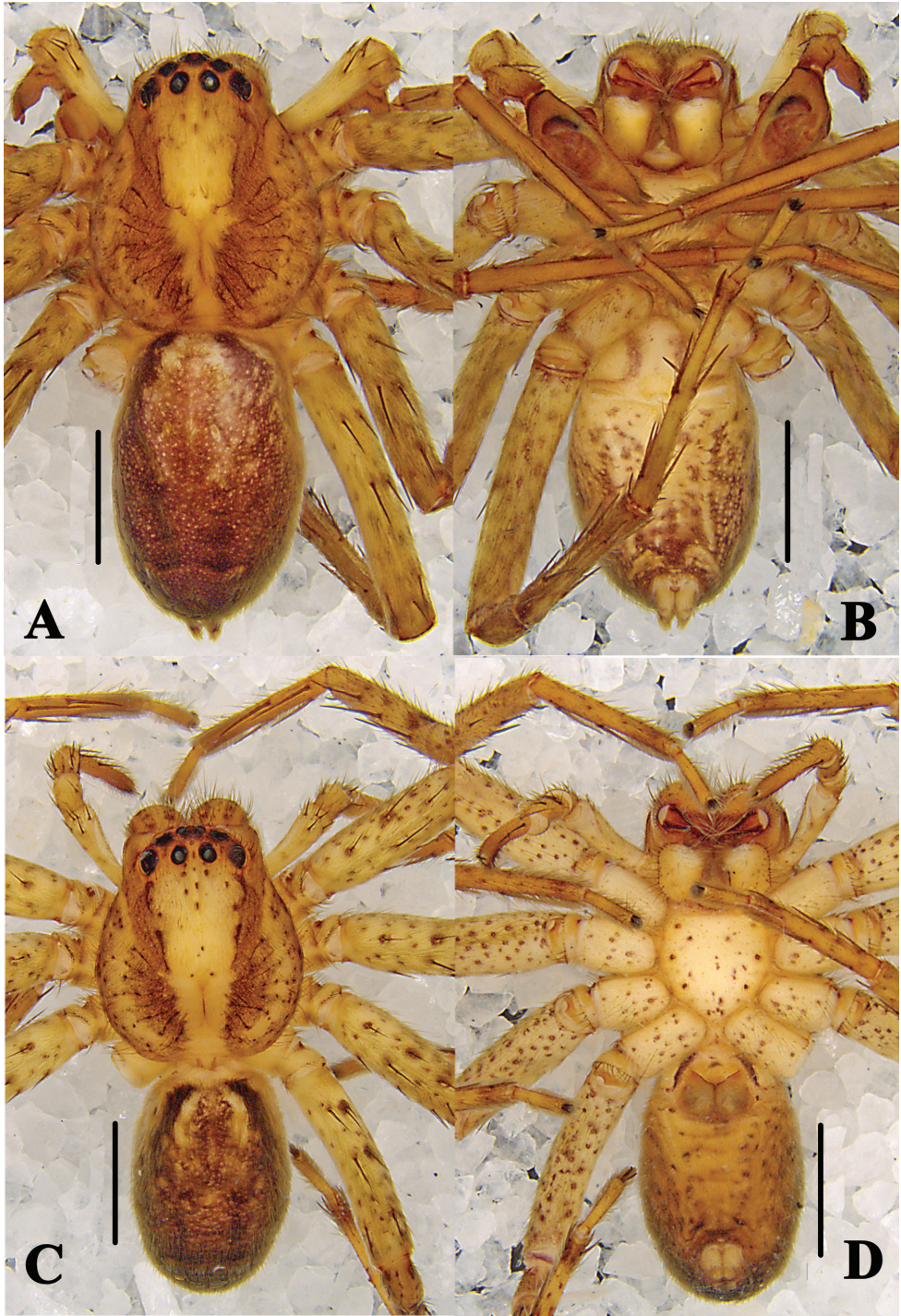


**Figure 4.** *Pseudopoda bibulba* Xu & Yin, 2000 **A, B** male habitus (**A** dorsal **B** ventral) **C, D** female habitus (**C** dorsal **D** ventral). Scale bars: 2 mm.

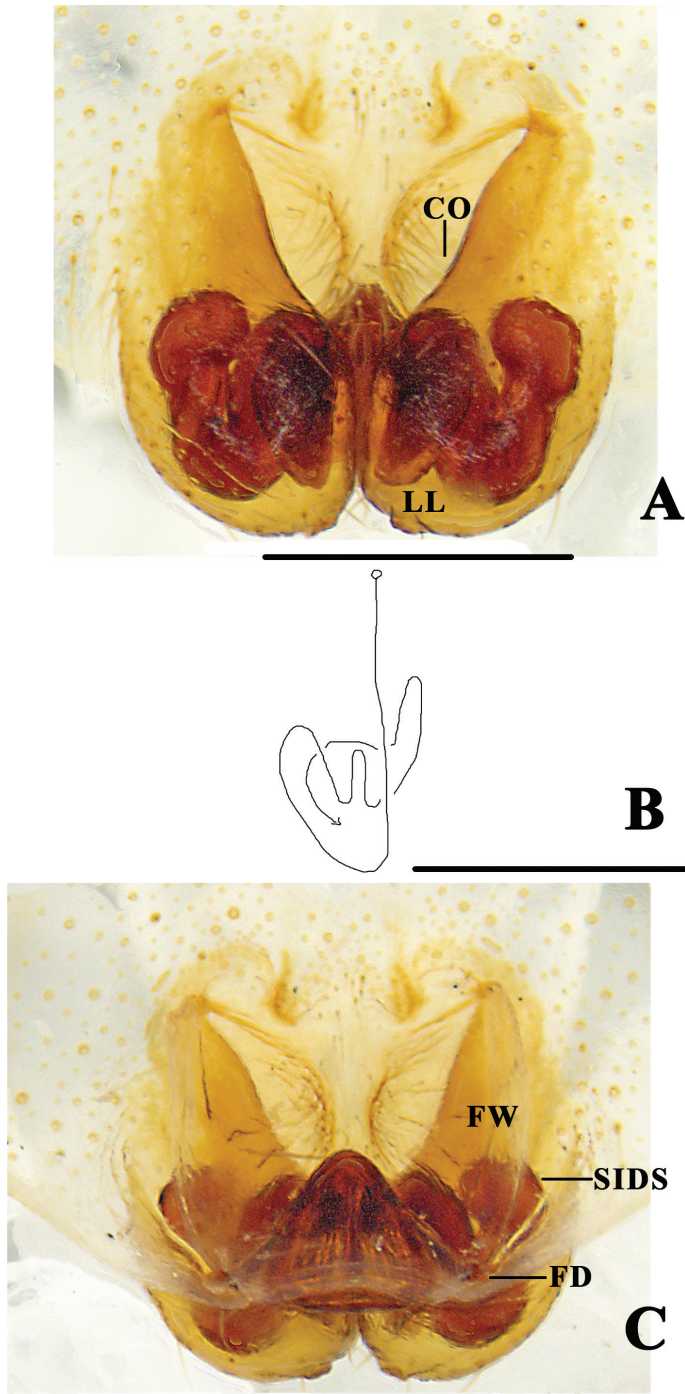


**Figure 5.** *Pseudopoda physematosa* sp. nov. **A** epigyne, ventral **B** schematic course of internal duct system, dorsal **C** vulva, dorsal. Abbreviations: CO—copulatory opening; FD—fertilisation duct; FW—first winding; LL—lateral lobes; SIDS—sclerotised internal duct system. Scale bars: 0.5 mm.

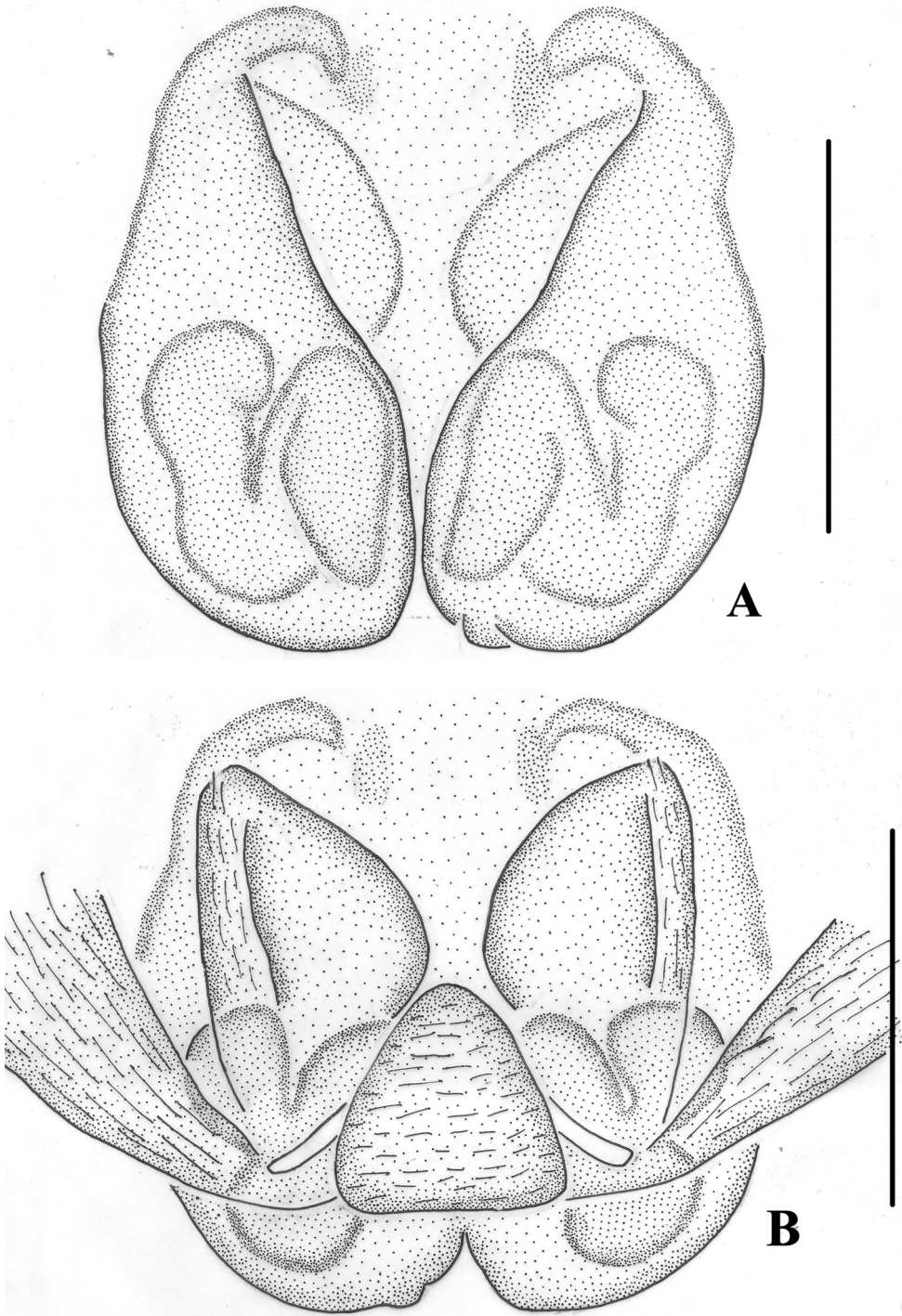


**Figure 6.** *Pseudopoda physematosa* sp. nov. **A** epigyne, ventral **B** vulva, dorsal. Scale bars: 0.5 mm.



**Figure 7.** *Pseudopoda physematosa* sp. nov. Female habitus (**A** dorsal **B** ventral). Scale bars: 2 mm.

**Diagnosis.** *Pseudopoda physematosa* sp. nov. differs from other species of the *P. signata* group, except *P. bibulba*, by the SIDS with well developed twisted loops, in ventral view. It can be distinguished from *P. bibulba* by the following characters: anterior margins of lateral lobes longer than half the width of epigynal field in *P. physematosa*, but shorter in *P. bibulba*; SIDS folded, with swollen tip in *P. physematosa*, but not in *P. bibulba* (Fig. 5A).

**Description.** **Male** unknown. **Female (holotype):** Measurements: small-sized Heteropodinae. Body length 8.6–9.9. DS length 4.4, width 3.3, OS length 5.5, width 3.6. Eyes: AME 0.24, ALE 0.31, PME 0.18, PLE 0.22, AME-AME 0.18, AME-ALE 0.11, PME-PME 0.15, PME-PLE 0.24, AME-PME 0.27, ALE-PLE 0.24, CH AME 0.35, CH ALE 0.28. Leg formula: II-I-IV-III. Spination: Pp 131, 101, 2121, 1014; Fe I-II 323, III 322, IV 322; Pa I-III 101, IV 100; Ti I-II 2228, III-IV 2126; Mt I-II 2024, III 3025, IV 3036. Measurement of palps and legs: Pp 4.5 (1.3, 0.5, 1.0, -, 1.7); I 12.8 (3.8, 1.9, 2.8, 3.1, 1.2); II 13.0 (4.0, 1.3, 3.0, 3.2, 1.5); III 11.1 (3.1, 1.6, 2.7, 2.6, 1.1); IV 11.6 (3.1, 1.7, 3.0, 2.7, 1.1). Promargin of chelicerae with three teeth, retromargin with four teeth, cheliceral furrow with ca. 32 denticles. Epigynal field almost as wide as long, with anterior bands included in the field. Epigyne with lateral lobes touching each other posteriorly. The anterior margins of lateral lobes forming a “V”. FW covering most of SIDS, the latter folded in the middle part (Fig. 5A–C). Col-

ouration in ethanol: DS yellow with irregular radially arranged dark spots and brown patterns. Fovea and radial furrows distinctly marked. OS dorsally with light yellow hairs and large patches of reddish brown spots, ventrally lighter with larger and sparser reddish brown marks (Fig. 7A, B).

**Distribution.** China (Yunnan) (Fig. 18).

***Pseudopoda semilunata* sp. nov.**

<http://zoobank.org/42780378-AF52-41DB-8447-C71F62523204>

Figs 8–11, 18

**Type material. Holotype male: CHINA: Yunnan Province:** Lijiang City, Black Dragon Pool Park, 26.89°N, 100.24°E, 2659 m, 20 May 2014, Yang Zhong & Xiaowei Cao leg. (CBEE, LJ01905); **Paratypes:** 7 males, 8 females, with same data as holotype. (CBEE, LJ01906-LJ01920); 2 males, 2 females, Diqing Tibetan Autonomous Prefecture, Deqin County, Fei Lai Temple scenic area, 28.42°N, 98.87°E, 3458m, 25 May 2014, Yang Zhong & Xiaowei Cao leg. (CBEE, LJ01921-LJ01924).

**Etymology.** The specific name is derived from the Latin adjective *semilunatus*, -a, -um, meaning lunate, referring to the shape of anterior margins of lateral lobes (Fig. 8B–D); adjective.

**Diagnosis.** *P. semilunata* sp. nov. differs from other members in this group by the following characters: dRTA with distinct sub-apical cavity, anterior margins of lateral lobes not strongly curved as in other species but together forming a semicircle. Males of this species are similar to those of *P. wu* in having a twisted embolus tip but can be distinguished by embolic tip forming a semicircle and conductor present (embolic tip forming a full circle, conductor entirely reduced in *P. wu*) (Figs 8A–D, 9A, B).

**Description. Male (holotype):** Measurements: small-sized Heteropodinae. Body length 7.0–9.5. DS length 4.1, width 3.5, OS length 5.0, width 3.4. Eyes: AME 0.16, ALE 0.23, PME 0.19, PLE 0.24, AME-AME 0.13, AME-ALE 0.21, PME-PME 0.24, PME-PLE 0.27, AME-PME 0.37, ALE-PLE 0.40, CH AME 0.26, CH ALE 0.21. Leg formula: II-I-IV-III. Spination: Pp 131, 101, 2121, 1014; Fe I–II 323, III 322, IV 322; Pa I–III 101, IV 100; Ti I–II 2228, III–IV 2126; Mt I–II 2024, III 3025, IV 3036. Measurement of palps and legs: Pp 5.0 (1.3, 0.6, 0.9, -, 2.2); I 13.9 (3.9, 1.0, 3.6, 4.0, 1.4); II 14.3 (4.1, 1.2, 4.2, 3.3, 1.5); III 12.2 (3.5, 0.9, 3.4, 3.0, 1.4); IV 13.7 (4.5, 1.2, 3.3, 3.2, 1.5). Promargin of chelicerae with three teeth, retromargin with four teeth, cheliceral furrow with ca. 20 denticles. Palp as in diagnosis. Conductor arising from tegulum at 12-o'clock-position, basally folded. Tegular outgrowth short, claviform. Embolus arising from tegulum at 8.30-o'clock-position, long, well developed, with abruptly tapering apical part with additional loop. Spermophore visible submarginally on retro-lateral tegulum in ventral view. RTA arising proximally on Ti, with broad ventral part, its distal end bent, bowl-shaped (Figs 8A, 9A, B). Colouration in ethanol: DS yellow with dark spots, two lateral bands, margin with thin dash line and brown patterns. Fovea and radial furrows distinctly marked. OS dorsally with lots of reddish brown dots, ventrally with reddish brown marks, regularly arranged (Fig. 11A, B).

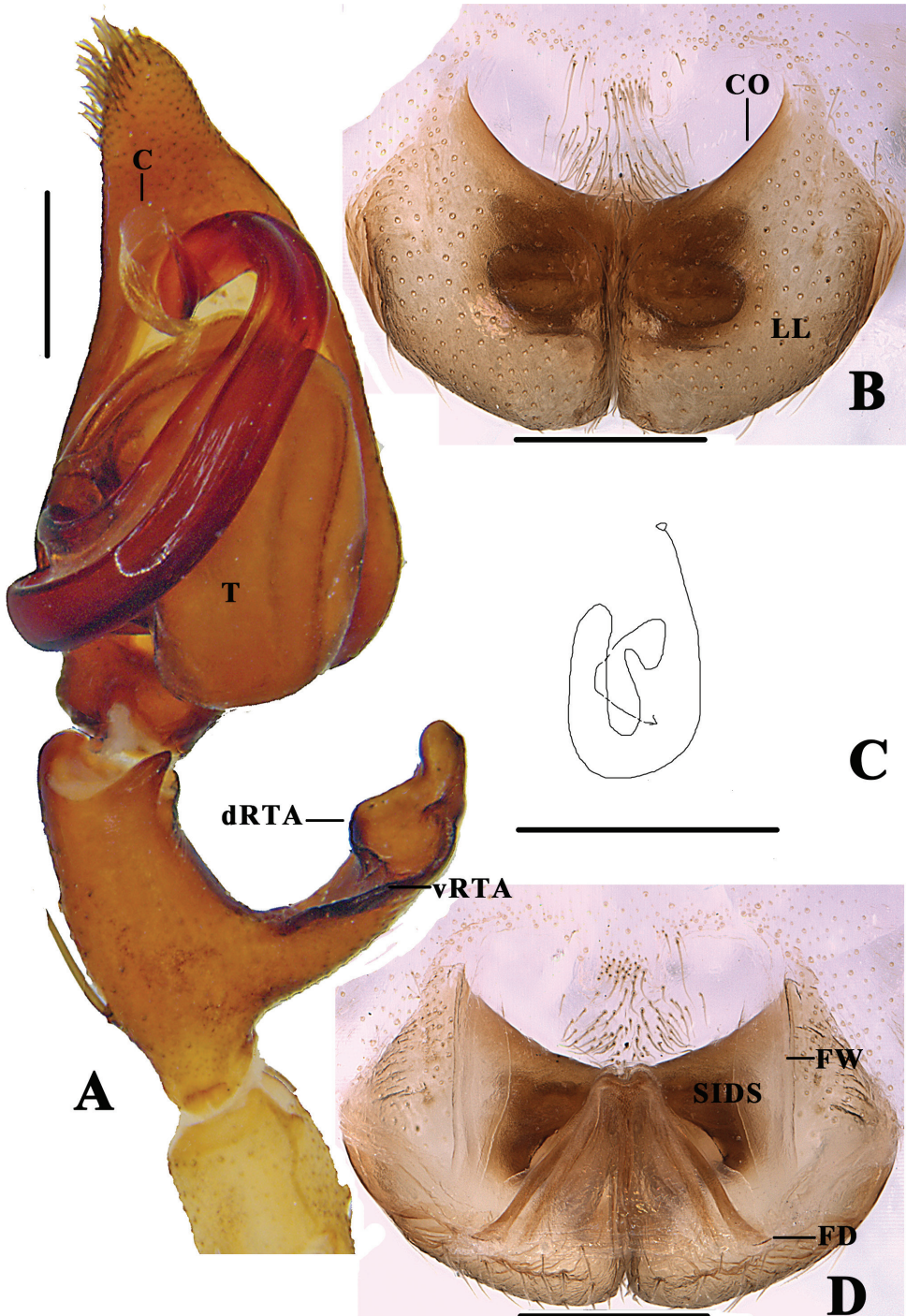


**Figure 8.** *Pseudopoda semilunata* sp. nov. **A** left male palp, ventral **B** epigyne, ventral **C** schematic course of internal duct system in right art, dorsal **D** vulva, dorsal. Abbreviations: C—conductor; dRTA—dorsal retrolateral tibial apophysis; T—tegulum; vRTA—ventral retrolateral tibial apophysis; CO—copulatory opening; LL—lateral lobes; FD—fertilisation duct; FW—first winding; SIDS—sclerotised internal duct system. Scale bars: 0.5 mm.

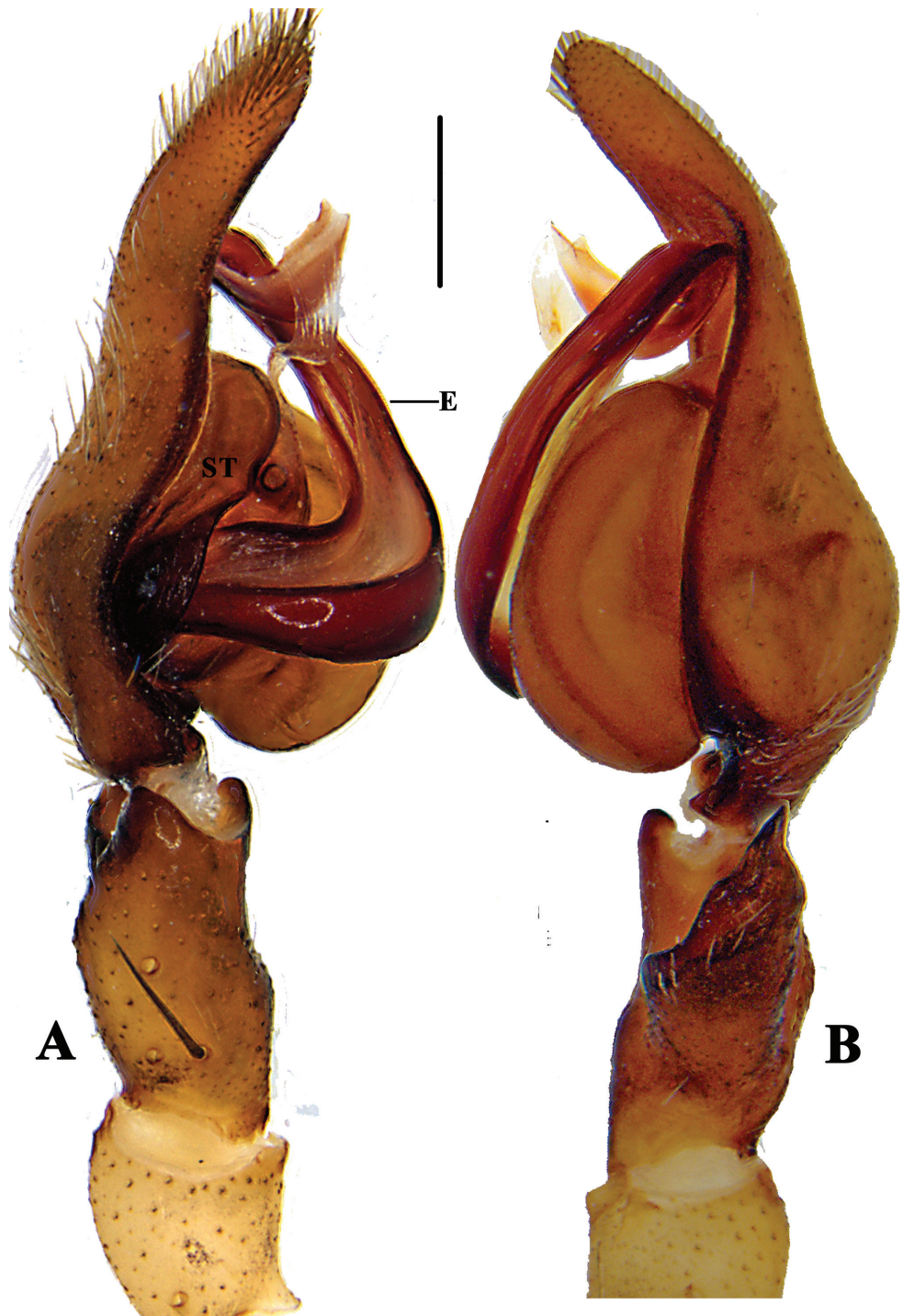


**Figure 9.** *Pseudopoda semilunata* sp. nov. **A** left male palp, prolateral **B** Same, retrolateral. Abbreviations: E-embolus; ST-subtegulum. Scale bar: 0.5 mm.

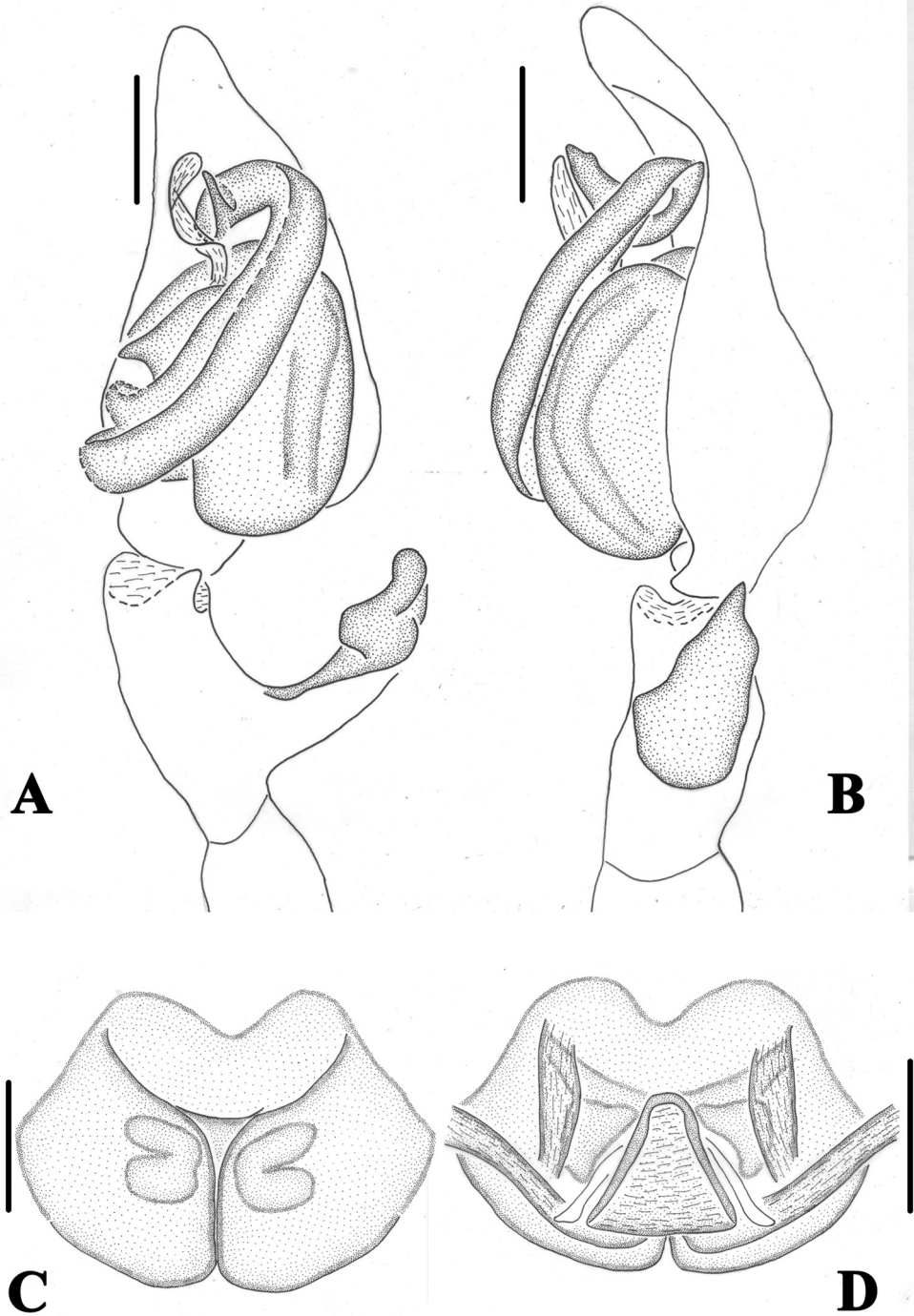


**Figure 10.** *Pseudopoda semilunata* sp. nov. **A, B** left male palp (**A** ventral **B** retrolateral) **C** epigyne, ventral **D** vulva, dorsal. Scale bars: 0.5mm.

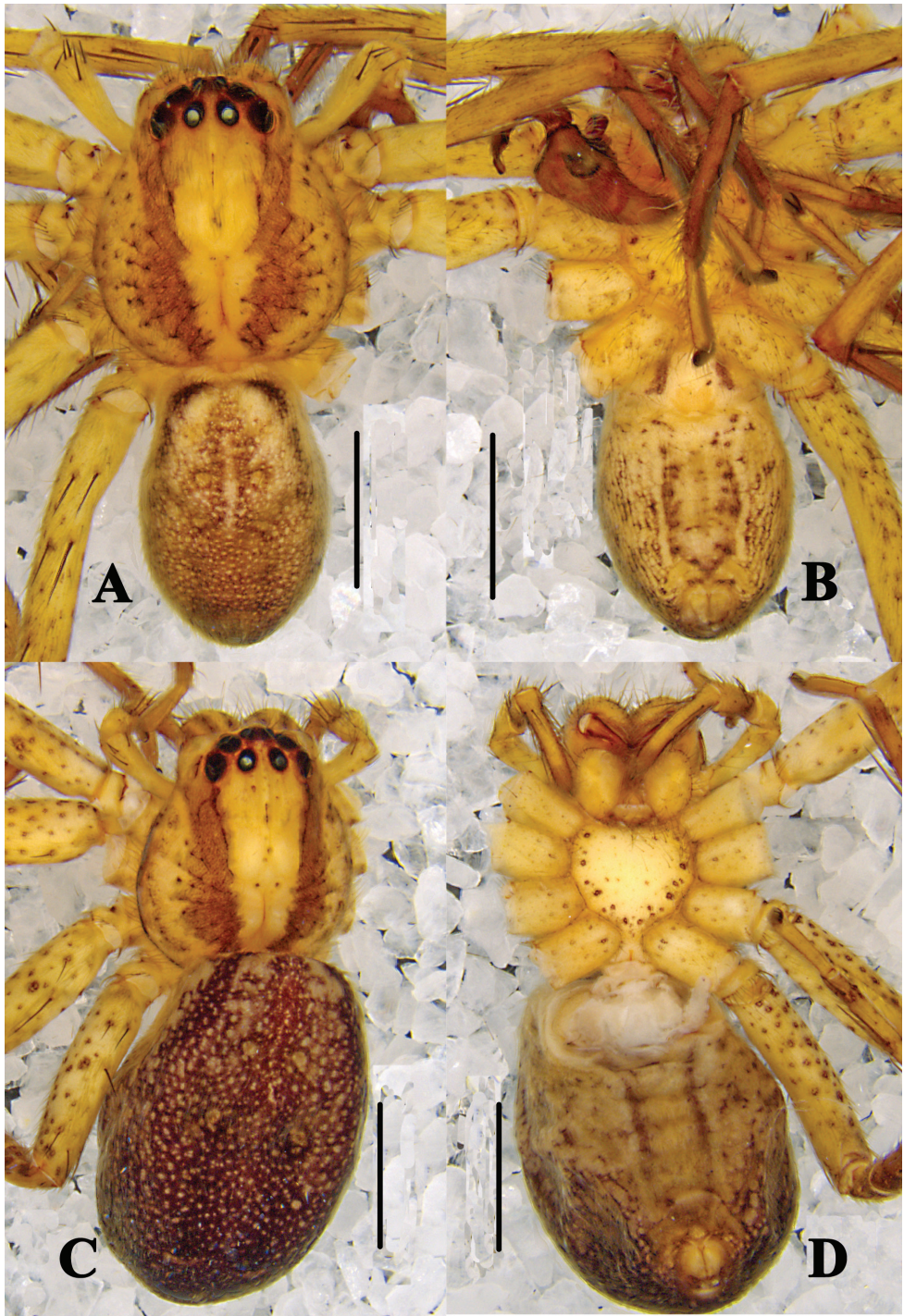


**Figure 11.** *Pseudopoda semilunata* sp. nov. **A, B** male habitus (**A** dorsal **B** ventral) **C, D** female habitus (**C** dorsal **D** ventral). Scale bars: 2 mm.

**Female:** Measurements: small-sized Heteropodinae. Body length 8.0–9.5. DS length 4.0, width 3.6, OS length 4.6, width 2.8. Eyes: AME 0.15, ALE 0.20, PME 0.16, PLE 0.20, AME-AME 0.27, AME-ALE 0.13, PME-PME 0.33, PME-PLE 0.41, AME-PME 0.35, ALE-PLE 0.32, CH AME 0.31, CH ALE 0.29. Leg formula: II-I-IV-III. Spination: Pp 131, 101, 2121, 1014; Fe I-II 323, III 322, IV 322; Pa I-III 101, IV 100; Ti I-II 2228, III-IV 2126; Mt I-II 2024, III 3025, IV 3036. Measurements of palps and legs: Pp 4.4 (1.3, 0.6, 0.9, -, 1.6); I 9.9 (3.1, 0.8, 2.6, 2.4, 1.0); II 10.9 (3.1, 1.2, 3.0, 2.6, 1.0); III 7.3 (1.9, 0.8, 2.2, 1.5, 0.9); IV 8.8 (2.8, 0.8, 2.4, 2.0, 0.8). Cheliceral furrow with three anterior and four posterior teeth, and with ca. 18 denticles. Epigynal field wider than long. Anterior and posterior margins of lateral lobes almost parallel. FW well developed, covering the entire sclerotised part of internal duct system, the latter folded. FD long, narrow (Fig. 8B–D). Colouration in ethanol: As in male, generally darker (Fig. 11C, D).

**Distribution.** China (Yunnan) (Fig. 18).

### *Pseudopoda signata* Jäger, 2001

Figs 12–14, 18

*Pseudopoda signata* Jäger, 2001: 50, f. 29h–j (description of female).

*Pseudopoda signata*: Jäger et al. 2015: 375, f. 55–90, 93–106 (description of male, re-description of female); Jäger, 2015: 349, fig. 98 (illustration of male).

**Material examined. CHINA, Yunnan Province:** 6 males, 7 females, Dali Bai Autonomous Prefecture, Cangshan Scenic Area, 25.01°N, 100.14°E, 2645 m, 17 May 2014, Yang Zhong & Xiaowei Cao leg. (CBEE, LJ01695-LJ01707); 12 males, 6 females, Chuxiong City, Zixishan Scenic Area, 25.01°N, 101.42°E, 2476 m, 15 May 2014, Yang Zhong & Xiaowei Cao leg. (CBEE, LJ01708-LJ01719, LJ01785-LJ01790).

**Diagnosis and Description.** See Jäger et al. (2015).

**Distribution.** China (Yunnan, new province record; Sichuan) (Fig. 18).

### *Pseudopoda yunnanensis* Yang & Hu, 2001

Figs 15–18

*Sinopoda yunnanensis* Yang & Hu, 2001: 18, figs 1–3 (description of female).

*Pseudopoda yunnanensis*: Jäger & Vedel, 2007: 17, figs 60–62 (Transfer from *Sinopoda*); Yang & Chen, 2008: 810, figs 1–13 (Description of male, redescription female).

**Material examined. CHINA, Yunnan Province:** 2 males, 2 females, Nujiang Lisu Autonomous Prefecture, Lanping Bai Nationality Autonomous Prefecture, Mt. Erwu, 26.43°N, 99.41°E, 2366 m, 28 May 2014, Yang Zhong & Xiaowei Cao leg. (CBEE, LJ01535-LJ01538); 42 males, 26 females, Diqing Tibetan Autonomous Prefecture, Shangri-La County, Mt. Wufeng, 27.18°N, 99.29°E, 3528 m, 23 May 2014, Yang

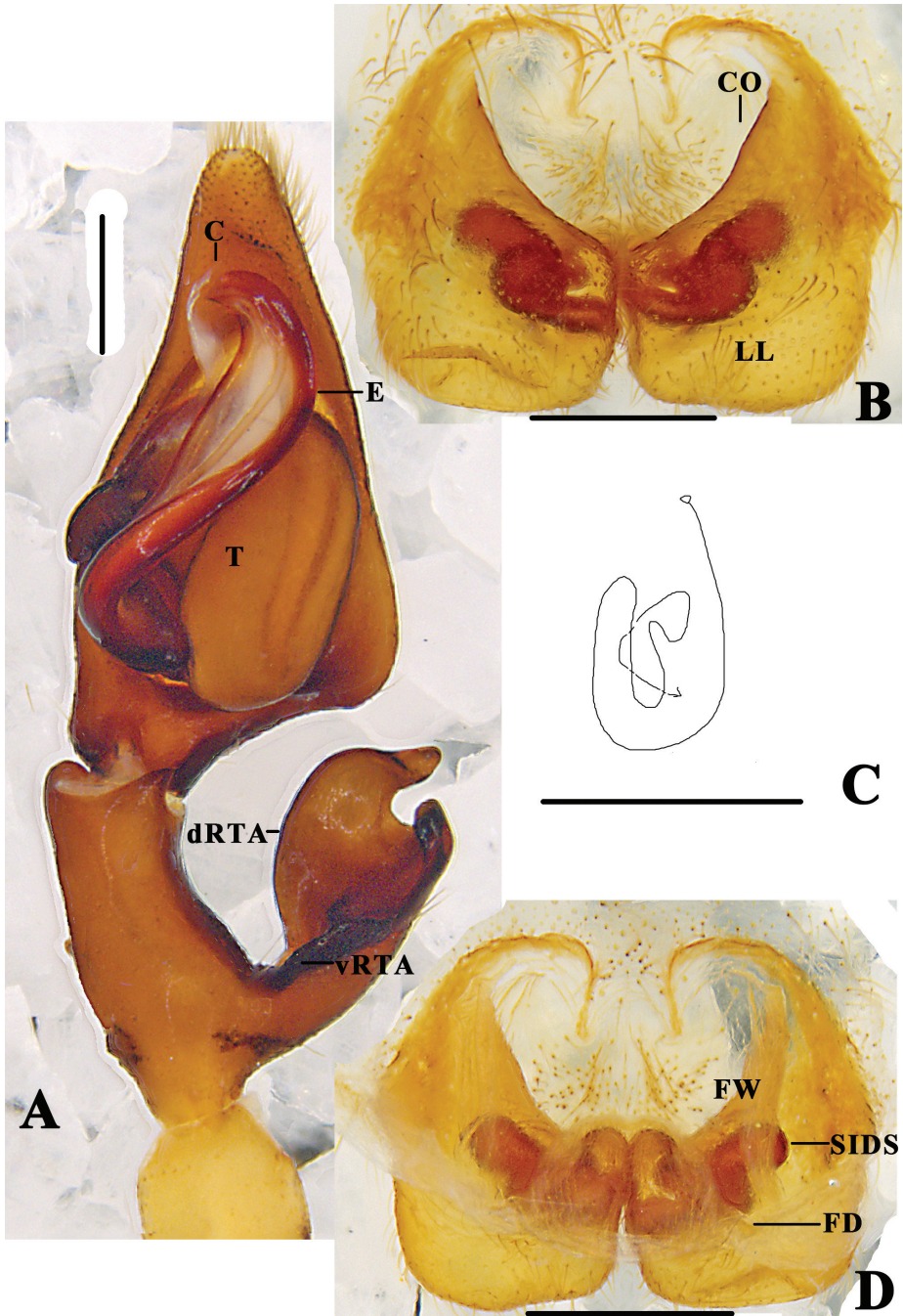


**Figure 12.** *Pseudopoda signata* Jäger, 2001 **A** left male palp, ventral **B** epigyne, ventral **C** schematic course of internal duct system in right part, dorsal **D** vulva, dorsal. Abbreviations: C—conductor; E—embolus; dRTA—dorsal retrolateral tibial apophysis; T—tegulum; vRTA—ventral retrolateral tibial apophysis; CO—copulatory opening; LL—lateral lobes; FD—fertilisation duct; FW—first winding; SIDS—sclerotised internal duct system. Scale bars: 0.5 mm.



**Figure 13.** *Pseudopoda signata* Jäger, 2001 **A** left male palp, prolateral **B** same, retrolateral. Abbreviation: ST—subtegulum. Scale bar: 0.5 mm.

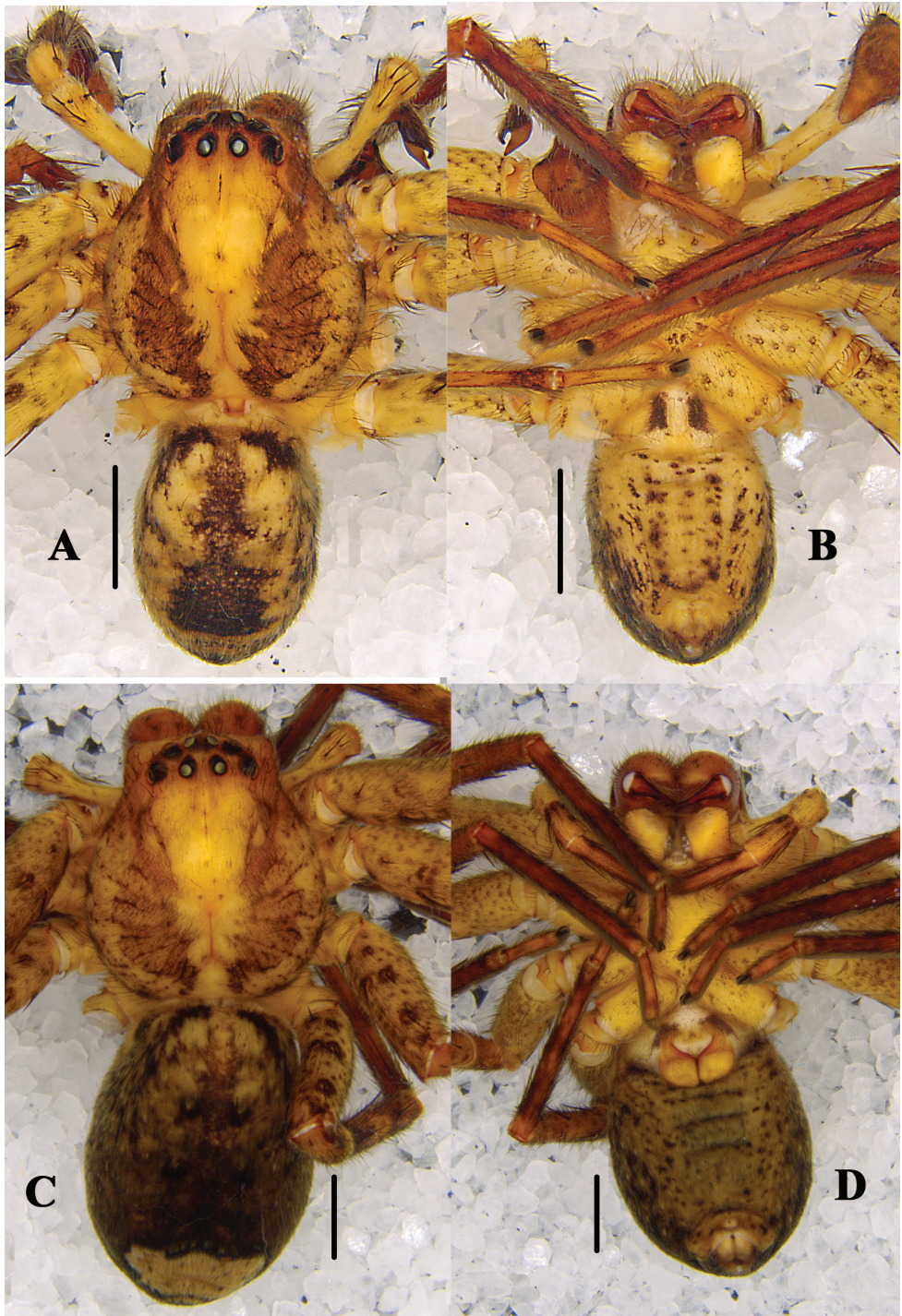


**Figure 14.** *Pseudopoda signata* Jäger, 2001 **A, B** male habitus (**A** dorsal **B** ventral) **C, D** female habitus (**C** dorsal **D** ventral). Scale bars: 2 mm

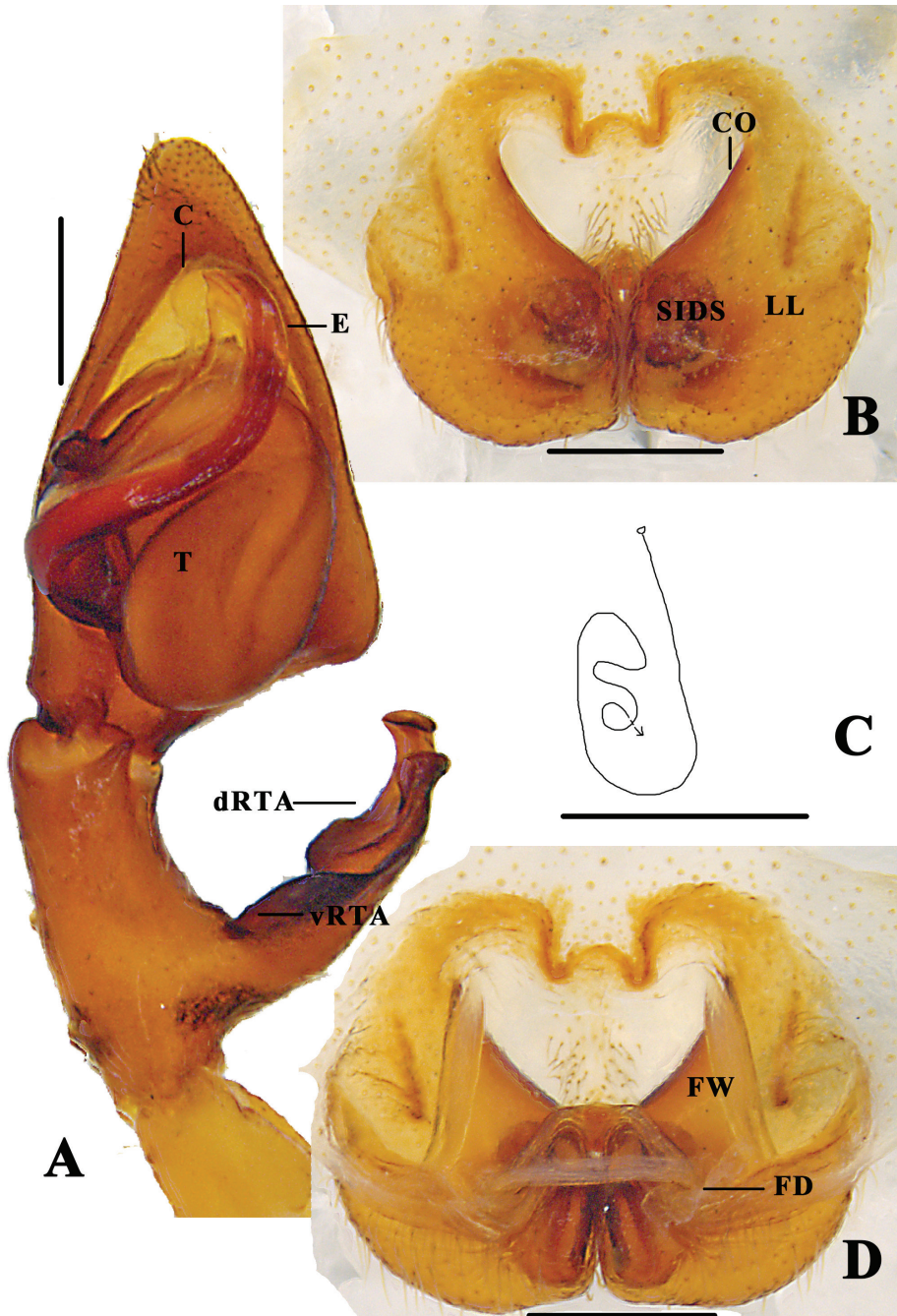


**Figure 15.** *Pseudopoda yunnanensis* Yang & Hu, 2001 **A** left male palp, ventral **B** epigyne, ventral **C** Schematic course of internal duct system in right part, dorsal **D** vulva, dorsal. Abbreviations: C—conductor; dRTA—dorsal retrolateral tibial apophysis; E—embolus; vRTA—ventral retrolateral tibial apophysis; T—tegulum; CO—copulatory opening; LL—lateral lobes; FD—fertilisation duct; FW—first winding; SIDS—sclerotised internal duct system. Scale bars: 0.5 mm.



**Figure 16.** *Pseudopoda yunnanensis* Yang & Hu, 2001 **A** left male palp, prolateral **B** same, retrolateral. Abbreviation: ST—subtegulum. Scale bar: 0.5mm.

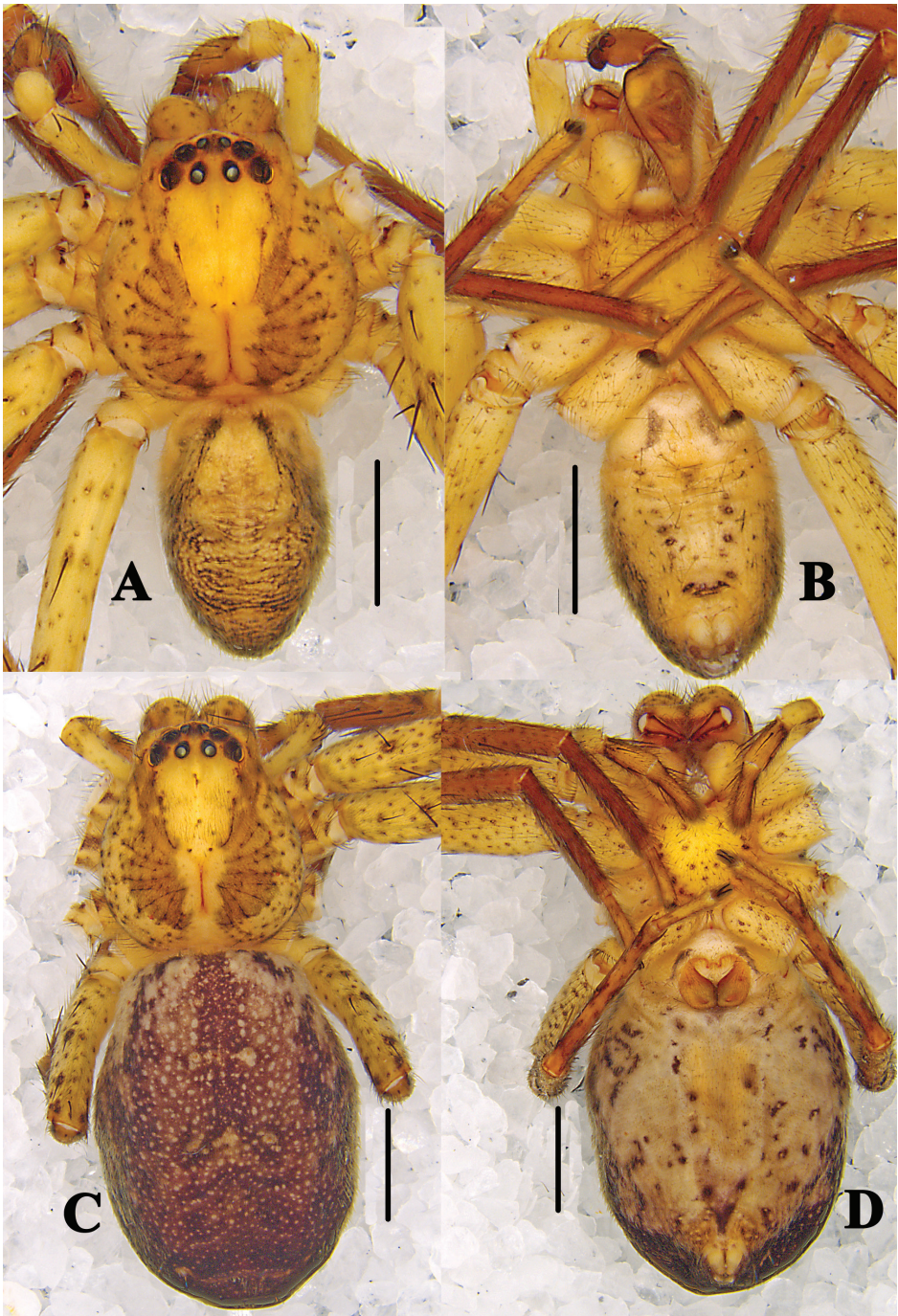


**Figure 17.** *Pseudopoda yunnanensis* Yang & Hu, 2001 **A, B** male habitus (**A** dorsal **B** ventral) **C, D** female habitus (**C** dorsal **D** ventral). Scale bars: 2 mm

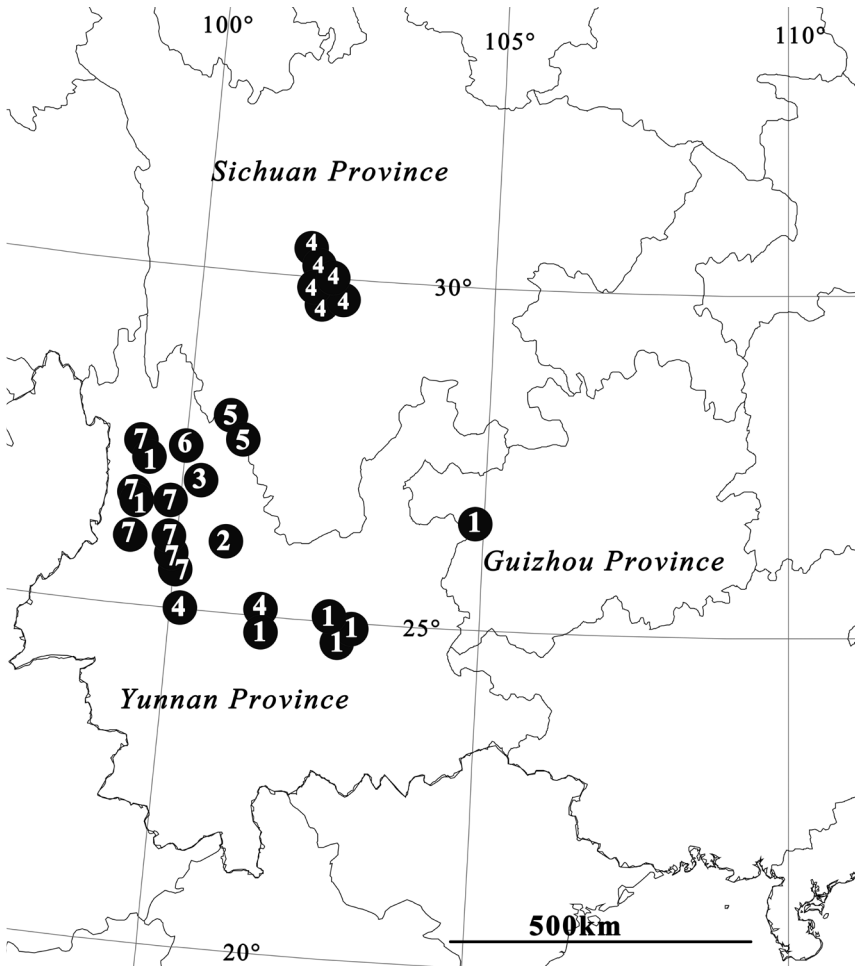


**Figure 18.** Locality records of *P. signata* group from China: 1 *P. bibulba* 2 *P. physematosa* sp. nov. 3 *P. semilunata* sp. nov. 4 *P. signata* 5 *P. wu* 6 *P. yinae* 7 *P. yunnanensis*.

Zhong & Xiaowei Cao leg. (CBEE, LJ01539-LJ01606); 18 males, 17 females, Dali Bai Autonomous Prefecture, Jianchuan County, Mt. Qianshi, 26.53°N, 99.88°E, 2647 m, 19 May 2014, Yang Zhong & Xiaowei Cao leg. (CBEE, LJ01501-LJ01534).

**Diagnosis and Description.** See Yang and Chen (2008).

**Distribution.** China (Yunnan) (Fig. 18).

## Acknowledgements

We thank Prof. Zhisheng Zhang (SWUC), Luyu Wang (SWUC), Yanchao Wang (SWUC), Kaiyi Xu (SWUC), Yang Zhong (HUST), Xiaowei Cao (CBEE), and Yang Zhu (CBEE) for providing Sparassidae specimens. We also thank Matjaž Kuntner (Evo-

lutionary Zoology Laboratory, Department of Organisms and Ecosystems Research, National Institute of Biology, Ljubljana, Slovenia) for help in improving this paper. The manuscript greatly benefited from comments by Dr Cristina Rheims (Instituto Butantan, Sao Paulo, Brazil), Dr Ivan L. F. Magalhaes (Museo Argentino de Ciencias Naturales “Bernardino Rivadavia”, Buenos Aires, Argentina), and Dr Majid Moradmand (University of Isfahan, Isfahan, Iran). This study was financially supported by the National Natural Sciences Foundation of China (NSFC-31572236/31970406/31772420).

## References

- Cao XW, Liu J, Chen J, Zheng G, Kuntner M, Agnarsson I (2016) Rapid dissemination of taxonomic discoveries based on DNA barcoding and morphology. *Scientific Reports* 6, 37066. <https://doi.org/10.1038/srep37066>
- Jäger P (2000) Two new heteropodine genera from southern continental Asia (Araneae: Sparassidae). *Acta Arachnologica* 49(1): 61–71. <https://doi.org/10.2476/asjaa.49.61>
- Jäger P (2001) Diversität der Riesenkrabbenspinnen im Himalaya – die Radiation zweier Gattungen in den Schneetropen (Araneae, Sparassidae, Heteropodinae). *Courier Forschungsinstitut Senckenberg* 232: 1–136.
- Jäger P (2015) Conductor-less and vertically niched: new species of the genus *Pseudopoda* (Araneae: Sparassidae: Heteropodinae) from Myanmar. *Arachnology* 16(9): 333–350. <https://doi.org/10.13156/ arac.2015.16.9.333>
- Jäger P, Li SQ, Krehenwinkel H (2015) Morphological and molecular taxonomic analysis of *Pseudopoda* Jäger, 2000 (Araneae: Sparassidae: Heteropodinae) in Sichuan Province, China. *Zootaxa* 3999(3): 363–392. <https://doi.org/10.11646/zootaxa.3999.3.3>
- Jäger P, Vedel V (2007) Sparassidae of China 4. The genus *Pseudopoda* (Araneae: Sparassidae) in Yunnan Province. *Zootaxa* 1623: 1–38. <https://doi.org/10.11646/zootaxa.1623.1.1>
- Jäger P, Yin C (2001) Sparassidae in China. 1. Revised list of known species with new transfers, new synonymies and type designations (Arachnida: Araneae). *Acta Arachnologica* 50: 123–134. <https://doi.org/10.2476/asjaa.50.123>
- Quan D, Zhong Y, Liu J (2014) Four *Pseudopoda* species (Araneae: Sparassidae) from southern China. *Zootaxa* 3754(5): 555–571. <https://doi.org/10.11646/zootaxa.3754.5.2>
- World Spider Catalog (2018) World Spider Catalog. Natural History Museum Bern. <http://wsc.nmbe.ch>, version 19.5 [Accessed on August 8, 2018]
- Xu X, Yin CM (2000) One new species of the genus *Heteropoda* from China (Araneae: Heteropodidae). *Acta Laser Biology Sinica* 9: 37–39.
- Yang Z, Chen L (2008) The first description of the female *Pseudopoda yunnanensis* (Araneae, Sparassidae). *Acta Zootaxonomica Sinica* 33: 810–812.
- Yang Z, Hu J (2001) A new species of the genus *Sinopoda* from China (Araneae: Heteropodidae). *Acta Arachnologica Sinica* 10(2): 18–20.
- Zhang H, Jäger P, Liu J (2017) One new *Pseudopoda* species group (Araneae: Sparassidae) from Yunnan Province, China, with description of three new species. *Zootaxa* 4318(2): 271–294. <https://doi.org/10.11646/zootaxa.4318.2.3>



# DNA barcoding of aphid-associated ants (Hymenoptera, Formicidae) in a subtropical area of southern China

Junaid Ali Siddiqui<sup>1,2</sup>, Zhilin Chen<sup>3</sup>, Qiang Li<sup>1,2</sup>, Jun Deng<sup>1,2</sup>,  
Xiaolan Lin<sup>1,2</sup>, Xiaolei Huang<sup>1,2</sup>

**1** State Key Laboratory of Ecological Pest Control for Fujian and Taiwan Crops, College of Plant Protection, Fujian Agriculture and Forestry University, Fuzhou 350002, China **2** Fujian Provincial Key Laboratory of Insect Ecology, Fujian Agriculture and Forestry University, Fuzhou 350002, China **3** Key Laboratory of Ecology of Rare and Endangered Species and Environmental Protection of Ministry of Education, Guangxi Normal University, Guilin 541004, China

Corresponding author: Xiaolei Huang ([huangxl@fafu.edu.cn](mailto:huangxl@fafu.edu.cn))

Academic editor: B. Lee Fisher | Received 12 September 2018 | Accepted 5 September 2019 | Published 9 October 2019

<http://zoobank.org/86A56794-6AD9-4275-942C-319EB72167F5>

**Citation:** Siddiqui JA, Chen Z, Li Q, Deng J, Lin X, Huang X (2019) DNA barcoding of aphid-associated ants (Hymenoptera, Formicidae) in a subtropical area of southern China. ZooKeys 879: 117–136. <https://doi.org/10.3897/zookeys.879.29705>

## Abstract

As one of the most abundant and complex groups of terrestrial insects, ants have associations with many other organismal groups, such as hemipteran insects producing honeydew. With the aim of expanding the knowledge base of ant species associated with aphids, this study analyzed mitochondrial COI barcodes of 301 ant samples for 37 aphid-associated ant species in a subtropical area of southern China. Sequence analyses revealed that the intraspecific and interspecific distances ranged from zero to 7.7% and 0.2 to 31.7%, respectively. Three barcoding approaches – Automatic Barcode Gap Discovery, Bayesian Poisson Tree Processes and Generalized Mixed Yule-coalescent – were used to help delimit ant species based on COI sequences, and their results corresponded well with most of the morphospecies. All three approaches indicate cryptic diversity may exist within *Tetramorium bicarinatum* and *Technomyrmex albipes*, with intraspecific genetic distances of 7.7% and 6.24%, respectively. Our analyses also reported five species for the first time from Fujian Province of China, and the COI sequences of nine species are newly added into the GenBank. This study provides information about species diversity of aphid-associated ants in subtropical China and compiles a DNA barcode reference library for future ant barcoding work.

## Keywords

cryptic diversity, DNA barcode, genetic distance, myrmecophily

## Introduction

Relationships between various organisms are crucial for upholding the ecological function of natural communities. The interactions between ants and aphids are classic examples of mutualism and are important to support ecosystem function (Fischer et al. 2015). The aphids have positive interactions with ants, which can play important role in their survival rate. The ant-aphid associations even have a great impact on local insect faunal diversity (Billick et al. 2007), especially dominant ants. They even determine the structure of the local ant community by interfering with the foraging of other ants (Carval et al. 2016). These interactions are very diverse and complex in nature. For a better understanding of their complex interactions, it is very important to know the species diversity of each part of this association. Ants are the part that collect honeydew of aphids and protect them from natural enemies (Stadler and Dixon 2005). The diversity of ants is highest in tropical regions, while aphids are supposed to be most diverse in temperate regions (Hölldobler and Wilson 1990, Heie 1994). As transition zones where the two groups encounter one another, subtropical regions may have an elevated diversity of ant-aphid associations. However, there have been no published studies focusing on diversity of both partners in this association. In this work, we tried to explore the diversity of aphid-associated ants in the subtropical Fujian in southern China.

Ants (Hymenoptera, Formicidae) are a dominant terrestrial insect group. They have colonized almost the entire world except Antarctica, especially in the tropical regions (Rizali et al. 2008). There are 17 subfamilies having about 13,500 described species worldwide (Bolton 2018). This group of insects has been present on Earth for about 120 Mya (Brady 2003). Ants play essential roles in seed dispersal (Hanzawa et al. 1988). Many grass species in fire-prone graze lands mainly depend on ants for their survival (Fisher et al. 2003). Also, they are efficient biocontrol agents and improve soil aeration as well (Hölldobler and Wilson 1990). For example, the predatory Asian weaver ants are the most efficient biocontrol agents of certain field crops and predatory ants of genus *Oecophylla* can control 50 different species of pests species feeding on eight tropical trees (Peng and Christian 2009, Offenberg 2014). Due to the obligatory interactions between ants, plants and other animals, the diversity of ants usually is a good indicator of the strength of ecosystems (Alonso and Agosti 2000).

Biological classification based on morphological characters has been a routine practice to identify biodiversity on the Earth. Nowadays, biodiversity quantification is a challenge for taxonomist if only based on morphological identification. The recognition of minute anatomical differences between closely related species sometimes is complicated morphologically (Ojha et al. 2014). Ants usually have different castes with apparent variations in their body structure within the same species, which makes them more diverse and challenging to identify. To overcome these problems, DNA barcoding has been shown to be a reliable technique for rapid and accurate species identification (Hebert et al. 2003a, Savolainen et al. 2005). Mitochondrial DNA (mtDNA) has been extensively used in molecular studies. A partial fragment of cytochrome c oxidase I gene (COI) is employed for easy identification of closely related or cryptic animal species along with biological diversity assessment (Hebert et al. 2004,

Ojha et al. 2014). The utility of DNA barcoding as a rapid and accurate tool for species identification is well recognized in a wide variety of animal taxa across the globe (<http://www.ibol.org/resources/>). DNA barcoding techniques have been used by some researchers in ant identification and phylogenetic analysis (Smith et al. 2005, Jansen et al. 2009, Ng'endo et al. 2013, Smith et al. 2013, Ojha et al. 2014, Chen and Zhou 2017). However, to our knowledge, little is known about the regional fauna of aphid-associated ants especially in subtropical areas.

The present study aimed to investigate the subtropical ant fauna associated with aphids with the help of DNA barcoding. Both the morphological and DNA barcoding approaches were used and results were compared. Our study provides information of species composition and species diversity of ants in a subtropical region, and a DNA library for future ant barcoding work.

## Materials and methods

### Sample collection

The ant specimens were collected from four localities (Fuzhou, Quanzhou, Shouning, Wuyishan) (Fig. 1) of the subtropical areas of Fujian Province in southern China. Specimens were collected during 2015–2017 by hand and camel hair brushes. Ant collection was based on the occurrence of aphids in different places. During our field collections, on the basis of visual observations, only the ant individuals attending aphid populations with obvious physical contact of beating aphid body by antenna and a consistent feeding on aphid honeydew were collected. All collected specimens were placed in 95% alcohol and kept in -20 °C until processed. Ant samples were identified morphologically first. The complete dataset comprises 301 individual specimens representing three subfamilies, 19 genera and 37 species (Suppl. material 2: Table S2).

### Morphological identification

The ant species were identified by Dr Chen Zhilin and Dr Zhou Shanyi (Guangxi Normal University, Guilin 541004, China). Both of them have described more than 100 ant species up till now. Their knowledge and expertise help guarantee the reliability of the morphological identification. The voucher specimens have been stored at the Insect Systematics and Diversity lab at Fujian Agriculture and Forestry University.

### DNA extraction and PCR amplification and sequencing

DNA was isolated from the leg or whole ant body using the Qiagen DNeasy kit following the manufacturer's protocols. Mainly a non-destructive DNA extraction method was used. In cases where numerous individuals from a colony were available, a destructive

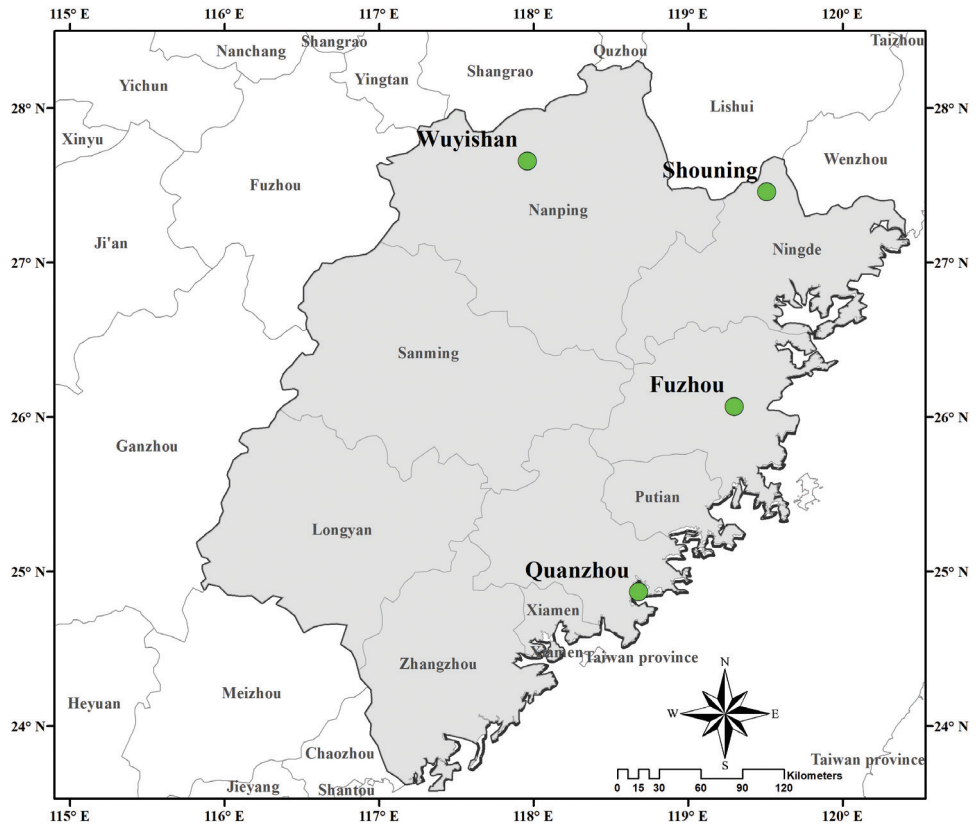


**Figure 1.** Map of Fujian Province showing the sampling sites.

technique (entire ant crushed) was preferred. Polymerase chain reactions (PCR) were carried out in a total reaction volume of 50  $\mu\text{L}$  containing 8  $\mu\text{L}$  of dNTP mixture (2.5 mM), 5  $\mu\text{L}$  of 10 $\times$  PCR buffer (25 mM  $\text{Mg}^{2+}$ ), 10 pmol of each primer and 1 unit of Taq DNA polymerase (TaKaRa Bio Inc., Otsu, Japan). The reaction conditions for the COI gene include: initial denaturation at 95  $^{\circ}\text{C}$  for 5 min; 35 cycles of 94  $^{\circ}\text{C}$  for 1 min, 50  $^{\circ}\text{C}$  for 1 min (denaturing) and 72  $^{\circ}\text{C}$  for 1 min (extension); a final elongation at 72  $^{\circ}\text{C}$  for 7 min reactions were done using the ProFlex PCR system. Standard primers used were: forward primer LepF1 (ATTCAACCAATCATAAAGATATTGG) and reverse primer LepR1 (TAAACTTCTGGATGTCCAAAAAATCA) (Hebert et al. 2003b). The amplified products were visualized on 1% agarose gel stained with ethidium bromide. PCR purified products were sent to a (Sangon Biotech (Shanghai) Co., Ltd) for bidirectional sequencing. Obtained sequences were manually edited in BioEdit version 7.0.5.0 (Hall 1999) and aligned with MAFFT v7 (Katoh et al. 2009). The resultant sequence fragments were around 600–700 base pairs (bp). These sequences were identified as COI fragments for the ants with BLAST procedure searched in public database (Altschul et al. 1990). The aligned sequences were 593 bp long and free from gaps after trimming. All sequences were deposited in the GenBank under accession number (MH754200–MH754506) and BOLD under process IDs (DBAFC001-19-DBAFC301-19).

## Sequence analysis and species delimitation

A total of 301 sequences from our study (Suppl. material 2: Table S2) and 52 COI sequences (mostly sequences with BLAST results) collected from GenBank were included in further analyses. Moreover, *Vespula germanica* (KR788643.1) and *Vespa velutina* (LC170010.1) were used as outgroups. Pairwise intraspecific genetic distance was calculated between all sequences of same species, while pairwise interspecific distance between species of the same genera and all species of a subfamily under Kimura-2-Parameter (K2P) and Proportional (p-distance) distances models were calculated using MEGA 7.0 (Kumar et al. 2016). The sequences were without stop codons, frameshift mutations or a high dN/dS ratio, which helped us to conclude that they were mitochondrial and not nuclear mitochondrial DNA segment (NUMTs) (Bensasson et al. 2001, Calvignac et al. 2011). Analyzing the unidentified NUMTs as the true mitochondrial sequences could result in the inappropriate identification of cryptic species (Song et al. 2008). Based on our analysis performed, we are confident that the sequences analyzed here are mitochondrial in origin.

Automatic Barcode Gap Discovery (ABGD) (Puillandre et al. 2012), Bayesian Poisson Tree Processes (bPTP) (Zhang et al. 2013) and Generalized Mixed Yule-coalescent (GMYC) (Pons et al. 2006) were used for species delimitation. The ABGD method was performed for detecting the barcode gaps and identification of distinct clusters of COI sequences. The maximum value of intraspecific divergence was fixed between 0.001 and 0.1. Moreover, the K2P model (Kimura 1980) was used along with the default gap width of  $X=1.5$ . In the PTP analysis, distinctive haplotype sequences were obtained using DnaSP 6.10 (Librado and Rozas 2009), then phylogenetic trees were constructed based on these haplotype sequences by using raxmlGUI v1.5 (Stamatakis 2014). The GTR+I+G model was the best model obtained by jModel test v2.1.7 (Posada 2008). This method is implemented in an online web server (<http://species.h-its.org/>). For the GMYC model, firstly a linearized Bayesian phylogenetic tree was calculated in BEAST v1.8.4 using a Yule pure birth model tree prior. Settings in BEAUTi v1.8.4 were: best substitution model, estimated base frequencies, four gamma categories. An uncorrelated relaxed log-normal clock model was used with a log-normal relaxed distribution. All further settings were left as defaults. The Markov Chain Monte Carlo length was 100,000,000 generations with log parameters every 10,000 generations. The evaluation of ESS values and trace files of runs were performed in Tracer v1.6. Tree files obtained from BEAST analysis were combined using the LogCombiner prior to generating the final ultra-metric tree with 20% burn-in, 0.5 posterior probability limit, and node heights of target tree were performed in TreeAnnotator v1.8.4. Single-threshold GMYC analyses were carried out in R studio using the PARAN, APE and SPLITS packages.

The maximum likelihood (ML) (Tamura et al. 2011) and Bayesian approaches (Huelsenbeck and Ronquist 2001) were also used to build phylogenetic trees. The ML tree was constructed based on haplotype sequences by using raxmlGUI v1.5 (Stamatakis 2014). The best nucleotide substitution model for the COI sequences for ML analysis was selected on the basis of the Bayesian information criterion value by jModeltest v2.1.7 (Posada 2008). The most suitable model for ML analysis was GTR+I+G for haplotypes among the 301 sequences identified by DnaSP 6.10 (Librado and Rozas 2009).

A BI tree was reconstructed under the GTR+I+G (Bollback 2002) model (obtained by jModel Test) for all sequence of current study and combined with GenBank sequences in MrBayes v3.2.6 (Ronquist et al. 2012) with two independent runs and each run employing four Metropolis Coupled Monte Carlo Markov chains (three heated and one cold). The number of generations for the total analysis was set at 100 million. The burn-in value was set as 25% and other parameters were left as default options. The evaluating effective sample size values were analyzed in Tracer v1.6 (Rambaut et al. 2014), and generated trees were visualized in FigTree v1.4.3 (<http://tree.bio.ed.ac.uk/software/figtree>) and edited in MEGA 7.0 (Kumar et al. 2016).

## Results

A total of 37 ant species associated with aphids were identified morphologically, belonging to 19 genera of three subfamilies, viz., Dolichoderinae (8), Formicinae (16) and Myrmicinae (13) (Suppl. material 2: Table S2). COI sequences were obtained from all the 301 samples used. The newly acquired 301 COI sequences were deposited in GenBank and BOLD. BLAST analysis in the NCBI database showed overall 84–100% nucleotide identity between the newly acquired sequences and the previously published COI sequences in GenBank. In this study, the COI sequences of nine species, namely *Aphaenogaster smythiesii*, *Crematogaster nicobarensis*, *C. vitiosus*, *C. egidyi*, *C. osakensis*, *Monomorium chinense*, *Pheidole fervida*, *P. smythiesii* and *Nylanderia flaviabdominis* were newly added in GenBank. Our results also found five species, namely *Formica sinae*, *N. flaviabdominis*, *Prenolepis emmae*, *C. egidyi*, and *Pheidole smythiesii* that were newly recorded from Fujian Province of China.

The specimens collected from the Wuyishan Nature Reserve showed maximum species diversity up to 21 species, whereas the other two localities, Shouning and Fuzhou, had almost similar species diversity with 18 and 16 species respectively. The subfamily Myrmicinae had highest number of taxa in our study, with seven genera and 13 species occupying 55.48% of the total 301 samples. The genus *Crematogaster* was the most dominate group representing 23% of total samples. Moreover, three ant species *P. punctatus*, *C. egidyi* and *P. noda* showed the most aphid associations with 17, 16 and 12 aphid species respectively (Suppl. material 1: Table S1).

## Genetic distances

Intraspecific divergences were calculated for all species except those with only one sequence while interspecific distances were calculated for subfamilies and genera using p-distance and K2P model (Table 1). Moreover, we found that the values of the genetic distance calculated by the K2P model were slightly higher than the p-distance. The results of both models (p-distance and K2P model) were similar (Suppl. material 3: Figure S1), so for further analysis the K2P distance only was used. The intraspecific

**Table 1.** COI K2P genetic distances for aphid-associated ant species in this study. Intraspecific distances were calculated within the same species and interspecific distances between species of same genus. Only species with two or more sequences were included.

Taxon name	Number of sequences	Intraspecific distance			Interspecific distance	Number of haplotypes
		min.	max.	mean	range	
<b>Dolichoderinae</b>					0.137–0.27	
<i>Iridomyrmex anceps</i>	7	0	0	0		1
<i>Liometopum sinense</i>	2	0	0	0		1
<i>Ochetellus glaber</i>	6	0	0.005	0.002		2
<i>Tapinoma melanocephalum</i>	9	0	0.034	0.008	0.139–0.258	2
<i>Technomyrmex albipes</i>	8	0	0.062	0.033		2
<b>Formicinae</b>					0.048–0.316	
<i>Camponotus japonicus</i>	9	0	0.007	0.003	0.195–0.251	5
<i>Camponotus mitis</i>	2		0.008	0.008	0.195–0.251	2
<i>Camponotus nicobarensis</i>	5	0	0.002	0.001	0.195–0.251	2
<i>Formica japonica</i>	14	0	0	0	0.002–0.005	1
<i>Formica sinae</i>	12	0	0.005	0.002	0.002–0.005	6
<i>Lepisiota rothmeyei</i>	2	0	0	0	0.002–0.005	1
<i>Nylanderia flavipes</i>	10	0	0.022	0.010	0.139–0.222	2
<i>Nylanderia bourbonica</i>	11	0	0.002	0.001	0.139–0.222	2
<i>Nylanderia flaviabdominis</i>	6	0	0.013	0.007	0.139–0.222	2
<i>Polyrhachis dives</i>	13	0	0.015	0.006	0.175–0.184	3
<i>Polyrhachis illaudata</i>	3	0	0.002	0.001	0.175–0.184	2
<i>Prenolepis emmae</i>	6	0	0.003	0.001		3
<b>Myrmicinae</b>					0.056–0.317	
<i>Aphaenogaster smythiesii</i>	2	0	0	0		1
<i>Crematogaster egidyi</i>	53	0	0.015	0.007	0.056–0.229	6
<i>Crematogaster osakensis</i>	5	0	0.003	0.001	0.056–0.229	3
<i>Crematogaster rogenhoferi</i>	10	0	0.005	0.002	0.056–0.229	2
<i>Monomorium chinense</i>	3	0	0	0	0.175	1
<i>Pheidole fervida</i>	2	0	0	0	0.167–0.199	1
<i>Pheidole noda</i>	30	0	0.020	0.009	0.167–0.199	5
<i>Pristomyrmex punctatus</i>	46	0	0.058	0.016		8
<i>Tetramorium wroughtonii</i>	2	0	0	0	0.169–0.218	1
<i>Tetramorium bicarinatum</i>	9	0	0.077	0.043	0.169–0.218	2
<i>Tetramorium caespitum</i>	3	0	0.020	0.013	0.169–0.218	2
<b>Total</b>					0.048–0.345	

distances for most species were lower than 1%, the maximum intraspecific distance varied from 1.3% (e.g., *N. flaviabdominis*) to 7.7% (*Tetramorium bicarinatum*), and the mean intraspecific distances varied from 0.01 (*Nylanderia flavipes*) to 0.043 (*Tetramorium bicarinatum*). The maximum interspecific distances for the three subfamilies were: Myrmicinae 31.7%, Formicinae 31.6% and Dolichoderinae 27%. For some abundant genera based on sample numbers, the interspecific distances were: *Camponotus* 0.195–0.251, *Crematogaster* 0.056–0.229, *Nylanderia* 0.139–0.222, *Tetramorium* 0.169–0.218, *Pheidole* 0.167–0.199, and *Formica* 0.002–0.005. Overall interspecific distance of the 301 COI sequences ranged from 0.048 to 0.345 (Table 1).

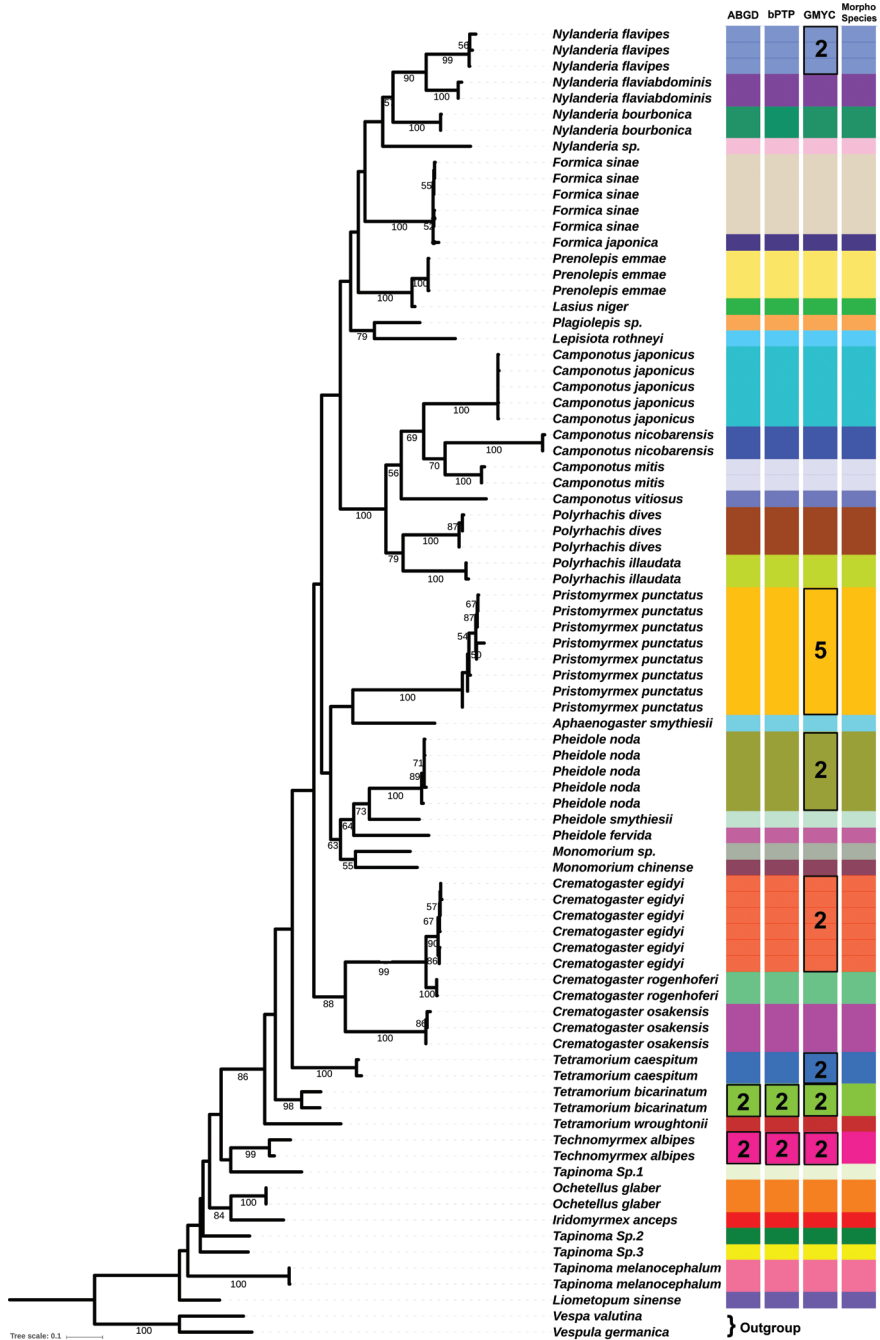


**Figure 2.** Maximum likelihood haplotype tree for the COI gene. Bootstrap values higher than 50 are displayed. Color strips on the right side represent the MOTUs produced by ABGD, bPPT and GMYC methods; extreme right one indicates the morphologically identified species. Black square around some bars indicates differences between the MOTUs and morphospecies. Values inside the square indicate the number of MOTUs produced by different approaches.

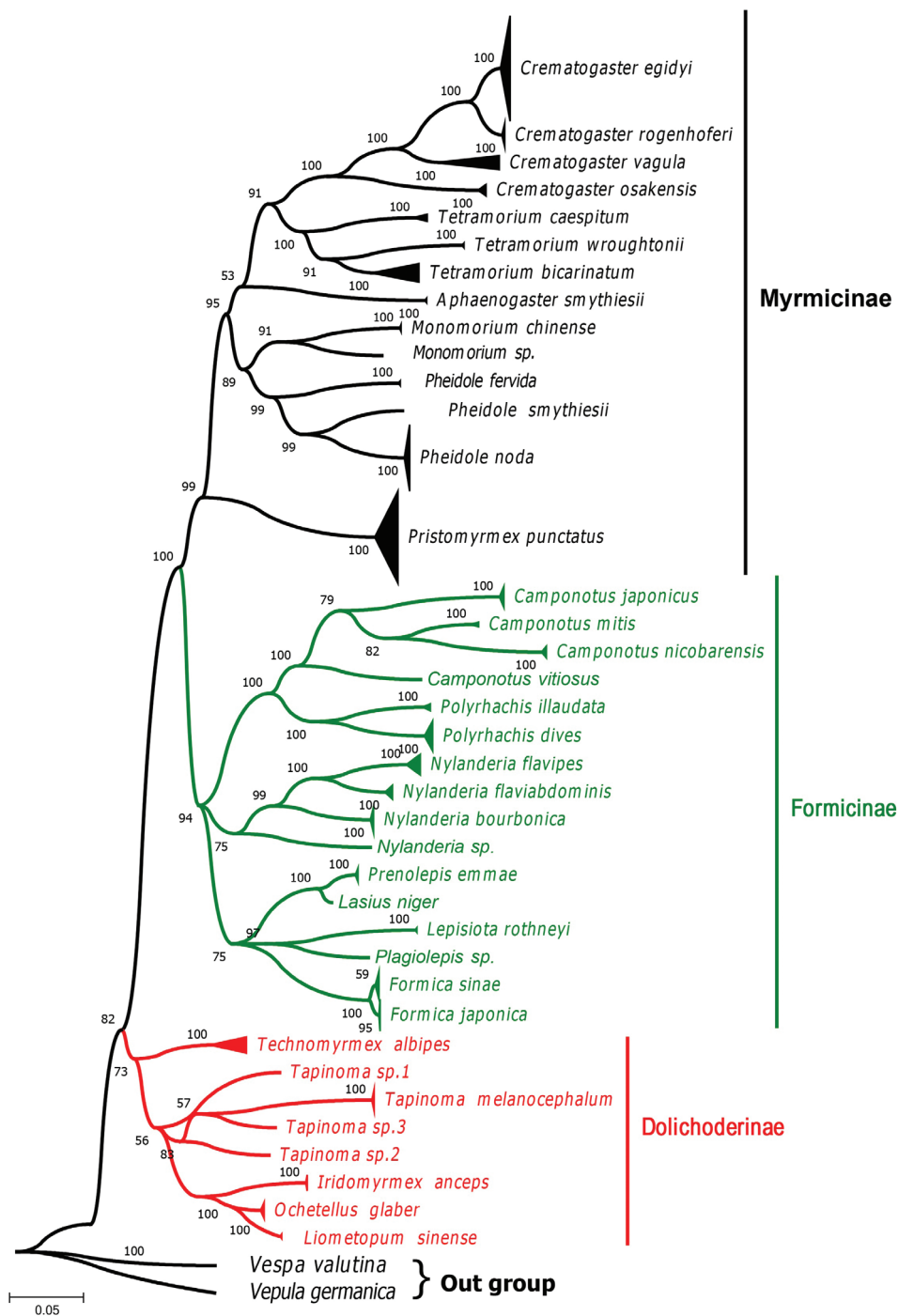


**Figure 3.** Bayesian inference tree for the COI gene. The numbers on the branches are Bayesian posterior probabilities. The black, green and red colours indicate the species under each subfamily, respectively.

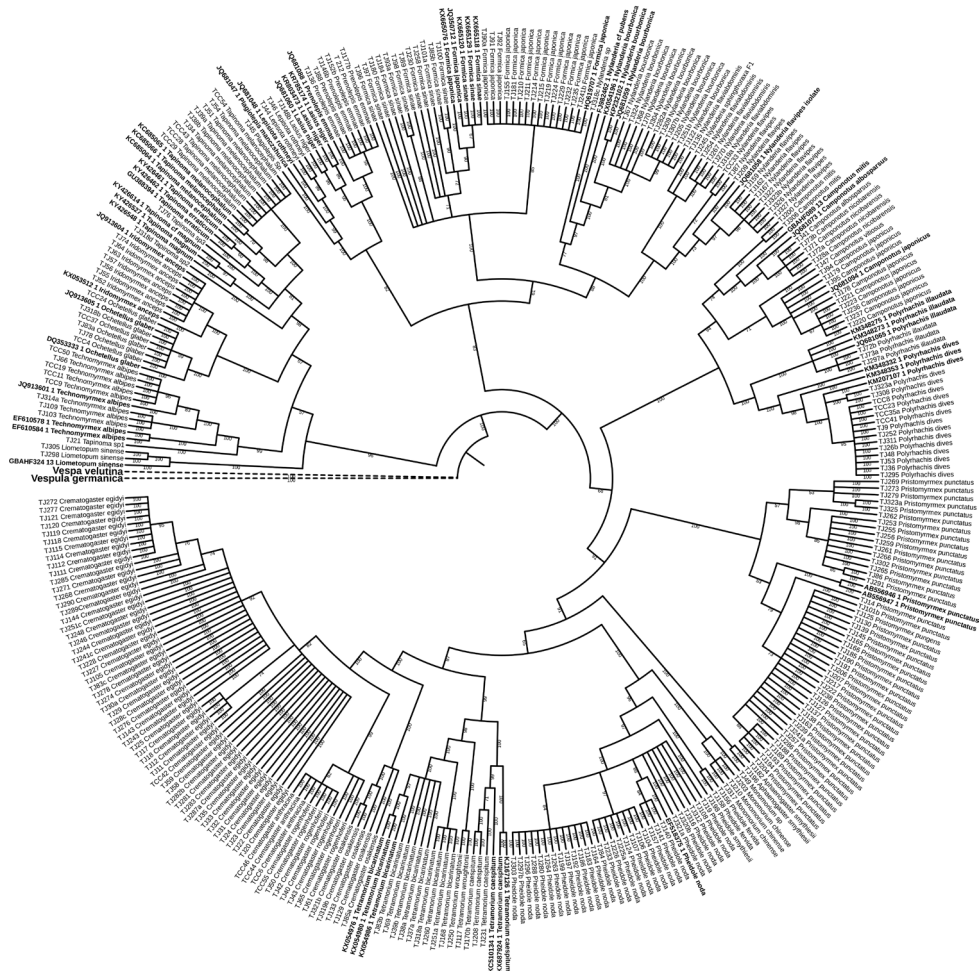


**Figure 4.** Bayesian Inference tree combined with 301 COI sequences from the current study and 52 COI sequences from the GenBank. Values besides the branches indicate Bayesian posterior probabilities. Dotted lines are indicating the outgroups. Bold labels indicate the sequences from the GenBank.

## Species delimitations

The ABGD approach produced 39 molecular operational taxonomic units (MOTUs) or genetic groups. Among them, 35 MOTUs matched with the morphospecies identification, which represented 89.7% of the morphospecies in total. The other four MOTUs might indicate species differentiation for some morphospecies (Fig. 2). These included *T. caespitum* and *T. albipes*, which were each divided into two groups. The bPTP approach yielded the same species delimitation result as the ABGD, also dividing the 301 sequences into 39 putative species and 35 of them corresponding well to morphological identifications. The GMYC method produced different results: the 301 sequences were grouped into 47 MOTUs; 30 MOTUs were congruent with the ABGD and bPTP as well as the morphospecies (Fig. 2). Contrary to the other two approaches, *P. punctatus*

was divided into five separate MOTUs. Moreover, species *C. egidyi*, *N. flavipes*, *P. noda*, *T. caespitum*, *T. albipes*, *T. bicarinatum* were each separated into two groups.

ML and Bayesian Inference analysis applied to all 303 sequences along with two outgroups created monophyletic groups. As the phylogenetic trees (Figs 2–4, Suppl. material 4: Figure S2) show, all the 37 morphospecies were clustered into three subfamilies, Dolichoderinae, Formicinae and Myrmicinae. The relationships between these three subfamilies revealed in our study were similar to those reported in previous studies (Kück et al. 2011, Reemer 2013). Different clades or groups in the phylogenetic trees corresponded well with the MOTUs produced by the ABGD, bPTP, and GMYC methods.

## Discussion

Ants are eusocial insects having the high degree of caste polymorphism with various distinct anatomical characters and size variations (Wheeler 1986, Mysore et al. 2009, Wills et al. 2018). The complexity of ant groups usually makes them difficult to identify to species only based on morphological characters. For example, species of genus *Crematogaster* have been reported to be morphologically diverse and having cryptic species with high genetic intraspecific variation (Blaimer 2012). There are few studies that combine morphological identification with DNA barcode analysis for ants (Ng'endo et al. 2013, Kanturski et al. 2018). However, various barcoding approaches of species delimitation can be more suitable and useful in describing ant species diversity (Smith et al. 2005, Ojha et al. 2014). Our paper may be the first study of a regional fauna of aphid-associated ants to use a combined species delimitation approach.

Most of the morphospecies identified were supported by DNA barcoding approaches. According to the Guénard and Dunn (2012) Fujian Province has 184 ant species and this study added five new ant species (*F. siniae*, *N. flaviabdominis*, *P. emmae*, *C. egidyi* and *P. smythiesii*) to the provincial ant fauna. Moreover, COI sequences of nine species (*C. nicobarensis*, *C. vitiosus*, *A. smythiesii*, *C. egidyi*, *C. osakensis*, *M. chinense*, *N. flaviabdominis*, *P. fervida* and *P. smythiesii*) were newly added into the GenBank and BOLD databases. Geographically, we also found highest species diversity in the Wuyishan Nature Reserve with 21 species. This is related to the fact that the Wuyishan Nature Reserve has the highest habit heterogeneity compared to the other three geographic areas (Ding et al. 2015).

In the present study, three ant species (*P. punctatus*, *C. egidyi* and *P. noda*) were found associated with a maximum number of aphid species on various host plants (Suppl. material 1: Table S1). All of them belong to the subfamily Myrmicinae. The parthenogenetic ant species *P. punctatus* is known as seed harvester ants; they are abundantly present in forests and natural vegetation (Satow et al. 2013; Zhu and Wang 2018). They have the ability to fuse their colony into neighbouring colonies of same species (Satow et al. 2013), which may make them more abundant. In a previous study *P. punctatus* was found to be the most dominant ant in natural grassland in Japan (Suetsugu 2015). In the current study this species is mainly found in natural vegetation in Shouning and Wuyishan Nature Reserve interacting with 17 aphid species. Due to their high abundance, this species was found as the most dominant aphid-associated

ant in our study areas. *Crematogaster egidyi* is known as an aggressive predatory arboreal ant species (Longino 2003). They are considered to be strong and aggressive towards other dominant ant species and compete for food and space (Richard et al. 2001). In the current study *C. egidyi* was found associated with 16 species of aphids. In our sampling sites this species was also found dominant and aggressive towards other ant foragers, which may influence the local ant diversity. *Pheidole noda* is a seed dispersal ant species mostly found in the open lands and forest vegetation (Yamawo et al. 2012) and mainly distributed in the east Asian countries (Sarnat et al. 2015). It has been found abundant from Iwo-jima island of Japan (Ikudome and Yamane 2007) and also reported from rainforest of Yuanan, China (Liu et al. 2015). In the current study, *P. noda* was also found abundantly associated with 12 aphid species on various host plants in the Wuyishan Nature Reserve and mountainous areas of Shouning. It was observed that these three species associated with the most aphids, mainly found in natural habitats, and therefore may influence other aphid-associated ant species.

Species delineation and identification on the basis of DNA sequence distance analysis, like the DNA barcoding gap (Hebert et al. 2003b, Hebert et al. 2004) and other related methodologies (Ferri et al. 2009), have been used repeatedly to develop effective standards for species delimitation. Genetic distance-based methods are regularly being used in DNA barcoding studies of various groups to indicate the possible incidence of cryptic species diversity among morphologically similar species (Lefébure et al. 2006), including termites (Roy et al. 2014), butterflies (Ashfaq et al. 2013) and snails (Prévot et al. 2013). Genetic divergence of ant species was previously calculated by different researchers on the basis of COI gene sequences, but they focused on ant groups solely (Ng'endo 2011, Ojha et al. 2014). Actually, the interactions between ants and other insect groups, for example aphids, are critical to regional community function. Considering that morphologically similar ant species may occur in a same area and sometimes co-occur with same aphid species, molecular identification is helpful to understand the regional diversity of aphid-associated ants. In this study, we observed that several morphospecies produced multiple MOTUs using the different barcoding methods; also, the MOTUs were separated in the phylogenetic tree analysis (Figs 2–4, Suppl. material 4: Figure S2). The ABGD, bPTP and GMYC methods all supported *T. albipes* and *T. bicarinatum* as each having two clear MOTUs. These two species showed higher mean (>3.34%) as well as maximum (>6.24%) intraspecific genetic distances. The GMYC method revealed five more species with multiple MOTUs: *P. punctatus*, *N. flavipes*, *P. noda*, *T. caespitum* and *C. egidyi*. The maximum intraspecific distances were 5.84%, 2.19%, 2.01%, 2.01% and 1.51% respectively; however, the mean intraspecific genetic distances were all below 1.55%, which is lower than the practical criterion for insect species delimitation (Footit et al. 2008). This may be the reason that the ABGD and bPTP methods found them each to be a single MOTUs.

The comparative performance of different algorithms to species delineation has been studied previously. ABGD considered as the most computationally effective approach. It needs a priori specification of an intraspecific distance threshold, and this method is based on the genetic distances calculated from a single locus (Puillandre et al. 2012). Empirical studies have revealed that the GMYC approach tends to over-split

species compared to alternative methods of species delimitation (Esselstyn et al. 2012, Paz and Crawford 2012, Sauer and Hausdorf 2012, Talavera et al. 2013). Other studies indicate that the ABGD and bPTP may be better strategies and that these encounter less computing errors than GMYC (Puillandre et al. 2012, Luo et al. 2018). Our study also showed GMYC delimited more MOTUs. However, considering GMYC combines the Yule model of species birth with neutral coalescent model of intraspecific branching, its results may also have implications for understanding population divergence for some species. For example, previous studies reported diverse cryptic species within the *T. caespitum* complex (Wagner et al. 2018). In this study, the individuals of *T. caespitum* were grouped into two MOTUs by GMYC, and the maximum intraspecific genetic distance was 2.0%, which may also indicate possible differentiation within this species.

The ML and BI phylogenetic analysis produced almost same topologies on the basis of the COI sequences and produced two discrete clades. One clade included two putative sister clades representing the subfamilies Myrmicinae and Formicinae (Figs 3, 4). It has been thought that the two subfamilies evolved from a common ancestor (Brady et al. 2006, LaPolla et al. 2010, Ward et al. 2015). Moreover, a second cluster comprised species of subfamily Dolichoderinae. The grouping of the six genera presented in this study was similar to that reported by Chiotis et al. (2000), but our DNA sequence data alone provide insufficient support to comment on relationships among the ant subfamilies. Leaving aside the assemblages supported by lower posterior probability values, on the basis of the sole barcode sequence data set, the three subfamilies (Dolichoderinae, Formicinae, and Myrmicinae) mostly appear as monophyletic. The overall topology of phylogenetic trees corresponds well with most results of ABGD, bPTP and GMYC species delimitation approaches. For the new MOTUs we found beyond the known morphospecies further DNA diagnostics based on more sampling and morphological work are needed to verify whether they can be well-defined species.

## Acknowledgements

We would like to thank help from Junjie Li, Qian Liu, Muhammad Qasim, Habib Ali and Mubasher Hussain during this work. This work was supported by National Key R&D Program of China (2016YFE0203100) and Open Fund of Fujian Provincial Key Laboratory of Insect Ecology, Fujian Agriculture and Forestry University.

## References

- Alonso LE, Agosti D (2000) Biodiversity studies, monitoring, and ants: an overview. *ants: standard methods for measuring and monitoring biodiversity*. Smithsonian Institution, Washington, 1–8.
- Altschul SF, Gish W, Miller W, Myers EW, Lipman DJ (1990) Basic local alignment search tool. *Journal of Molecular Biology* 215: 403–410. [https://doi.org/10.1016/S0022-2836\(05\)80360-2](https://doi.org/10.1016/S0022-2836(05)80360-2)

- Ashfaq M, Akhtar S, Khan AM, Adamowicz SJ, Hebert PDN (2013) DNA barcode analysis of butterfly species from Pakistan points towards regional endemism. *Molecular Ecology Resources* 13: 832–843. <https://doi.org/10.1111/1755-0998.12131>
- Bensasson D, Zhang D-X, Hartl DL, Hewitt GM (2001) Mitochondrial pseudogenes: evolution's misplaced witnesses. *Trends in Ecology & Evolution* 16: 314–321. [https://doi.org/10.1016/S0169-5347\(01\)02151-6](https://doi.org/10.1016/S0169-5347(01)02151-6)
- Billick I, Hammer S, Reithel JS, Abbot P (2007) Ant–aphid interactions: Are ants friends, enemies, or both? *Annals of the Entomological Society of America* 100: 887–892. [https://doi.org/10.1603/0013-8746\(2007\)100\[887:AIAAFE\]2.0.CO;2](https://doi.org/10.1603/0013-8746(2007)100[887:AIAAFE]2.0.CO;2)
- Blaimer BB (2012) Acrobat ants go global – Origin, evolution and systematics of the genus *Crematogaster* (Hymenoptera: Formicidae). *Molecular Phylogenetics and Evolution* 65: 421–436. <https://doi.org/10.1016/j.ympev.2012.06.028>
- Bollback JP (2002) Bayesian model adequacy and choice in phylogenetics. *Molecular Biology and Evolution* 19: 1171–1180. <https://doi.org/10.1093/oxfordjournals.molbev.a004175>
- Bolton B (2018) An online Catalog of the Ants of the World. <https://www.antweb.org/world.jsp>
- Brady SG (2003) Evolution of the army ant syndrome: The origin and long-term evolutionary stasis of a complex of behavioral and reproductive adaptations. *Proceedings of the National Academy of Sciences* 100: 6575–6579. <https://doi.org/10.1073/pnas.1137809100>
- Brady SG, Schultz TR, Fisher BL, Ward PS (2006) Evaluating alternative hypotheses for the early evolution and diversification of ants. *Proceedings of the National Academy of Sciences* 103: 18172–18177. <https://doi.org/10.1073/pnas.0605858103>
- Brown DJ, Heal G (1979) Equity, efficiency and increasing returns. *The Review of Economic Studies* 46: 571. <https://doi.org/10.2307/2297028>
- Calvignac S, Konecny L, Malard F, Douady CJ (2011) Preventing the pollution of mitochondrial datasets with nuclear mitochondrial paralogs (numts). *Mitochondrion* 11: 246–254. <https://doi.org/10.1016/j.mito.2010.10.004>
- Carval D, Cotté V, Resmond R, Perrin B, Tixier P (2016) Dominance in a ground-dwelling ant community of banana agroecosystem. *Ecology and Evolution* 6: 8617–8631. <https://doi.org/10.1002/ece3.2570>
- Chen Y, Zhou S (2017) Phylogenetic relationships based on DNA barcoding among 16 species of the ant genus *Formica* (Hymenoptera: Formicidae) from China. *Journal of Insect Science* 17: 117. <https://doi.org/10.1093/jisesa/iex092>
- Chiotis M, Jermiin LS, Crozier RH (2000) A Molecular framework for the phylogeny of the ant subfamily Dolichoderinae. *Molecular Phylogenetics and Evolution* 17: 108–116. <https://doi.org/10.1006/mpev.2000.0821>
- Ding H, Yang YF, Xu HG (2015) Species composition and community structure of the typical evergreen broad-leaved forest in the Wuyi Mountains of southeastern China. *Acta Ecologica Sinica* 35: 1142–1154. <https://doi.org/10.5846/stxb201305050924>
- Esselstyn JA, Evans BJ, Sedlock JL, Anwarali Khan FA, Heaney LR (2012) Single-locus species delimitation: a test of the mixed Yule-coalescent model, with an empirical application to Philippine round-leaf bats. *Proceedings of the Royal Society B: Biological Sciences* 279: 3678–3686. <https://doi.org/10.1098/rspb.2012.0705>
- Ferri E, Barbuto M, Bain O, Galimberti A, Uni S, Guerrero R, Ferté H, Bandi C, Martin C, Casiraghi M (2009) Integrated taxonomy: traditional approach and DNA barcoding for

- the identification of filarioid worms and related parasites (Nematoda). *Frontiers in Zoology* 6: 1. <https://doi.org/10.1186/1742-9994-6-1>
- Fischer CY, Vanderplanck M, Lognay GC, Detrain C, Verheggen FJ (2015) Do aphids actively search for ant partners? *Insect Science* 22: 283–288. <https://doi.org/10.1111/1744-7917.12125>
- Fisher R, Vigilante T, Yates C, Russell-Smith J (2003) Patterns of landscape fire and predicted vegetation response in the North Kimberley region of Western Australia. *International Journal of Wildland Fire* 12: 369. <https://doi.org/10.1071/WF03021>
- Footitt RG, Maw HEL, Von Dohlen OHLEN CD, Hebert PDN (2008) Species identification of aphids (Insecta: Hemiptera: Aphididae) through DNA barcodes. *Molecular Ecology Resources* 8: 1189–1201. <https://doi.org/10.1111/j.1755-0998.2008.02297.x>
- Guénard B, Dunn RR (2012) A checklist of the ants of China. *Zootaxa* 3558: 1–77. <https://doi.org/10.11646/zootaxa.3558.1.1>
- Hall TA (1999) BioEdit: a user-friendly biological sequence alignment editor and analysis program for Windows 95/98/NT. *Nucleic Acids Symposium Series* 41: 95–98.
- Hanzawa FM, Beattie AJ, Culver DC (1988) Directed dispersal: demographic analysis of an ant-seed mutualism. *The American Naturalist* 131: 1–13. <https://doi.org/10.1086/284769>
- Hebert PDN, Cywinska A, Ball SL, deWaard JR (2003a) Biological identifications through DNA barcodes. *Proceedings of the Royal Society B: Biological Sciences* 270: 313–21. <https://doi.org/10.1098/rspb.2002.2218>
- Hebert PDN, Ratnasingham S, de Waard JR (2003b) Barcoding animal life: cytochrome c oxidase subunit 1 divergences among closely related species. *Proceedings of the Royal Society B: Biological Sciences* 270: 96–99. <https://doi.org/10.1098/rsbl.2003.0025>
- Hebert PDN, Stoeckle MY, Zemplak TS, Francis CM (2004) Identification of birds through DNA barcodes. *PLoS Biology* 2: e312. <https://doi.org/10.1371/journal.pbio.0020312>
- Heie OE (1994) Aphid ecology in the past and a new view on the evolution of Macrosiphini. Individuals, populations and patterns in ecology. Intercept Ltd, Andover, Hampshire, 409–418.
- Hölldobler B, Wilson EO (1990) *The ants*. Belknap Press of Harvard University Press, 732 pp.
- Huelsenbeck JP, Ronquist F (2001) MRBAYES: Bayesian inference of phylogenetic trees. *Bioinformatics* 17: 754–755. <https://doi.org/10.1093/bioinformatics/17.8.754>
- Ikudome S, Yamane S (2007) Ants, wasps and bees of Iwo Jima, Northern Ryukyus, Japan (Hymenoptera, Aculeata). *Bulletin of the Institute, Minami-Kyushu Regional Science, Kagoshima Women's Junior College* 23: 1–7.
- Jansen G, Savolainen R, Vepsäläinen K (2009) DNA barcoding as a heuristic tool for classifying undescribed Nearctic *Myrmica* ants (Hymenoptera: Formicidae). *Zoologica Scripta* 38: 527–536. <https://doi.org/10.1111/j.1463-6409.2009.00386.x>
- Kanturski M, Lee Y, Choi J, Lee S (2018) DNA barcoding and a precise morphological comparison revealed a cryptic species in the *Nippolachnus piri* complex (Hemiptera: Aphididae: Lachninae). *Scientific Reports* 8: 8998. <https://doi.org/10.1038/s41598-018-27218-2>
- Katoh K, Asimenos G, Toh H (2009) Multiple alignment of DNA sequences with MAFFT. In: Posada D (Ed.) *Bioinformatics for DNA sequence analysis*. Humana Press, Totowa, NJ, 39–64. [https://doi.org/10.1007/978-1-59745-251-9\\_3](https://doi.org/10.1007/978-1-59745-251-9_3)
- Kimura M (1980) A simple method for estimating evolutionary rate of base substitutions through comparative studies of nucleotide sequences. *Journal of Molecular Evolution* 16: 111–120. <https://doi.org/10.1007/BF01731581>

- Kück P, Garcia FH, Misof B, Meusemann K (2011) Improved phylogenetic analyses corroborate a plausible position of *martialis* heureka in the ant tree of life. PLoS ONE 6: e21031. <https://doi.org/10.1371/journal.pone.0021031>
- Kumar S, Stecher G, Tamura K (2016) MEGA7: molecular evolutionary genetics analysis version 7.0 for bigger datasets. Molecular Biology and Evolution 33: 1870–1874. <https://doi.org/10.1093/molbev/msw054>
- LaPolla JS, Cheng CH, Fisher BL (2010) Taxonomic revision of the ant (Hymenoptera: Formicidae) genus *Paraparatrechina* in the Afrotropical and Malagasy regions. Zootaxa 2387: 1–27. <https://doi.org/10.11646/zootaxa.2387.1.1>
- Lefébure T, Douady CJ, Gouy M, Gibert J (2006) Relationship between morphological taxonomy and molecular divergence within Crustacea: Proposal of a molecular threshold to help species delimitation. Molecular Phylogenetics and Evolution 40: 435–447. <https://doi.org/10.1016/j.ympev.2006.03.014>
- Librado P, Rozas J (2009) DnaSP v5: a software for comprehensive analysis of DNA polymorphism data. Bioinformatics 25: 1451–1452. <https://doi.org/10.1093/bioinformatics/btp187>
- Liu C, Guénard B, Garcia FH, Yamane S, Blanchard B, Yang D-R, Economo E (2015) New records of ant species from Yunnan, China. ZooKeys: 17–78. <https://doi.org/10.3897/zookeys.477.8775>
- Longino JT (2003) The *Crematogaster* (Hymenoptera, Formicidae, Myrmicinae) of Costa Rica. Zootaxa 150: 1–150. <https://doi.org/10.11646/zootaxa.151.1.1>
- Luo A, Ling C, Ho SYW, Zhu C-D (2018) Comparison of methods for molecular species delimitation across a range of speciation scenarios. Systematic Biology 67: 830–846. <https://doi.org/10.1093/sysbio/syy011>
- Mindell DP (1997) Phylogenetic relationships among and within select avian orders based on mitochondrial DNA. Avian Molecular Evolution and Systematics: 211–247. <https://doi.org/10.1016/B978-012498315-1/50014-5>
- Mysore K, Subramanian KA, Sarasij RC, Suresh A, Shyamala B V, VijayRaghavan K, Rodrigues V (2009) Caste and sex specific olfactory glomerular organization and brain architecture in two sympatric ant species *Camponotus sericeus* and *Camponotus compressus* (Fabricius, 1798). Arthropod Structure & Development 38: 485–497. <https://doi.org/10.1016/j.asd.2009.06.001>
- Ng'endo RN (2011) Phylogenetic community structure of ants in secondary tropical forests in Brazil. PhD Thesis, Philipps-University Marburg, Marburg.
- Ng'endo RN, Osiemo ZB, Brandl R, Kondo T (2013) DNA barcodes for species identification in the hyperdiverse ant genus *Pheidole* (Formicidae: Myrmicinae). Journal of Insect Science 13: 1–13. <https://doi.org/10.1673/031.013.2701>
- Offenberg J (2014) The use of artificial nests by weaver ants: A preliminary field observation. Asian Myrmecology 6: 119–128.
- Ojha R, Jalali SK, Ali TMM, Venkatesan T, Prosser SW, Kumar NKK (2014) DNA barcoding of Indian ant species based on *cox1* gene. Indian Journal of Biotechnology 13: 165–171. [https://doi.org/10.1007/978-81-322-2089-3\\_2](https://doi.org/10.1007/978-81-322-2089-3_2)
- Paz A, Crawford AJ (2012) Molecular-based rapid inventories of sympatric diversity: A comparison of DNA barcode clustering methods applied to geography-based vs clade-based

- sampling of amphibians. *Journal of Biosciences* 37: 887–896. <https://doi.org/10.1007/s12038-012-9255-x>
- Peng RK, Christian K (2009) Determination and management of weaver ant, *Oecophylla smaragdina* (Fabricius) (Hymenoptera: Formicidae), marks on mango fruit in the Northern Territory of Australia. *International Journal of Pest Management* 55: 27–30. <https://doi.org/10.1080/09670870802450227>
- Pons J, Barraclough TG, Gomez-Zurita J, Cardoso A, Duran DP, Hazell S, Kamoun S, Sumlin WD, Vogler AP, Hedin M (2006) Sequence-based species delimitation for the DNA taxonomy of undescribed insects. *Systematic Biology* 55: 595–609. <https://doi.org/10.1080/10635150600852011>
- Posada D (2008) jModelTest: phylogenetic model averaging. *Molecular Biology and Evolution* 25: 1253–1256. <https://doi.org/10.1093/molbev/msn083>
- Prévot V, Jordaens K, Sonet G, Backeljau T (2013) Exploring species level taxonomy and species delimitation methods in the facultatively self-fertilizing land snail genus *Rumina* (Gastropoda: Pulmonata). *PLoS ONE* 8: e60736. <https://doi.org/10.1371/journal.pone.0060736>
- Puillandre N, Lambert A, Brouillet S, Achaz G (2012) ABGD, Automatic Barcode Gap Discovery for primary species delimitation. *Molecular Ecology* 21: 1864–1877. <https://doi.org/10.1111/j.1365-294X.2011.05239.x>
- Rambaut A, Drummond AJ, Suchard M (2014) Tracer v1. 6 <http://beast.bio.ed.ac.uk> [visited on 2017-06-12]
- Reemer M (2013) Review and phylogenetic evaluation of associations between microdontinae (Diptera: Syrphidae) and ants (Hymenoptera: Formicidae). *Psyche* 2013: 538316. <https://doi.org/10.1155/2013/538316>
- Richard FJ, Fabre A, Dejean A (2001) Predatory behavior in dominant arboreal ant species: The case of *Crematogaster* sp. (Hymenoptera: Formicidae). *Journal of Insect Behavior* 14: 271–282. <https://doi.org/10.1023/A:1007845929801>
- Rizali A, Bos MM, Buchori D, Yamane S, Schulze CH (2008) Ants in tropical urban habitats: The Myrmecofauna in a densely populated area of Bogor, West Java, Indonesia. *HAYATI Journal of Biosciences* 15: 77–84. <https://doi.org/10.4308/hjb.15.2.77>
- Ronquist F, Teslenko M, Van Der Mark P, Ayres DL, Darling A, Höhna S, Larget B, Liu L, Suchard MA, Huelsenbeck JP (2012) MrBayes 3.2: efficient Bayesian phylogenetic inference and model choice across a large model space. *Systematic Biology* 61: 539–542. <https://doi.org/10.1093/sysbio/sys029>
- Roy V, Constantino R, Chassany V, Giusti-Miller S, Diouf M, Mora P, Harry M (2014) Species delimitation and phylogeny in the genus *Nasutitermes* (Termitidae: Nasutitermitinae) in French Guiana. *Molecular Ecology* 23: 902–920. <https://doi.org/10.1111/mec.12641>
- Sarnat EM, Fischer G, Guénard B, Economo EP (2015) Introduced phaidole of the world: Taxonomy, biology and distribution. *ZooKeys* 2015: 1–109. <https://doi.org/10.3897/zookeys.543.6050>
- Satoh S, Satoh T, Hirota T (2013) Colony fusion in a parthenogenetic ant, *Pristomyrmex punctatus*. *Journal of Insect Science* 13: 1–16. <https://doi.org/10.1673/031.013.3801>
- Sauer J, Hausdorf B (2012) A comparison of DNA-based methods for delimiting species in a Cretan land snail radiation reveals shortcomings of exclusively molecular taxonomy. *Cladistics* 28: 300–316. <https://doi.org/10.1111/j.1096-0031.2011.00382.x>

- Savolainen V, Cowan RS, Vogler AP, Roderick GK, Lane R (2005) Towards writing the encyclopedia of life: an introduction to DNA barcoding. *Philosophical Transactions of the Royal Society B: Biological Sciences* 360: 1805–11. <https://doi.org/10.1098/rstb.2005.1730>
- Smith MA, Fisher BL, Hebert PDN (2005) DNA barcoding for effective biodiversity assessment of a hyperdiverse arthropod group: the ants of Madagascar. *Philosophical Transactions of the Royal Society B: Biological Sciences* 360: 1825–1834. <https://doi.org/10.1098/rstb.2005.1714>
- Smith MA, Hallwachs W, Janzen DH, Segura RB (2013) Dna barcoding a collection of ants (Hymenoptera: Formicidae) from Isla Del Coco, Costa Rica. *Florida Entomologist* 96: 1500–1507. <https://doi.org/10.1653/024.096.0431>
- Song H, Buhay JE, Whiting MF, Crandall KA (2008) Many species in one: DNA barcoding overestimates the number of species when nuclear mitochondrial pseudogenes are coamplified. *Proceedings of the National Academy of Sciences* 105: 13486–13491. <https://doi.org/10.1073/pnas.0803076105>
- Stadler B, Dixon AFG (2005) Ecology and evolution of aphid-ant interactions. *Annual Review of Ecology, Evolution, and Systematics* 36: 345–372. <https://doi.org/10.1146/annurev.ecolsys.36.091704.175531>
- Stamatakis A (2014) RAxML version 8: A tool for phylogenetic analysis and post-analysis of large phylogenies. *Bioinformatics* 30: 1312–1313. <https://doi.org/10.1093/bioinformatics/btu033>
- Suetsugu K (2015) Seed dispersal of the hemiparasitic plant *Thesium chinense* by *Tetramorium tsushimae* and *Pristomyrmex punctatus*. *Entomological Science* 18: 523–526. <https://doi.org/10.1111/ens.12148>
- Talavera G, Dincă V, Vila R (2013) Factors affecting species delimitations with the GMYC model: insights from a butterfly survey. *Methods in Ecology and Evolution* 4: 1101–1110. <https://doi.org/10.1111/2041-210X.12107>
- Tamura K, Peterson D, Peterson N, Stecher G, Nei M, Kumar S (2011) MEGA5: Molecular evolutionary genetics analysis using maximum likelihood, evolutionary distance, and maximum parsimony methods. *Molecular Biology and Evolution* 28: 2731–2739. <https://doi.org/10.1093/molbev/msr121>
- Wagner HC, Gamisch A, Arthofer W, Moder K, Steiner FM, Schlick-Steiner BC (2018) Evolution of morphological crypsis in the *Tetramorium caespitum* ant species complex (Hymenoptera: Formicidae). *Scientific Reports* 8: 12547. <https://doi.org/10.1038/s41598-018-30890-z>
- Ward PS, Brady SG, Fisher BL, Schultz TR (2015) The evolution of myrmicine ants: Phylogeny and biogeography of a hyperdiverse ant clade (Hymenoptera: Formicidae). *Systematic Entomology* 40: 61–81. <https://doi.org/10.1111/syen.12090>
- Wheeler DE (1986) Developmental and physiological determinants of caste in social Hymenoptera: Evolutionary implications. *The American Naturalist* 128: 13–34. <https://doi.org/10.1086/284536>
- Wills BD, Powell S, Rivera MD, Suarez AV (2018) Correlates and consequences of worker polymorphism in ants. *Annual Review of Entomology* 63: 575–598. <https://doi.org/10.1146/annurev-ento-020117-043357>

- Yamawo A, Suzuki N, Tagawa J, Hada Y (2012) Leaf ageing promotes the shift in defence tactics in *Mallotus japonicus* from direct to indirect defence. *Journal of Ecology* 100: 802–809. <https://doi.org/10.1111/j.1365-2745.2011.01934.x>
- Zhang J, Kapli P, Pavlidis P, Stamatakis A (2013) A general species delimitation method with applications to phylogenetic placements. *Bioinformatics* 29: 2869–2876. <https://doi.org/10.1093/bioinformatics/btt499>
- Zhu Y, Wang D (2018) Leaf volatiles from two *Corydalis* species Lure a keystone seed-dispersing ant and enhance seed retrieval. *Sociobiology* 65: 370. <https://doi.org/10.13102/sociobiology.v65i3.2726>

## Supplementary material 1

### Table S1. Ant and associated aphid species collected from different localities of Fujian Province of southern China

Authors: Junaid Ali Siddiqui, Zhilin Chen, Qiang Li, Jun Deng, Xiaolan Lin, Xiaolei Huang

Data type: species data

Copyright notice: This dataset is made available under the Open Database License (<http://opendatacommons.org/licenses/odbl/1.0/>). The Open Database License (ODbL) is a license agreement intended to allow users to freely share, modify, and use this Dataset while maintaining this same freedom for others, provided that the original source and author(s) are credited.

Link: <https://doi.org/10.3897/zookeys.879.29705.suppl1>

## Supplementary material 2

### Table S2. Analyzed samples of ant species with information on sampling location, GenBank accession number, BOLD process ID, morphological species identification, collection date, voucher specimen number, latitude and longitude

Authors: Junaid Ali Siddiqui, Zhilin Chen, Qiang Li, Jun Deng, Xiaolan Lin, Xiaolei Huang

Data type: species data

Copyright notice: This dataset is made available under the Open Database License (<http://opendatacommons.org/licenses/odbl/1.0/>). The Open Database License (ODbL) is a license agreement intended to allow users to freely share, modify, and use this Dataset while maintaining this same freedom for others, provided that the original source and author(s) are credited.

Link: <https://doi.org/10.3897/zookeys.879.29705.suppl2>

### **Supplementary material 3**

#### **Figure S1. Line chart of genetic distance of different taxonomic level based on p-distance and K2P model**

Authors: Junaid Ali Siddiqui, Zhilin Chen, Qiang Li, Jun Deng, Xiaolan Lin, Xiaolei Huang

Data type: molecular data

Copyright notice: This dataset is made available under the Open Database License (<http://opendatacommons.org/licenses/odbl/1.0/>). The Open Database License (ODbL) is a license agreement intended to allow users to freely share, modify, and use this Dataset while maintaining this same freedom for others, provided that the original source and author(s) are credited.

Link: <https://doi.org/10.3897/zookeys.879.29705.suppl3>

### **Supplementary material 4**

#### **Figure S2. Bayesian Inference tree of the 301 COI sequences from our study**

Authors: Junaid Ali Siddiqui, Zhilin Chen, Qiang Li, Jun Deng, Xiaolan Lin, Xiaolei Huang

Data type: phylogenetic tree

Explanation note: The values besides the branches indicate Bayesian posterior probabilities. The dotted lines indicate the outgroups.

Copyright notice: This dataset is made available under the Open Database License (<http://opendatacommons.org/licenses/odbl/1.0/>). The Open Database License (ODbL) is a license agreement intended to allow users to freely share, modify, and use this Dataset while maintaining this same freedom for others, provided that the original source and author(s) are credited.

Link: <https://doi.org/10.3897/zookeys.879.29705.suppl4>

# First mitochondrial genome from Yponomeutidae (Lepidoptera, Yponomeutoidea) and the phylogenetic analysis for Lepidoptera

Mingsheng Yang<sup>1</sup>, Bingyi Hu<sup>1</sup>, Lin Zhou<sup>1</sup>, Xiaomeng Liu<sup>1</sup>, Yuxia Shi<sup>1</sup>,  
Lu Song<sup>1</sup>, Yunshan Wei<sup>2</sup>, Jinfeng Cao<sup>3</sup>

**1** College of Life Science and Agronomy, Zhoukou Normal University, Zhoukou, Henan, 466000, China

**2** Chifeng Agricultural and Animal Husbandry Scientific Research Institute, Chifeng, Neimenggu, 024031, China **3** Cangzhou Academy of Agriculture and Forestry Sciences, Cangzhou, Hebei, 061001, China

Corresponding author: Mingsheng Yang ([yms-888@163.com](mailto:yms-888@163.com))

---

Academic editor: Thomas Simonsen | Received 2 April 2019 | Accepted 18 September 2019 | Published 9 October 2019

---

<http://zoobank.org/EEE86198-06CF-415A-A70D-F2944FBF5A52>

---

**Citation:** Yang M, Hu B, Zhou L, Liu X, Shi Y, Song L, Wei Y, Cao J (2019) First mitochondrial genome from Yponomeutidae (Lepidoptera, Yponomeutoidea) and the phylogenetic analysis for Lepidoptera. ZooKeys 879: 137–156. <https://doi.org/10.3897/zookeys.879.35101>

---

## Abstract

The complete mitochondrial genome (mitogenome) of *Yponomeuta montanatus* is sequenced and compared with other published yponomeutoid mitogenomes. The mitogenome is circular, 15,349 bp long, and includes the typical metazoan mitochondrial genes (13 protein-coding genes, two ribosomal RNA genes, and 22 transfer RNA genes) and an A + T-rich region. All 13 protein-coding genes use a typical start codon ATN, the one exception being *cox1*, which uses CGA across yponomeutoid mitogenomes. Comparative analyses further show that the secondary structures of tRNAs are conserved, including loss of the Dihydrouridine (DHU) arm in *trnS1* (AGN), but remarkable nucleotide variation has occurred mainly in the DHU arms and pseudouridine (T $\psi$ C) loops. A + T-rich regions exhibit substantial length variation among yponomeutoid mitogenomes, and conserved sequence blocks are recognized but some of them are not present in all species. Multiple phylogenetic analyses confirm the position of *Y. montanatus* in Yponomeutoidea. However, the superfamily-level relationships in the Macroheterocera clade in Lepidoptera recovered herein show considerable difference with that recovered in previous mitogenomic studies, raising the necessity of extensive phylogenetic investigation when more mitogenomes become available for this clade.

## Keywords

Mitogenome evolution, next-generation sequencing, protein-coding genes

## Introduction

The mitochondrial genome (mitogenome) is a circular and double-stranded molecule that usually encodes 37 genes (13 protein-coding genes (PCGs), two ribosomal RNA genes (rRNAs), 22 transfer RNA genes (tRNAs)), and an A + T-rich region (Boore 1999). Characterized by cellular abundance, absence of introns, rapid evolution, and a lack of extensive recombination, mitogenome sequences can be easily amplified and has been extensively employed in evolutionary studies in past decades (Cameron et al. 2014; Curole et al. 2014). Additionally, the mitogenome often exhibits some characters such as gene rearrangement that have been widely used to infer genome evolution and phylogeny for multiple groups. For instance, comparative analyses of lepidopteran mitogenomes showed the gene order *trnM-trnI-trnQ* is present in more derived ditrysian lineage and its close relatives Tischerioidea and Palaephatoidea, in contrast to the ancestral *trnI-trnQ-trnM* in other lepidopterans such as *Thitarodes renzhiensis* (Yang, 1991) and *T. yunnanensis* (Yang, 1992) (Cao et al. 2012; Timmermans et al. 2014).

Lepidoptera is the second largest insect order after Coleoptera, with more than 157,000 extant species in 43 superfamilies (van Nieuwerkerken et al. 2011; Mitter et al. 2017). To date, mitogenomes of more than 400 lepidopteran species or subspecies have been sequenced (<https://www.ncbi.nlm.nih.gov>; last visited on March 2019). Relative to other species-rich orders, however, the current number of sequenced mitogenomes is still limited. Moreover, deep-level lepidopteran phylogeny is still poorly understood despite previous investigations based on various data including mitogenome sequences (Mitter et al. 2017). The superfamily Yponomeutoidea, with approximately 1,800 described species, represents one of the earliest diverging lineages of ditrysian Lepidoptera and includes many notable pest species (van Nieuwerkerken et al. 2011; Sohn et al. 2013). In Yponomeutoidea, 11 families were recognized based on a multiple-gene dataset (Sohn et al. 2013), but phylogenetic relationships among yponomeutoid families still need further investigation (Mitter et al. 2017). To date, mitogenomes of only three yponomeutoid species representing three families have been published. According to the classification system proposed by Sohn et al. (2013), they are *Prays oleae* (Bernard, 1788) (Praydidae) (van Asch et al. 2016), *Plutella xylostella* (Linnaeus, 1758) (Plutellidae) (Wei et al. 2013; Dai et al. 2016), and *Leucoptera malifoliella* (Costa, 1836) (Lyonetiidae) (Wu et al. 2012). Thus, the number of reported yponomeutoid mitogenomes is quite limited. Moreover, a comparative analysis among the published mitogenomes has never been conducted.

Mitogenomic data of major Yponomeutoidea lineages would play an important role for better understanding the evolution of the superfamily or even Lepidoptera as a whole. In the present study, we sequenced the complete mitogenome of *Yponomeuta montanatus* Moriuti, 1977, the first mitogenome from the family Yponomeutidae. Moreover, detailed comparative analyses were conducted based on this and all other published yponomeutoid mitogenomes. In addition, extensive phylogenetic analyses using three different datasets and three different tree-constructed methods were performed to test phylogenetic implications of the *Y. montanatus* mitogenome in Lepidoptera phylogeny. This study contributes to further understanding the mitogenome evolution and phylogeny of the Yponomeutoidea and Lepidoptera.

## Materials and methods

### Sample collection, identification and DNA extraction

Adult *Y. montanatus* specimens were sampled by light trap at Mountain Jigongshan, Henan, China in May 2018. Fresh specimens were stored in 95–100% ethanol in the field and then maintained at  $-80^{\circ}\text{C}$  until used for DNA extraction. Dry specimens were identified based on the morphological description and illustrations provided by Byun and Bae (2013). In addition, molecular identification was performed by blasting the standard *cox1* barcode sequence in GenBank. Thorax muscle tissues were used to extract genomic DNA with the DNeasy tissue kit (Qiagen, Hilden, Germany) according to the manufacturer's instructions. Voucher specimens are deposited in the Biology Laboratory of Zhoukou Normal University, China.

### Mitogenome sequencing and assembly

Next-generation sequencing methods were used to obtain the complete mitogenome sequence of *Y. montanatus*. Briefly, total genomic DNA was firstly quantified and fragmented to an average size of 400 bases using Covaris M220 system with the Whole Genome Shotgun method (Covaris, Woburn, MA, USA). Then, a library was constructed using the TruSeq DNA PCR-Free Sample Preparation Kit (Illumina, USA). Lastly, Illumina HiSeq 2500 was used for sequencing with the strategy of 251 paired-ends.

A total of 3,707,876 raw paired reads were retrieved for *Y. montanatus*. FastQC (<http://www.bioinformatics.babraham.ac.uk/projects/fastqc>) was used for quality control (avg. Q20 > 95.1%, avg. Q30 > 88.65%). After processing with AdapterRemoval v. 2 (Mikkelsen et al., 2016) and SOAPdenovo v. 2.01 (Luo et al. 2012), the raw paired reads were filtered into a total of 2,582,644 high-quality reads. Then, the A5-miseq v20150522 (Coil et al. 2015) and SPAdes v. 3.9.0 (Bankevich et al. 2012) were used in de novo assembly, generating contig and scaffold sequences. Lastly, the mitochondrial sequences were identified using blastn method, and the mummer v. 3.1 (Kurtz et al. 2004) was used to establish the position relationships among the contig sequences and to fill in the possible gaps.

### Mitogenome annotation and comparative analysis

The MITOS webserver was employed to annotate the complete mitogenome sequence with the invertebrate genetic code (Bernt et al. 2013). The tRNAScan-SE server v. 1.21 (Lowe and Eddy 1997) was used to re-identify the 22 tRNAs as well as to reconfirm their secondary structures. Gene boundaries were re-identified by aligning the new mitogenome with previously reported yponomeutoid mitogenomes using MEGA v. 6.06 (Tamura et al. 2013). To ensure the correct reading frame, nucleotide sequences of the 13 PCGs were translated with both the programs Primer Premier v. 5.00 (Pre-

mier Biosoft International, Palo Alto, CA) and MEGA v. 6.06 (Tamura et al. 2013) with invertebrate mitochondrial genetic code. Tandem repeat elements in the A + T-rich region were identified using the Tandem Repeats Finder program (<http://tandem.bu.edu/trf/trf.html>) (Benson 1999). All other published yponomeutoid mitogenomes, along with the one sequenced in this study were compiled for comparative analysis. Base composition and the relative synonymous codon usage (RSCU) were calculated using MEGA v. 6.06 (Tamura et al. 2013). Strand asymmetry was calculated according to the formulas:  $AT\text{-skew} = [A - T]/[A + T]$  and  $GC\text{-skew} = [G - C]/[G + C]$  (Perna and Kocher 1995). The nucleotide diversity and the ratio of non-synonymous substitution ( $K_a$ ) to synonymous substitution ( $K_s$ ) were calculated with DNASP v. 5.0 (Librado and Rozas 2009).

### Phylogenetic analyses

To investigate phylogenetic implications of the *Y. montanatus* mitogenome in Lepidoptera phylogeny, a total of 33 mitogenomes representing 15 lepidopteran superfamilies with mitogenome available (Suppl. material 1, Table S1) were sampled for phylogenetic analyses. Two additional trichopteran mitogenomes were selected as outgroups. Sequence alignment was conducted on the TranslatorX online platform (Abascal et al. 2010) for 13 PCGs. The two rRNAs and 22 tRNAs were aligned with the Q-INS-i algorithm implemented in the MAFFT online platform (Katoh et al. 2017). MEGA v. 6.06 (Tamura et al. 2013) was used to check all alignments. Then, MEGA v. 6.06 (Tamura et al. 2013) was also used to generate three different datasets: PCG123 (all codon positions of 13 PCGs), PCG123R (PCG123 dataset plus two rRNAs and 22 tRNAs), and PCGAA (amino acid sequences translated from 13 PCGs). Nucleotide sequence substitution model was selected using PartitionFinder v. 1.1.1 (Lanfear et al. 2012), with the Bayesian Information Criterion (BIC) algorithm under a greedy search. The best partition scheme and corresponding models are shown in Suppl. material 1, Tables S2 and S3.

Maximum likelihood (ML) analyses were conducted using two methods. The raxmlGUI version 1.539 interface (Silvestro and Michalak 2012) of RAxML version 7.2.6 (Stamatakis 2006) was used under the GTRGAMMAI model for PCG123 and PCG123R datasets, and the model MtArt + I + G for PCGAA dataset. Node reliability was assessed using the ML + rapid bootstrap algorithm with 100 replicates. IQ-TREE 1.6.7.1 (Nguyen et al. 2015) was used with the models determined by PartitionFinder for PCG123 and PCG123R datasets, and the model MtArt + I + G for PCGAA dataset. Node support was assessed using 1,000 ultrafast bootstrap replicates.

Bayesian inference (BI) analysis was performed using MrBayes v. 3.1.2 (Ronquist and Huelsenbeck 2003). For the PCG123 and PCG123R datasets, the model determined by PartitionFinder was used, and for PCGAA dataset with the model MtRev + I + G. Two independent Markov chain Monte Carlo (MCMC) runs were performed for 1,000,000–3,000,000 generations sampling per 100 generations. The convergence

between the two runs was established by the Tracer v. 1.6 (Effective sample sizes >200) (Rambaut et al. 2014). After the first 25% of the yielded trees were discarded as burn-in, a 50% majority-rule consensus tree with the posterior probability was generated from the remaining trees.

## Results and discussion

### General characteristics of the *Y. montanatus* mitogenome

The complete mitogenome of *Y. montanatus* (GenBank accession number: MK256747) is circular, double-stranded, and 15,349 bp long (Fig. 1, Table 1). This length is shortest amongst published yponomeutoid mitogenomes. The typical 37 mitochondrial genes (13 PCGs, 22 tRNAs, and two rRNAs) and an A + T-rich region are included. Among them, 23 (nine PCGs and 14 tRNAs) are encoded on majority strand (J-strand), and the remaining 14 are located on minority strand (N-strand). As in most ditrysian members of Lepidoptera, the *trnM-trnI-trnQ* can be recognized in Yponomeutoidea, in contrast to the *trnI-trnQ-trnM* in most non-ditrysian lineage such as the Hepialoidea (Cao et al. 2012), and in the ancestral arthropod mitogenome (*Drosophila yakuba*) (Clary and Wolstenholme 1985).

As in other insect mitogenomes (Boore 1999), high A + T content is recognized across Yponomeutoidea mitogenomes, which ranges from 81% in *P. lutella* (KM023645) to 82.5% in *L. malifoliella* (Table 2). In addition to the A + T content, AT-skew and GC-skew are also routinely used to characterize base composition of mitogenomes (Perna and Kocher 1995; Wei et al. 2010). The negligible AT-skew (0.0037) and moderate GC-skew (-0.164) (Suppl. material 1, Table S4) in *Y. montanatus* mitogenome are similar to other Lepidoptera and most insect species (Cameron and Whiting 2008).

### Protein-coding genes

The total length of the 13 PCGs in *Y. montanatus* mitogenome is 11,183 bp, approximately accounting for 72.9% of the whole mitogenome (Table 2). Identical to other yponomeutoid mitogenomes, nine of the 13 PCGs are encoded on J-strand, and the other four are located on N-strand. In yponomeutoid mitogenomes, the A + T content of the 13 PCGs varies from 79.1% in *P. oleae* to 80.7% in *L. malifoliella*. The codon positions show unequal A + T content (Suppl. material 1, Table S5). The third codon positions have the highest A + T content (93.4% on average), followed by first codon positions (74.9% on average) and second codon positions (70.7% on average). To characterize codon frequencies across yponomeutoid mitogenomes, relative synonymous codon usages (RSCU) were calculated and drawn for all five yponomeutoid mitogenomes. As shown in Figure 2 and Suppl. material 1, Table S6, the codon usage

**Table I.** Summary of the *Yponomeuta montanatus* mitogenome.

Feature	Strand	Location	Size (bp)	Start codon	Stop codon	Anticodon	Intergenic nucleotides
<i>trnM</i>	J	1–67	67			CAT	0
<i>trnI</i>	J	68–136	69			GAT	–3
<i>trnQ</i>	N	134–202	69			TTG	49
<i>nad2</i>	J	252–1265	1014	ATT	TAA		–2
<i>trnW</i>	J	1264–1331	68			TCA	–8
<i>trnC</i>	N	1324–1385	62			GCA	11
<i>trnY</i>	N	1397–1460	64			GTA	2
<i>cox1</i>	J	1463–2998	1536.9	CGA	TAA		–5
<i>trnL2</i> (UUR)	J	2994–3059	66			TAA	0
<i>cox2</i>	J	3060–3744	685	ATG	T		–3
<i>trnK</i>	J	3742–3812	71			CTT	–1
<i>trnD</i>	J	3812–3876	65			GTC	0
<i>atp8</i>	J	3877–4035	159	ATT	TAA		–7
<i>atp6</i>	J	4029–4706	678	ATG	TAA		–1
<i>cox3</i>	J	4706–5497	792	ATG	TAA		2
<i>trnG</i>	J	5500–5565	66			TCC	0
<i>nad3</i>	J	5566–5919	354	ATT	TAA		2
<i>trnA</i>	J	5922–5984	63			TGC	–1
<i>trnR</i>	J	5984–6050	67			TCG	8
<i>trnN</i>	J	6059–6123	65			GTT	–1
<i>trnS1</i> (AGN)	J	6123–6188	66			GCT	0
<i>trnE</i>	J	6189–6250	62			TTC	–1
<i>trnF</i>	N	6250–6315	66			GAA	22
<i>nad5</i>	N	6338–8050	1713	ATT	TAA		12
<i>trnH</i>	N	8063–8129	67			GTG	0
<i>nad4</i>	N	8130–9468	1339	ATG	T		0
<i>nad4I</i>	N	9469–9756	288	ATG	TAA		7
<i>trnT</i>	J	9764–9828	65			TGT	0
<i>trnP</i>	N	9829–9894	66			TGG	2
<i>nad6</i>	J	9897–10430	534	ATT	TAA		9
<i>cob</i>	J	10440–11591	1152	ATG	TAA		–2
<i>trnS2</i> (UCN)	J	11590–11657	68			TGA	35
<i>nad1</i>	N	11693–12631	939	ATG	TAA		1
<i>trnL1</i> (CUN)	N	12633–12699	67			TAG	0
<i>rrnL</i>	N	12700–14073	1374				0
<i>trnV</i>	N	14072–14135	64			TAC	–1
<i>rrnS</i>	N	14135–14903	769				0
A + T-rich region		14904–15349	446				

Note: the “J” indicates the majority strand and the “N” indicates the minority strand in the strand column.

pattern is generally similar among them such as the most frequently used codons (i.e., UUA, AUU, UUU, AUA, and AAU). In the *Y. montanatus* mitogenome, a number of 3,727 amino acids are translated, of which 1,787 (47.9%) are encoded by the five frequently used codons above. However, the codons absent in yponomeutoid mitogenomes are different, but most of them are rich in C/G nucleotides. In general, the high A/T content in frequently used codons effectively contributes to the high A + T composition in PCGs and the whole mitogenome.

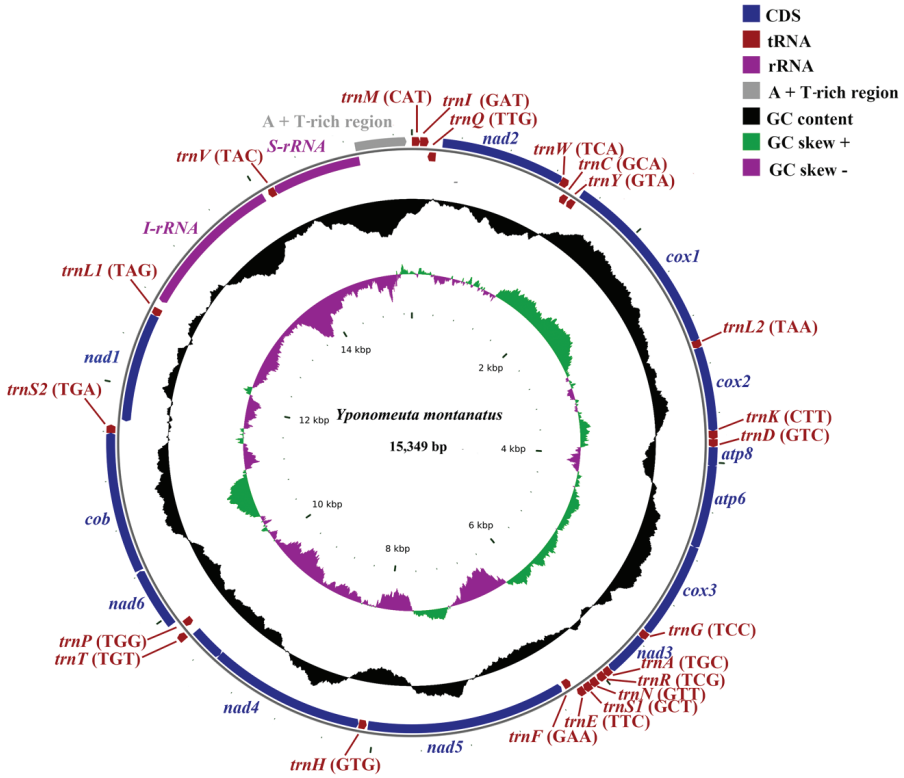
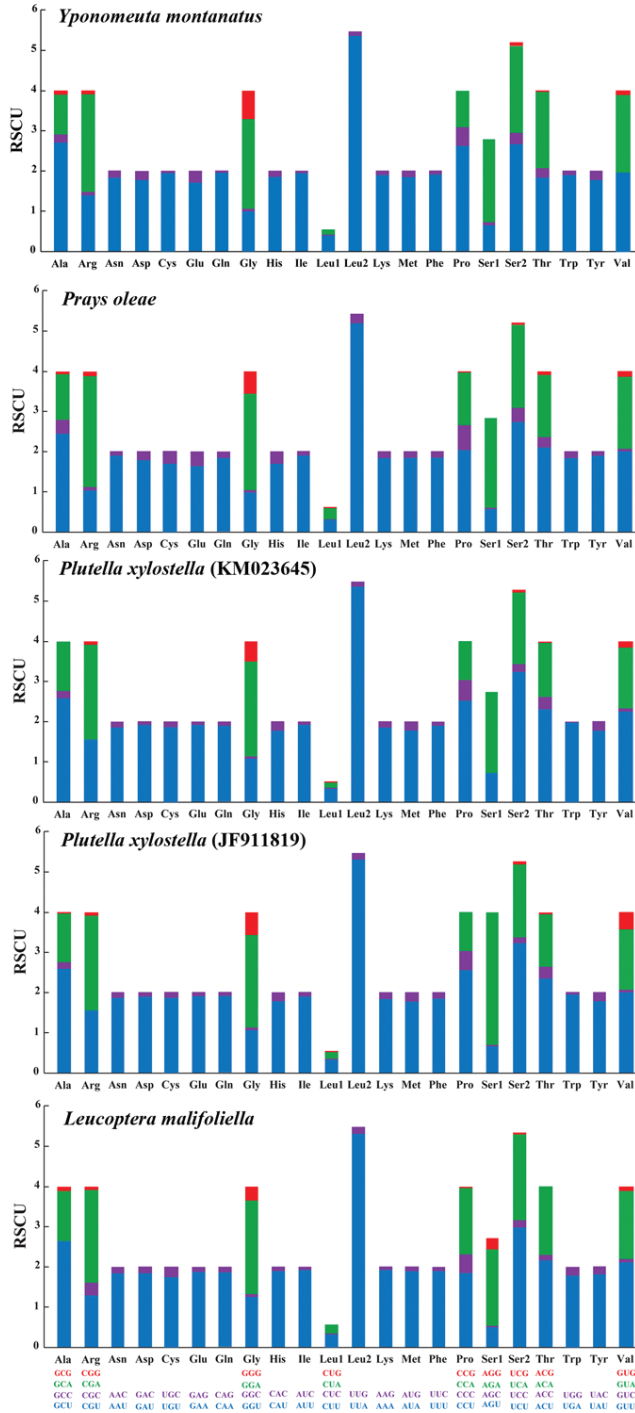


Figure 1. Mitochondrial genome map of the *Yponomeuta montanatus*.

Table 2. Base composition of the five sequenced yponomeutoid mitogenomes.

Taxon	Size (bp)	A + T (%)	PCGs No. of codon A + T (%)	<i>rrnS</i>	<i>rrnL</i>	tRNAs	A + T-rich region	GenBank accession no.
				RNA Size (bp) A + T (%)	RNA Size (bp) A + T (%)	Size (bp) A + T (%)	Size (bp) A + T (%)	
<b>Yponomeutidae</b>								
<i>Yponomeuta montanatus</i>	15,349	81.08	3,727 79.6	769 85.7	1,374 85.1	1,453 80.8	446 96.2	MK256747
<b>Praydidae</b>								
<i>Prays oleae</i>	16,499	81.8	3,720 79.1	773 85	1,372 85	1,486 81.3	1,483 96.3	KM874804
<b>Plutellidae</b>								
<i>Plutella xylostella</i>	16,014	81	3,731 79.4	783 86.1	1,382 85.1	1,465 81.2	888 93.1	KM023645
<i>Plutella xylostella</i>	16,179	81.4	3,729 79.4	783 86.1	1,415 84.9	1,468 81.3	1,081 n.a.	JF911819
<b>Lyonetiidae</b>								
<i>Leucoptera maliifoliella</i>	15,646	82.5	3,719 80.7	770 87.1	1,351 85.5	1,488 83.7	733 95.3	JN790955

Note: n.a. indicates not available.



**Figure 2.** Relative synonymous codon usages (RSCU) in PCGs of *Yponomeuta montanatus* and other published yponomeutoid mitogenomes. Codon families are indicated below the X-axis.

Most PCGs in yponomeutoid mitogenomes use the conventional ATN start codon (Table 1, Suppl. material 1, Table S7). The unconventional CGA was consistently found in only the *cox1* gene, a common feature for lepidopteran mitogenomes (Wu et al. 2016). TAA is employed as stop codon in most PCGs, but two other kinds of stop codons were recognized. One is the TAG for *nad4l* and *nad6* genes in *L. malifoliella*; the other is the incomplete termination codon T which is commonly used in yponomeutoid mitogenomes. Actually, the incomplete termination codon can be also commonly recognized across arthropod mitogenomes, which may be related to the post transcriptional modification during the mRNA maturation process (Ojala et al. 1981).

To investigate evolutionary patterns of all PCGs, nucleotide diversity and the ratio of Ka to Ks were calculated for each PCG. As shown in Figure 3 and Suppl. material 1, Table S8, *nad6* and *cox1* genes show the highest and lowest nucleotide diversity respectively. The Ka/Ks values are the highest in *atp8* genes and the lowest is for *cox1* gene. Notably, the Ka/Ks values for all PCGs are lower than one, indicating that they are evolving under the purifying selection and are suitable for investigating phylogenetic relationships within Yponomeutoidea.

### Transfer and ribosomal RNA genes

The *Y. montanatus* mitogenome contains 22 tRNAs with the length ranging from 62 bp (*trnC*, *trnE*) to 71 bp (*trnK*) (Fig. 4, Table 1). Among them, eight tRNAs are encoded by N-strand and the remaining 14 by J-strand. The total length of tRNAs is 1,453 bp, which is shortest among yponomeutoid mitogenomes, which otherwise range from 1,465 bp in *P. xylostella* (KM023645) to 1,488 in *L. malifoliella* (Table 2). As shown in Fig. 4, all tRNAs exhibit typical clover-leaf secondary structure but *trnS1* (AGN) lacks the DHU arm, a feature generally present in all Lepidoptera insects as well as in other metazoan mitogenomes (Garey and Wolstenholme 1989; Lavrov et al. 2000). In tRNAs of the *Y. montanatus* mitogenome, we recognized 22 unmatched base pairs, of which 18 are non-canonical G-U pairs, and the remaining four are mis-

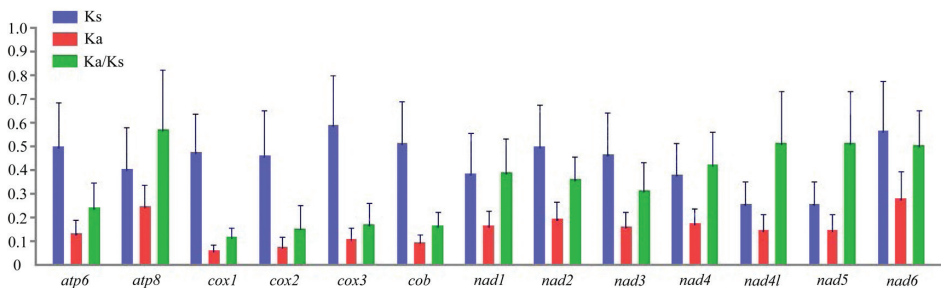


**Figure 3.** Evolutionary rate of each PCG among yponomeutoid mitogenomes. Ka, non-synonymous substitution; Ks, synonymous substitution.

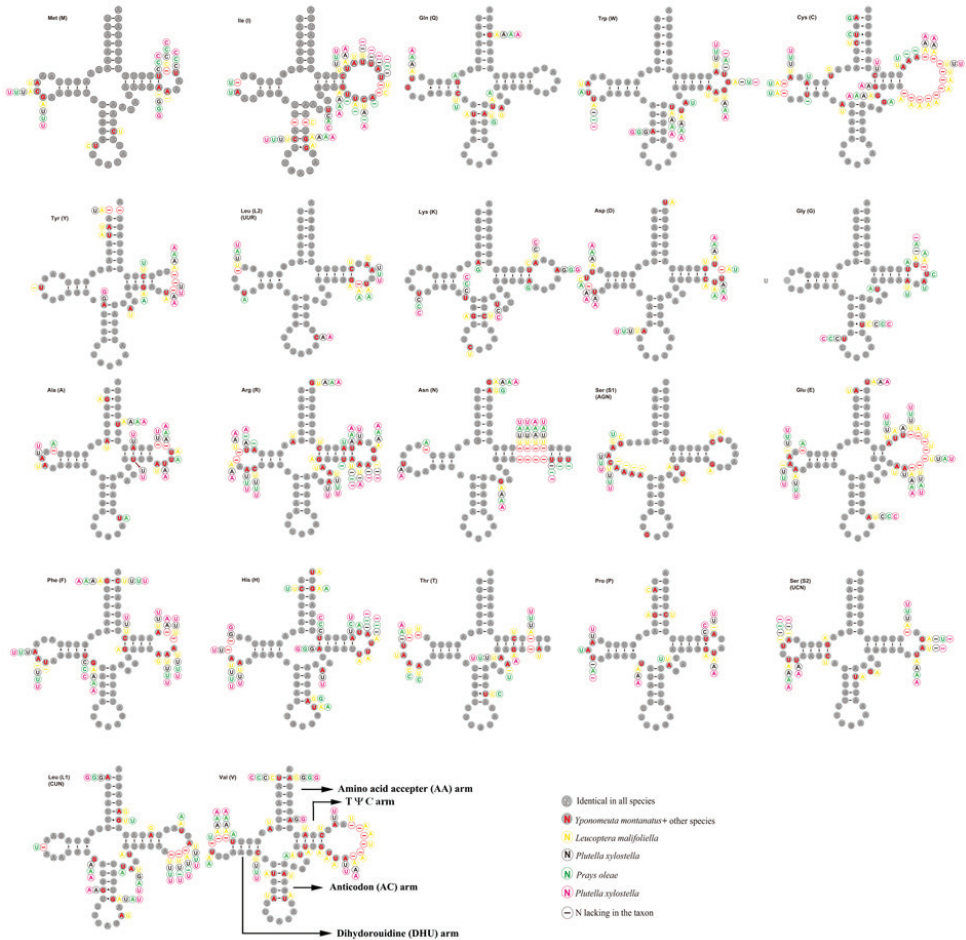


**Figure 4.** Putative secondary structures of tRNAs from *Yponomeuta montanatus* mitogenome. The tRNAs are labeled with the abbreviations of their corresponding amino acids. The tRNA arms are illustrated as for *trnV*. Dashes indicate the Watson-Crick base pairs; dots indicate the wobble GU pairs; and the other non-canonical pairs are not marked. The nucleotides marked indicate the variable sites among published yponomeutoid mitogenomes.

matched base pairs U-U. The overrepresented non-canonical G-U pairs in tRNAs is commonly present in insect mitogenomes (Salvato et al. 2008; Chen et al. 2016; Chen and Du 2017).

Comparative tRNA analyses among yponomeutoid mitogenomes found that each tRNA structure is highly conserved, including the loss of the DHU arm in *trnS1* (AGN). However, substantial nucleotide variation exists, most of which occurred in the DHU arm and TΨC loops (Fig. 4). Interestingly, in *L. malifoliella*, the anticodons for both *trnK* and *trnS1* (AGN) were rarely mutated relative to other yponomeutoid

species. For *trnS1* (AGN), the TCT is used instead of routinely used codon GCT. This phenomenon has been recognized in previous reports such as two species of Helioloidea and three species of Noctuoidea (Li et al. 2018). In *trnK*, the mostly used anticodon CTT was changed to TTT (Wu et al. 2012), which is, to our knowledge, extremely rare in Lepidoptera and insects in general.

Similar to other yponomeutoid mitogenomes, two rRNA genes, *rrnS* and *rrnL*, were recognized in the *Y. montanatus* mitogenome (Fig. 1, Table 1). The *rrnS* is 769 bp long, which is located between *trnV* and A + T-rich region; the *rrnL* is 1,374 bp long, being present between *trnV* and *trnL1*. The lengths of *rrnS* and *rrnL* are comparable to those of other reported yponomeutoid mitogenomes, which are from 770 bp in *L. malifoliella* to 783 bp in *P. xylostella*, and from 1,351 bp in *L. malifoliella* to 1,415 bp in *P. xylostella* (JF911819), respectively.

### Gene overlapping and intergenic regions

In the *Y. montanatus* mitogenome, 36 gene overlapping sites were recognized across 13 gene junctions from one to eight bp in length (Table 1). Comparative mitogenome analyses showed that gene overlapping region only between *atp8* and *atp6* is consistently present across reported yponomeutoid mitogenomes. This 7-bp motif of “ATGATAA” (Fig. 5A) is actually a common feature for Lepidoptera and other insects, such as *Taeniopteryx ugola* Ricker & Ross, 1968 (Plecoptera) (Chen and Du 2017).

In addition to the A + T-rich region, a total of 162 intergenic nucleotides across 13 gene junctions from one to 49 bp were identified in *Y. montanatus* mitogenome (Table 1). Among the 13 intergenic regions or site, three are conserved among the reported yponomeutoid mitogenomes, and they are located between the *nad6* and *cob* genes (Fig. 5B), the *trnQ* and *nad2* genes (Fig. 5C), and the *trnS2* and *nad1* genes (Fig. 5D). The one between the *nad6* and *cob* genes ranges from four to 41 bp in length across yponomeutoid mitogenomes. A remarkable feature for this region is that both mitogenomes of *P. xylostella* contain microsatellite (TA)<sub>n</sub> sequence but with different repeat numbers. *P. xylostella* is an important agricultural pest, and this microsatellite (TA)<sub>n</sub> sequence may be used as a candidate marker to test the population structure for pest management. The one between the *trnQ* and *nad2* genes exhibits substantial sequence variation (except two sequences for *P. xylostella*) among reported yponomeutoid mitogenomes. This intergenic region is also widely present in other lepidopterans such as those in the Lasiocampidae (Kim et al. 2017) and Noctuidae (Chai and Du 2012), and may even be regarded as an autapomorphy of Lepidoptera (Cao et al. 2014). Also, the intergenic region between *trnS2* and *nad1* is commonly present in insect mitogenomes (Cameron and Whiting 2008). Although the length varies among yponomeutoid mitogenomes, a conserved motif “ATACTAA” could be identified, which has been reported related to mitochondrion transcription (Taanman 1999).

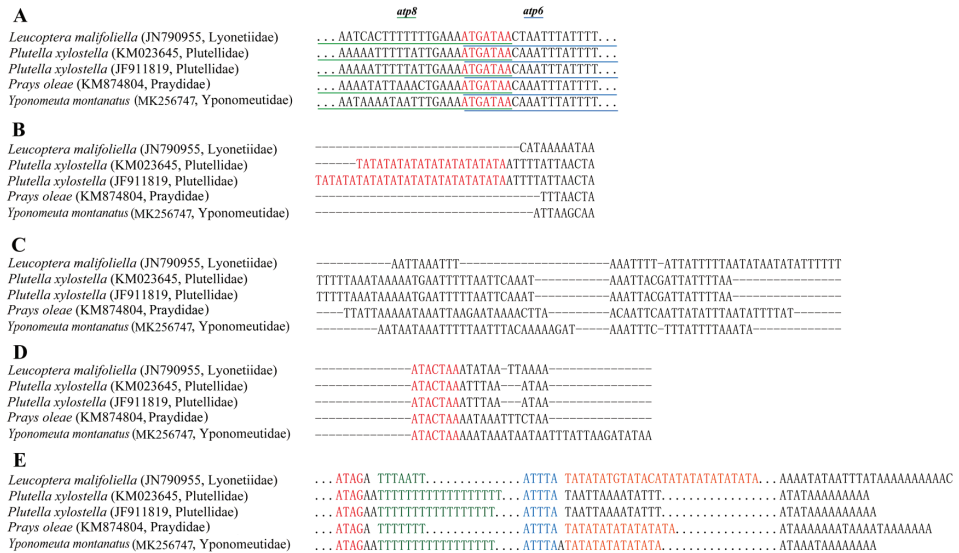


**Figure 5. A** The overlapping region between *atp8* and *atp6*. The nucleotides colored red indicate the sequence of overlapping region; the nucleotides with green underline indicate partial sequence of the *atp8* gene, and the nucleotides with blue underline indicate the partial sequence of the *atp6* gene **B** The intergenic region between *nad6* and *cob*. The microsatellite (TA)<sub>n</sub> are marked red **C** The intergenic region between *trnQ* and *nad2* **D** The intergenic region between *trnS2* and *nad1*. The nucleotides colored red indicate the conserved motif sequence **E** Schematic illustration of the A + T-rich region from all yponomeutoid mitogenomes. The conserved motif ATAG (colored red) and subsequent poly-T stretch (colored green), the conserved motif ATTTA (colored blue) and subsequent (TA)<sub>n</sub> sequence (colored orange) are emphasized. Dots indicate omitted sequences, and the number of dot is not proportional to nucleotide number of corresponding part.

## A + T-rich region

As in other yponomeutoid mitogenomes, the A + T-rich region of the *Y. montanatus* mitogenome is located between the *rrnS* and *trnM* genes (Fig. 1, Table 1). These regions of the published yponomeutoid mitogenomes are remarkably variable in length. The shortest one, consisting of 446 nucleosides, is recognized in the *Y. montanatus* mitogenome. In contrast, the *P. oleae* mitogenome contains the longest one with up to 1,438 bp, and in this region, several tandem repeat elements can be recognized (van Asch et al. 2016). The A + T content of the A + T-rich region among yponomeutoid mitogenomes ranges from 93.1% in *P. xylostella* to 96.3% in *P. oleae*, and all species show the highest A + T content within the whole mitogenome.

Insect mitochondrial A + T-rich region is usually structured in base composition, mainly exhibiting the existence of conserved sequence blocks responsible for mitogenome replication and transcription (Zhang and Hewitt 1997). In the mitogenomes of *Y. montanatus* and other reported yponomeutoids, several conserved sequence blocks could be recognized (Fig. 5E). These blocks include (from 5' to 3' end) the motif

“ATAG” and subsequent poly-T structure, the motif “ATTTA” and followed microsatellite (TA)<sub>n</sub> element and an “A”-rich 3’ end upstream of the *trnM* gene. However, in *L. malifoliella* and *P. xylostella*, we did not recognize the poly-T structure and microsatellite (TA)<sub>n</sub> element, respectively. Also, insect A + T-rich region is generally characterized by the presence of multiple tandem repeat elements (Vila and Björklund 2004). In yponomeutoid mitogenomes, this character can be recognized in *P. oleae* (van Asch et al. 2016) and *L. malifoliella* (Wu et al. 2012). However, in mitogenomes of *Y. montanatus* sequenced herein and *P. xylostella* (Dai et al. 2016), no tandem repeat elements were identified.

### Phylogenetic analyses

To investigate phylogenetic implications of the *Y. montanatus* mitogenome in Yponomeutoidea and Lepidoptera, we constructed the superfamily-level relationships within Lepidoptera using three inference methods and three different datasets.

As shown in Figures 6–8. and S1–S3, relationships among the four yponomeutoid families involved herein were consistently recovered as Lyonetiidae + (Praydidae + (Yponomeutidae + Plutellidae)), which is consistent with that of Sohn et al. (2013) based on multiple-gene data. *Y. montanatus* is nested within Yponomeutoidea, confirming its phylogenetic position using mitogenomic data. In previous studies, the Yponomeutoidea is recovered either sister to Gracillarioidea (Heikkilä et al. 2015) or paraphyletic with respect to Gracillarioidea (Regier et al. 2013; Sohn et al. 2013). Most mitogenome-based phylogenetic studies of Lepidoptera scarcely sampled representatives of Gracillarioidea. As an exception, Timmermans et al. (2014) revealed that Gracillarioidea are nested in the Yponomeutoidea. The same results are recovered in this study. The only representative of Gracillarioidea is consistently sister to *L. malifoliella* in Yponomeutoidea, rendering the Yponomeutoidea paraphyletic.

Regarding the phylogenetic pattern of other superfamilies, mostly identical results were obtained by different analyses, which are also similar to other mitogenome-based studies (Clary and Wolstenholme 1985; Timmermans et al. 2014; Bao et al. 2018). We noticed that the minor topology difference across our analyses mainly occurred in the position of the Papilionoidea, Gelechioidea and Cossoidea. These results are similar to other mitogenome-based studies (Clary and Wolstenholme 1985; Bao et al. 2018) as well as multiple-gene-based study (Heikkilä et al. 2015) where the positions of these superfamilies are unstable or weakly supported, respectively. Within Macroheterocera, Noctuoidea + (Geometroidea + Bombycoidea) were recovered by studies based on various data, such as mitogenome sequences (Kim et al. 2011; Yang et al. 2015), multi-gene sequences (Regier et al. 2013) and 741 genes from transcriptome sequences (Bazin et al. 2013). Interestingly, our analyses consistently recovered Bombycoidea + (Geometroidea + Noctuoidea), which was identical to that of Kawahara and Breinholt (Kawahara and Breinholt 2014). This result suggests the necessity of extensive phylogenetic investigation when more mitogenomes become available for this clade.

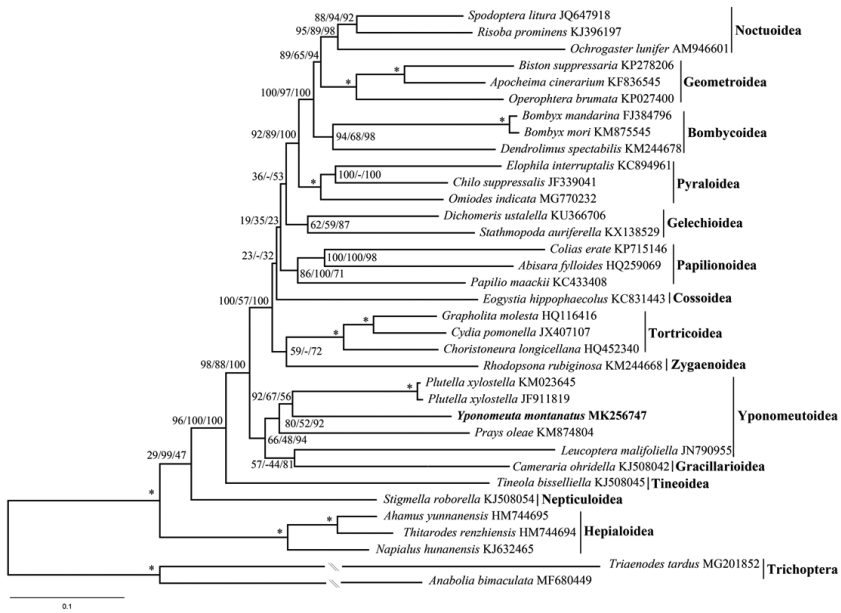


**Figure 6.** ML tree inferred from RAxML method based on PCG123R dataset. Numbers separated by slash (/) on node represent bootstrap replicates based on PCG123, PCGAA and PCG123R datasets, respectively. The dash (-) represents unrecovered node in ML tree based on the PCG123 or PCGAA dataset.

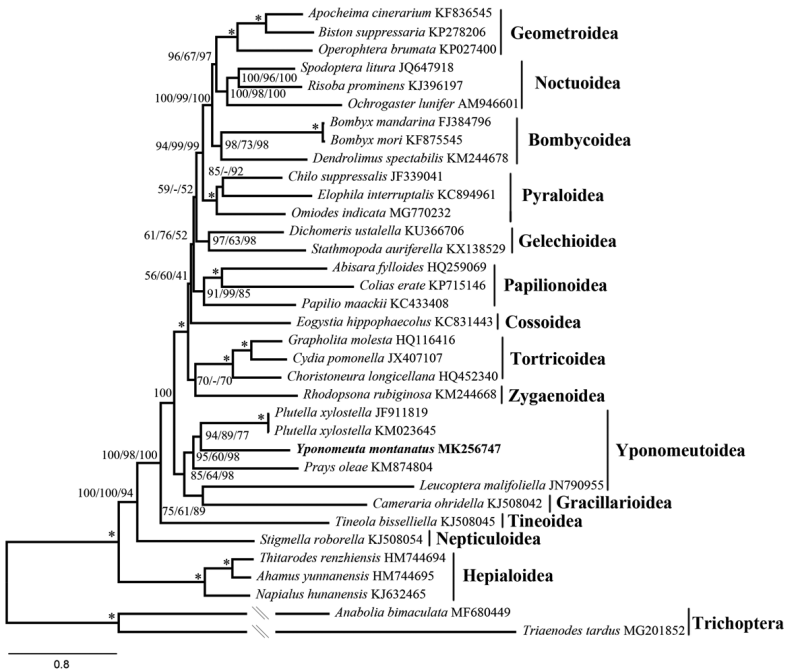


**Figure 7.** ML tree inferred from IQ-TREE method based on PCG123R dataset. Numbers separated by slash (/) on node represent bootstrap replicates based on PCG123, PCGAA and PCG123R datasets, respectively. The dash (-) represents unrecovered node in ML tree based on the PCG123 or PCGAA dataset.

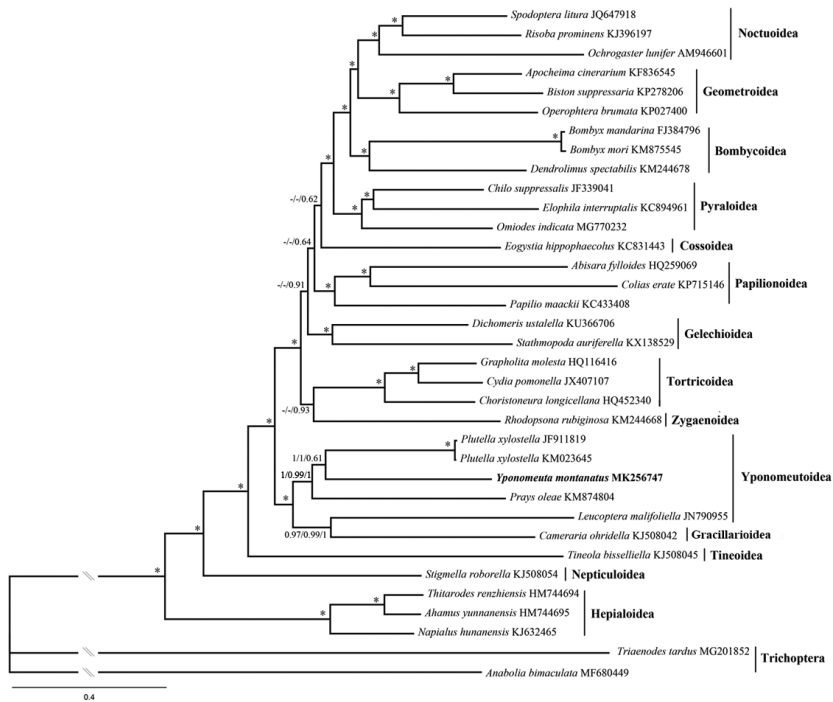


**Figure 8.** BI tree inferred from MrBayes method based on PCG123R dataset. Numbers separated by slash (/) on node represent posterior probabilities based on PCG123, PCGAA and PCG123R datasets, respectively. The dash (-) represents unrecovered node in BI tree based on the PCG123 or PCGAA dataset.

## Acknowledgements

We sincerely appreciate the anonymous reviewers for comments on this manuscript. This work was supported by the National Natural Science Foundation of China (31702046), Scientific and Technological Innovation Talent Project of Henan Province (19HASTIT015) and Science and Technology Program of Henan Province (182106000047).

## References

- Abascal F, Zardoya R, Telford MJ (2010) TranslatorX: multiple alignment of nucleotide sequences guided by amino acid translations. *Nucleic Acids Research* 38: W7–W13. <https://doi.org/10.1093/nar/gkq291>
- Bankevich A, Nurk S, Antipov D, Smoot M, Shumway M, Antonescu C, Salzberg SL (2012) SPAdes: a new genome assembly algorithm and its applications to single-cell sequencing. *Journal of Computational Biology* 19: 455–477. <https://doi.org/10.1089/cmb.2012.0021>
- Bao L, Zhang YH, Gu X, Gao YF, Yu YB (2018) The complete mitochondrial genome of *Eterusia aedea* (Lepidoptera, Zygaenidae) and comparison with other zygaenid moths. *Genomics* 111: 1043–1052. <https://doi.org/10.1016/j.ygeno.2018.06.007>

- Bazinnet AL, Cummings MP, Mitter KT, Mitter C (2013) Can RNA-Seq resolve the rapid radiation of advanced moths and butterflies (Hexapoda: Lepidoptera: Apoditrysia)? An exploratory study. PLoS ONE 8: e82615. <https://doi.org/10.1371/journal.pone.0082615>
- Benson G (1999) Tandem repeats finder: a program to analyze DNA sequences. Nucleic Acids Research 27: 573–580. <https://doi.org/10.1093/nar/27.2.573>
- Bernt M, Donath A, Jühling F, Externbrink F, Florentz C, Fritzsche G, Pütz J, Middendorf M, Stadler PF (2013) MITOS: improved de novo metazoan mitochondrial genome annotation. Molecular Phylogenetics and Evolution 69: 313–319. <https://doi.org/10.1016/j.ympev.2012.08.023>
- Boore JL (1999) Animal mitochondrial genomes. Nucleic Acids Research 27: 1767–1780. <https://doi.org/10.1093/nar/27.8.1767>
- Byun B-K, Bae Y-S (2013) Systematic review of the genus *Yponomeuta* L. (Lepidoptera: Yponomeutidae) in Korea. Insect Koreana 20: 227–237.
- Cameron SL (2014) Insect mitochondrial genomics: implications for evolution and phylogeny. Annual Review of Entomology 59: 95–117. <https://doi.org/10.1146/annurev-ento-011613-162007>
- Cameron SL, Whiting MF (2008) The complete mitochondrial genome of the tobacco hornworm, *Manduca sexta* (Insecta: Lepidoptera: Sphingidae), and an examination of mitochondrial gene variability within butterflies and moths. Gene 40: 112–123. <https://doi.org/10.1016/j.gene.2007.10.023>
- Cao SS, Yu WW, Sun M, Du YZ (2014) Characterization of the complete mitochondrial genome of *Tryporyza incertulas*, in comparison with seven other Pyraloidea moths. Gene 533: 356–365. <https://doi.org/10.1016/j.gene.2013.07.072>
- Cao YQ, Ma C, Chen JY, Yang DR (2012) The complete mitochondrial genomes of two ghost moths, *Thitarodes renzhiensis* and *Thitarodes yunnanensis*: the ancestral gene arrangement in Lepidoptera. BMC Genomics 13: 376. <https://doi.org/10.1186/1471-2164-13-276>
- Chai H-N, Du Y-Z (2012) The complete mitochondrial genome of the pink stem borer, *Sesamia inferens*, in comparison with four other noctuid moths. International Journal of Molecular Sciences 13: 10236–10256. <https://doi.org/10.3390/ijms130810236>
- Chen S, Li F-H, Lan X-E, You P (2016) The complete mitochondrial genome of *Pycnarmon lactiferalis* (Lepidoptera: Crambidae). Mitochondrial DNA Part B 1: 638–639. <https://doi.org/10.1080/23802359.2016.1214551>
- Chen Z-T, Du Y-Z, (2017) The first two mitochondrial genomes from Taeniopterygidae (Insecta: Plecoptera): structural features and phylogenetic implications. International Journal of Biological Macromolecules 111: 70–76. <https://doi.org/10.1016/j.ijbiomac.2017.12.150>
- Clary DO, Wolstenholme DR (1985) The ribosomal RNA genes of *Drosophila* mitochondrial DNA. Nucleic Acids Research 13: 4029–4045. <https://doi.org/10.1093/nar/13.11.4029>
- Coil D, Jospin G, Darling AE (2015) A5-miseq: an updated pipeline to assemble microbial genomes from Illumina MiSeq data. Bioinformatics 31: 587–589. <https://doi.org/10.1093/bioinformatics/btu661>
- Curole JP, Kocher TD (1999) Mitogenomics: digging deeper with complete mitochondrial genomes. Trends in Ecology & Evolution 14: 394–398. [https://doi.org/10.1016/S0169-5347\(99\)01660-2](https://doi.org/10.1016/S0169-5347(99)01660-2)

- Dai L-S, Zhu B-J, Qian C, Zhang C-F, Li J, Wang L, Wei G-Q, Liu C-L (2016) The complete mitochondrial genome of the diamondback moth, *Plutella xylostella* (Lepidoptera: Plutellidae). *Mitochondrial DNA Part A* 27: 1512–1513. <https://doi.org/10.3109/19401736.2014.953116>
- Garey JR, Wolstenholme DR (1989) Platyhelminth mitochondrial DNA: evidence for early evolutionary origin of a tRNA<sup>Ser</sup>AGN that contains a dihydrouridine arm replacement loop, and of serine-specifying AGA and AGG codons. *Journal of Molecular Evolution* 28: 374–387. <https://doi.org/10.1007/BF02603072>
- Heikkilä M, Mutanen M, Wahlberg N, Sihvonen P, Kaila L (2015) Elusive ditrysian phylogeny: an account of combining systematized morphology with molecular data (Lepidoptera). *BMC Evolutionary Biology* 15: 260. <https://doi.org/10.1186/s12862-015-0520-0>
- Katoh K, Rozewicki J, Yamada KD (2017) MAFFT online service: multiple sequence alignment, interactive sequence choice and visualization. *Briefings in Bioinformatics*. <https://doi.org/10.1093/bib/bbx108>
- Kawahara AY, Breinholt JW (2014) Phylogenomics provides strong evidence for relationships of butterflies and moths. *Proceedings of the Royal Society B: Biological Sciences* 281: 20140970. <https://doi.org/10.1098/rspb.2014.0970>
- Kim MJ, Jeong JS, Kim JS, Jeong SY, Kim I (2017) Complete mitochondrial genome of the lappet moth, *Kunugia undans* (Lepidoptera: Lasiocampidae): genomic comparisons among macroheteroceran superfamilies. *Genetics and Molecular Biology* 40: 717–723. <https://doi.org/10.1590/1678-4685-GMB-2016-0298>
- Kim MJ, Kang AR, Jeong HC, Kim KG, Kim I (2011) Reconstructing intraordinal relationships in Lepidoptera using mitochondrial genome data with the description of two newly sequenced lycaenids, *Spindasis takanonis* and *Protantigius superans* (Lepidoptera: Lycaenidae). *Molecular Phylogenetics and Evolution* 61: 436–445. <https://doi.org/10.1016/j.ympev.2011.07.013>
- Kurtz S, Phillippy A, Delcher AL, Smoot M, Shumway M, Antonescu C, Salzberg SL (2004) Versatile and open software for comparing large genomes. *Genome Biology* 5: R12. <https://doi.org/10.1186/gb-2004-5-2-r12>
- Lanfear R, Calcott B, Ho SY, Guindon S (2012) Partitionfinder: combined selection of partitioning schemes and substitution models for phylogenetic analyses. *Molecular Biology and Evolution* 29: 1695–1701. <https://doi.org/10.1093/molbev/mss020>
- Lavrov DV, Brown WM, Boore JL (2000) A novel type of RNA editing occurs in the mitochondrial tRNAs of the centipede *Lithobius forficatus*. *Proceedings of the National Academy of Sciences of the United States of America* 97: 13738–13742.
- Li J, Zhao Y, Lin R, Zhang Y, Hu K, Li Y, Huang Z, Peng S, Ding J, Geng X, Zhang H, Xu Z (2018) Mitochondrial genome characteristics of *Somena scintillans* (Lepidoptera: Erebidae) and comparison with other Noctuoidea insects. *Genomics*: <https://doi.org/10.1016/j.ygeno.2018.08.003>
- Librado P, Rozas J (2009) DnaSP v5: a software for comprehensive analysis of DNA polymorphism data. *Bioinformatics* 25: 1451–1452. <https://doi.org/10.1093/bioinformatics/btp187>
- Lowe T.M, Eddy SR (1997) tRNAscan-SE: A program for improved detection of transfer RNA genes in genomic sequence. *Nucleic Acids Research* 25: 955–964. <https://doi.org/10.1093/nar/25.5.0955>

- Luo R, Liu B, Xie Y, Li Z, Huang W, Yuan J, He G, Chen Y, Pan Q, Liu Y, Tang J, Wu G, Zhang H, Shi Y, Liu Y, Yu C, Wang B, Lu Y, Han C, Cheung DW, Yiu SM, Peng S, Xiaoqian Z, Liu G, Liao X, Li Y, Yang H, Wang J, Lam TW, Wang J (2012) SOAPdenovo2: an empirically improved memory-efficient short-read de novo assembler. *GigaScience* 1: 18. <https://doi.org/10.1186/2047-217x-1-18>
- Mikkel S, Lindgreen S, Orlando L (2016) AdapterRemoval v2: rapid adapter trimming, identification, and read merging. *BMC research notes* 9: 88. <https://doi.org/10.1186/s13104-016-1900-2>
- Mitter C, Davis DR, Cummings MP (2017) Phylogeny and evolution of Lepidoptera. *Annual Review of Entomology* 62: 265–283. <https://doi.org/10.1146/annurev-ento-031616-035125>
- Nguyen LT, Schmidt HA, von Haeseler A, Minh BQ (2015) IQ-TREE: a fast and effective stochastic algorithm for estimating maximum-likelihood phylogenies. *Molecular Biology and Evolution* 32: 268–274. <https://doi.org/10.1093/molbev/msu300>
- Ojala D, Montoya J, Attardi G (1981) tRNA punctuation model of RNA processing in human mitochondria. *Nature* 290: 470–474. <https://doi.org/10.1038/290470a0>
- Perna NT, Kocher TD (1995) Patterns of nucleotide composition at fourfold degenerate sites of animal mitochondrial genomes. *Journal of Molecular Evolution* 41: 353–358. <https://doi.org/10.1007/BF01215182>
- Rambaut A, Suchard MA, Xie D, Drummond AJ (2014) Tracer v1.6. <http://tree.bio.ed.ac.uk/software/tracer/>
- Regier JC, Mitter C, Zwick A, Bazinet AL, Cummings MP, Kawahara AY, Sohn J-C, Zwickl DJ, Cho S, Davis DR, Baixeras J, Brown J, Parr C, Weller S, Lees DC, Mitter KT (2013) A large-scale, higher-level, molecular phylogenetic study of the insect order Lepidoptera (moths and butterflies). *PLoS ONE* 8: e58568. <https://doi.org/10.1371/journal.pone.0058568>
- Ronquist F, Huelsenbeck JP (2003) MrBayes3: Bayesian phylogenetic inference under mixed models. *Bioinformatics* 19: 1572–1574. <https://doi.org/10.1093/bioinformatics/btg180>
- Sohn JC, Regier JC, Mitter C, Davis D, Landry J-F, Zwick A, Cummings MP (2013) A molecular phylogeny for Yponomeutoidea (Insecta, Lepidoptera, Ditrysia) and its implications for classification, biogeography and the evolution of host plant use. *PLoS ONE* 8: e55066. <https://doi.org/10.1371/journal.pone.0055066>
- Salvato P, Simonato M, Battisti A, Negrisolo E (2008) The complete mitochondrial genome of the bag-shelter moth *Ochrogaster lunifer* (Lepidoptera, Notodontidae). *BMC Genomics* 9: 331. <https://doi.org/10.1186/1471-2164-9-331>
- Silvestro D, Michalak I (2012) raxmlGUI: a graphical front-end for RAxML. *Organisms Diversity & Evolution* 12: 335–337. <https://doi.org/10.1007/s13127-011-0056-0>
- Stamatakis A (2006) RAxML-VI-HPC: maximum likelihood-based phylogenetic analyses with thousands of taxa and mixed models. *Bioinformatics* 22: 2688–2690. <https://doi.org/10.1093/bioinformatics/btl446>
- Taanman JW (1999) The mitochondrial genome: structure, transcription, translation and replication. *Biochim Biophys Acta* 1410: 103–123. [https://doi.org/10.1016/S0005-2728\(98\)00161-3](https://doi.org/10.1016/S0005-2728(98)00161-3)

- Tamura K, Stecher G, Peterson D, Filipiński A, Kumar S (2013) MEGA6: Molecular evolutionary genetics analysis version 6.0. *Molecular Biology and Evolution* 30: 2725–2729. <https://doi.org/10.1093/molbev/mst197>
- Timmermans MJTN, Lees DC, Simonsen TJ (2014) Towards a mitogenomic phylogeny of Lepidoptera. *Molecular Phylogenetics and Evolution* 79: 169–178. <https://doi.org/10.1016/j.ympev.2014.05.031>
- van Asch B, Blibech I, Pereira-Castro I, Rei FT, da Costa LT (2016) The mitochondrial genome of *Prays oleae* (Insecta: Lepidoptera: Praydidae). *Mitochondrial DNA Part A, DNA Mapping, Sequencing, and Analysis* 27: 2108–2109. <https://doi.org/10.3109/19401736.2014.982579>
- van Nieuwerkerken EJ, Kaila L, Kitching IJ, Kristensen NP, Lees DC, Minet J, Mitter C, Mutanen M, Regier JC, Simonsen TJ, Wahlberg N, Yen SH, Zahiri R, Adamski D, Baixeras J, Bartsch D, Bengtsson BÅ, Brown JW, Bucheli SR, Davis DR, de Prins J, de Prins W, Epstein ME, Gentili-Poole P, Gielis C, Hättenschwiler P, Hausmann A, Holloway JD, Kallies A, Karsholt O, Kawahara AY, Koster S, Kozlov M, Lafontaine J D, Lamas G, Landry J-F, Lee S, Nuss M, Park K-T, Penz C, Rota J, Schintlmeister A, Schmidt BC, Sohn J-C, Solis MA, Tarmann GM, Warren AD, Weller S, Yakovlev RV, Zolotuhin VV, Zwick, A (2011) Order Lepidoptera Linnaeus, 1758. *Zootaxa* 3148: 212–221. <https://doi.org/10.11646/zootaxa.3148.1.41>
- Vila M, Björklund M (2004) The utility of the neglected mitochondrial control region for evolutionary studies in Lepidoptera (Insecta). *Journal of Molecular Evolution* 58: 280–290. <https://doi.org/10.1007/s00239-003-2550-2>
- Wei S-J, Shi B-C, Gong Y-J, Li Q, Chen X-X (2013) Characterization of the mitochondrial genome of the diamondback moth *Plutella xylostella* (Lepidoptera: Plutellidae) and phylogenetic analysis of advanced moths and butterflies. *DNA and Cell Biology* 32: 173–187. <https://doi.org/10.1089/dna.2012.1942>
- Wei SJ, Shi M, Chen XX, Sharkey M.J., van Achterberg C, Ye GY, He JH (2010) New views on strand asymmetry in insect mitochondrial genomes. *PLoS ONE* 5: e12708. <https://doi.org/10.1371/journal.pone.0012708>
- Wu Y-P, Zhao J-L, Su T-J, Li J, Yu F, Chesters D, Fan R-J, Chen M-C, Wu C-S, Zhu C-D (2012) The complete mitochondrial genome of *Leucoptera malifoliella* Costa (Lepidoptera: Lyonetiidae). *DNA and Cell Biology* 31: 1508–1522. <https://doi.org/10.1089/dna.2012.1642>
- Wu YP, Zhao J-L, Su T-J, Luo A-R, Zhu C-D (2016) The complete mitochondrial genome of *Choristoneura longicellana* (Lepidoptera: Tortricidae) and phylogenetic analysis of Lepidoptera. *Gene* 591: 161–176. <https://doi.org/10.1016/j.gene.2016.07.003>
- Yang X, Cameron SL, Lees DC, Xue D, Han H (2015) A mitochondrial genome phylogeny of owlet moths (Lepidoptera: Noctuoidea), and examination of the utility of mitochondrial genomes for lepidopteran phylogenetics. *Molecular Phylogenetics and Evolution* 85: 230–237. <https://doi.org/10.1016/j.ympev.2015.02.005>
- Zhang D-X, Hewitt GM (1997) Insect mitochondrial control region: a review of its structure, evolution and usefulness in evolutionary study. *Biochemical Systematics and Ecology* 25: 99–120. [https://doi.org/10.1016/s0305-1978\(96\)00042-7](https://doi.org/10.1016/s0305-1978(96)00042-7)

## Supplementary material 1

### Supplementary Tables S1–S8

Authors: Mingsheng Yang, Bingyi Hu, Lin Zhou, Xiaomeng Liu, Yuxia Shi, Lu Song, Yunshan Wei, Jinfeng Cao

Data type: molecular data

Explanation note: **Table S1.** List of Lepidoptera species used in phylogenetic analyses.

**Table S2.** The best scheme and substitution models for the PCG123R dataset.

**Table S3.** The best scheme and substitution models for for the PCG123 dataset. **Table S4.** AT-skew and GC-skew of the *Yponomeuta montanatus* mitogenome.

**Table S5.** A + T content (%) in three codon positions in mitochondrial protein-coding genes of reported yponomeutoid mitogenomes.

**Table S6.** Codon usage in mitochondrial protein-coding genes of the *Yponomeuta montanatus*.

**Table S7.** Start and stop codons of mitochondrial protein-coding genes of four yponomeutoid species. **Table S8.** Evolutionary rates of mitochondrial protein-coding genes among reported yponomeutoid mitogenomes.

Copyright notice: This dataset is made available under the Open Database License (<http://opendatacommons.org/licenses/odbl/1.0/>). The Open Database License (ODbL) is a license agreement intended to allow users to freely share, modify, and use this Dataset while maintaining this same freedom for others, provided that the original source and author(s) are credited.

Link: <https://doi.org/10.3897/zookeys.879.35101.suppl1>

## Supplementary material 2

### Supplementary Figures S1–S3

Authors: Mingsheng Yang, Bingyi Hu, Lin Zhou, Xiaomeng Liu, Yuxia Shi, Lu Song, Yunshan Wei, Jinfeng Cao

Data type: molecular data

Explanation note: **Figure S1.** ML trees inferred from RAxML method based on PCG123 (A) and PCGAA (B) datasets. Number on node represents bootstrap replicate.

**Figure S2.** ML trees inferred from IQ-TREE method based on PCG123 (A) and PCGAA (B) datasets. Number on node represents bootstrap replicate.

**Figure S3.** BI trees inferred from MrBayes method based on PCG123 (A) and PCGAA (B) datasets. Number on node represents posterior probability.

Copyright notice: This dataset is made available under the Open Database License (<http://opendatacommons.org/licenses/odbl/1.0/>). The Open Database License (ODbL) is a license agreement intended to allow users to freely share, modify, and use this Dataset while maintaining this same freedom for others, provided that the original source and author(s) are credited.

Link: <https://doi.org/10.3897/zookeys.879.35101.suppl2>